DEVELOPMENT AND DISEASE: QUANTIFICATION OF INHIBITORY AND EXCITATORY SYNAPTIC STRUCTURES IN PRIMARY AUDITORY CORTEX DURING ADOLESCENCE AND IN SCHIZOPHRENIA

by

Caitlin Elizabeth Moyer

Bachelor of Arts in Biology, St. Mary's College of Maryland, 2007

Submitted to the Graduate Faculty of

University of Pittsburgh School of Medicine in partial fulfillment

of the requirements for the degree of

Doctor of Philosophy

University of Pittsburgh

2013

UNIVERSITY OF PITTSBURGH

School of Medicine

This dissertation was presented

by

Caitlin Elizabeth Moyer

It was defended on

August 28, 2013

and approved by

Kenneth N. Fish, PhD, Assistant Professor, Dept. of Psychiatry

Lori L. Holt, PhD, Professor, Dept. of Psychology, Carnegie Mellon University,

and Adjunct Professor, Dept. of Neuroscience

Daniel C. Javitt, MD, PhD, Professor, Dept. of Psychiatry and Neuroscience,

Columbia University

Edda Thiels, PhD, Assistant Professor, Dept. of Neurobiology

Committee Chair: Etienne L. Sibille, PhD, Associate Professor, Dept. of Psychiatry

Dissertation Advisor: Robert A. Sweet, MD, Professor, Dept. of Psychiatry and Neurology

DEVELOPMENT AND DISEASE: QUANTIFICATION OF INHIBITORY AND EXCITATORY SYNAPTIC STRUCTURES IN PRIMARY AUDITORY CORTEX DURING ADOLESCENCE AND IN SCHIZOPHRENIA

Caitlin Elizabeth Moyer, Ph.D.

University of Pittsburgh, 2013

Individuals with schizophrenia demonstrate auditory processing impairments that localize to primary auditory cortex, and likely contribute to disruptions of higher level processes and resultant disability. To inform the development of new treatments and preventative measures, we sought to understand which synapse populations contribute to primary auditory cortex pathology. We used quantitative fluorescence microscopy to assess intracortical excitatory, thalamocortical, and inhibitory boutons in primary auditory cortex deep layer 3 of individuals with schizophrenia. We found that intracortical excitatory and thalamocortical boutons are unaltered in schizophrenia despite reduced density of dendritic spines, their primary postsynaptic targets. However, levels of the 65 kiloDalton isoform of glutamate decarboxylase (GAD65) protein are reduced within inhibitory boutons in primary auditory cortex of subjects with schizophrenia. Further, reductions in within-bouton GAD65 protein are correlated with previously measured reductions in spine density.

As the onset of schizophrenia typically occurs during late adolescence and young adulthood, adolescence represents a potential window of opportunity for preventing the pathophysiology underlying symptom onset. However, adolescent trajectories of auditory cortex synaptic components and associated auditory cortex functional changes that could be targeted for prevention have not been characterized. In mouse auditory cortex, we found that spine and

excitatory bouton numbers decrease between early adolescence and young adulthood, followed by reduction of within-bouton GAD65 protein levels between late adolescence and young adulthood. As a behavioral readout of auditory cortex function, we measured gap-mediated prepulse inhibition of the acoustic startle reflex (gap-PPI) in mice between early adolescence and young adulthood. Gap-PPI responses increase during adolescence, suggesting that adolescent development of auditory cortex synapses contributes to auditory cortex functional maturation.

Our findings suggest that spine and within-bouton GAD65 protein deficits are related pathological features of primary auditory cortex in schizophrenia, and that within-bouton GAD65 protein declines subsequent to the onset of auditory cortex spine pruning between early adolescence and young adulthood. From these observations, we propose a model where excessive spine pruning in auditory cortex leads to an excessive reduction in within-bouton GAD65 protein. Testing this model will promote development of strategies to prevent auditory cortex pathophysiology and downstream perceptual and cognitive deficits in schizophrenia.

TABLE OF CONTENTS

LIST OF TABLES

LIST OF FIGURES

ACKNOWLEDGEMENTS

First of all, I thank my mentor, Dr. Rob Sweet, for taking me on as a graduate student, and for the time and energy he has put into my graduate training. Rob's dedication to his research, clinical work, and family is inspiring, and I have learned so much from him as both a scientist and a person. I am grateful to the members of my committee Dr. Etienne Sibille, Dr. Ken Fish, Dr. Floh Thiels and Dr. Lori Holt for the guidance, insights and enthusiasm they have provided to help shape and enrich my dissertation project. I would especially like to thank Ken for the time he spent teaching me quantitative microscopy techniques, and Floh for her guidance on the mouse behavioral studies. Finally, I would like to thank Dr. Dan Javitt, for taking the time to participate in my dissertation defense as external examiner. Over the years I have enjoyed reading about Dr. Javitt's contributions to the field of sensory dysfunction in schizophrenia, and it was an honor to have him as a member of my committee.

I thank all the past and current members of the Sweet lab for years of technical support and helpful discussions. I thank my labmates Caitlin Kirkwood, Isaac Goldszer, and Patrick Murray for their encouragement and friendship. I am grateful to Ruth Henteleff, for patiently teaching me the fundamentals of immunohistochemistry, and to Kristen Delevich, who contributed to data collection and analysis in the studies presented in chapters 2 and 3. I thank Dr. Susan Erickson, who has provided me with invaluable advice on countless occasions, and I am especially grateful for her help maintaining and generating the mice I needed for the studies

in chapters 4 and 5. Finally, I thank Eloise Peet, for technical support while I was carrying out the behavioral experiments, and for her friendship during the long days I spent in the RBAC.

I would like to thank all the members of the Translational Neuroscience Program, for their support and feedback over the years. I would especially like to thank everyone on the Brain Bank team for their efforts to generate and maintain high-quality tissue resources. I also would like to acknowledge the CNUP students and faculty for fostering a positive and collaborative graduate school environment. I am so grateful for the opportunities and interactions that I have experienced here. I also thank the CNUP administrative staff, especially Patti Argenzio, for patiently answering many questions and making sure I stayed on track.

I am grateful to all my friends and family who have provided me with motivation and support during my graduate studies. I am especially grateful to my friends and CNUP classmates, Amanda Kinnischtzke and Erin Kirschmann, who have been sources of fun and friendship since our first year. I thank my boyfriend Adam Hartman for the love and understanding that keeps me going every day. I thank my family, especially my parents Braxton Moyer and Donna Goletz for encouraging me to succeed academically and for providing me with opportunities that allowed me to reach my goals.

Lastly, I would like to acknowledge the families who gave consent for tissue donation, for without their generosity this research would not be possible.

1.0 INTRODUCTION

Schizophrenia is a chronic illness associated with lifelong debilitation and reduced quality of life that affects approximately 0.7% of the world's population (World Health Organization, 2013). Age of onset, defined by the first appearance of psychotic symptoms (American Psychiatric Association, 1994) is typically during the late adolescent to early adult years; generally between 18 and 30 years of age (Tandon et al., 2009). Disease onset in males is about 4 years earlier than in females (Hafner et al., 1993), and females also exhibit a second peak in age of onset later in life, between age 45 and 55 (Hafner et al., 1991). Individuals with schizophrenia have an increased risk for comorbid illnesses and death by suicide, and overall the lifespan in individuals with schizophrenia is reduced by approximately 15-20 years (Auquier et al., 2007). The debilitating consequences of schizophrenia coupled with the typically young age of onset illustrate the devastating impact on the life of affected individuals.

A definite cause of schizophrenia has yet to be identified. Evidence suggests a strong role of genetics in the etiology of schizophrenia, as monozygotic twins demonstrate 45-60% concordance for schizophrenia and the estimate of heritability is about 80% (Sullivan et al., 2003). A number of potential schizophrenia susceptibility genes have been identified (Owen et al., 2004), but no one genetic factor appears to be responsible. This suggests that risk for schizophrenia is likely to be conferred through the converging effects of multiple genes (Gottesman and Shields, 1967). The fact that the concordance rate between monozygotic twins

is not 100% also suggests that environmental influences contribute to the likelihood of developing schizophrenia. Many environmental risk factors for developing schizophrenia have been identified (Brown, 2011), and include prenatal exposure to maternal infection (Brown and Derkits, 2010), obstetric complications (Cannon et al., 2003), birth during winter or early spring (Davies et al., 2003), urban upbringing (Vassos et al., 2012), and cannabis use (Smit et al., 2004). Taken together, this suggests that both genetics and environmental factors contribute to the etiology of schizophrenia.

Schizophrenia is characterized by a variety of symptoms, which can be categorized into positive, negative, and cognitive domains (Tandon et al., 2008; Tandon et al., 2009). Positive symptoms describe the presence of perceptions or behaviors involving distortions of reality, including disorganized thought processes, delusions, and hallucinations. Hallucinations may occur in any sensory modality, but are typically auditory and verbal in nature. Negative symptoms refer to the absence of behaviors which should be present, including alogia (absence of speech), avolition (absence of motivation), anhedonia (inability to experience pleasure), and flattened affect (inability to express emotion). Negative symptoms have been shown to contribute to occupational impairments (Lysaker and Bell, 1995). Cognitive symptoms include impairments in memory performance, executive function, attention, as well as poor language and reading ability (Salisbury, 2008), and impaired social cognition (Green et al., 2008). Deficits in cognition are highly prevalent, and are present to some degree in the pre-morbid phase of the illness, in addition to being observed in first-degree relatives, suggesting that these symptoms are related to the etiology of schizophrenia and are not a consequence of long-term illness (Tandon et al., 2009). Although evidence for a strong link between positive symptoms and functional outcome is lacking (Green, 1996), symptoms such as hallucinations are debilitating, and

psychotic symptoms do contribute to reduced occupational functioning (Racenstein et al., 2002). However, positive symptoms are relatively well controlled by current antipsychotic medications (Miyamoto et al., 2005), while current available treatments do not reduce the impact of negative or cognitive symptoms on the life of an affected individual (Keshavan et al., 2008). Therefore, we need to increase our understanding of the neuropathological processes that contribute to negative and cognitive symptoms in order to implement more effective treatments.

Abnormal functioning of the auditory system could contribute to all three symptom domains. For example, auditory verbal hallucinations may arise in part from increased activity of the primary auditory cortex (Dierks et al., 1999). As we will review in the following sections, disruptions in auditory processing can hinder verbal communication, which could contribute to negative symptoms such as social withdrawal, and cognitive impairments including language and reading impairments and decreases in social cognition. As auditory processing impairments seem to contribute to multiple symptom domains, a more complete understanding of the neurobiological contributions to these impairments may ultimately allow for design of novel treatments which address more than just the positive symptoms.

This thesis investigates the contribution of excitatory and inhibitory synapse impairments to auditory cortex pathology in schizophrenia, as well as the developmental trajectories of excitatory and inhibitory synapse components during adolescence, a key time period for schizophrenia symptom emergence, and finally the behavioral correlates of auditory cortex adolescent development. In the following sections, we will begin by reviewing the basic organization of the cortical auditory regions, which will inform a discussion of auditory behavioral, electrophysiological and anatomical abnormalities observed in individuals with schizophrenia. We will then discuss what is known about excitatory and inhibitory synapse

development in the cortex during adolescence, a key developmental period for symptom onset, and discuss a relevant genetic animal model that can be used to study altered adolescent cortical synapse development.

1.1 ORGANIZATION OF THE AUDITORY CORTEX

1.1.1 Auditory cortical regions

In primate cortex, there are three hierarchical auditory processing areas: the core, the belt, and the parabelt (Kaas and Hackett, 2000). In humans, the anatomical location of the core, belt and parabelt regions are Heschl's gyrus, the banks of Heschl's sulcus, and the planum temporale, respectively (Sweet et al., 2005). Heschl's gyrus extends transversely across the superior temporal plane, within the sylvian fissure. The core corresponds to Brodmann's area 41 (Garey, 1999) and exhibits characteristics attributable to primary sensory cortex, including short latency responses to pure tones. The core also possesses biochemical characteristics of primary sensory regions, such as prominent expression of cytochrome oxidase, parvalbumin, and acetylcholinesterase in the middle cortical layers (Tootell et al., 1985; Hackett et al., 1998). Auditory projections from the ventral subdivision of the medial geniculate nucleus (MGNv) terminate in the core region, which is the primary auditory region. Neurons in the belt receive extensive feedforward projections from the core, and respond to higher-order characteristics of auditory stimuli, such as narrow frequency bands of noise rather than tones (Rauschecker et al., 1995). The parabelt receives information from the core, via the belt, and functional studies suggest activity in the parabelt is consistent with its role as a tertiary auditory region (Molinari et

al., 1995; Hackett et al., 1998; Griffiths and Warren, 2002). The parabelt sends projections to nearby areas in the parietal and temporal lobes, as well as to regions of the frontal cortex (Hackett et al., 1999), where presumably, multimodal integration and higher-order processing can occur.

1.1.2 Auditory cortex circuitry

The laminar organization of primary auditory cortex (**Figure 1.1**) is generally similar to the organization reported for other primary sensory regions (Rockel et al., 1980), but there are some notable differences (Read et al., 2002; Linden and Schreiner, 2003). The principal sensory thalamocortical projections (also referred to as the lemniscal pathway) arise from the MGNv. The primary cells receiving thalamocortical input are pyramidal neurons in deep layer 3 and layer 4, rather than spiny stellate cells as in layer 4 of the primary visual cortex (Smith and Populin, 2001). The medial division of the MGN (MGNm) projects to layers 1 and 6 (Winer and Larue, 1989), while the dorsal division of the MGN (MGNd) projects to layers 1, 2, 5, and 6 (Winer, 1985; Winer and Prieto, 2001). Following the initial activation of thalamocortical synapses, information flows to supragranular layers 2 and 3, which are densely packed and supply corticocortical projections, including projections to the contralateral primary auditory cortex, a feature of primary auditory cortex that is not shared by the primary visual cortex (Linden and Schreiner, 2003). In contrast with other sensory cortices, layer 2/3 pyramidal neurons also send projections back to layer 4 (Barbour and Callaway, 2008). From the supragranular layers, information flows to the infragranular layers. Layer 5 is relatively sparsely populated and contains large pyramidal neurons which project to all divisions of the MGN (Winer and Prieto, 2001; Winer et al., 2001), as well as to the inferior colliculus (Mitani and

Shimokouchi, 1985; Winer et al., 1998) and the dorsal cochlear nucleus (Weedman and Ryugo, 1996). Layer 6 supplies feedback projections to the MGNv, which are thought to modulate thalamic responses (Villa et al., 1991; Zhang and Suga, 1997; Yan and Ehret, 2002).

1.1.3 Role of primary auditory cortex excitation and inhibition in auditory processing

Excitation and inhibition in the auditory cortex help to shape responses to auditory stimuli. Excitatory responses in primary auditory cortex neurons can be elicited via two broad classifications of glutamatergic input, thalamocortical and intracortical. Tone-evoked excitatory responses are reported to be about 60% attributable to thalamic inputs, as opposed to excitation arising within the cortex (Liu et al., 2007). Intracortical excitatory transmission is thought to play a role in amplification and sharpening of auditory cortex neuron responses (Liu et al., 2007). Approximately 20% of auditory cortex neurons are GABAergic (Prieto et al., 1994), and inhibition that balances excitation is also important for frequency tuning and temporal precision of auditory cortex responses (Wehr and Zador, 2003; Wu et al., 2008). The primary auditory cortex is specialized for processing fast temporal information, and inhibitory responses in auditory cortex are faster than in other cortical areas (Hefti and Smith, 2000). Evidence suggests that delayed inhibition from GABAergic inhibitory synapses increases the precision of excitatory neuron firing (Wehr and Zador, 2003) and helps to refine frequency tuning curves of neurons in primary auditory cortex, as tuning curves can be broadened or narrowed through application of $GABA_A$ receptor antagonists and agonists, respectively (Wang et al., 2000; Wang et al., 2002; Kaur et al., 2005). One model suggests that inhibition which is more broadly tuned than excitation will narrow the recipient neuron's tuning curve by generating relatively more inhibition than excitation at the lateral "edges" of the frequency tuning curve (Wu et al., 2008).

Together, evidence suggests that both excitation and inhibition in primary auditory cortex are important for generating refined responses to acoustic stimuli.

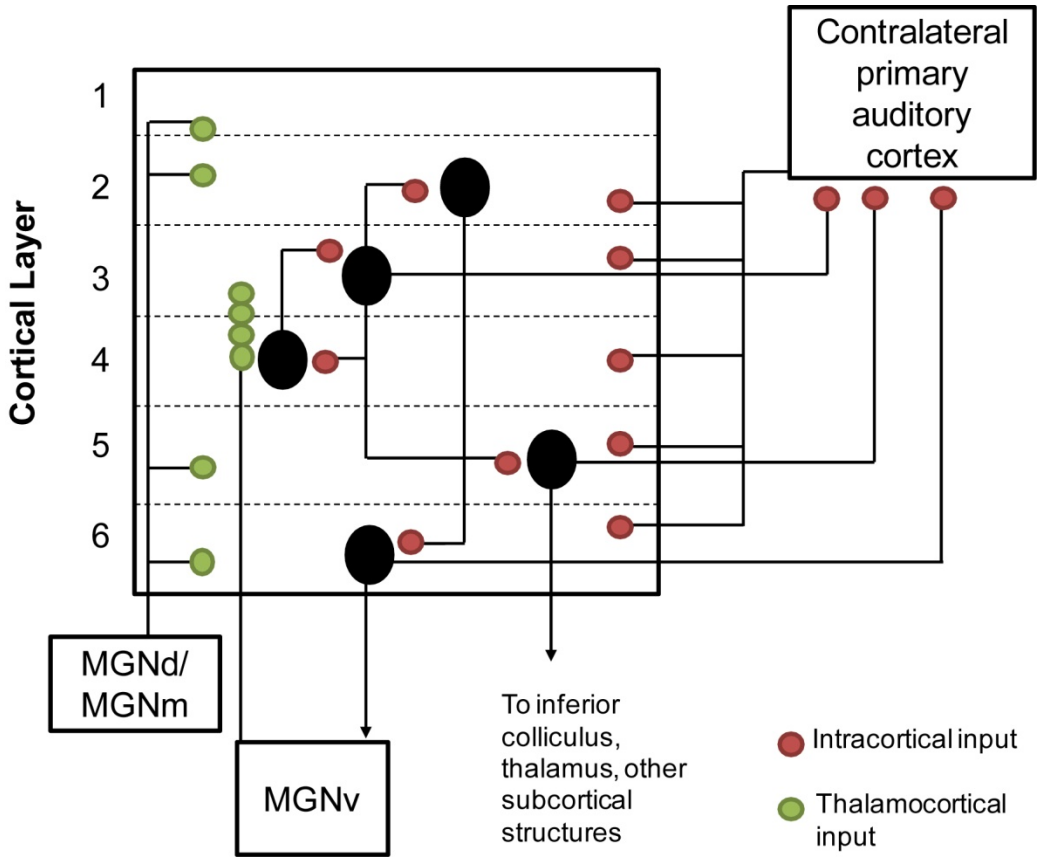

Figure 1.1. Schematic depicting primary auditory cortex circuitry. Black ovals represent pyramidal neurons, small spheres represent thalamocortical (green) or intracortical (red) excitatory inputs to primary auditory cortex. Modified from Linden and Schreiner (2003).

1.2 DYSFUNCTIONAL AUDITORY PROCESSING IN SCHIZOPHRENIA

1.2.1 Auditory perceptual impairments in schizophrenia: contribution to negative and cognitive symptoms and functional outcome

Correlative studies suggest that basic auditory processing dysfunction in schizophrenia may contribute to symptoms. Individuals with schizophrenia show reduced ability to match two tones separated by a brief interval, suggesting that tone discrimination ability and/or auditory sensory memory may be impaired (Strous et al., 1995). Correlated with these tone discrimination deficits, individuals with schizophrenia also exhibit poor recognition of vocally expressed emotion across a range of emotions (Leitman et al., 2010a). Deficits in emotion identification appear to be derived from an inability to utilize pitch-based acoustic features and frequency modulation as cues (Leitman et al., 2010a; Kantrowitz et al., 2013). Inability to interpret emotion in spoken language would be expected to substantially impact social communication and may lead to social withdrawal and impaired social cognition.

However, the role of vocal pitch extends further than the expression of emotion by the speaker. In many non-Western languages, modulation of vocal pitch is essential for communication of semantic meaning. In Mandarin-speaking patients with schizophrenia, impaired tone matching performance is associated with poor word identification and discrimination between words (Yang et al., 2012). Even in non-tonal languages, prosodic phrasing of sentences contributes heavily to interpretation of meaning (Frazier et al., 2006) and informs the listener about whether a phrase is a question or a statement. Further, variations in pitch are used in language to distinguish phonemes, the simplest components of speech. For example, relatively subtle differences in formant pitch, and formant pitch of preceding and

subsequent syllables, allow for categorical perception of syllables such as *ga* and *da* (Holt and Lotto, 2008). Therefore, difficulty discriminating between closely related pitches would impact phoneme identification and speech comprehension (Javitt, 2009). This evidence suggests that impairments in very basic auditory perception exert a detrimental effect on both the emotional and semantic aspects of verbal communication. It is possible that these deficits lead to the reading impairments observed in schizophrenia (Revheim et al., 2006), and ultimately to impairments in verbal learning and memory (Kawakubo et al., 2007).

Evidence suggests that the negative and cognitive aspects of schizophrenia, including impairment in social cognition, contribute to long-term functional outcome (Green, 1996; Evans et al., 2004; Schmidt et al., 2011). Further in support of a link between auditory processing deficits and disease severity, tone matching performance is severely impaired in patients with poor long term outcome, such as in those who need long-term residential care (Rabinowicz et al., 2000). Also, groups at high risk of developing schizophrenia demonstrate impairments in auditory working memory, verbal memory, and verbal processing (Simon et al., 2007). This suggests that these deficits are not simply a consequence of long-term illness and represent the pathophysiology of schizophrenia. Finally, auditory training paradigms have been shown to increase verbal memory and cognition (Adcock et al., 2009), further suggesting that auditory processing contributes to cognitive function. Taken together, this evidence suggests that auditory processing impairments exert effects on the functional outcome and quality of life of individuals with schizophrenia.

1.2.2 Electrophysiological measures of disrupted auditory processing in schizophrenia

The function of the auditory system can also be evaluated using auditory event related potentials (ERPs), which can be measured non-invasively in humans using electroencephalography (EEG) or magnetoencephalography (MEG). One index of early auditory sensory processing is the N100, or N1, an auditory evoked potential that is indicative of auditory stimulus detection, reflects early cortical activity to an auditory stimulus (Naatanen and Picton, 1987), and is reported to be abnormal in schizophrenia (Saletu et al., 1971). The MEG equivalent M100 response to pairs of syllables differing in voice onset time (VOT) (for example, *ba* has a short VOT and *pa* has a long VOT), is abnormal in the presence of background noise in individuals with schizophrenia (Dale et al., 2010). VOT is the duration of time between the offset of the consonant and onset of low-frequency speech sound, and responses to VOT have been recorded in monkey and human primary auditory cortex (Steinschneider et al., 1994; Steinschneider et al., 1995; Steinschneider et al., 1999). Perception of VOT is related to and may rely on mechanisms similar to those for detection of silent gaps embedded in acoustic stimuli (Elangovan and Stuart, 2008) which are also encoded to some extent in primary auditory cortex (Eggermont, 1999; Eggermont, 2000; Kirby and Middlebrooks, 2012). This demonstrates electrophysiological evidence for impaired language perception in schizophrenia, and implies that disruption in primary auditory cortex function underlies these deficits.

The mismatch negativity response (MMN), another index of early auditory processing is also impaired in schizophrenia. MMN reflects activity in the auditory cortex in response to an infrequent stimulus presented during a series of repetitive stimuli. As the response can be evoked regardless of whether the subject is paying attention to the stimuli or is distracted with another task, it is thought to represent pre-attentive auditory sensory memory (Naatanen et al.,

1989; Alho et al., 1994; Winkler et al., 1996). Individuals with schizophrenia exhibit MMN impairments when the auditory stimuli are deviant for duration (Shelley et al., 1991) or pitch (tone frequency) (Javitt et al., 1993). Subsequent MMN deficits have also been reported when the auditory stimulus is deviant in intensity, location, or by insertion of a silent gap in a tone (Thonnessen et al., 2008), suggesting impairment in discrimination of a variety of acoustic stimulus features. The reductions in the MMN response to frequency deviants are correlated with impairments in pure tone frequency discrimination (Javitt et al., 1994; Javitt et al., 2000; Naatanen and Kahkonen, 2009; Leitman et al., 2010b), suggesting that altered auditory physiology underlies the behavioral observations in individuals with schizophrenia. Further, duration-MMN is not impaired in individuals with bipolar disorder, suggesting specificity for the disease process of schizophrenia (Catts et al., 1995). When phonemes are used as stimuli in a MMN paradigm, patients with schizophrenia demonstrate impaired MMN responses (Kasai et al., 2002), suggesting inability to distinguish between changes in the basic elements that contribute to speech. Finally, greater duration-MMN responses are associated with better daily functioning and social cognition (Wynn et al., 2010), suggesting that MMN impairments contribute to deficits that have an impact on disease outcome.

Animal studies indicate that both frequency discrimination and MMN are dependent upon the supragranular auditory cortex (Javitt et al., 1994; Javitt et al., 1996; Tramo et al., 2002; Kaur et al., 2005; Molholm et al., 2005; Liu et al., 2007). Intracortical recordings in non-human primate auditory cortex during an MMN paradigm indicate that while the initial thalamocortical responses are similar for the standard and the deviant stimuli, the change detection signal appears to be represented by increased excitatory activity in primary auditory cortex layers 2 and 3 in response to the deviant stimulus (Javitt et al., 1994). Further, application of PCP and MK-801,

antagonists of the NMDA subtype of ionotropic glutamate receptors, prevent the increased supragranular response to the deviant stimulus (Javitt et al., 1996). In contrast, application of the $GABA_A$ receptor antagonist bicuculline generally enhanced activity levels, and the pan-glutamatergic antagonist kynurenic acid reduced activity in supragranular layers to the standard stimuli, rather than specifically reducing the response to the deviant. This suggests that there are alterations in the circuitry, specifically NMDA-mediated glutamatergic circuitry, in supragranular primary auditory cortex in subjects with schizophrenia that may contribute to functional deficits in early auditory processing.

Another auditory evoked potential found to be impaired in individuals with schizophrenia is the auditory steady state response (aSSR), which reflects the synchronized response of neurons to a temporally modulated auditory stimulus (for example, clicks or tones repeated at a rapid rate, amplitude modulated tones). Individuals with schizophrenia exhibit reduced aSSR power in response to a 40 Hz click train (Kwon et al., 1999b; Light et al., 2006), as well as reduced aSSR theta (5 Hz) and gamma (80 Hz) levels of entrainment to modulated noise stimuli (Hamm et al., 2011). Mean power in the gamma range (40 Hz) is also reduced in response to an unmodulated pure tone stimuli in subjects with schizophrenia, suggesting that impairment in auditory cortex oscillatory activity is not restricted to steady state responses to auditory stimuli (Krishnan et al., 2009). Further, impairments in the 40 Hz response are reported to be present in first episode patients (Spencer et al., 2008), and also in first degree relatives of patients (Hong et al., 2004), suggesting that auditory functional impairments are not a consequence of long-term illness or medication, and are a primary pathological feature of schizophrenia. The aSSR response is thought to be generated by the primary auditory cortex (Pastor et al., 2002; Picton et al., 2003). As GABAergic interneurons play a role in the generation of gamma oscillations by

synchronizing firing rates of pyramidal neurons (Whittington et al., 2000; Vierling-Claassen et al., 2008), these functional deficits provide evidence for primary auditory cortex inhibitory neuron pathology in schizophrenia.

1.3 ALTERATIONS OF AUDITORY CORTEX IN SCHIZOPHRENIA

1.3.1 In vivo imaging evidence of auditory cortex alterations in schizophrenia

The functional impairments in auditory processing in individuals with schizophrenia described above are highly suggestive of disruptions in primary auditory cortex. Gray matter volume of the superior temporal gyrus (STG) is consistently reported to be reduced in subjects with schizophrenia (Shenton et al., 2001; Rajarethinam et al., 2004). The STG contains Heschl's gyrus and sulcus, as well as the planum temporale, which are the anatomical locations of primary and non-primary auditory cortices, respectively. Reductions in gray matter volume of Heschl's gyrus and planum temporale are reported in patients in both cross-sectional and longitudinal studies (Kwon et al., 1999a; Hirayasu et al., 2000; Kasai et al., 2003; Smiley et al., 2009). Further, reduction in volume of Heschl's gyrus is specific for schizophrenia, as first-psychotic episode manic bipolar patients or first episode patients with affective psychosis showed no change in Heschl's gyrus volume (Hirayasu et al., 2000; Kasai et al., 2003; McCarley et al., 2008). The changes in gray matter volume likely have functional consequences, as reductions in MMN responses to frequency and duration deviants are correlated with reduced volume of Heschl's gyrus (Rasser et al., 2011). Also, evidence suggests that Heschl's gyrus volume is reduced around the time of the first psychotic episode, and correlated with MMN amplitude

(Salisbury et al., 2007; McCarley et al., 2008). However, MMN impairment is not present at the first psychotic episode (Salisbury et al., 2002), but emerges over the next year (McCarley et al., 2008), as the reductions in Heschl's gyrus volume and MMN responses get worse as the illness progresses (Salisbury et al., 2007). This indicates that structural changes in the auditory cortex precede and may play a causal role in the onset of electrophysiological auditory processing disturbances. Taken together, this evidence suggests that abnormalities of primary auditory cortex gray matter are related to the onset and progression of schizophrenia, are not a consequence of long term illness or a general feature of psychosis, and likely contribute to auditory processing deficits.

1.3.2 Post-mortem evidence for auditory cortex alterations in schizophrenia

In addition to overall gray matter volume changes, evidence suggests that circuit and synapse level changes are present in auditory cortex of subjects with schizophrenia. For example, disruptions in hemispheric asymmetries in microcolumns are reported in Heschl's gyrus and the planum temporale (Chance et al., 2008). Microcolumns are considered the smallest units of cortical processing (Jones, 2000) and consist of locally interacting inhibitory and excitatory neurons. Disruptions in microcolumn spacing could be indicative of changes in volume taken up by different circuit components, such as cell bodies of neurons and glia, axons, and dendrites. Pyramidal neuron cell volume is reduced in deep layer 3 of primary auditory cortex and auditory association cortex of subjects with schizophrenia (Sweet et al., 2003; Sweet et al., 2004), but not in layer 5 of auditory association cortex (Sweet et al., 2004) suggesting that feedforward but not feedback circuits are affected. However, the number of pyramidal neurons in deep layer 3 of primary auditory cortex is unchanged in schizophrenia (Dorph-Petersen et al., 2009b), indicating

that pyramidal cell reduction does not contribute to gray matter loss; however, reductions in other components such as dendrites, spines, and axons could be reduced in schizophrenia to contribute to the gray matter volume reduction in primary auditory cortex. Reduced dendritic spine density in deep layer 3 of subjects with schizophrenia, identified by immunoreactivity for spinophilin (Sweet et al., 2009), suggests a deficiency in excitatory synapses, as spines are the most common postsynaptic target for glutamatergic boutons in the cortex. Axon bouton densities identified with the presynaptic terminal marker synaptophysin are reduced in deep layer 3 of primary auditory cortex of subjects with schizophrenia (Sweet et al., 2007). As synaptophysin is expressed in all classical neurotransmitter releasing boutons in the cortex (Navone et al., 1986), reduction in density of synaptophysin expressing boutons could indicate general bouton loss or a specific reduction in density of a particular population of boutons, such as excitatory or inhibitory boutons. However, it is not known whether excitatory and inhibitory boutons are affected in the primary auditory cortex of subjects with schizophrenia.

1.4 RELEVANCE OF ADOLESCENT DEVELOPMENT TO SCHIZOPHRENIA ONSET

The onset of schizophrenia symptoms typically occurs during late adolescence or young adulthood (Tandon et al., 2009), an observation which has led to the hypothesis that abnormal developmental processes in regions undergoing relatively protracted maturation may contribute to the emergence of schizophrenia symptoms during late adolescence (Feinberg, 1982; McGlashan and Hoffman, 2000). Throughout the late teen years and early twenties, certain brain regions continue to mature via the refinement of synaptic connections and myelination of fiber

tracts (Paus et al., 2008). In humans, prefrontal and superior temporal cortices are among the last brain regions to mature, and their development is not complete until the third decade of life (Huttenlocher and Dabholkar, 1997; Gogtay et al., 2004; Shaw et al., 2008). Protracted maturation in these regions may leave them vulnerable to disruptive insults during development, and in support of this, these cortical regions are heavily implicated in the neuropathology of schizophrenia (Lewis and Sweet, 2009).

Imaging studies of adolescent subjects transitioning to schizophrenia reveal excessive gray matter loss in prefrontal cortex (Pantelis et al., 2007). In addition, first episode psychosis patients and ultra-high risk individuals who later develop psychosis show longitudinal reductions in STG gray matter that correlate with severity of delusions (Takahashi et al., 2009). Together, this suggests that excessive gray matter loss during adolescence may precipitate the emergence of schizophrenia symptoms. A key adolescent neurodevelopmental process is the pruning of synapses in the cortex, where synapse density peaks prior to adolescence, then declines during adolescence before reaching stable adult levels (Rakic et al., 1986; Zecevic et al., 1989; Huttenlocher and Dabholkar, 1997; Glantz et al., 2007). It has been proposed that excessive elimination of synapses during adolescence could contribute to the pathophysiology of schizophrenia (Feinberg, 1982).

1.4.1 Synapse pruning in the cortex during adolescence

In mammalian cortex, synapse density peaks prior to adolescence, then declines by approximately 30% during adolescence before reaching stable adult levels (Huttenlocher, 1979; Rakic et al., 1986; Glantz et al., 2007). In humans, synapse elimination appears to occur earlier in auditory than in frontal cortex, and earlier still in visual cortex compared to auditory,

suggesting heterochronicity in postnatal maturation of different brain regions (**Figure 1.2**) (Huttenlocher and Dabholkar, 1997). In dorsolateral prefrontal cortex of mice, there is a 20% loss of dendritic spines over the month following the peak in spine density at postnatal day (P) 28, corresponding to the beginning of adolescence (Zuo et al., 2005), and spine density stabilizes by the 16th postnatal week (Alvarez and Sabatini, 2007). Adolescent synapse pruning occurs after mature activity-dependent connections have already been formed, as excitatory synapse properties of pre-adolescent monkeys are already similar to synapse properties of adults, indicating that adolescent pruning is independent of maturation of individual synapses (Gonzalez-Burgos et al., 2008). Increased synapse pruning during adolescence could lead to reduced density of cortical excitatory synapses and decreased gray matter volume in individuals with schizophrenia (Bennett, 2011; Kasai et al., 2003).

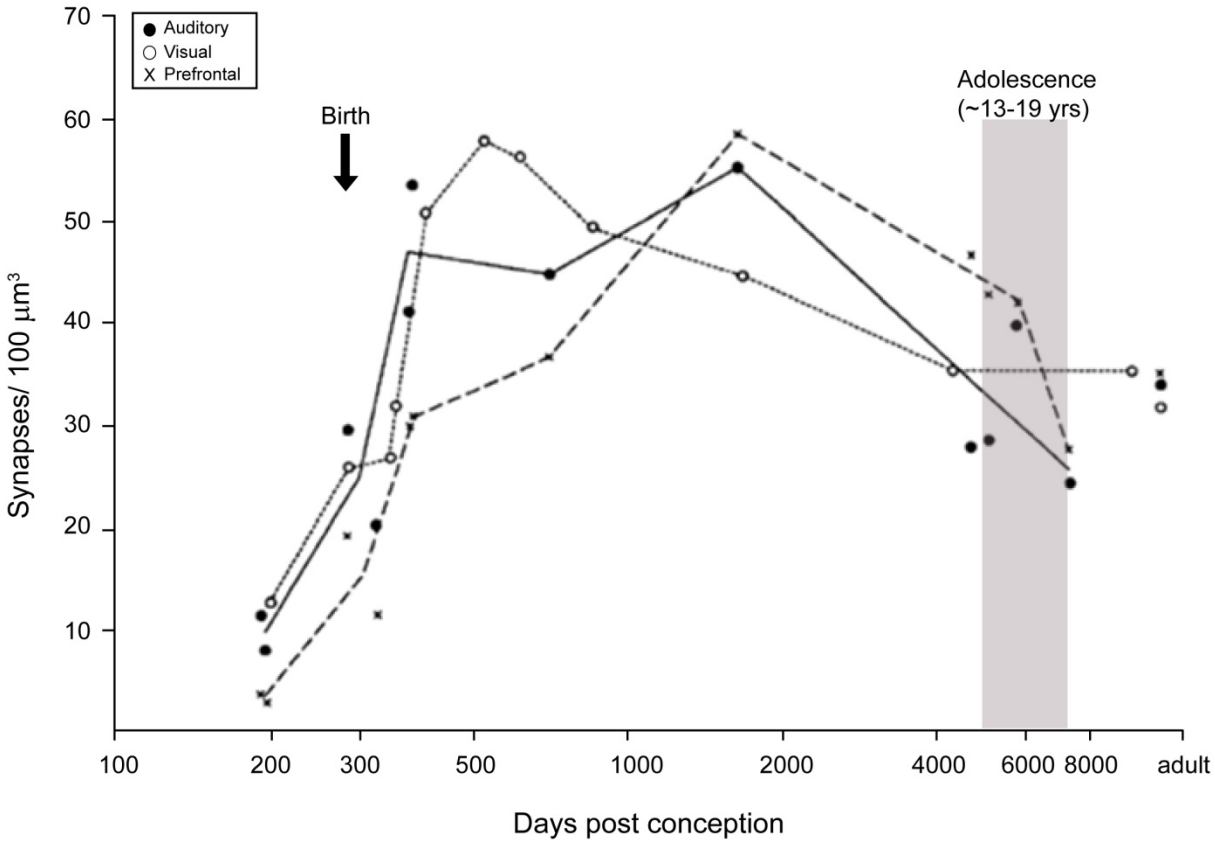

Figure 1.2. Postnatal trajectories of synapse density in human prefrontal (x), auditory (filled circles), and visual (open circles) cortex. Gray shaded region represents adolescence. Modified from (Huttenlocher and Dabholkar, 1997).

Most evidence from non-human primates suggest that cortical inhibitory synapses do not undergo extensive pruning during adolescence. Inhibitory contacts are reported to remain relatively unchanged in monkey somatosensory and visual cortex across development (Zecevic and Rakic, 1991; Bourgeois and Rakic, 1993). Accordingly, in the monkey prefrontal cortex, the density of boutons expressing the GABA plasma membrane transporter (GAT-1) does not change across development (Erickson and Lewis, 2002). However, in parallel with spine pruning in monkey prefrontal cortex, there is a decrease in the density of parvalbumin-expressing axon boutons of the chandelier subtype of interneuron, suggesting that pruning of inhibitory synapses does occur during adolescence (Anderson et al., 1995), but may be limited to certain subtypes of inhibitory neurons. Conflicting reports of postnatal changes in inhibitory synapses have been reported in rodents. For example, in rat visual cortex the number of type II synapses, which would include inhibitory synapses among other non-glutamatergic synapses, decreases substantially between P28 and P90 (Blue and Parnavelas, 1983). A small decrease in symmetric (non-glutamatergic) synapse density is also reported during this time in mouse somatosensory cortex (De Felipe et al., 1997), although synapse reduction in this study was first and foremost attributable to asymmetric (glutamatergic) synapses. In contrast, another report indicates that inhibitory synapse numbers do not decrease in rat somatosensory cortex between postnatal days 30 and 60 (Micheva and Beaulieu, 1996). Changes in presynaptic markers of inhibitory boutons, such as the GABA synthesizing enzymes, glutamate decarboxylase (GAD; GAD65 and GAD67) may also be indicative of inhibitory bouton loss or stability. In human visual cortex, GAD67 protein levels appear to remain stable throughout the lifespan, which is consistent with the idea that inhibitory boutons are not pruned, while GAD65 levels reach a peak around age 20 and then begin to slowly decline through old age (Pinto et al., 2010). This could indicate loss of boutons

expressing only GAD65 beginning in young adulthood, or a reduction in GAD65 protein levels within boutons during adulthood. Thus, there is evidence both for stability of inhibitory synapses across development, and for changes in inhibitory synapses during postnatal development which may be restricted to certain interneuron subtypes.

Reduced dendritic spine density occurs in multiple cortical regions in schizophrenia (Lewis and Sweet, 2009), and reduced expression of GABAergic markers is also conserved across cortical regions (Hashimoto et al., 2008). Together with evidence for changes in excitatory and inhibitory synaptic components during adolescence, this raises the possibility that adolescence represents a dynamic period for cortical excitatory and inhibitory synapses. During adolescence, excitatory and inhibitory synapses may be vulnerable to environmental and genetic insults which could give rise to disruptions in primary auditory cortex circuitry in schizophrenia. However, relatively little is known about excitatory and inhibitory synapse development in the auditory cortex during adolescence. Determining how excitatory and inhibitory synaptic components change during adolescence will increase our understanding of developmental processes which may be affected in schizophrenia.

1.4.2 Kalirin: a schizophrenia-relevant mediator of dendritic spine development

Findings of reduced dendritic spine density in the cortex of subjects with schizophrenia suggest that molecular regulators of spine development could be involved in schizophrenia pathophysiology (Penzes et al., 2013). A number of studies have uncovered evidence supporting spine plasticity mediators as schizophrenia susceptibility genes (Bennett, 2011). One such mediator is kalirin, a Rac/Rho guanine nucleotide (GTP/GDP) exchange factor (GEF) (Penzes and Remmers, 2012). Given the observation of extensive dendritic spine pruning which takes

place in the cortex during adolescence, and the interaction between kalirin and proteins involved in spine plasticity and remodeling, it is possible that kalirin plays a role in the adolescent pruning process. In fact, mice lacking kalirin protein (kalirin KO mice) have reduced frontal cortex dendritic spine density in young adulthood, but not prior to the onset of synapse pruning, suggesting that kalirin is important for maintaining normal dendritic spine density in frontal cortex during adolescence (Cahill et al., 2009).

Spine morphology and dynamics play an important role in influencing the plasticity of excitatory circuits in the cortex. Small GTPases are important effectors of spine plasticity and actin remodeling (Penzes and Rafalovich, 2012). Kalirin is able to activate members of the Rho family of GTPases, such as Rac1 and RhoA. Activation of Rac1 increases dendritic spine stability and spine growth (Yoshihara et al., 2009b) while RhoA is involved in the regulation of dendritic growth (Rabiner et al., 2005), but also destabilizes spines (Newey et al., 2005). Kalirin has been shown to play an important role in experience dependent spine plasticity (Newey et al., 2005; Xie et al., 2007). Upon activation of NMDA receptors, kalirin-7 is phosphorylated by CAMKII and is able to activate Rac1 (Newey et al., 2005; Xie et al., 2007). Further, kalirin interacts with the GluR1 subunit of AMPA receptors, and is necessary for activity-dependent localization of AMPA receptors to dendritic spines (Newey et al., 2005; Xie et al., 2007), which is a key mechanism for regulating synaptic strength (Xie et al., 2007; Anggono and Huganir, 2012).

The kalirin gene encodes several different isoforms via alternative splicing mechanisms. The kalirin-7 isoform is the most abundant in the adult CNS (Johnson et al., 2000) where it is localized to the postsynaptic density (Penzes et al., 2001; Ma et al., 2008). Levels of kalirin-7 are low at birth and increase at the beginning of the second postnatal week, during the time

corresponding to postnatal synaptogenesis (Xie et al., 2007). Kalirin-7 contains a single GEF domain, and is able to activate Rac1 (Penzes and Jones, 2008). Kalirin-9 has been shown to be localized to axonal and dendritic processes, and growth cones in developing neurons (Johnson et al., 2000), and is also expressed outside the central nervous system, in pituitary, liver, aorta, and skeletal muscle (Mandela et al., 2012). Recently, kalirin-9 has been shown to localize to dendritic spines (Deo et al., 2012). In contrast, kalirin-12 is localized to the cell soma in cortex and cerebellum, although it is reported to localize to spines in hippocampal neuron culture (Ma et al., 2003). The kalirin-9 and -12 isoforms are already at detectable levels in rat CNS by birth (Ma et al., 2003). Kalirin-9 and -12 contain a second GEF domain, which activates RhoA (Johnson et al., 2000), and so may play different roles than kalirin-7 in regulating dendritic spine and circuit dynamics. Kalirin mRNA levels are highest in layers 2-4 and layer 6 of the cortex, while protein expression is greatest in the soma and dendrites of layer 5 pyramidal neurons (Ma et al., 2001). High levels of kalirin mRNA and protein are also found in the hippocampus, and in the cerebellum, although it is expressed at varying levels in other mid-brain and brainstem structures. It is important to note that kalirin protein is localized to both pyramidal and non-pyramidal neurons. Kalirin also influences dendritic arborization and formation of excitatory synapses onto GABAergic interneurons (Ma et al., 2008), where it influences the expression of GAD65 (Ma et al., 2011).

Several lines of evidence suggest a role for kalirin in schizophrenia. Associations have been identified between the kalirin gene and schizophrenia in genome wide association studies (Ikeda et al., 2011). In addition, rare (< 1%) mutations specific for the kalirin-9 and -12 isoforms have been found to be associated with schizophrenia (Kushima et al., 2012). In layer 3 of dorsolateral prefrontal cortex of subjects with schizophrenia, kalirin mRNA is reduced and

correlated with reduced dendritic spine density (Hill et al., 2006). A more recent Western blot study also suggests that levels of kalirin-7 (called Duo in humans) protein are reduced in anterior cingulate and dorsolateral prefrontal cortex (Rubio et al., 2012). Together, this evidence supports a role for kalirin in dendritic spine impairment in the frontal cortex of subjects with schizophrenia. However, in the primary auditory cortex of subjects with schizophrenia, levels of kalirin-7 protein are unchanged, and levels of kalirin-9 are actually increased (Deo et al., 2012). The observation of differential changes in kalirin between frontal and auditory cortex in subjects with schizophrenia suggests that loss of kalirin may have different effects in different cortical areas. While a role for kalirin in mediating adolescent spine elimination has been established in the frontal cortex (Cahill et al., 2009), and suggests that reduced kalirin expression could lead to spine over-pruning in prefrontal cortex in schizophrenia, it is not known if kalirin contributes to adolescent synapse pruning in the auditory cortex.

1.5 GOALS AND RELEVANCE OF THIS DISSERATION

In summary, we have presented evidence that auditory processing impairments could contribute to some of the more debilitating negative and cognitive symptoms of schizophrenia. Further, evidence from *in vivo* imaging and postmortem studies suggest auditory cortex alterations contribute to functional impairments in auditory processing. Finally, protracted gray matter and synapse development in the cortex during adolescence and young adulthood, when schizophrenia symptoms typically emerge, suggests that abnormal developmental processes could lead to alterations in primary auditory cortex in subjects with schizophrenia. Based on this evidence, we propose a model (**Figure 1.3**), where genetic and/or environmental risk factors for schizophrenia

contribute to abnormal adolescent auditory cortex development, leading to auditory cortex pathology. Alterations in auditory cortex in subjects with schizophrenia lead to abnormal auditory processing, which contributes to some of the observed symptoms.

As we have alluded to in the above sections, evidence suggests that primary auditory cortex synapses are disrupted in schizophrenia, but we do not know which synapse populations are responsible. Correlated reductions in presynaptic boutons and postsynaptic dendritic spines (Sweet et al., 2007; Sweet et al., 2009) suggest a decrease in excitatory synapses in the auditory cortex of individuals with schizophrenia. However, as electrophysiological evidence points to impairments in physiological processes thought to be mediated by inhibitory as well as excitatory transmission, there may also be disruptions in inhibitory synapse components. As dendritic spine density is reduced in the auditory cortex, and is hypothesized to result from over pruning of excitatory synapses during adolescence, it is important for our understanding of the pathophysiology of schizophrenia that we interpret synaptic alterations in the auditory cortex in schizophrenia in the context of how these synaptic elements change during the highly dynamic period of adolescence, when symptoms typically emerge. Therefore, the goals of the research outlined in this dissertation (see **Figure 1.3**) are first, to determine whether disruptions in excitatory (Chapter 2) and inhibitory (Chapter 3) synapse components contribute to the disruptions of primary auditory cortex circuitry observed in individuals with schizophrenia; second, to determine the temporal relationship between excitatory and inhibitory synapse component developmental trajectories in the auditory cortex between adolescence and young adulthood (Chapter 4); and third, to determine how development of synapse components over adolescence affects auditory cortex function (Chapter 5). We hypothesize 1) that excitatory and inhibitory presynaptic components contribute to pathology of primary auditory cortex in

individuals with schizophrenia, and 2) reductions in excitatory synapse components in primary auditory cortex precede changes in inhibitory synapse components during adolescence, and maturation of these synapse components is important for developmental improvement in auditory processing during adolescence. The experimental chapters are briefly summarized in the following sections.

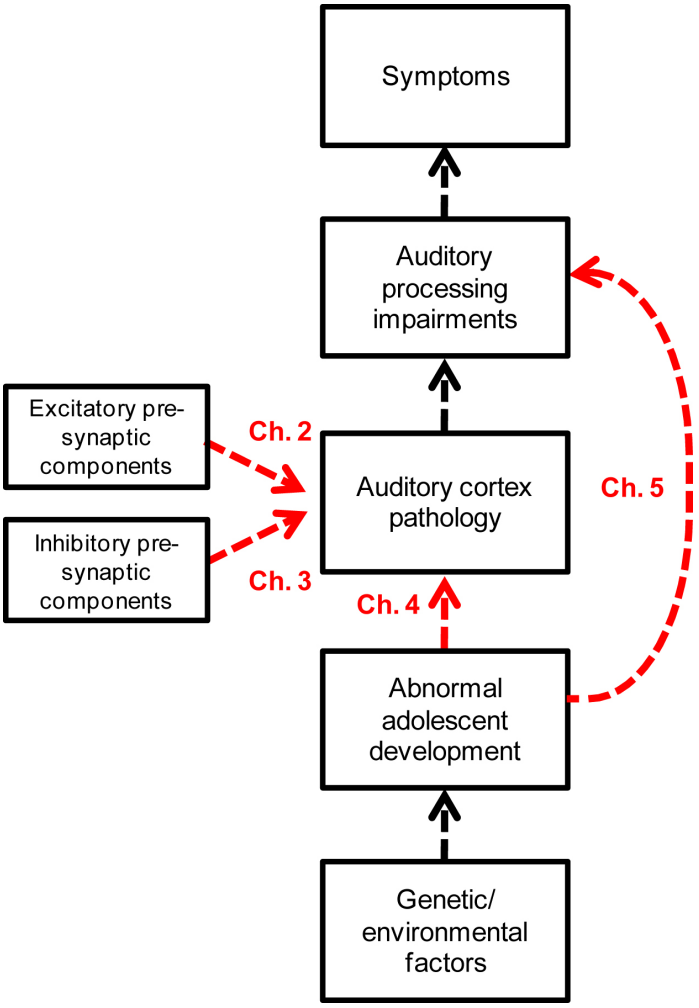

Figure 1.3. Schematic of the contribution of experimental chapters to overall model. Contributions of experimental chapters are denoted by red arrows. In chapter 1, we reviewed evidence which supports a contribution of auditory processing impairments to the symptoms of schizophrenia. Alterations in auditory cortex structure and function may contribute to those auditory processing deficits. We propose that abnormalities of adolescent cortical synapse development, presumably mediated by some combination of genetic and environmental factors, leads to the alterations in synapse components in primary auditory cortex in schizophrenia. In chapter 2, we will determine whether intracortical excitatory or thalamocortical boutons are disrupted in the primary auditory cortex in schizophrenia. In chapter 3, we will determine whether alterations of GAD65-expressing inhibitory boutons

contribute to auditory cortex synaptic alterations in schizophrenia. In chapter 4, we will determine how pre- and postsynaptic components of primary auditory cortex excitatory and inhibitory synapses change during normal adolescence, and in mice lacking kalirin. Finally, in chapter 5, we will explore how auditory cortex function changes during adolescence, and whether disrupted development of auditory cortex induced by the absence of kalirin impairs behavioral maturation of auditory cortex.

1.5.1 Intracortical excitatory and thalamocortical boutons are intact in primary auditory cortex in schizophrenia

Given the reduction of dendritic spine density in auditory cortex of schizophrenia, we hypothesized that excitatory presynaptic boutons would be reduced to a similar degree in the primary auditory cortex of subjects with schizophrenia. The primary auditory cortex receives extensive excitatory projections from the thalamus, as well as excitatory projections arising from within the cortex. Therefore, we took advantage of the differential expression of two isoforms of the vesicular glutamate transporters (VGluT) between these two populations to ask whether the density, number, and vesicular glutamate transporter levels within VGluT1-expressing intracortical excitatory and VGluT2-expressing thalamocortical excitatory boutons are altered in deep layer 3 of primary auditory cortex of subjects with schizophrenia. Surprisingly, we found no alterations in either population, suggesting excitatory presynaptic boutons are not reduced despite reduced density of dendritic spines, their primary postsynaptic targets.

1.5.2 Reduced glutamate decarboxylase 65 protein in primary auditory cortex inhibitory boutons in schizophrenia

Electrophysiological abnormalities in the aSSR response and auditory stimulus evoked oscillatory activity suggest inhibitiory neurotransmission might be impaired in the primary auditory cortex in subjects with schizophrenia. As rapid modulation of inhibition is necessary for oscillatory activity, we hypothesized that inhibitory boutons expressing GAD65 would be affected in schizophrenia, as GAD65 mediates rapid activity dependent up-regulation of GABA synthesis. In this study, we used immunohistochemistry and quantitative confocal microscopy to examine density, number, and GAD65 protein content within GAD65-expressing boutons in deep layer 3 of the primary auditory cortex of individuals with schizophrenia. We found that density and number of GAD65-expressing inhibitory boutons are unchanged in schizophrenia; however, the within-bouton GAD65 protein content is reduced by approximately 40%. Further, we observed that the reduction in within-bouton GAD65 protein was correlated with previously measured reduction in dendritic spine density in deep layer 3. Our findings suggest that dendritic spine reduction and within-bouton GAD65 protein reduction are related pathological features of primary auditory cortex of subjects with schizophrenia.

1.5.3 Developmental trajectories of excitatory synaptic components and within-bouton GAD65 protein in mouse auditory cortex between early adolescence and young adulthood

Our observation of correlated disruptions of dendritic spines and levels of GAD65 protein within boutons in the primary auditory cortex of individuals with schizophrenia (**1.5.2**) suggests a relationship between excitatory and inhibitory synapse pathology. Based on the relationship

between dendritic spines and GAD65 protein levels, we hypothesized that a decrease in levels of GAD65 protein may occur subsequent to spine pruning during adolescence in auditory cortex. We utilized the kalirin KO mouse to determine how genetically-mediated dendritic spine disruption impacts development of excitatory and inhibitory synapse components in auditory cortex during adolescence. We hypothesized that excessive spine pruning occurs in the auditory cortex of kalirin KO mice, as has been observed in frontal cortex. Our findings suggest that levels of within-bouton GAD65 protein decline between late adolescence and young adulthood, while spine pruning occurred between early adolescence and young adulthood, suggesting changes in GAD65 protein levels occurs subsequent to spine pruning. Surprisingly, there were only subtle alterations in excitatory synapse components in the mice lacking kalirin, indicating that molecular regulators of spine pruning may be slightly different in auditory compared to frontal cortex. Together, we see that components of excitatory and inhibitory synapses in the auditory cortex continue to develop through adolescence and young adulthood, and that inhibitory bouton changes appear to follow excitatory synapse pruning.

1.5.4 Development of prepulse inhibition of the acoustic startle reflex by silent gaps across adolescence in mice

Individuals with schizophrenia exhibit alterations in inhibitory and excitatory synapse components in primary auditory cortex, as well as basic auditory processing impairments. In the mouse auditory cortex, we observed that numbers and molecular features of pre- and postsynaptic components of excitatory and inhibitory synapses change between early adolescence and young adulthood (**1.5.3**). We hypothesized that auditory cortex function improves over adolescence, in parallel with maturation of auditory cortex synaptic components.

We also hypothesized that auditory cortex improvement would be blunted in mice lacking kalirin, as maturation of synaptic components during adolescence also exhibited subtle disruptions. Using gap-mediated prepulse inhibition of the acoustic startle reflex (gap-PPI) as a readout of auditory cortex function, we determined that gap-PPI responses increase during adolescence in wild type mice, but not in mice lacking kalirin. This suggests that adolescent auditory cortex synapse refinement during adolescence is important for normal development of auditory cortex function, and is disrupted in kalirin KO mice.

2.0 INTRACORTICAL EXCITATORY AND THALAMOCORTICAL BOUTONS ARE INTACT IN PRIMARY AUDITORY CORTEX IN SCHIZOPHRENIA

This chapter has been previously published as:

Moyer CE, Delevich KM, Fish KN, Asafu-Adjei JK, Sampson AR, Dorph-Petersen KA, Lewis DA, Sweet RA. 2013. Intracortical excitatory and thalamocortical boutons are intact in primary auditory cortex in schizophrenia. *Schizophrenia Research*, 149:127-134.

It is unchanged in content, with the exception of minor formatting alterations and moving supplemental methods to the main body of the article to satisfy the requirements for this dissertation.

My contributions include participation in study design, data collection and analysis, and writing the manuscript under the direction of Dr. Sweet. Kristen Delevich assisted with data collection. Dr. Fish contributed to study design and data analysis. Dr. Asafu-Adjei and Dr. Sampson assisted with statistical analysis, Dr. Dorph-Petersen assisted with stereological methods and analysis. Dr. Lewis contributed to study design and data analysis. All authors contributed to and approved the final manuscript.

Abstract. Schizophrenia is associated with auditory processing impairments that could arise as a result of primary auditory cortex excitatory circuit pathology. We have previously reported a deficit in dendritic spine density in deep layer 3 of primary auditory cortex in subjects with schizophrenia. As boutons and spines can be structurally and functionally co-regulated, we asked whether the densities of intracortical excitatory or thalamocortical presynaptic boutons are also reduced. We studied 2 cohorts of subjects with schizophrenia and matched controls, comprising 27 subject pairs and assessed the density, number, and within-bouton vesicular glutamate transporter (VGluT) protein level of intracortical excitatory (VGluT1-immunoreactive) and thalamocortical (VGluT2-immunoreactive) boutons in deep layer 3 of primary auditory cortex using quantitative confocal microscopy and stereologic sampling methods. We found that VGluT1- and VGluT2-immunoreactive puncta densities and numbers were not altered in deep layer 3 of primary auditory cortex of subjects with schizophrenia. Our results indicate that reduced dendritic spine density in primary auditory cortex of subjects with schizophrenia is not matched by a corresponding reduction in excitatory bouton density. This suggests excitatory boutons in primary auditory cortex in schizophrenia may synapse with structures other than spines, such as dendritic shafts, with greater frequency. The discrepancy between dendritic spine reduction and excitatory bouton preservation may contribute to functional impairments of the primary auditory cortex in subjects with schizophrenia.

2.1 INTRODUCTION

Individuals with schizophrenia exhibit impairments in auditory processing, including pure tone frequency discrimination (Javitt et al., 2000; Leitman et al., 2010b). Electrophysiological

deficits observed during auditory processing tasks, such as reduction in the mismatch negativity (MMN) response to stimulus changes during a repetitive acoustic stimulus presentation (Javitt et al., 1994; Javitt et al., 2000; Naatanen and Kahkonen, 2009), are also observed in schizophrenia. In addition to functional abnormalities, gray matter volume loss is consistently reported in the anatomical region of the primary auditory cortex in the superior temporal gyrus (STG) (McCarley et al., 1999; Rajarethinam et al., 2004) and Heschl's gyrus (Hirayasu et al., 2000; Kasai et al., 2003; Salisbury et al., 2007; Takahashi et al., 2009) of subjects with schizophrenia and high-risk individuals.

Evidence suggests that alterations of excitatory, glutamatergic synapses could underlie the structural and functional abnormalities in the auditory cortex in schizophrenia. For example, the MMN response is disrupted by blocking the NMDA subtype of ionotropic glutamate receptor (Javitt et al., 1996; Gunduz-Bruce et al., 2012). In subjects with schizophrenia, spinophilin-immunoreactive (-IR) puncta density (a marker of dendritic spines) is reduced in the primary auditory cortex (Sweet et al., 2009), suggesting that the density of postsynaptic components of excitatory synapses in the auditory cortex is reduced. Trans-synaptic communication coordinates functional and structural changes between pre- and postsynaptic elements, as indicated by reports that postsynaptic alterations such as AMPA receptor removal (Ripley et al., 2011) or protein synthesis inhibition (McCann et al., 2007) lead to presynaptic bouton loss. Therefore, reduced dendritic spine density in schizophrenia may be indicative of a coordinated reduction in excitatory bouton density. Alternatively, if excitatory bouton density is unchanged, then this could indicate that the distribution of their postsynaptic targets is altered. For example, excitatory boutons may synapse with dendritic shafts with greater frequency, which occurs following spine loss in culture (Mateos et al., 2007; Woods et al., 2011). Here, we asked

whether the density of excitatory boutons in deep layer 3 of primary auditory cortex is reduced in individuals with schizophrenia.

Glutamatergic inputs to the primary auditory cortex can be broadly classified into two groups: thalamocortical inputs primarily to layer 4 and deep layer 3 from the medial geniculate nucleus of the thalamus, and intracortical excitatory inputs originating within primary auditory cortex and from other cortical regions. It is important to distinguish between the two populations because alterations of excitatory synapses in the primary auditory cortex may have different functional consequences depending on whether thalamocortical boutons or intracortical excitatory boutons are affected. The two populations can be differentiated at the molecular level by the presence of different isoforms of the vesicular glutamate transporter (VGluT). Most reports indicate that VGluT1 is preferentially expressed in neurons in the cortex and hippocampus, and VGluT2 is preferentially expressed in neurons located in subcortical structures, including some nuclei of the thalamus (Fremeau, Jr. et al., 2001; Kaneko and Fujiyama, 2002; Fremeau, Jr. et al., 2004a; Fremeau, Jr. et al., 2004b). Levels of VGluT protein have also been shown to be correlated with glutamate release and synaptic strength (Wilson et al., 2005), and so changes in within-bouton levels of these proteins may indicate functional impairments of these synapses.

We used quantitative fluorescence confocal microscopy to examine VGluT1- and VGluT2-immunoreactive puncta in primary auditory cortex of two cohorts of subjects, comprising a total of 27 subjects with schizophrenia and an equal number of matched controls. We found that densities and numbers of thalamocortical and intracortical excitatory boutons, and within-bouton VGluT protein levels were not altered in deep layer 3 of primary auditory cortex of subjects with schizophrenia. Taken together with our previous finding of reduced dendritic

spine density in this region, our data suggest that excitatory boutons may aberrantly target non-spine postsynaptic structures, such as dendritic shafts. A shift in the distribution of excitatory synapses away from spines and onto dendritic shafts could alter excitatory circuit function in the primary auditory cortex.

2.2 MATERIALS AND METHODS

2.2.1 Subjects and animals

We studied two cohorts (**Table 2.1** and **Appendix Table A.1**) of subjects diagnosed with schizophrenia or schizoaffective disorder and matched controls included in our previous studies (Sweet et al., 2004; Sweet et al., 2007; Sweet et al., 2009; Dorph-Petersen et al., 2009b; Moyer et al., 2012). We also studied a cohort of four male macaque monkeys (*Macaca fascicularis*) chronically exposed to haloperidol decanoate, and four control macaques matched for sex and weight (Sweet et al., 2007).

All of the brain specimens were collected during autopsies conducted at the Allegheny County Medical Examiner's Office with permission obtained from the subjects' next-of-kin. The protocol used to obtain consent was approved by the University of Pittsburgh Institutional Review Board and Committee for Oversight of Research Involving the Dead. An independent committee of experienced clinicians made consensus diagnoses (American Psychiatric Association, 1994) for each subject, using information obtained from clinical records and structured interviews with surviving relatives. These procedures were IRB approved.

Table 2.1. Summary of subject characteristics for cohorts 1 and 2. Each subject in cohorts 1 and 2 was previously matched to a normal comparison subject based on sex, and as closely as possible for age, postmortem interval (PMI), and group matched for handedness. There were no diagnostic group differences in age ($t_{52} = 0.517$, $p = 0.608$) or PMI ($t_{52} = 0.584$, $p = 0.561$) or in the distribution of handedness between diagnostic groups ($\chi^2 = 1.46$, $df = 1$, $p = 0.314$). Mean storage time did not differ between diagnostic groups (Cohort1: $t_{28} = 0.040$, $p = 0.968$; Cohort 2: $t_{22} = 0.596$, $p = 0.557$). Tobacco use at time of death was more frequent in the schizophrenia group compared to the control group ($\chi^2 = 5.28$, $df = 1$, $p = 0.022$). Abbreviations: SD, standard deviation; F/M, female/male; R/L/A/U, right-handed/left-handed/ambidextrous/unknown; mos, months; yrs, years; N, number; ATOD, at time of death; Y/N/U, yes/no/unknown.

	COHORT 1		COHORT 2		TOTAL	
	Control	Schizophrenia	Control	Schizophrenia	Control	Schizophrenia
N	15	15	12	12	27	27
Mean Age (SD)	46.8 (8.3)	47.6 (5.5)	45.1 (12.9)	47.3 (13.4)	46.0 (10.4)	47.4 (9.6)
Range	27-64	38-63	19-65	25-71	19-65	25-71
Sex (F/M)	6/9	6/9	4/8	4/8	10/17	10/17
Handedness (R/L/M/U)	10/4/0/1	7/3/1/4	11/1/0/0	6/2/1/3	21/5/0/1	13/5/2/7
PMI (SD)	13.9 (5.5)	15.9 (6.6)	18.0 (6.6)	17.9 (8.8)	15.7 (6.3)	16.8 (7.6)
Storage Time, mos (SD)	168 (29)	167 (26)	111 (27)	102 (30)	142 (40)	138 (43)
Illness Duration, yrs (SD)		24.9 (5.6)		22.1 (14.6)		23.7 (10.6)
Range		14-34		3-50		3-50
Suicide, N (%)		3 (20%)		2 (17%)		5 (19%)
Schizoaffective, N (%)		3 (20%)		4 (33%)		7 (26%)
Living independently ATOD, N (%)		7 (47%)		2 (17%)		9 (33%)
Alcohol/Substance abuse ATOD, N (%)		9 (60%)		7 (58%)		16 (59%)
Antipsychotic ATOD, N (%)		13 (87%)		11 (92%)		24 (89%)
Tobacco use ATOD (Y/N/U)	3/4/8	9/2/4	4/6/2	8/3/1	7/10/10	17/5/5

2.2.2 Tissue processing

2.2.2.1 Cohort 1 tissue processing

Brains from individuals in cohort 1 were bisected and the left hemisphere of each subject was cut coronally into 1-2 cm-thick blocks, which were then immersed in cold 4% paraformaldehyde in phosphate buffer for 48 hours, equilibrated in a series of graded sucrose solutions, and stored at -30ºC in an antifreeze solution (30% glycerol and 30% ethylene glycol in phosphate-buffered saline). Superior temporal gyrus (STG)- containing blocks were generated as described previously (Sweet et al., 2003; Sweet et al., 2004) and 40 μm coronal cryostat sections were cut and then stored in antifreeze solution at -30ºC until use in this study.

2.2.2.2 Cohort 2 tissue processing

Brain specimens from individuals in cohort 2 were harvested, bisected, blocked coronally, and stored in antifreeze solution at -30ºC as described for cohort 1 (Sweet et al., 2005; Dorph-Petersen et al., 2009b). The entirety of the left STG of each subject was dissected from the fixed coronal blocks. The pial surfaces of the STG blocks were painted with hematoxylin to facilitate identification of the pial surface later during tissue processing, and the blocks were reassembled in 7% low-melt agarose in their *in vivo* orientation. The reassembled STG was cut into systematic uniformly random 3 mm slabs orthogonal to the long axis of Heschl's gyrus. Every other slab with a random start was selected for mapping the boundaries of primary auditory cortex and the remaining slabs were stored in antifreeze solution until use. Mapping slabs were cut on a cryostat at 60 μm, and three consecutive sections from each slab were stained for parvalbumin (PV) immunoreactivity, acetylcholinesterase activity, and Nissl substance. These sections were used to determine whether primary auditory cortex was present in a given slab, to

estimate the volume of primary auditory cortex, and to delineate the boundaries of primary auditory cortex. The boundaries of primary auditory cortex determined using the mapping slabs were applied to the unused set of slabs, such that boundaries of primary auditory cortex on a mapping slab were applied to the adjacent unused slab immediately rostral. The primary auditory cortex was dissected from the unused slabs, and further subdivided into 3 mm wide blocks. Blocks from the most rostral and caudal slabs containing the region of interest were weighted at 1/3 relative to the weight of other blocks to account for the fact that these blocks only partially contained the region of interest. This weighting method has been previously published (Dorph-Petersen et al., 2009b). Briefly, it is needed because the end blocks only partially represent the region of interest (on average less than half due to the positive curvature of the boundary of the region of interest in 3 dimensions) and therefore should not have the same weight as the other blocks. However, there is no way to know the precise weight without knowing the exact fraction of the region of interest and the N_v of the region of interest as well as that of the neighboring region within each block in question. Because the positive curvature is best approximated by a cone or a pyramid, it would take up 1/3 of the volume, leading to our weighting. Block weights were factored into calculations of bouton number (Dorph-Petersen et al., 2009b). Each primary auditory cortex block was then placed pial surface down in a layer of optimal cutting temperature compound (OCT) on a stainless steel block. A hollow cylinder was placed on the block over the tissue, and the cylinder was filled with OCT and allowed to freeze at -20^{o}C. The block of tissue encased in OCT was then removed from the cylinder and placed in a stainless steel well where it was randomly rotated and fixed in its orientation with OCT. The primary auditory cortex block was then sectioned at 50 μm in this orientation perpendicular to the pial surface, and sections were stored at -30^{o}C in antifreeze solution until use in this study.

2.2.2.3 Antipsychotic-exposed macaque cohort tissue processing

In order to account for possible effects of antipsychotic medications, we studied a previously described cohort (Sweet et al., 2007) of four male macaque monkeys (*Macaca fascicularis*) chronically exposed to haloperidol decanoate, and four control macaques matched for sex and weight. All procedures were approved by the University of Pittsburgh's Institutional Animal Care and Use Committee. Animals received injections of haloperidol (mean (standard deviation) = 16.0 (2.1) mg/kg) every four weeks, maintaining trough serum levels of haloperidol of 4.3 (1.1) ng/ml, on average. Following 9-12 months of haloperidol exposure, animals were euthanized with an overdose of pentobarbital, and brains were removed and immersed in 4% paraformaldehyde following a 45 min post mortem interval (PMI). Free-floating sections from the four matched pairs were processed together within immunohistochemistry runs, and procedures were identical to those described for human tissue immunohistochemistry.

2.2.3 Immunohistochemistry

Auditory cortex containing tissue sections (3 from each subject in cohort 1, and 4 from each subject in cohort 2) from matched pairs were processed together in immunohistochemistry runs. In order to identify excitatory glutamatergic axon boutons in deep layer 3 of the primary auditory cortex, we utilized two antibodies directed against two isoforms of the vesicular glutamate transporter (VGluTs 1 and 2). Auditory cortex containing tissue sections from matched pairs were processed together in immunohistochemistry runs. Free-floating sections were rinsed in 0.1 M phosphate buffered saline (PBS), and then incubated in 1% $NaBH_4$ in phosphate buffer for 30 minutes to reduce tissue autofluorescence. Sections were rinsed again in PBS and incubated for 3 hours in blocking buffer containing 0.3% Triton-X, 5% normal human serum, 5% normal goat

serum, 1% bovine serum albumin, 0.1% lysine, and 0.1% glycine in PBS. Sections were then incubated with a 1:500 dilution of guinea pig anti-VGluT1 primary antibody and a 1:10,000 dilution of rabbit anti-VGluT2 primary antibody in blocking buffer for 96 hours at 4ºC. After rinsing in PBS, sections were incubated overnight with 1:500 dilutions of Alexa Fluor 568 conjugated goat anti-guinea pig and Alexa Fluor 488 conjugated anti-rabbit secondary antibodies (Invitrogen, Carlsbad, CA). Sections were rinsed, mounted on gelatin-coated slides, allowed to dry for 1 hour, rehydrated for 10 min in distilled water, and coverslipped with Vectashield Hard Set mounting medium (Vector Laboratories, Burlingame, CA).

VGluT1 was detected using a guinea pig anti-VGluT1 antibody (AB5905, Millipore, Billerica, MA), and VGluT2 was detected using a rabbit anti-VGluT2 antibody (V2514, HY-19; Sigma-Aldrich, St. Louis, MO). Although some evidence suggests that mRNA for these transporters may be co-expressed (De Gois et al., 2005; Graziano et al., 2008; Hackett et al., 2011), VGluT1 and 2 proteins demonstrate non-overlapping and complimentary patterns of expression throughout the brain. VGluT1 is the predominant vesicular glutamate transporter in corticocortical and corticothalamic neurons, while VGluT2 is the predominant transporter expressed in thalamocortical neurons (Fremeau, Jr. et al., 2001; Fremeau, Jr. et al., 2004a; Fremeau, Jr. et al., 2004b; Hackett et al., 2011). In monkey and human auditory cortex, we observed the expected pattern of VGluT1 immunoreactivity across all cortical layers, and an apparent increase in VGluT2 immunoreactivity in the thalamocortical termination zone in deep layer 3 and layer 4 (**Figure 2.1A and 2.1B**). In addition, we observed minimal colocalized labeling of puncta with these anti-VGluT1 and -VGluT2 antibodies, although both markers showed extensive colocalization with an antibody targeting the presynaptic bouton marker synaptophysin (**Figure 2.1C and 2.1D**). Also, we observed no colocalization of VGluT1- and

VGluT2-immunoreactive (IR) puncta with a marker of inhibitory GABAergic presynaptic boutons, glutamate decarboxylase-65 (Moyer et al., 2012).

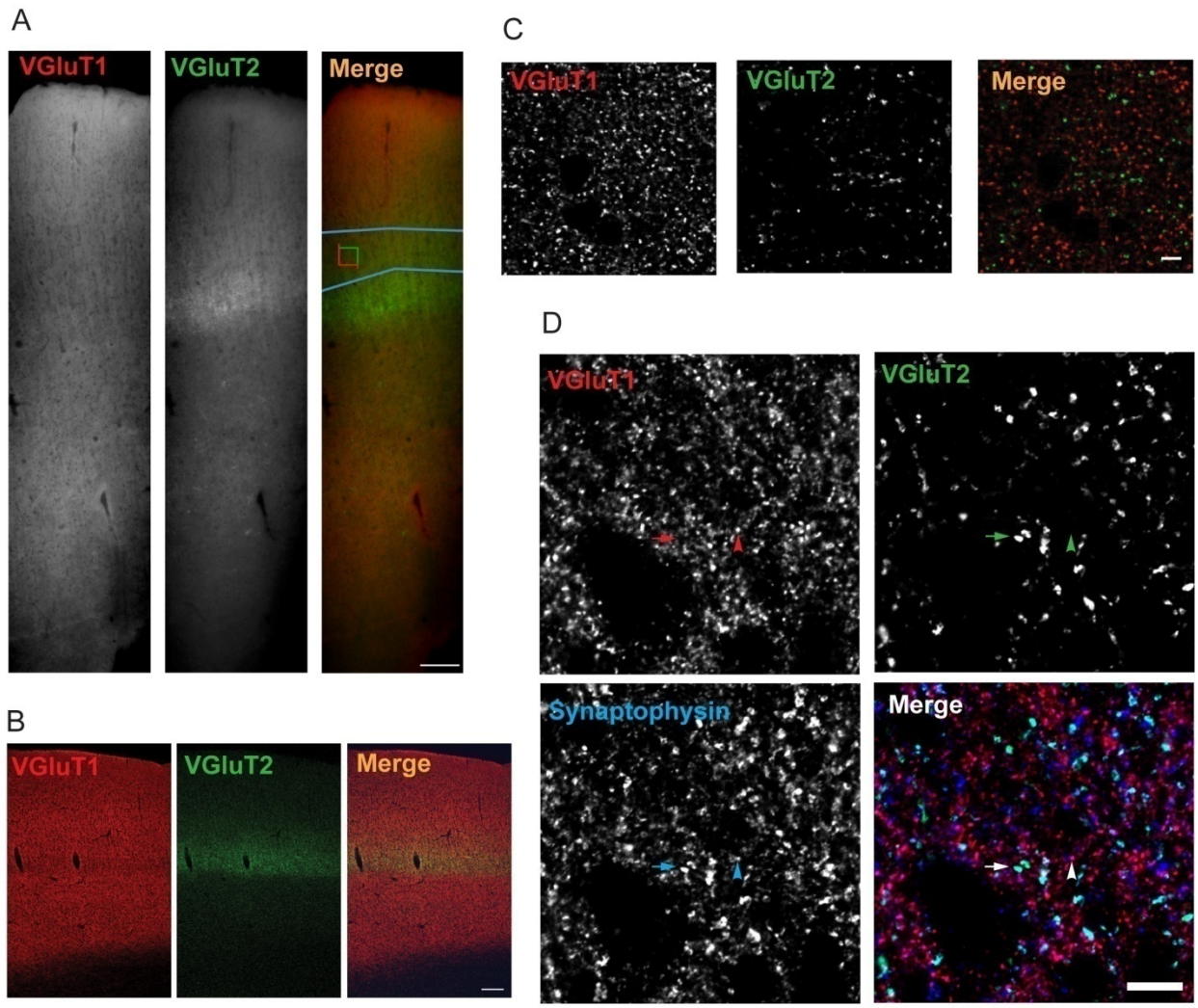

Figure 2.1. Specificity of antibodies used to identify VGluT1- and VGluT2-immunoreactive puncta. A. VGluT1 and VGluT2 immunoreactivity across all cortical layers of primary auditory cortex of one human subject from cohort 2. Blue outline in "Merge" panel represents the deep layer 3 contour, and the counting frame represents a sampling site. Scale bar is 200 µm. B. VGluT1 and VGluT2 immunoreactivity across all cortical layers of primary auditory cortex of a macaque. Image was taken using a laser scanning confocal. Scale bar is 200 µm. C. The antibodies directed against VGluT1 and VGluT2 label two separate bouton populations with no observable colocalization of markers. Scale bar is 10 µm. D. The VGluT1 and VGluT2 antibodies demonstrate overlap with an antibody directed against synaptophysin, a protein found in all classical neurotransmitter releasing boutons. The arrowheads indicate a bouton that is immunoreactive for VGluT1 and synaptophysin and arrows indicate a bouton that is immunoreactive for VGluT2 and synaptophysin. Scale bar is 10 µm.

2.2.4 Image collection

Sections were coded so that the experimenter was blind to diagnostic or drug exposure group, and sections were organized into sets so that sections from paired subjects were imaged during the same imaging session. Images were collected using a 1.42 NA 60X oil objective on an Olympus BX51 upright microscope (Olympus, Center Valley, PA) equipped with an Olympus DSU spinning disk confocal, a Hamamatsu C4742-98 CCD camera (Hamamatsu, Bridgewater, NJ), Olympus mercury light source, excitation/emission filter wheels, a 89000 Sedat Quad ET filter set (Chroma Technology Corp, Bellows Falls, VT), and high precision Prior Scientific motorized XY stage (Prior Scientific, Inc., Rockland, MD) equipped with a linear XYZ encoder (Ludl Electronic Products, Ltd., Hawthorne, NY). Image collection was controlled using SlideBook version 4.1 software (Intelligent Imaging Innovations, Denver, CO). At each sampling site, the tissue thickness (Z axis depth) was measured and recorded, and tissue thickness did not differ between diagnostic groups ($t_{52} = 0.844$, $p = 0.402$). Image stacks were collected with a step size of 0.22 μm between Z axis planes in the stack, starting from 10 μm below the tissue surface closest to the coverglass and stepping up until the tissue surface was reached, yielding a 10 μm thick (Z axis depth) stack comprised of 46 individual 2-dimensional planes. Collected image planes were 512 x 512 pixels with 2 x 2 binning, and exposure times were adjusted to optimize the spread of the intensity histogram and to ensure that none of the pixels in the image stack were saturated. Although mean exposure time was not significantly different between diagnostic groups [Mean (SD): 568 channel: Control, 308 (174) ms; Schizophrenia, 309 (184) ms; $t_{52} = -0.02$, $p = 0.983$; 488 channel: Control, 222 (51) ms; Schizophrenia, 230 (53) ms; $t_{52} = -0.52$, $p = 0.607$] any potential contributions of differences in sampling site exposure time to our outcome variables were corrected for by including exposure

times in statistical models. For the monkey group mean exposure time did not differ between groups for VGluT1-IR boutons [Mean (SD): 568 channel: Control, 147 (55) ms; Antipsychotic, 141 (27) ms; t_{196} = 1.03, p = 0.301] and was significantly lower for antipsychotic exposed monkeys than control monkeys for VGluT2-IR boutons [Mean (SD): 488 channel: Control, 237 (74) ms; Antipsychotic, 212 (67) ms; t_{194} = 2.45; p = 0.02]; however, contributions of differences in exposure time were corrected for by including exposure time in statistical models.

2.2.5 Image processing

Collected image stacks were post-processed offline, using SlideBook and Automation Anywhere software (Automation Anywhere, Inc., San Jose, CA) to automate keystrokes and increase image processing efficiency. The background fluorescence intensity of each stack was determined as the mode value of the intensity histogram in each of the two channels. Background subtraction was done by subtracting the mode intensity (gray scale) value from all pixel intensities in that channel. Images were then deconvolved with a constrained iterative algorithm using a calculated point spread function, a maximum of 20 iterations, and 3D frequency filtering enabled. The background subtracted and deconvolved image stack was then subject to intensity segmentation coupled with morphological selection using our iterative masking approach (Fish et al., 2008). For VGluT1-immunoreactive puncta, the initial intensity threshold was set at 105% of the background intensity level determined above, and with each subsequent iteration the intensity threshold was increased by 5%, until a maximum of 12,000 gray levels was reached. For VGluT2-IR puncta, the initial intensity threshold was set at 180% of the background intensity, and with each subsequent iteration the intensity threshold was increased by 25% until a maximum of 12,000 gray levels was reached. After each segmentation step, mask objects with

volumes ranging from 0.2 to 2.0 μm^3 (VGluT1) or 0.05 to 2.0 μm^3 (VGluT2) were selected and merged with the mask generated in the prior segmentation step. VGluT1- and VGluT2-IR bouton data (mean intensity, mean volume, mean surface area) were extracted from these image stacks using the generated masks to identify objects of interest. VGluT1-IR mask objects were selected for final analysis if the mean intensity of the object was greater than or equal to a 20% increase over the background fluorescence (mode value of histogram). This further eliminated falsely detected background signal collected as a result of our small intensity threshold step size in this channel. VGluT1- and VGluT2-IR puncta were counted automatically by determining whether the centroid of each automatically detected object was inside the disector. This corresponds to the so-called "associated point rule" (Baddeley and Jensen, 2004), which is an unbiased alternative to the unbiased counting frame (Gundersen, 1977). Guard zones of 10 pixels were applied around all edges in the X and Y dimensions of each stack, and 10 Z planes starting 10 planes below the coverglass were included in analysis, as antibody penetration was uniform (puncta counts and intensities were uniform) across these Z axis depths (10 planes x 0.22 μm step size = 2.20 μm disector height).

2.2.6 Quantification of VGluT1- and VGluT2-IR puncta

VGluT1- and VGluT2-IR puncta within deep layer 3 of primary auditory cortex were quantified in this study using spinning disk confocal microscopy. Stereologic sampling, confocal imaging, and image processing were conducted as described previously (Moyer et al., 2012). Mean puncta fluorescence intensity, and mean density and number of puncta in deep layer 3 were determined for VGluT1- and VGluT2-IR puncta.

Densities reported were calculated individually at each site in order to include exposure time as a covariate in our analyses, as exposure time varied on a site-by-site basis. The density of mask objects at each site was determined by dividing the number of objects counted at each site by the product of the disector height (2.2 μm) and the area of the counting frame (2553 μm^2), and then multiplying that by the measured tissue thickness at each site divided by the cryostat block advance (40 μm (cohort1 and monkey cohort) or 50 μm (cohort 2)) (Dorph-Petersen et al., 2001) to correct for tissue shrinkage. It should be noted that the disector height of 2.2 μm used in the current study is very low and could only be implemented robustly because we used confocal microscopy allowing for a high number of thin focal planes; and because we performed a careful analysis of the distribution of the boutons along the Z axis (see Fig. 4 of (Dorph-Petersen et al., 2009a)). We determined the position of the disector and corresponding guard zones post hoc ensuring that boutons were only sampled in the zone with uniform bouton counts. Such sampling was possible due to the high number of automatically detected boutons—for example, on average 59,208 VGluT1-IR and 11,495 VGluT2-IR puncta were detected per subject in cohort 1 and of these an average of 2,566 VGluT1-IR and 2,292 VGluT2-IR puncta per subject were sampled by the disector. Thus, while a disector height of only 2.2 μm should be avoided in a standard brightfield microscopy study with manual counts, we were able to robustly implement such a disector in the current study.

For cohort 2 subjects, we were also able to estimate VGluT1- and VGluT2-IR bouton number because of the tissue processing methods used to generate auditory cortex tissue sections. To do this, mean object densities were calculated as described in equations 4 and 5 of Dorph-Petersen et al. (Dorph-Petersen et al., 2009b) using the numerical density (N_V) approach with the following modification: the distances of each individual mask object from the central

axis were not included in the calculation under the reasonably robust assumption of homogeneity on the scale of the sampling site (~50 μm). Instead, object counts at each sampling site were weighted by multiplying object count at each site by the distance of the sampling site from the central axis. Deep layer 3 volumes for each subject were calculated as described in equations 1-3 of Dorph-Petersen et al. (Dorph-Petersen et al., 2009b) by multiplying the volume fraction of deep layer 3 sampled by the total primary auditory cortex volume. Bouton number for each subject was then generated by multiplying the N_V by the total deep layer 3 volume (Dorph-Petersen et al., 2009b).

Mean puncta volume and surface area of puncta in deep layer 3 were calculated in SlideBook for VGluT1- and VGluT2-IR puncta. The surface area is determined from the surface areas of the exposed voxel faces of each object. Puncta shape complexity was calculated as the inverse of puncta sphericity (Wadell, 1935), determined with the following equation:

$$\text{Sphericity} = (\pi^{1/3} (6V_p)^{2/3})/A_p$$

Where V_p is the IR puncta volume and A_p is the IR puncta surface area.

2.2.7 Statistical analyses

For each human and macaque subject, mean density, fluorescence intensity, and volume of VGluT1- and VGluT2-IR puncta in deep layer 3 of primary auditory cortex were calculated. Among the human subjects, the analyses of VGluT1- and VGluT2-IR bouton volume, surface area, shape complexity, density, and mean intensity were conducted separately using two multivariate analysis of covariance (MANCOVA) models: a primary model that included diagnosis and cohort as fixed effects, subject pair (nested in cohort) as a blocking factor, and tissue storage time and exposure time as covariates; and a secondary model without subject pair

as a blocking factor, that included diagnosis, sex, and cohort as fixed effects and age, PMI, tissue storage time, and exposure time as covariates. To help satisfy the normality requirement for MANCOVA models, mean fluorescence intensity was analyzed on the natural logarithm scale. To account for the correlation among sampling sites within each subject and among sampling sites within each section for each subject, site and section nested in subject were included as random effects in each MANCOVA model. Inclusion of tissue thickness, subject handedness, or immunohistochemistry assay order in the models had negligible impact on diagnostic group differences and, thus, the results reported are from MANCOVA models omitting these factors.

The analysis of VGluT1- and VGluT2-IR bouton number (cohort 2 subjects only) was conducted using two analysis of covariance (ANCOVA) models: a primary model that included diagnosis and pair as fixed effects, and tissue storage time as a covariate; and a secondary model without pair as a factor that included diagnosis and sex as fixed effects, and age, PMI, and tissue storage time as covariates.

Diagnostic comparison results were compared from both primary and secondary models for consistency. Due to the consistency of comparisons found in our analyses, p-values and 95% confidence intervals for the estimated mean difference in response between subjects with schizophrenia and control subjects provided in the text are based on the primary model.

Based on the mean densities, fluorescence intensities, volumes, surface areas, and bouton shape complexity for each subject, two sample t tests were used to determine the effect of the following: independent living status, antipsychotic use, co-morbid alcohol or substance abuse, death by suicide, and diagnosis of schizoaffective disorder. In these analyses, the percent changes of bouton density, fluorescence intensity, volume, surface area, and shape complexity in

subjects with schizophrenia (relative to healthy controls) within each subject pair were the response variables of interest.

To compare mean bouton density, fluorescence intensity, volume, surface area, and shape complexity between antipsychotic exposed and control macaques, MANCOVA models were used, each of which included drug treatment as a fixed effect, pair as a blocking factor, and exposure time as a covariate, and site and section nested in animal were included as random effects. Due to the similarity of storage time within each pair, storage time was not included as a covariate.

All statistical tests were two-sided and conducted at the 0.05 significance level.

2.3 RESULTS

2.3.1 VGluT1-IR puncta

The density of VGluT1-IR puncta was not significantly different between subjects with schizophrenia and control subjects ($F_{(1, 23.2)} = 0.34$, $p = 0.568$, 95% CI: (-0.001, 0.002)) (**Figure 2.2A**). Because we have previously determined the total volume of primary auditory cortex layer 3 for cohort 2 subjects (Dorph-Petersen et al., 2009b), we were able to estimate the total number of VGluT1-IR puncta in primary auditory cortex deep layer 3 for the 12 subject pairs of cohort 2 and we found that the absolute number of VGluT1-IR puncta was not different in schizophrenia ($F_{(1, 10)} = 0.003$, $p = 0.956$, 95% CI: (-1.62×10^8, 1.54×10^8)) (**Figure 2.2B**). Because of the differences in tissue processing methods, we were not able to estimate puncta number in subject pairs from cohort 1. We observed no significant alterations in primary

auditory cortex deep layer 3 VGluT1-IR puncta fluorescence intensity ($F_{(1, 149)} = 0.42$, $p = 0.518$, 95% CI: (-0.09, 0.18)), indicating that relative levels of within-bouton VGluT1 protein are not different between schizophrenia and control subjects (**Figure 2.2C**).

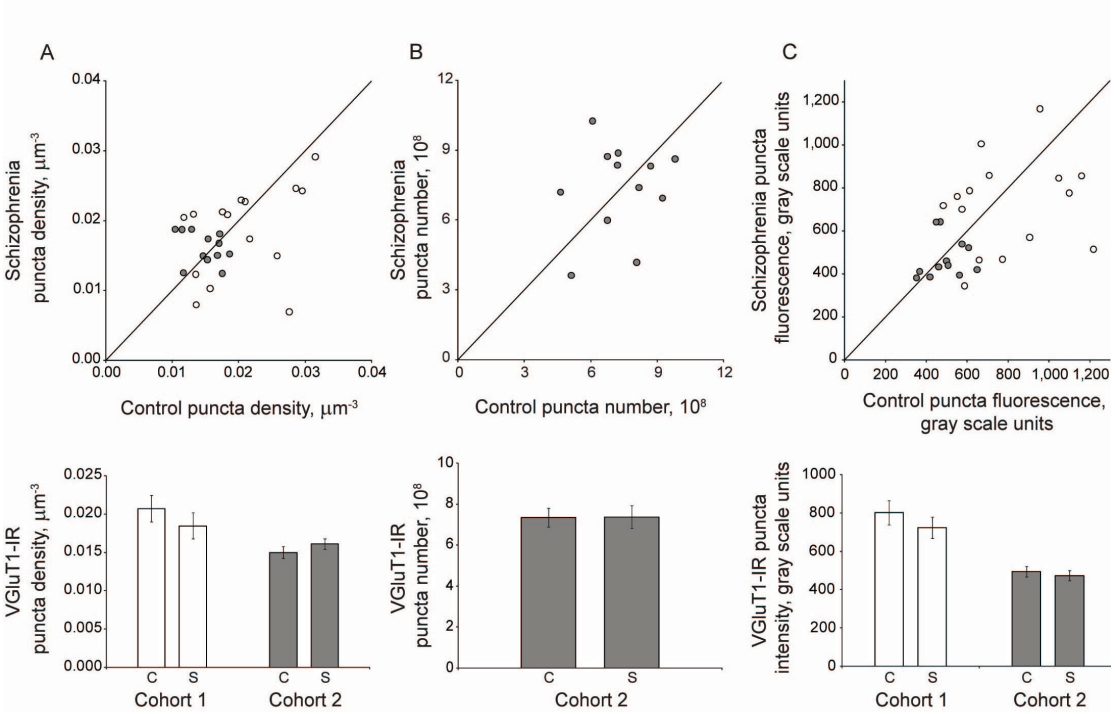

Figure 2.2. VGluT1-IR puncta density, number, and mean fluorescence intensity are unaltered in deep layer 3 of primary auditory cortex of subjects with schizophrenia. A. (Top) VGluT1-IR puncta density for subjects in cohort 1 (open circles) and cohort 2 (gray circles). Reference line represents schizophrenia = control values, where points below the line indicate a pair where control > schizophrenia, and points above the line indicate schizophrenia > control. (Bottom) Diagnostic group mean puncta density for control (c) and schizophrenia (s) subjects in cohort 1 (open bars) and cohort 2 (gray bars). Error bars are +/-SEM. B. (Top) VGluT1-IR puncta number for subjects in cohort 2. Reference line represents schizophrenia = control values, where points below the line indicate a pair where control > schizophrenia, and points above the line indicate schizophrenia > control. (Bottom) Diagnostic group mean puncta number for control (c) and schizophrenia (s) subjects in cohort 2. Error bars are +/-SEM. C. (Top) VGluT1-IR puncta fluorescence intensity for subjects in cohort 1 (open circles) and cohort 2 (gray circles). Reference line represents schizophrenia = control values, where points below the line indicate a pair where control > schizophrenia, and points above the line indicate schizophrenia > control. (Bottom) Diagnostic group mean puncta fluorescence intensity for control (c) and schizophrenia (s) subjects in cohort 1 (open bars) and cohort 2 (gray bars). Error bars are ± SEM.

We observed no effect of chronic haloperidol exposure on density ($F_{(1, 17.3)} = 0.95$; $p = 0.343$, 95% CI: (-0.003, 0.01)) or intensity ($F_{(1, 18.6)} = 0.36$; $p = 0.554$, 95% CI: (-0.11, 0.21)), of VGluT1-IR puncta in deep layer 3 of primary auditory cortex of antipsychotic-exposed macaques (**Figure 2.3**).

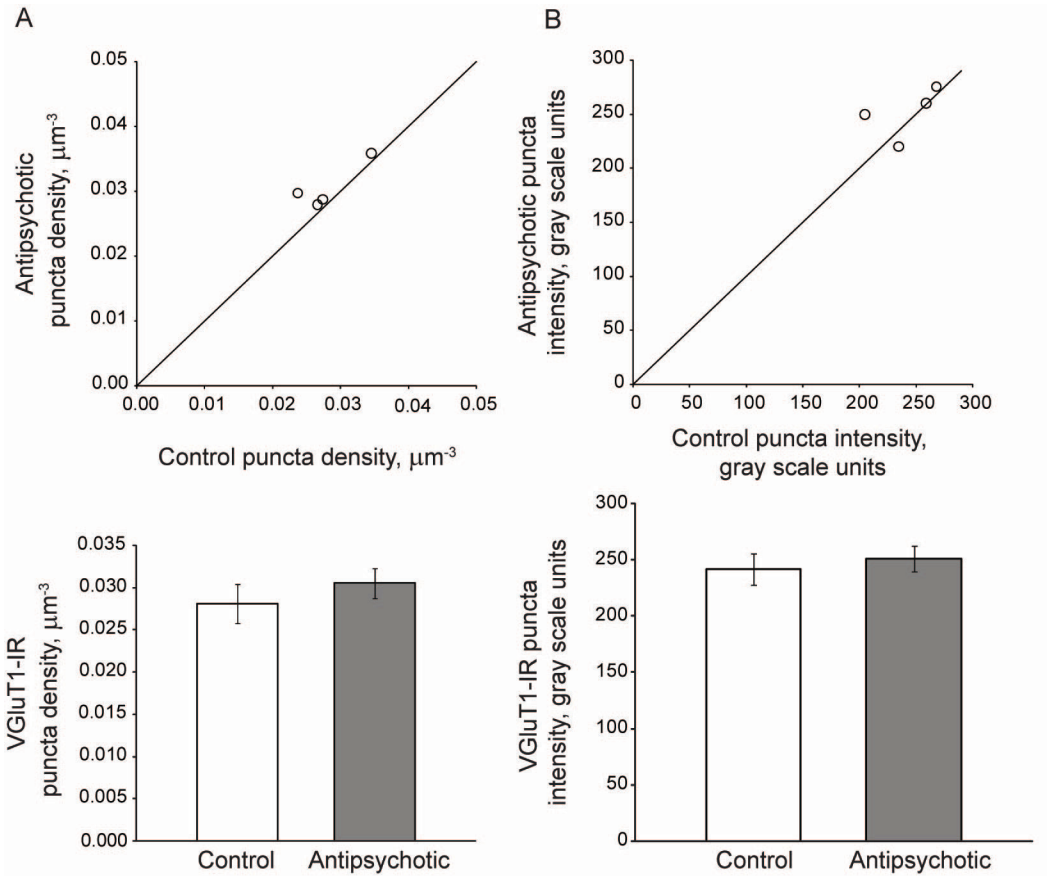

Figure 2.3. Chronic antipsychotic exposure does not alter VGluT1-IR puncta mean density or fluorescence intensity. (Top) VGluT1-IR puncta mean density (A) or fluorescence intensity (B) for monkey cohort. Reference line represents antipsychotic = control values, where points below the line indicate a pair where control > antipsychotic-exposed, and points above the line indicate antipsychotic-exposed > control. (Bottom) Group means for control (open bars) and antipsychotic-exposed (gray bars) animals. Error bars are ± SEM.

2.3.2 VGluT2-IR puncta

We observed no significant change in primary auditory cortex deep layer 3 VGluT2-IR puncta density ($F_{(1,\ 23.3)} = 0.97$, p = 0.335, 95% CI: (-0.0003, 0.001)) in subjects with schizophrenia (**Figure 2.4A**). Similarly, we found that the absolute number of VGluT2-IR puncta was not altered in cohort 2 schizophrenia subjects relative to matched controls ($F_{(1,\ 10)} = 0.153$, p = 0.704, 95% CI: (-1.11×10^8, 1.58×10^8)) (**Figure 2.4B**). There were also no diagnostic group differences in primary auditory cortex deep layer 3 VGluT2-IR puncta fluorescence intensity ($F_{(1,\ 23.2)} = 0.69$, p = 0.413, 95% CI: (-0.09, 0.04)) (**Figure 2.4C**).

We observed trends toward increased VGluT2-IR puncta fluorescence intensity ($F_{(1,\ 20.6)} = 3.05$, p = 0.096, 95% CI: (-0.02, 0.17)) and increased VGluT2-IR bouton puncta density ($F_{(1,\ 20.5)} = 3.64$, p = 0.071, 95% CI: (-0.0002, 0.003)) in haloperidol-exposed macaques, although neither reached statistical significance (**Figure 2.5**).

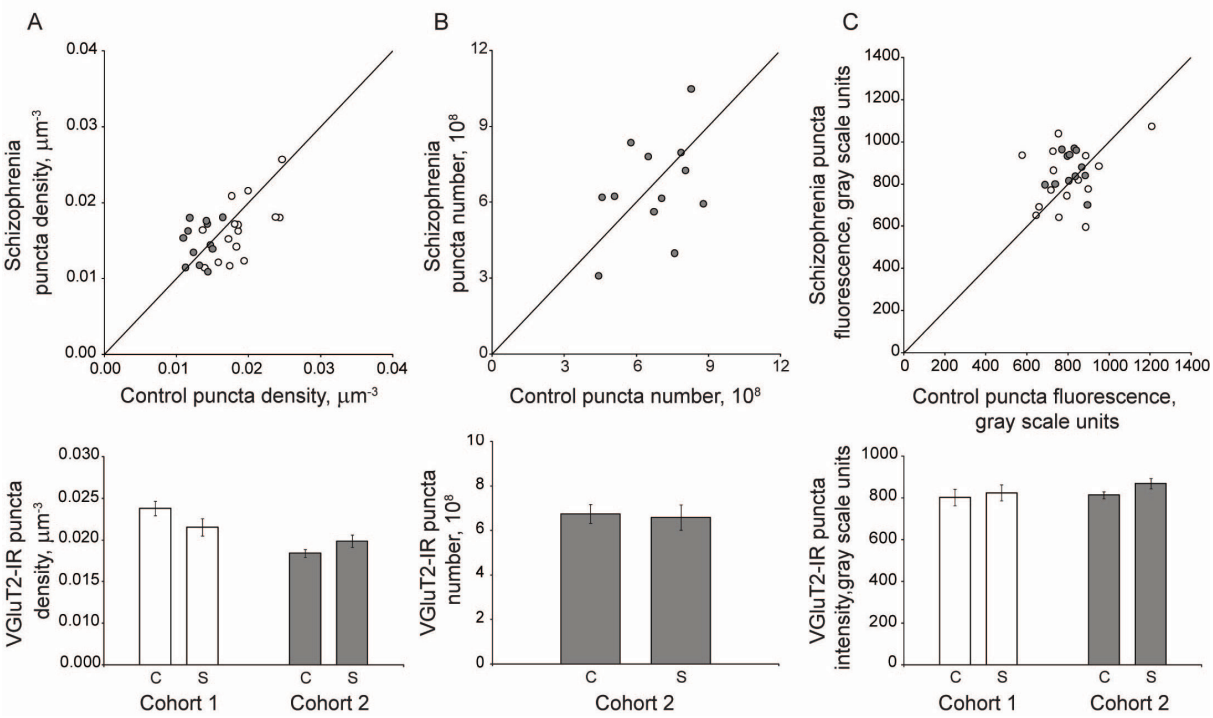

Figure 2.4. VGluT2-IR bouton density, number, and mean fluorescence intensity are unaltered in deep layer 3 of primary auditory cortex of subjects with schizophrenia. A. (Top) VGluT2-IR puncta density for subjects in cohort 1 (open circles) and cohort 2 (gray circles). Reference line represents schizophrenia = control values, where points below the line indicate a pair where control > schizophrenia, and points above the line indicate schizophrenia > control. (Bottom) Diagnostic group mean puncta density for control (c) and schizophrenia (s) subjects in cohort 1 (open bars) and cohort 2 (gray bars) Error bars are +/-SEM. B. (Top) VGluT2-IR puncta number for subjects in cohort 2. Reference line represents schizophrenia = control values, where points below the line indicate a pair where control > schizophrenia, and points above the line indicate schizophrenia > control. (Bottom) Diagnostic group mean puncta number for control (c) and schizophrenia (s) subjects in cohort 2. Error bars are +/-SEM. C. (Top) Mean VGluT2-IR puncta fluorescence intensity for each schizophrenia-control subject pair in cohort 1 (open circles) and cohort 2 (gray circles). Reference line represents schizophrenia = control values, where points below the line indicate a pair where control > schizophrenia, and points above the line indicate schizophrenia > control. (Bottom) Diagnostic group mean puncta fluorescence intensity for control (c) and schizophrenia (s) subjects in cohort 1 (open bars) and cohort 2 (gray bars). Error bars are ± SEM.

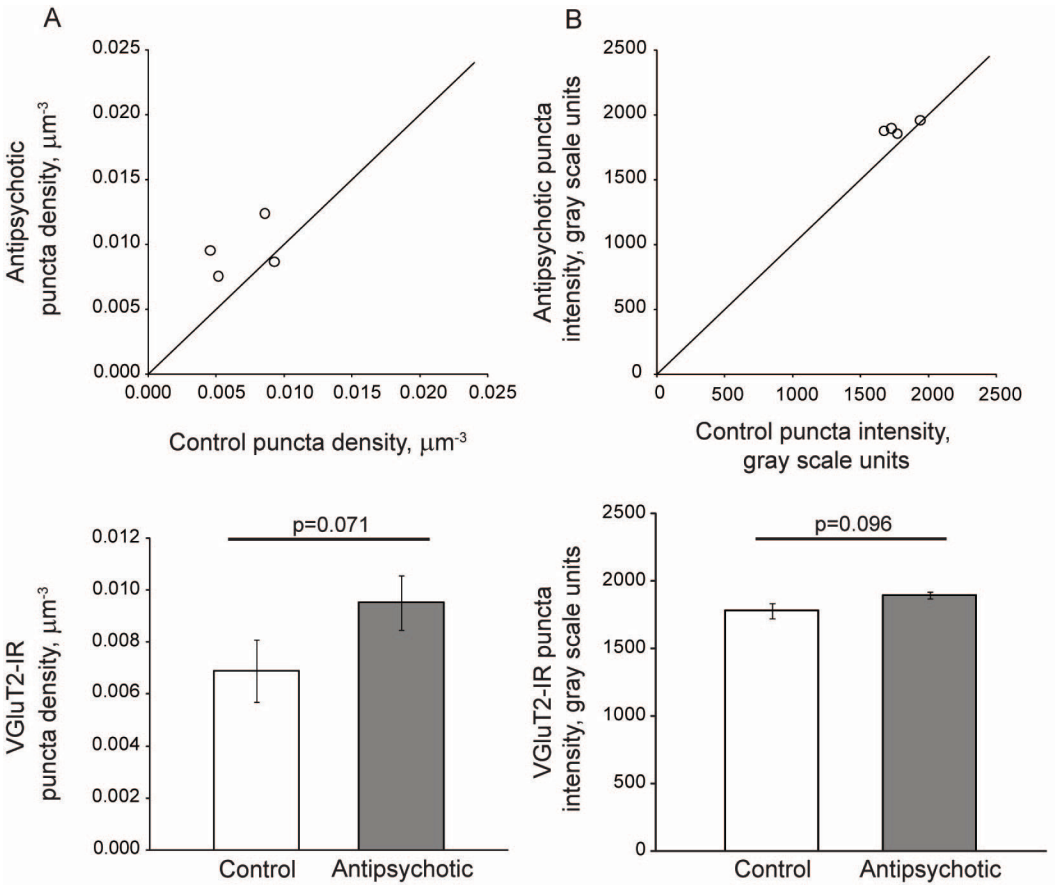

Figure 2.5. Chronic antipsychotic exposure does not alter VGluT2-IR puncta mean density or fluorescence intensity. (Top) VGluT2-IR puncta mean density (A) or fluorescence intensity (B) for monkey cohort. Reference line represents antipsychotic = control values, where points below the line indicate a pair where control > antipsychotic-exposed, and points above the line indicate antipsychotic-exposed > control. (Bottom) Group means for control (open bars) and antipsychotic-exposed (gray bars) animals. Error bars are ± SEM.

2.4 DISCUSSION

Here we asked whether there are alterations in intracortical excitatory or thalamocortical boutons in deep layer 3 of the primary auditory cortex of subjects with schizophrenia. We report that neither VGluT1-IR intracortical excitatory nor VGluT2-IR thalamocortical boutons are altered in density or number. To the best of our knowledge, no studies have examined densities of these two bouton populations in schizophrenia, although the question of whether VGluT1 or VGluT2 mRNA or protein levels are altered has been asked. Conflicting studies of VGluT1 expression in schizophrenia report reduced mRNA in prefrontal cortex and hippocampus (Eastwood and Harrison, 2005), no change in mRNA in the prefrontal cortex (Oni-Orisan et al., 2008; Fung et al., 2011), and increased mRNA and protein in anterior cingulate cortex (Oni-Orisan et al., 2008). Studies of VGluT2 expression in schizophrenia have found that mRNA and protein are unaltered in anterior cingulate and prefrontal cortices (Oni-Orisan et al., 2008), and that mRNA expression in inferior temporal cortex is reduced (Uezato et al., 2009). In the present study, we did not find VGluT1-or VGluT2-IR puncta fluorescence intensities to be altered, suggesting that within-bouton VGluT protein levels are unchanged in subjects with schizophrenia. This indicates that our ability to detect immunoreactive puncta was unimpaired by any changes in VGluT protein levels within presumptive boutons. This also suggests that excitatory boutons in the auditory cortex of subjects with schizophrenia are not impaired in terms of their VGluT protein content. However it remains possible that levels of other proteins involved in glutamate release are altered within excitatory boutons, as reductions in mRNA expression of other presynaptic release machinery genes have been reported in schizophrenia (Mirnics et al., 2000).

2.4.1 Possible implications of spine loss and excitatory bouton preservation

Together with our previous study (Sweet et al., 2009) we found that spine density is reduced in auditory cortex of subjects with schizophrenia but excitatory bouton density is not reduced. One interpretation of our result is that the primary auditory cortex in subjects with schizophrenia has a normal complement of excitatory boutons but that some of these lack postsynaptic contacts. Evidence of boutons which lack postsynaptic contacts has been reported in electron microscopy studies (Jones et al., 1997; Shepherd and Harris, 1998) which suggests that boutons are stable in the absence of a post-synaptic contact. However, chronic *in vivo* imaging studies demonstrate varying rates of turnover for presynaptic boutons in the cortex (De Paola et al., 2006). This would suggest that boutons do not persist without postsynaptic contacts, but instead undergo formation and elimination such that a cross-sectional microscopy analysis will uncover a certain percentage of boutons which appear to not contact postsynaptic structures.

Probably the most parsimonious explanation for the observed deficit in dendritic spines but not excitatory boutons in the primary auditory cortex in schizophrenia is that a greater proportion of excitatory boutons form synapses with dendritic shafts rather than spines. This could result from a failure in the down-regulation of shaft synapses relative to spine synapses during early development, as occurs during the first few postnatal weeks in the rat hippocampus (Boyer et al., 1998; Fiala et al., 1998). Alternatively, several lines of experimental evidence suggest that the prevalence of excitatory shaft synapses may increase when dendritic spines are lost. In the hippocampus, spine loss leads to an increase in the number of synapses occurring on dendritic shafts (Mateos et al., 2007), and an enrichment of PSD-95 in the dendritic shaft (Woods et al., 2011). Whether due to a developmental disturbance or to spine loss, it is tempting to speculate that individuals with schizophrenia may demonstrate an increased proportion of shaft

synapses relative to spine synapses. Indeed, recent electron microscopy evidence has revealed an increased proportion of asymmetric synapses formed with dendritic shafts in the anterior cingulate cortex of subjects with schizophrenia (Barksdale et al., 2012). Future studies could examine if VGluT-IR boutons in the auditory cortex of subjects with schizophrenia demonstrate a relative increase in frequency of apposition to dendritic shaft postsynaptic densities, which would suggest an increased prevalence of shaft-targeting excitatory synapses. It would also be of interest to determine if expression of proteins which have been shown to mediate shaft synapse formation, such as GRIP1 and ephrinB3 (Aoto et al., 2007), are altered in this cortical region. Finally, emphasis should be placed on characterizing animal models of structural excitatory synapse pathology relevant to schizophrenia. For example, models of increased adolescent spine elimination such as the kalirin knockout mouse (Cahill et al., 2009), could be evaluated to determine whether excitatory boutons persist despite reduction in cortical spine density, and whether the proportions of shaft and spine synapses are altered.

The functional implications of a relative increase in shaft synapses concurrent with a reduction in spine synapses are not fully understood. Spines play important roles in segregating frequency inputs within the auditory cortex (Chen et al., 2011b) and serve to normalize the magnitude of inputs occurring at different distances from the soma (Harnett et al., 2012). In addition there is a reduction in dendritic length and branching in the cortex of individuals with schizophrenia (Glantz and Lewis, 2000; Broadbelt et al., 2002) that would be expected to alter excitatory input summation, EPSP magnitude (Jaslove, 1992), summation of responses at the soma (Shepherd et al., 1989), and neuron firing rates (Tsay and Yuste, 2004). Determining whether these alterations can account for impaired frequency discrimination and reduced

auditory event related potentials observed in individuals with schizophrenia, however, will require analysis in animal models that recapitulate these structural changes.

2.4.2 Non-glutamatergic bouton populations in auditory cortex may be affected

Previously, we reported that the density of synaptophysin-IR puncta is reduced in deep layer 3 of primary auditory cortex of subjects with schizophrenia (Sweet et al., 2007). Synaptophysin is a vesicular protein that is found in classical neurotransmitter-releasing boutons (Navone et al., 1986); therefore, this finding could represent a relative density reduction of many different types of boutons. We have previously determined that the density of GAD65-IR puncta is unchanged in deep layer 3 of primary auditory cortex (Moyer et al., 2012) (see chapter 3), and here we report that the densities of presumptive intracortical and thalamocortical glutamatergic boutons are also unchanged. However, densities of other potential synaptophysin-IR bouton types have not yet been evaluated in primary auditory cortex in schizophrenia. For example, boutons of the chandelier cell population of inhibitory neurons, which appear to be affected in schizophrenia (Lewis, 2011), have been shown to express only the 67 kDa isoform of GAD (Fish et al., 2011) and thus would not have been quantified in our previous study. Also, recent evidence suggests that a sub-population of inhibitory boutons originating from somatostatin-expressing interneurons, another population which has been implicated in the neuropathology of schizophrenia (Morris et al., 2008), may express only GAD67 (Rocco and Fish, 2010). Finally, it is possible that the densities of non-glutamatergic, non-GABAergic boutons, such as cholinergic, serotonergic, or dopaminergic boutons, which are present in primary auditory cortex (Campbell et al., 1987), are reduced in schizophrenia.

2.4.3 Use of VGluTs as markers of intracortical excitatory and thalamocortical boutons

Several potential methodological limitations are important to consider. We identified presumptive intracortical and thalamocortical boutons on the basis of their VGluT1 and VGluT2 immunoreactivity. Most reports indicate complementary and non-overlapping expression of VGluT1 and VGluT2 in the neocortex and subcortical structures (Fremeau, Jr. et al., 2001; Kaneko and Fujiyama, 2002; Fremeau, Jr. et al., 2004a; Fremeau, Jr. et al., 2004b). Congruent with these reports, we observed little to no colocalization of VGluT1 and VGluT2-immunoreactivity in human and monkey auditory cortex tissue sections (**Figure 2.1D and 2.1E**; also see (Sweet et al., 2010)). Based on this evidence, we conclude that the failure to observe differences in intracortical excitatory and thalamocortical bouton characteristics between control and schizophrenia subjects is not due to lack of specificity of the two bouton population markers. However, it should be noted that VGluT1 and VGluT2 can be colocalized in boutons in neocortical cultures and in layer 4 of the somatosensory cortex (De Gois et al., 2005; Graziano et al., 2008), and VGluT1 and VGluT2 mRNA expression may overlap in the medial geniculate nucleus (Hackett et al., 2011) (but see (Fremeau, Jr. et al., 2004b)), suggesting that both proteins could be coexpressed in thalamocortical projections to the auditory cortex. Therefore, it is not impossible that some VGluT1-IR puncta identified in our study could actually be thalamocortical rather than intracortical excitatory boutons. In addition, although the medial geniculate nucleus is likely to contribute the majority of subcortical inputs to the primary auditory cortex, it is possible that VGluT2-IR inputs from other subcortical structures are included in our presumptive thalamocortical bouton analyses. For example, the rodent primary auditory cortex receives input from the hypothalamus and the paraventricular nuclei of the thalamus (Budinger et al., 2008). It is possible that quantifying other subcortical excitatory inputs could have masked alterations

which are specific to VGluT2-IR boutons originating from the auditory thalamus but are not present in VGluT2-IR boutons from other sources.

2.4.4 Conclusions

In summary, we report that intracortical excitatory and thalamocortical boutons are unaltered in their density, number, and level of VGluT protein in deep layer 3 of primary auditory cortex of individuals with schizophrenia. Thus, presynaptic excitatory boutons appear to be preserved in the primary auditory cortex, despite reduced density of postsynaptic dendritic spines. Further investigation is needed to understand whether excitatory boutons have intact expression of proteins influencing glutamate release and to evaluate the functional implications of a discrepancy between preservation of boutons and loss of spines. Future studies in postmortem human tissue and animal models will aid the development of treatments aimed at normalizing the function of excitatory circuitry in schizophrenia.

3.0 REDUCED GLUTAMATE DECARBOXYLASE 65 PROTEIN IN PRIMARY AUDITORY CORTEX INHIBITORY BOUTONS IN SCHIZOPHRENIA

This chapter has been previously published as:

Moyer CE, Delevich KM, Fish KN, Asafu-Adjei JK, Sampson AR, Dorph-Petersen KA, Lewis DA, Sweet RA. 2012. Reduced glutamate decarboxylase 65 protein in primary auditory cortex inhibitory boutons in schizophrenia. *Biological Psychiatry*, 72(9):734-43.

It is unchanged in content, with the exception of minor formatting alterations and moving supplemental methods to the main body of the article to satisfy the requirements for this dissertation.

My contributions include participation in study design, data collection and analysis, and writing the manuscript under the direction of Dr. Sweet. Kristen Delevich assisted with data collection. Dr. Fish contributed to study design and data analysis. Dr. Asafu-Adjei and Dr. Sampson assisted with statistical analysis, Dr. Dorph-Petersen assisted with stereological methods and analysis. Dr. Lewis contributed to study design and data analysis. All authors contributed to and approved the final manuscript.

Abstract

Background: Schizophrenia is associated with perceptual and physiological auditory processing impairments which may result from primary auditory cortex excitatory and inhibitory circuit pathology. High-frequency oscillations are important for auditory function, and are often reported to be disrupted in schizophrenia. These oscillations may in part depend on up-regulation of GABA synthesis by glutamate decarboxylase 65 (GAD65) in response to high interneuron firing rates. It is not known whether levels of GAD65 protein, or GAD65-expressing boutons, are altered in schizophrenia.

Methods: Two cohorts of subjects with schizophrenia and matched controls, comprising 27 pairs of subjects, were studied and relative fluorescence intensity, density, volume, and number of GAD65 immunoreactive boutons in primary auditory cortex were measured using quantitative confocal microscopy and stereologic sampling methods. Bouton fluorescence intensities were used to compare the relative expression of GAD65 protein within boutons between diagnostic groups. Additionally, we assessed the correlation between previously-measured dendritic spine densities and GAD65-immunoreactive bouton fluorescence intensities.

Results: GAD65-immunoreactive bouton fluorescence intensity was reduced by 40% in subjects with schizophrenia, was correlated with previously-measured reduced spine density, and the reduction was greater in subjects who were not living independently at time of death. In contrast, immunoreactive bouton density and number were not altered in deep layer 3 of primary auditory cortex of subjects with schizophrenia.

Conclusions: Decreased expression of GAD65 protein within inhibitory boutons could contribute to auditory impairments in schizophrenia. The correlated reductions in dendritic

spines and GAD65 protein suggest a relationship between inhibitory and excitatory synapse pathology in primary auditory cortex.

3.1 INTRODUCTION

Individuals with schizophrenia exhibit basic auditory processing deficits (McCarley et al., 1991) that contribute to debilitating negative and cognitive symptoms. One such deficit is impaired tone frequency discrimination (Javitt et al., 2000; Leitman et al., 2010b), assessed either behaviorally or as reductions in the mismatch negativity (MMN) response of the auditory event related potential (ERP) (Javitt et al., 1994; Javitt et al., 2000; Naatanen and Kahkonen, 2009). The inability to properly discriminate between different frequencies may make phoneme identification difficult, translating to impaired speech comprehension in subjects with schizophrenia (Kasai et al., 2002; Javitt, 2009). Evidence suggests that features of schizophrenia stemming from disrupted tone processing have a significant impact on patients' quality of life, as tone matching performance is severely impaired in subjects who require long-term residential care (Rabinowicz et al., 2000). Correlated with tone matching deficits, subjects with schizophrenia show reduced ability to use pitch-based acoustic cues to recognize vocally expressed emotion (Leitman et al., 2005; Leitman et al., 2010b). Consequently, inability to recognize emotional components of speech, a negative symptom of schizophrenia (Shea et al., 2007), contributes to dysfunction in social interactions (Leitman et al., 2006). Thus, basic impairments in tone frequency discrimination likely impair higher-order functions downstream of auditory stimulus processing, contributing to some of the signs and symptoms of schizophrenia.

Studies in animals suggest that the ability to discriminate frequency depends on auditory cortex function (Heffner and Heffner, 1986; Rybalko et al., 2006). The primary auditory cortex is located on Heschl's gyrus, found within the Sylvian fissure on the superior temporal gyrus (STG). Reduction of STG gray matter volume is one of the most consistently reported gray matter volume change findings in schizophrenia subjects (McCarley et al., 1999) and those who are genetically at-risk (Rajarethinam et al., 2004). Specifically, findings include reductions of gray matter volume in Heschl's gyrus in both cross-sectional analyses of subjects with schizophrenia (Hirayasu et al., 2000; Kasai et al., 2003; Salisbury et al., 2007) and longitudinal studies of high risk individuals (Takahashi et al., 2009).

One measure of auditory neurophysiology known to depend on the integrity of the primary auditory cortex is the auditory steady state response (aSSR) (Pastor et al., 2002; Picton et al., 2003; Jeschke et al., 2008). Many studies have found the aSSR to be abnormal in patients with schizophrenia (Kwon et al., 1999b; Brenner et al., 2003; Light et al., 2006; Spencer et al., 2008; Krishnan et al., 2009). SSRs are generated in response to temporally modulated stimuli, are based on the synchronized activity of large populations of neurons, and represent the ability of neural circuits to oscillate at different frequencies (Brenner et al., 2009). Subjects with schizophrenia exhibit abnormal aSSR entrainment to tones and white noise bursts modulated at gamma-range frequencies (30-80 Hz) (Brenner et al., 2003; Hamm et al., 2011). Individuals with schizophrenia also demonstrate reduced power of induced gamma-range oscillatory activity in response to an unmodulated pure tone (Krishnan et al., 2009). Altered high frequency oscillatory activity may reflect a physiological impairment of auditory cortex circuitry that contributes to reduced ability to discriminate the features of auditory stimuli (Lenz et al., 2008).

Inhibitory γ-amino butyric acid (GABA)-ergic interneurons contribute to the generation of neural oscillatory activity through the production of rhythmic inhibitory postsynaptic potentials in excitatory neurons, inducing synchronization of their firing (Cobb et al., 1995; Uhlhaas and Singer, 2010). It has been shown that rapid adjustments to levels of inhibition are required for controlling changes in oscillation frequency (Atallah and Scanziani, 2009). This necessity of rapid adjustments to levels of inhibition suggests that modulation of the amount of GABA synthesized for release might be crucial for the ability of interneurons to mediate oscillatory activity. The GABA-producing activity of the 65 kDa isoform of glutamate decarboxylase (GAD65) is rapidly upregulated via binding to its cofactor pyridoxal-5'-phosphate (PLP) under conditions of increased neural activity (Martin et al., 1991; Patel et al., 2006). Mice lacking GAD65 demonstrate reduced GABA release during sustained activation of inhibitory neurons (Tian et al., 1999). GAD65 may therefore be particularly important for rapidly modulating GABA synthesis to maintain gamma range oscillatory activity in the cortex during conditions of sustained high interneuron firing rates (Gonzalez-Burgos and Lewis, 2008). Thus, impaired gamma-range oscillatory activity in auditory cortex in schizophrenia could indicate that GAD65-mediated GABA synthesis in inhibitory boutons is impaired in such a way as to be unable to keep up with the necessary high firing rates.

In the present study, we asked whether the relative level of GAD65 protein is reduced in the auditory cortex of subjects with schizophrenia. As auditory cortex circuitry is thought to participate in the generation of both aSSRs and the MMN component of the auditory ERP (Pastor et al., 2002; Picton et al., 2003; Kaur et al., 2005; Liu et al., 2007; Jeschke et al., 2008), and MMN reflects activity of the supragranular cortical layers (Javitt et al., 1994; Javitt et al., 1996), we wanted to determine whether GAD65 protein was reduced in this sub-region of

auditory cortex, specifically at its site of action: the bouton. To address this, we used quantitative fluorescence microscopy to assess levels of GAD65 protein within deep cortical layer 3 inhibitory boutons. We found that whereas the number and density of GAD65-expressing inhibitory boutons in deep layer 3 of primary auditory cortex were unaltered, these boutons contained less GAD65 protein, suggesting that the amount of GABA available for release when auditory cortex interneurons are firing at high rates may be reduced in subjects with schizophrenia.

3.2 MATERIALS AND METHODS

3.2.1 Subjects and animals

We studied two cohorts (**Table 3.1** and **Appendix Table A.1**) of subjects diagnosed with schizophrenia or schizoaffective disorder and matched controls included in our previous studies (Sweet et al., 2004; Sweet et al., 2007; Sweet et al., 2009; Dorph-Petersen et al., 2009b). All of the brain specimens were collected during autopsies conducted at the Allegheny County Medical Examiner's Office, with permission obtained from the subjects' next-of-kin. The protocol used to obtain consent was approved by the University of Pittsburgh Institutional Review Board and Committee for Oversight of Research Involving the Dead. An independent committee of experienced clinicians made consensus diagnoses (American Psychiatric Association, 1994) for each subject, using information obtained from clinical records and structured interviews with surviving relatives. These procedures were IRB approved. We also studied a cohort of four male macaque monkeys (*Macaca fascicularis*) chronically exposed to haloperidol decanoate, and

four control macaques matched for sex and weight (Sweet et al., 2007). All procedures were approved by the University of Pittsburgh's Institutional Animal Care and Use Committee.

Table 3.1. Summary of subject characteristics for cohorts 1 and 2. Each subject in cohorts 1 and 2 was previously matched to a normal comparison subject based on sex and as closely as possible for age and postmortem interval and group matched for handedness. There were no diagnostic group differences in age [$t_{(52)} = 0.517$, $p = 0.608$] or postmortem interval [$t_{(52)} = 0.584$, $p = 0.561$] or in the distribution of handedness between diagnostic groups ($\chi^2 = 1.46$, $df = 1$, $p = 0.314$). Mean storage time did not differ between diagnostic groups [cohort 1: $t_{(28)} = 0.040$, $p = 0.968$; cohort 2: $t_{(22)} = 0.596$, $p = 0.557$].A, ambidextrous; ATOD, at time of death; F, female; L, left-handed; M, male; PMI, postmortem interval; R, right-handed; U, unknown.

	COHORT 1		COHORT 2		TOTAL	
	Control	Schizophrenia	Control	Schizophrenia	Control	Schizophrenia
N	15	15	12	12	27	27
Mean Age (SD)	46.8 (8.3)	47.6 (5.5)	45.1 (12.9)	47.3 (13.4)	46.0 (10.4)	47.4 (9.6)
Range	27-64	38-63	19-65	25-71	19-65	25-71
Sex (F/M)	6/9	6/9	4/8	4/8	10/17	10/17
Handedness (R/L/A/U)	10/4/0/1	7/3/1/4	11/1/0/0	6/2/1/3	21/5/0/1	13/5/2/7
PMI (SD)	13.9 (5.5)	15.9 (6.6)	18.0 (6.6)	17.9 (8.8)	15.7 (6.3)	16.8 (7.6)
Storage Time, mos (SD)	168 (29)	167 (26)	111 (27)	102 (30)	142 (40)	138 (43)
Illness Duration, yrs (SD)		24.9 (5.6)		22.1 (14.6)		23.7 (10.6)
Range		14-34		3-50		3-50
Suicide, N (%)		3 (20%)		2 (17%)		5 (19%)
Schizoaffective, N (%)		3 (20%)		4 (33%)		7 (26%)
Living independently ATOD, N (%)		7 (47%)		2 (17%)		9 (33%)
Alcohol/Substance abuse ATOD, N (%)		9 (60%)		7 (58%)		16 (59%)
History of cannabis use, N (%)		3 (20%)		5 (42%)		8 (30%)
Antipsychotic ATOD, N (%)		13 (87%)		11 (92%)		24 (89%)
Benzodiazepine ATOD, N (%)	1 (7%)	5 (33%)		1 (8%)	1 (4%)	6 (22%)
Anticonvulsant ATOD, N (%)		3 (20%)		4 (33%)		7 (26%)
Antidepressant ATOD, N (%)		5 (33%)		4 (33%)		9 (33%)

3.2.2 Tissue processing

3.2.2.1 Cohort 1 tissue processing

Brains from individuals in cohort 1 were bisected and the left hemisphere of each subject was cut coronally into 1-2 cm-thick blocks, which were then immersed in cold 4% paraformaldehyde in phosphate buffer for 48 hours, equilibrated in a series of graded sucrose solutions, and stored at -30ºC in an antifreeze solution (30% glycerol and 30% ethylene glycol in phosphate-buffered saline). Superior temporal gyrus (STG)- containing blocks were generated as described previously (Sweet et al., 2003; Sweet et al., 2004) and 40 μm coronal cryostat sections were cut and then stored in antifreeze solution at -30ºC until use in this study.

3.2.2.2 Cohort 2 tissue processing

Brain specimens from individuals in cohort 2 were harvested, bisected, blocked coronally, and stored in antifreeze solution at -30ºC as described for cohort 1 (Sweet et al., 2005; Dorph-Petersen et al., 2009b). The entirety of the left STG of each subject was dissected from the fixed coronal blocks. The pial surfaces of the STG blocks were painted with hematoxylin to facilitate identification of the pial surface later during tissue processing, and the blocks were reassembled in 7% low-melt agarose in their *in vivo* orientation. The reassembled STG was cut into systematic uniformly random 3 mm slabs orthogonal to the long axis of Heschl's gyrus. Every other slab with a random start was selected for mapping the boundaries of primary auditory cortex and the remaining slabs were stored in antifreeze solution until use. Mapping slabs were cut on a cryostat at 60 μm, and three consecutive sections from each slab were stained for parvalbumin (PV) immunoreactivity, acetylcholinesterase activity, and Nissl substance. These sections were used to determine whether primary auditory cortex was present in a given slab, to

estimate the volume of primary auditory cortex, and to delineate the boundaries of primary auditory cortex. The boundaries of primary auditory cortex determined using the mapping slabs were applied to the unused set of slabs, such that boundaries of primary auditory cortex on a mapping slab were applied to the adjacent unused slab immediately rostral. The primary auditory cortex was dissected from the unused slabs, and further subdivided into 3 mm wide blocks. Blocks from the most rostral and caudal slabs containing the region of interest were weighted at 1/3 relative to the weight of other blocks to account for the fact that these blocks only partially contained the region of interest. This weighting method has been previously published (Dorph-Petersen et al., 2009b). Briefly, it is needed because the end blocks only partially represent the region of interest (on average less than half due to the positive curvature of the boundary of the region of interest in 3 dimensions) and therefore should not have the same weight as the other blocks. However, there is no way to know the precise weight without knowing the exact fraction of the region of interest and the Nv of the region of interest as well as that of the neighboring region within each block in question. Because the positive curvature is best approximated by a cone or a pyramid, it would take up 1/3 of the volume, leading to our weighting. Block weights were factored into calculations of bouton number (Dorph-Petersen et al., 2009b). Each primary auditory cortex block was then placed pial surface down in a layer of optimal cutting temperature compound (OCT) on a stainless steel block. A hollow cylinder was placed on the block over the tissue, and the cylinder was filled with OCT and allowed to freeze at -20^{o}C. The block of tissue encased in OCT was then removed from the cylinder and placed in a stainless steel well where it was randomly rotated and fixed in its orientation with OCT. The primary auditory cortex block was then sectioned at 50 μm in this orientation perpendicular to the pial surface, and sections were stored at -30^{o}C in antifreeze solution until use in this study.

3.2.2.3 Antipsychotic-exposed macaque cohort tissue processing

In order to account for possible effects of antipsychotic medications, we studied a previously described cohort (Sweet et al., 2007) of four male macaque monkeys (*Macaca fascicularis*) chronically exposed to haloperidol decanoate, and four control macaques matched for sex and weight. Animals received injections of haloperidol (mean (standard deviation) = 16.0 (2.1) mg/kg) every four weeks, maintaining trough serum levels of haloperidol of 4.3 (1.1) ng/ml, on average. Following 9-12 months of haloperidol exposure, animals were euthanized with an overdose of pentobarbital, and brains were removed and immersed in 4% paraformaldehyde following a 45 min post mortem interval (PMI). Free-floating sections from the four matched pairs were processed together within immunohistochemistry runs, and procedures were identical to those described for human tissue immunohistochemistry.

3.2.3 Immunohistochemistry

In order to identify axon boutons of inhibitory GABAergic neurons in the primary auditory cortex, we utilized an antibody directed against GAD65. GAD65 is highly expressed in GABAergic boutons, with minimal expression in interneuron cell bodies (Erlander et al., 1991). The antibody we selected (mouse anti-GAD65 monoclonal, Millipore, MAB351) is a clone of the monoclonal GAD-6 antibody developed by Chang and Gottlieb that recognizes only the lower molecular weight band of GAD in Western blots (Chang and Gottlieb, 1988). We have verified this by Western blot, and also found that this antibody does not label brain homogenate from GAD65 knockout mice (**Figure B.1A**). In immunohistochemistry, labeling with this antibody has been reported to colocalize with punctate structures immunoreactive for GAD67, cannabinoid receptor 1 (CB1) and parvalbumin (PV) (presumably inhibitory boutons) (Fish et

al., 2011), and in immunoelectron microscopy has been reported to label symmetrical synapses (Hagiwara et al., 2005), as well as punctate structures closely apposed to puncta immunoreactive for the α1 subunit of the $GABA_A$ receptor (Marty et al., 2004). Qualitatively, we observed no colocalization of puncta labeled with the GAD65 antibody and antibodies against vesicular glutamate transporters (VGluT1 and VGluT2), which label intracortical and thalamocortical excitatory boutons, respectively (**Figure B.1B**). In summary, this evidence suggests that this antibody is specific for GAD65, and in immunohistochemistry is specific for non-glutamatergic boutons and labels structures colocalized with or closely apposed to other GABAergic synaptic markers.

Auditory cortex containing tissue sections from matched pairs were processed together in immunohistochemistry runs. Free-floating sections were rinsed in 0.1 M phosphate buffered saline (PBS), and then incubated in 1% $NaBH_4$ in phosphate buffer for 30 minutes to reduce tissue autofluorescence. Sections were rinsed again in PBS and incubated for 3 hours in blocking buffer containing 0.3% Triton-X, 5% normal human serum, 5% normal goat serum, 1% bovine serum albumin, 0.1% lysine, and 0.1% glycine in PBS. Sections were then incubated with a 1:500 dilution of anti-GAD65 primary antibody (MAB351) in blocking buffer for 96 hours at 4°C. After rinsing in PBS, sections were incubated overnight with a 1:500 dilution of Alexa 405 goat anti-mouse secondary antibody (Invitrogen, Carlsbad, CA). Sections were rinsed, mounted on gelatin-coated slides, allowed to dry for 1 hour, rehydrated for 10 min in distilled water, and coverslipped with Vectashield Hard Set mounting medium (Vector Laboratories, Burlingame, CA).

3.2.4 Image collection

Sections were coded so that the experimenter was blind to diagnostic or drug exposure group, and sections were organized into sets so that sections from paired subjects were imaged during the same imaging session. Images were collected using a 1.42 NA 60X oil objective on an Olympus BX51 upright microscope (Olympus, Center Valley, PA) equipped with an Olympus DSU spinning disk confocal, a Hamamatsu C4742-98 CCD camera (Hamamatsu, Bridgewater, NJ), Olympus mercury light source, excitation/emission filter wheels, a 89000 Sedat Quad ET filter set (Chroma Technology Corp, Bellows Falls, VT), and high precision Prior Scientific motorized XY stage (Prior Scientific, Inc., Rockland, MD) equipped with a linear XYZ encoder (Ludl Electronic Products, Ltd., Hawthorne, NY). Image collection was controlled using SlideBook version 4.1 software (Intelligent Imaging Innovations, Denver, CO). At each sampling site, the tissue thickness (Z axis depth) was measured and recorded, and tissue thickness did not differ between diagnostic groups ($t_{52} = 0.844$, $p = 0.402$). Image stacks were collected with a step size of 0.22 μm between Z axis planes in the stack, starting from 10 μm below the tissue surface closest to the coverglass and stepping up until the tissue surface was reached, yielding a 10 μm thick (Z axis depth) stack comprised of 46 individual 2-dimensional planes. Collected image planes were 512 x 512 pixels with 2 x 2 binning, and exposure times were adjusted to optimize the spread of the intensity histogram and to ensure that none of the pixels in the image stack were saturated. Although mean exposure time was not significantly different between diagnostic groups (Means: Control, 1643 ms; Schizophrenia, 1796 ms; $t_{52} = 0.45$, $p = 0.654$), differences were corrected for by including exposure times in statistical models.

3.2.5 Image processing

Collected image stacks were post-processed offline, using SlideBook and Automation Anywhere software (Automation Anywhere, Inc., San Jose, CA) to automate keystrokes and increase image processing efficiency. Images were deconvolved with a constrained iterative algorithm using a calculated point spread function, a maximum of 20 iterations, 3D frequency filtering enabled, and Gaussian noise smoothing with a radius of 0.5. The background fluorescence intensity of each smoothed and deconvolved image stack was determined as the mode value of the intensity histogram. Background subtraction was done by subtracting the mode intensity (gray scale) value from all pixel intensities in the image stack. This deconvolved, smoothed, and background subtracted image stack was then subject to intensity segmentation coupled with morphological selection using our iterative masking approach (Fish et al., 2008). For each image stack, the initial intensity threshold was set at 105% of the background intensity level determined above, and with each subsequent iteration the intensity threshold was increased by 10%, until either a maximum of 5000 gray levels was reached or a maximum of 60 iterations occurred. After each segmentation step, mask objects with volumes ranging from 0.06 μm^3 to 1.0 μm^3 were selected and merged with the mask generated in the prior segmentation step. The resulting mask was then copied back onto the original image stack which had been deconvolved as described above, but without the Gaussian smoothing step, in order to obtain accurate pixel intensity information. GAD65-IR bouton data (mean intensity, mean volume) were extracted from these image stacks using the generated mask to identify objects of interest. Mask objects were selected for final analysis if the intensity gray level range within the object (maximum voxel intensity minus minimum voxel intensity) was greater than 50. This further eliminated falsely detected background signal, as objects identified from background noise are likely to have less intensity

variation between highest and lowest intensity gray scale pixels. GAD65-IR puncta were counted automatically by determining whether the centroid of each automatically detected object was inside the disector. This corresponds to the so-called "associated point rule" (Baddeley and Jensen, 2004, page 69), which is an unbiased alternative to the unbiased counting frame (Gundersen, 1977). Guard zones of 10 pixels were applied around all edges in the X and Y dimensions of each stack, and 10 Z planes starting 10 planes below the coverglass were included in analysis, as antibody penetration was uniform (puncta counts and intensities were uniform) across these Z axis depths (10 planes x 0.22 μm step size = 2.20 μm disector height).

3.2.6 Quantification of GAD65-IR puncta

GAD65-immunoreactive (IR) boutons within deep cortical layer 3 of primary auditory cortex were quantified using stereologic sampling as shown in **Figure 3.1**. Densities reported were calculated individually at each site in order to include exposure time as a covariate in our analyses, as exposure time varied on a site-by-site basis. The density of mask objects at each site was determined by dividing the number of objects counted at each site by the product of the the disector height (2.2 μm) and the area of the counting frame (2553 μm^2), and then multiplying that by the measured tissue thickness at each site divided by the cryostat block advance (40 or 50 μm) (Dorph-Petersen et al., 2001) to correct for tissue shrinkage. It should be noted that the disector height of 2.2 μm used in the current study is very low and could only be implemented robustly because we used confocal microscopy allowing for a high number of thin focal planes; and because we performed a careful analysis of the distribution of the boutons along the Z axis (see Fig. 4 of (Dorph-Petersen et al., 2009a)). We determined the position of the disector and corresponding guard zones post hoc ensuring that boutons were only sampled in the zone with

uniform bouton counts. Such sampling was possible due to the high number of automatically detected boutons—on average 23,037 boutons were detected per subject and of these an average of 5,742 per subject were sampled by the disector. Thus, while a disector height of only 2.2 μm should be avoided in a standard brightfield microscopy study with manual counts, we were able to robustly implement such a disector in the current study.

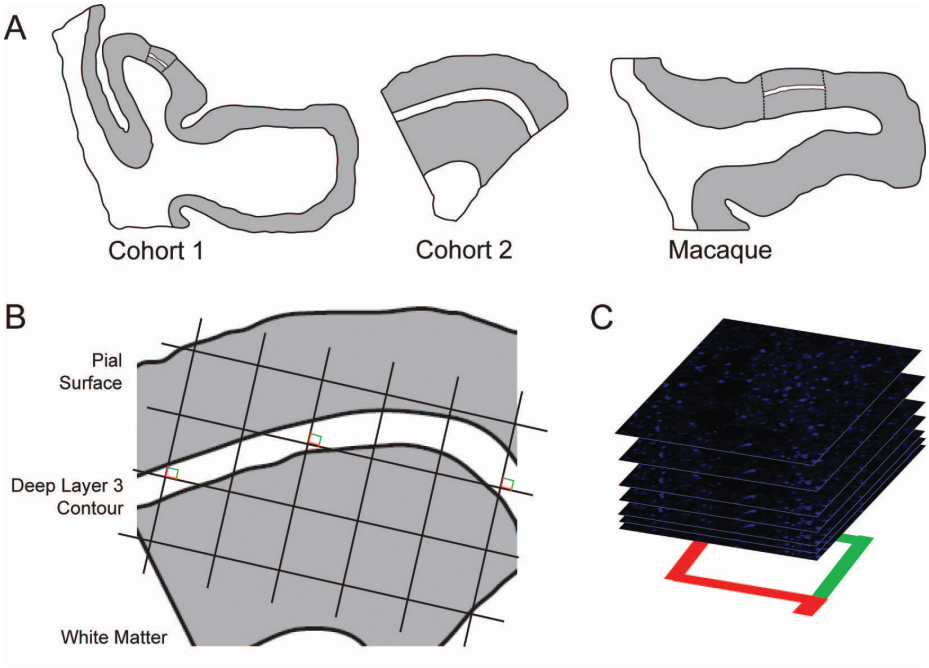

Figure 3.1. Sampling of glutamate decarboxylase 65-immunoreactive boutons in primary auditory cortex deep layer 3. (A) Illustration of delineation of primary auditory cortex deep layer 3 on sections containing auditory cortex for human and antipsychotic exposed macaque cohorts. (Left) Cohort 1: Previously, every tenth section with a random start was selected from superior temporal gyrus blocks and processed for Nissl staining, and primary auditory cortex (Brodmann area 41) was identified using cytoarchitectonic criteria (Sweet et al., 2004). Three Nissl-stained sections in which primary auditory cortex was cut perpendicular to the pial surface were selected for each subject, and sections adjacent to or nearby these sections were chosen for immunohistochemistry. (Middle) Cohort 2: Four primary auditory cortex blocks per subject were selected using a systematic uniformly random sampling scheme (Gundersen, 2002), designed to sample four primary auditory cortex blocks from each subject with equal probability. The central section of each block was stained for Nissl substance and used to delineate the cortical layer boundaries. From each selected block, one section adjacent to or nearby the center Nissl section was used in the present study. (Right) Antipsychotic-exposed macaques: Left hemisphere coronal superior temporal gyrus sections were generated similar to cohort 1 sections. Cytoarchitectonic criteria were used to identify primary auditory cortex, and three primary auditory cortex containing sections from each animal were selected for immunohistochemistry (Sweet et al., 2007; Sweet et al., 2009). For each human and monkey subject, the borders of layers 2/3 and 3/4 were

identified on each of the adjacent Nissl-stained sections to determine the total layer 3 area for each subject. A contour outline (white) of the deepest one third of layer 3 was drawn in Stereo Investigator (MicroBrightField Inc., Colchester, Vermont). The contours were aligned with the glutamate decarboxylase 65-labeled tissue sections using pial surface fiduciaries traced from the Nissl-stained sections. (B) A sampling grid was generated in Stereo Investigator to generate 12 to 14 sampling sites for each human subject and approximately 20 sites for each nonhuman primate subject. The grid size was determined based on the total deep layer 3 area across all tissue sections for a subject and the desired number of sampling sites per subject (12 for cohort 1 and 14 for cohort 2). The grid was then randomly rotated over the contour, and a sampling site was marked at every intersection between the grid and the deep layer 3 contour (shown as counting frames for the purpose of illustration; see text for description of the associated point rule used in this study). (C) At each sampling site, a 10 μm-thick stack of 46 image planes, each separated by 0.22 μm, was collected using spinning disk confocal microscopy.

For cohort 2 subjects, we were also able to estimate GAD65-IR bouton number because of the tissue processing methods used to generate auditory cortex tissue sections. To do this, mean object densities were calculated as described in equations 4 and 5 of Dorph-Petersen et al. (Dorph-Petersen et al., 2009b) using the numerical density (N_V) approach with the following modification: the distances of each individual mask object from the central axis were not included in the calculation under the reasonably robust assumption of homogeneity on the scale of the sampling site (~50 μm). Instead, object counts at each sampling site were weighted by multiplying object count at each site by the distance of the sampling site from the central axis. Deep layer 3 volumes for each subject were calculated as described in equations 1-3 of Dorph-Petersen et al. (2009b) by multiplying the volume fraction of deep layer 3 sampled by the total primary auditory cortex volume. Bouton number for each subject was then generated by multiplying the N_V by the total deep layer 3 volume (Dorph-Petersen et al., 2009b).

3.2.7 Statistical analyses

For each human and macaque subject, mean density, fluorescence intensity, and volume of GAD65-IR puncta in deep layer 3 of primary auditory cortex were calculated. Among the human subjects, the analyses of GAD65-IR bouton volume, density, and mean intensity were conducted separately using two multivariate analysis of covariance (MANCOVA) models: a primary model that included diagnosis and cohort as fixed effects, subject pair (nested in cohort) as a blocking factor, and tissue storage time and exposure time as covariates; and a secondary model without subject pair as a blocking factor, that included diagnosis, sex, and cohort as fixed effects and age, PMI, tissue storage time, and exposure time as covariates. To help satisfy the normality requirement for MANCOVA models, mean fluorescence intensity was analyzed on the natural logarithm scale. To account for the correlation among sampling sites within each subject and among sampling sites within each section for each subject, site and section nested in subject were included as random effects in each MANCOVA model. Inclusion of tissue thickness, subject handedness, or immunohistochemistry assay order in the models had negligible impact on diagnostic group differences and, thus, the results reported are from MANCOVA models omitting these factors.

The analysis of GAD65-IR bouton number (cohort 2 subjects only) was conducted using two analysis of covariance (ANCOVA) models: a primary model that included diagnosis and pair as fixed effects, and tissue storage time as a covariate; and a secondary model without pair as a factor that included diagnosis and sex as fixed effects, and age, PMI, and tissue storage time as covariates. Correlations between dendritic spine density and GAD65-IR bouton fluorescence intensity or density for cohort 1 subjects (as spine density measures were not available for cohort 2 subjects) (Sweet et al., 2009) were assessed using Pearson's correlation.

Based on the mean densities, fluorescence intensities, and volumes for each subject, two sample t tests were used to determine the effect of the following: antipsychotic use, co-morbid alcohol or substance abuse, independent living status at time of death, history of cannabis use, death by suicide, diagnosis of schizoaffective disorder, and benzodiazepine, antidepressant, or anticonvulsant medication status at time of death. In these analyses, the percent changes of bouton density, fluorescence intensity, and volume in subjects with schizophrenia (relative to normal controls) within each subject pair were the response variables of interest.

To compare mean bouton density, fluorescence intensity, and volume between antipsychotic exposed and control macaques, MANCOVA models were used, each of which included drug treatment as a fixed effect, pair as a blocking factor, and exposure time as a covariate, and site and section nested in animal were included as random effects. Due to the similarity of storage time within each pair, storage time was not included as a covariate.

All statistical tests were two-sided and conducted at the 0.05 significance level

3.3 RESULTS

3.3.1 GAD65-IR bouton density, intensity, and volume

The fluorescence intensity of GAD65-IR puncta in deep layer 3 of the primary auditory cortex of subjects with schizophrenia was significantly decreased in both the primary ($F_{(1, 25.2)} = 12.52$, $p = 0.002$) and secondary statistical models $F_{(1, 46.5)} = 15.74$, $p = 0.0002$; **Figure 3.2**). Estimated mean (95% CI) fluorescence intensities derived from the primary model were 5.94 (5.73, 6.15) and 5.42 (5.21, 5.64) gray scale units on the natural logarithm scale in normal controls and

subjects with schizophrenia, respectively, reflecting a 40.5% reduction in relative fluorescence intensity in subjects with schizophrenia.

The density of GAD65-IR puncta was not significantly altered in subjects with schizophrenia compared to controls, in either the primary ($F_{(1, 24)} = 0.84$, $p = 0.369$) or secondary ($F_{(1,46.8)} = 0.22$, $p = 0.641$) statistical models (**Figure 3.3A**).

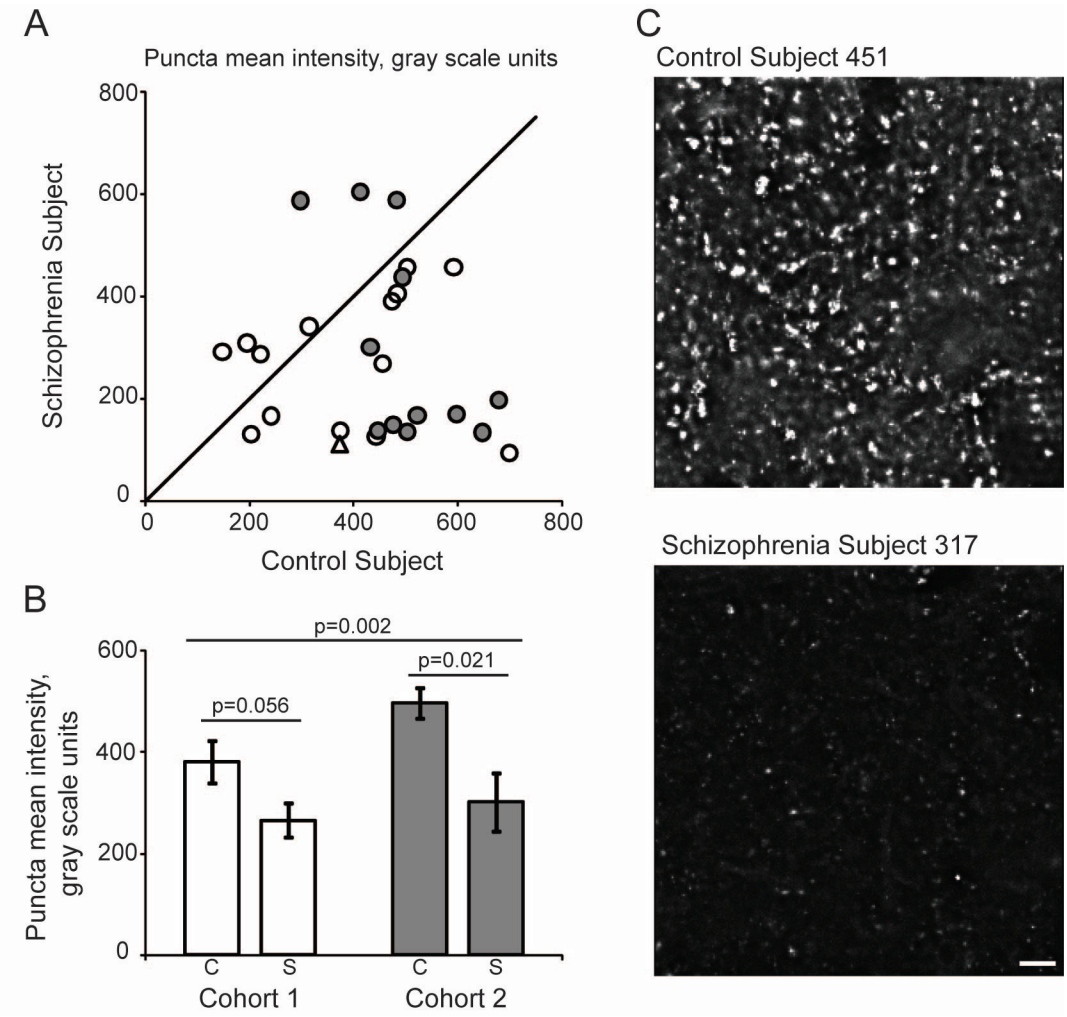

Figure 3.2. Within-bouton level of glutamate decarboxylase 65 protein is reduced in subjects with schizophrenia. (A) Mean puncta fluorescence intensity for each schizophrenia-control subject pair in cohort 1 (open circles and triangle) and cohort 2 (filled circles). Reference line represents schizophrenia = control subject values, where points below the line indicate a pair where control subject > schizophrenia and points above the line indicate schizophrenia > control subject. (B) Diagnostic group mean puncta fluorescence intensity for control (C) and schizophrenia (S) subjects in cohorts 1 (open bars) and 2 (gray bars). Error bars are ± SEM. (C) Representative projection image of glutamate decarboxylase 65-immunoreactive boutons from control subject 451 and schizophrenia subject 317 (cohort 1, pair 9, represented by open triangle in [A]). Scale bar represents 10 μm. Images are displayed across equivalent gray scale ranges.

The reduction of GAD65-IR puncta volume in subjects with schizophrenia relative to normal controls was nearly statistically significant in the primary model ($F_{(1, 26.6)} = 3.75$, $p = 0.063$), and was statistically significant in the secondary model ($F_{(1, 49.6)} = 4.80$, $p = 0.033$; **Figure 3.3B**). This effect was largely driven by the cohort 2 subject pairs in both the primary ($F_{(1, 10.7)} = 11.24$, $p = 0.007$) and secondary ($F_{(1, 17.8)} = 10.72$, $p = 0.004$) statistical models. Estimated mean (95% CI) volumes derived from the primary model were 0.499 (0.484, 0.515) and 0.465 (0.449, 0.481) μm^3 for control subjects and subjects with schizophrenia in cohort 2, respectively, reflecting a 6.8% reduction in subjects with schizophrenia. Because we suspected that the volume decrease in cohort 2 might be driven by the significant decrease in fluorescence intensity, we repeated the primary and secondary MANCOVA models for volume with mean intensity as a covariate, using both cohorts. There was a highly significant effect of intensity (primary model: $F_{(1,655)} = 114.16$, $p < 0.001$; secondary model: $F_{(1,669)} = 102.78$, $p < 0.001$), but the effect of diagnosis on bouton volume was still significant (primary model: $F_{(1, 25.1)} = 8.39$, $p = 0.008$; secondary model: $F_{(1, 44.8)} = 11.16$, $p = 0.002$).

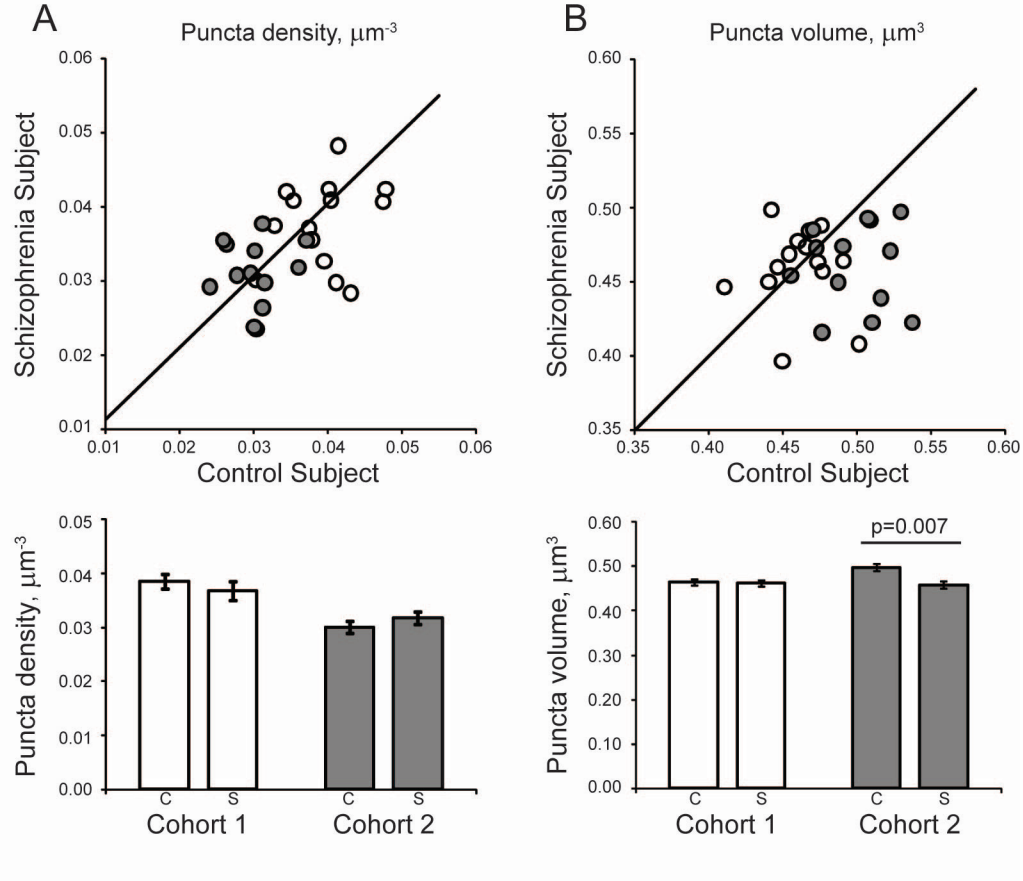

Figure 3.3. Glutamate decarboxylase 65-immunoreactive puncta density and volume in deep layer 3 of primary auditory cortex of subjects with schizophrenia. (A) (Top) Mean puncta density for each schizophrenia-control subject pair in cohort 1 (open circles) and cohort 2 (filled circles). Reference line represents schizophrenia = control subject values, where points below the line indicate a pair where control subject > schizophrenia and points above the line indicate schizophrenia > control subject. (Bottom) Diagnostic group mean puncta density for control (C) and schizophrenia (S) subjects in cohorts 1 (open bars) and 2 (gray bars). (B) (Top) Mean puncta volume for each schizophrenia-control subject pair in cohort 1 (open circles) and cohort 2 (filled circles). Reference line represents schizophrenia = control subject values, where points below the line indicate a pair where control subject > schizophrenia and points above the line indicate schizophrenia > control subject. (Bottom) Diagnostic group mean puncta volume for control (C) and schizophrenia (S) subjects in cohorts 1 (open bars) and 2 (gray bars). Error bars are ± SEM.

3.3.2 Independent living status

We found that the percent reduction in mean GAD65-IR bouton fluorescence intensity relative to matched controls was significantly greater for schizophrenia subjects who were not living independently at time of death than for those who were ($t_{24} = 2.77$, $p = 0.011$; **Figure 3.4**). In contrast, there was no significant relationship between independent living status and the percent changes in GAD65-IR bouton density or volume relative to controls.

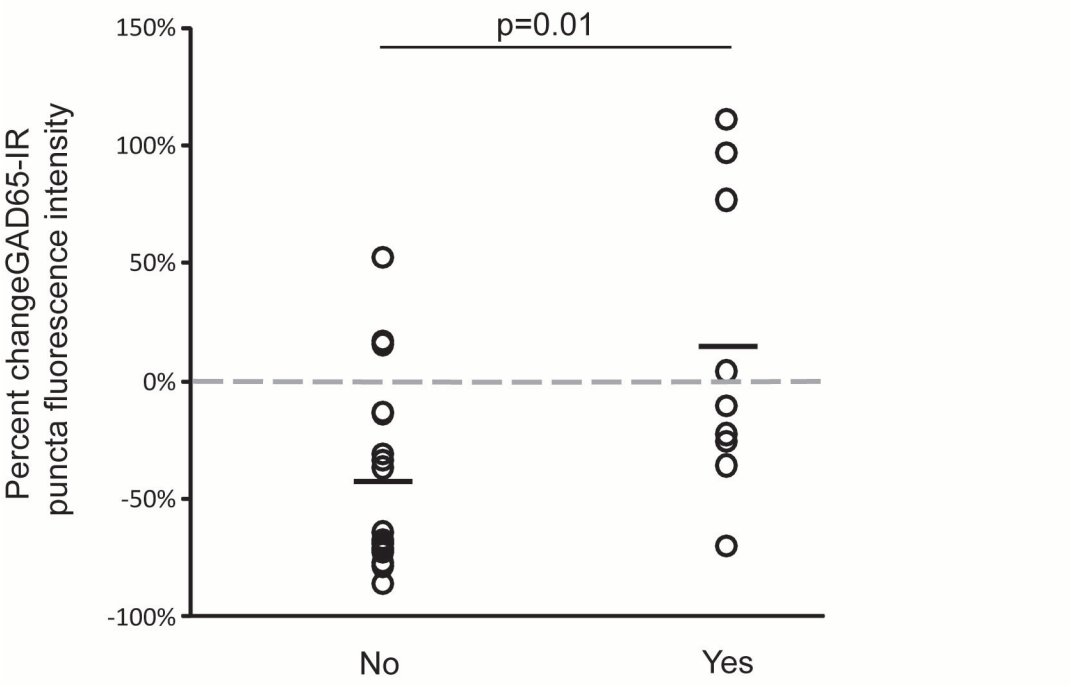

Figure 3.4. Relationship between independent living status of schizophrenia subjects and the reduction in mean glutamate decarboxylase 65-immunoreactive (GAD65-IR) bouton fluorescence intensity. The percent change in GAD65-IR bouton fluorescence intensity in subjects with schizophrenia is significantly greater in pairs where the schizophrenia subject was not living independently at time of death [$t_{(24)} = 2.77$, $p = 0.011$]. Horizontal lines indicate mean pairwise percent change relative to control subjects. Gray dashed line indicates zero percent change. There was no significant relationship between independent living status and percent change in GAD65-IR bouton density [$t_{(24)} = 0.09$, $p = 0.925$] or volume [$t_{(24)} = 1.86$, $p = 0.075$] relative to control subjects (data not shown).

3.3.3 Clinical factors

We tested for associations between GAD65-IR mean bouton density, fluorescence intensity, or volume and a number of clinical factors. We identified a significantly greater percent increase in GAD65-IR bouton density in subjects who were taking benzodiazepines at time of death (See **Appendix B.1** and **Appendix Figure B.2** for details).

3.3.4 Correlation between dendritic spine density and GAD65-IR bouton fluorescence intensity and density in cohort 1 subjects

Given the importance of balanced excitatory and inhibitory neurotransmission in neural processing of auditory stimuli (Wehr and Zador, 2003; Wu et al., 2008), and in modulating neural oscillations (Atallah and Scanziani, 2009), we hypothesized that there are concurrent reductions in inhibitory and excitatory components of primary auditory cortex circuitry. We examined whether GAD65-IR bouton mean intensity was correlated with previously measured spinophilin-IR puncta density in deep layer 3 of primary auditory cortex for cohort 1 subjects (Sweet et al., 2009). We found that GAD65-IR bouton fluorescence intensity is significantly correlated with dendritic spine density in this cohort of subjects ($r = 0.525$, $p = 0.003$; **Figure 3.5A**). The strength of the correlation was observed to be greater for schizophrenia subjects compared to control subjects (Control: $r = 0.379$, $p = 0.162$; Schizophrenia: $r = 0.505$, $p = 0.055$). In addition, we found a significant correlation between the percent changes in GAD65-IR puncta fluorescence intensity and dendritic spine density in schizophrenia subjects ($r = 0.745$, $p = 0.001$; **Figure 3.5B**). Similarly, we observed a correlation between GAD65-IR bouton density and spinophilin-IR spine density ($r = 0.457$, $p = 0.01$; **Appendix Figure B.3**). The strength of this

correlation was also greater for schizophrenia subjects than control subjects (Control: $r = 0.351$, $p = 0.2$; Schizophrenia: $r = 0.583$, $p = 0.02$). Finally, the percent reductions in GAD65-IR boutons and spinophilin-IR spine densities in schizophrenia subjects relative to controls were significantly correlated ($r = 0.718$, $p = 0.003$; **Appendix Figure B.3**).

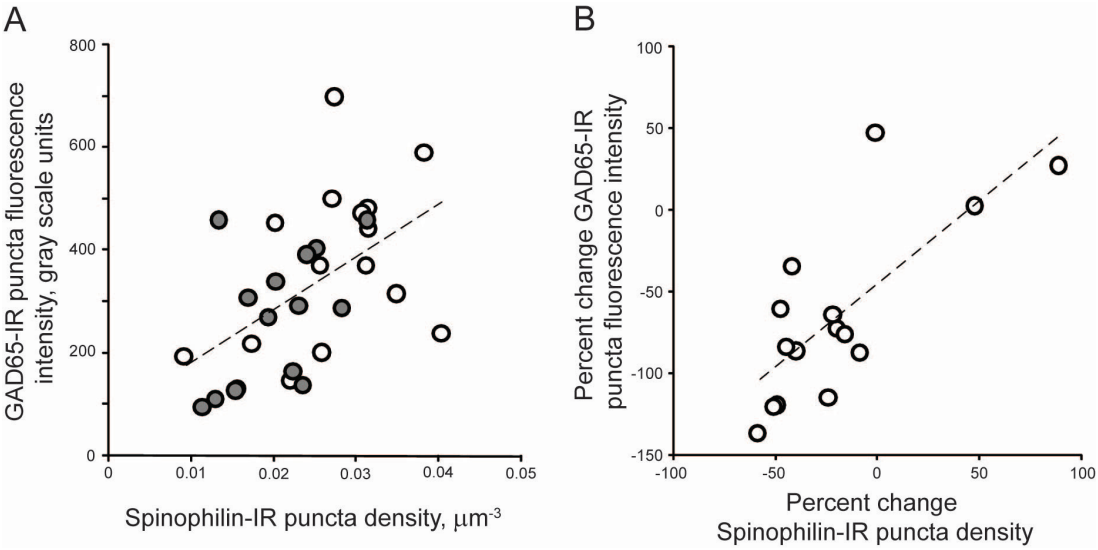

Figure 3.5. Correlations between mean and percent change in glutamate decarboxylase 65-immunoreactive (GAD65-IR) puncta fluorescence intensity and spine density in primary auditory cortex. (A) Mean GAD65-IR puncta fluorescence plotted as a function of spinophilin-immunoreactive (IR) puncta density for each subject in cohort 1. Open circles = control subject, filled circles = schizophrenia subject. Dashed line represents the regression line. (Pearson r = 0.525, p = 0.003). (B) The percent change in GAD65-IR puncta mean fluorescence intensity plotted as a function of the percent change in spinophilin-IR puncta density for pairs in cohort 1 (schizophrenia subjects relative to matched control subjects). Dashed line represents the regression line. (Pearson r = 0.745, p = 0.001).

3.3.5 Estimation of GAD65-IR bouton number in cohort 2 subjects

We were able to estimate the total number of GAD65-IR puncta in primary auditory cortex deep layer 3 for the 12 subject pairs of cohort 2 and found that the absolute numbers of GAD65-IR boutons were not altered in schizophrenia in either the primary ($F_{(1, 10)} = 0.644$, $p = 0.441$) or secondary ($F_{(1, 18)} = 0.065$, $p = 0.802$) ANCOVA models (**Figure 3.6**). Because of the differences in tissue processing methods, we were not able to estimate bouton number in subject pairs from cohort 1.

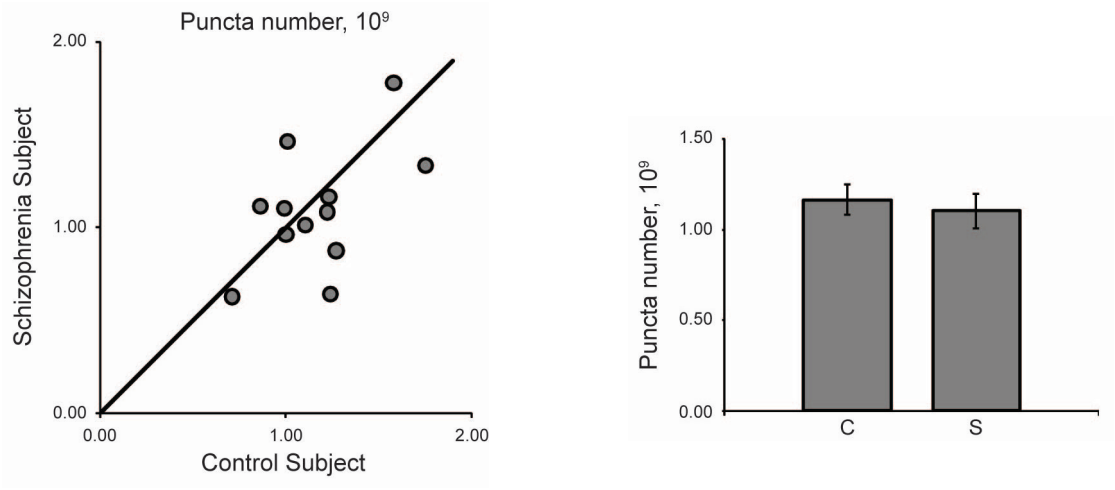

Figure 3.6. Glutamate decarboxylase 65-immunoreactive puncta number in deep layer 3 of primary auditory cortex of subjects with schizophrenia. (Left) Mean puncta number for each schizophrenia-control subject pair in cohort 2. Reference line represents schizophrenia = control subject values, where points below the line indicate a pair where control subject > schizophrenia and points above the line indicate schizophrenia > control subject. (Right) Diagnostic group mean puncta number for control (C) and schizophrenia subjects (S). Error bars are ± SEM.

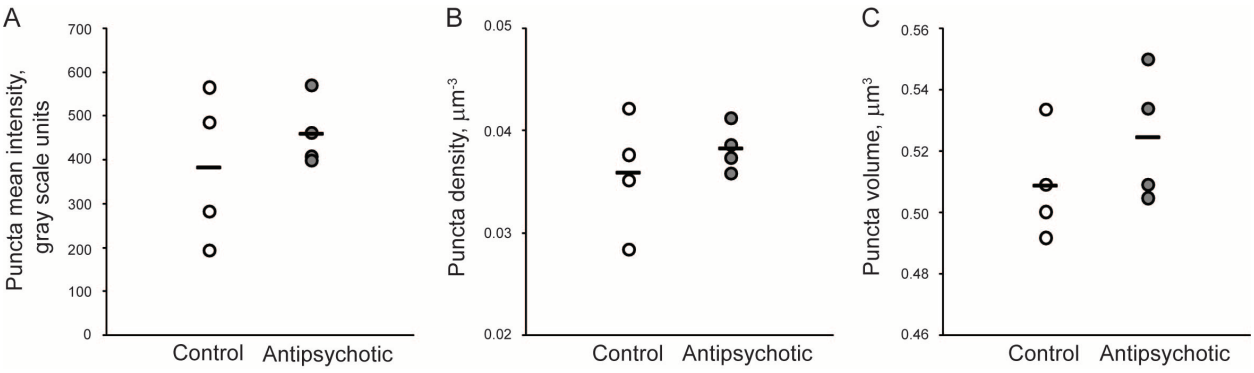

Figure 3.7. Chronic antipsychotic exposure does not alter glutamate decarboxylase 65-immunoreactive puncta mean intensity (A), density (B), or volume (C) in adult male macaques. Horizontal lines indicate group means.

3.3.6 Antipsychotic exposed monkeys

We observed no effect of chronic haloperidol exposure on relative fluorescence intensity ($F_{(1,3)}$=1.72; p=0.281), density ($F_{(1,\ 18.6)}$=0.51; p=0.483), or volume ($F_{(1,\ 2.88)}$=2.82; p=0.195) of GAD65-IR puncta in deep layer 3 of primary auditory cortex (**Figure 3.7**).

3.4 DISCUSSION

We found that GAD65-IR bouton fluorescence intensity was decreased within deep layer 3 in 27 subjects with schizophrenia relative to matched control subjects. Because the intensity data that we collect using our microscopy and image processing methods are linearly related to underlying

object fluorophore content (Fish et al., 2008), we interpret the decrease in bouton fluorescence intensity as a decrease in within-bouton GAD65 protein content. However, caution must be used in interpretation of the magnitude of protein reduction, as the stoichiometry of the binding of this antibody to GAD65 protein in tissue is not known for certain to be linear. The reductions in GAD65-IR bouton fluorescence and decreased spine density were correlated within subjects in the 15 subject pairs for whom both measures were available. Finally, we report that the reductions in GAD65-IR bouton fluorescence intensity were larger in those subjects who were not living independently at time of death.

3.4.1 GAD65 protein studies

The few prior studies that have examined GAD65 protein levels in the cortex of subjects with schizophrenia report mixed results. Assessments of protein by Western blot suggest that GAD65 protein level is unchanged in prefrontal and occipital cortices in subjects with schizophrenia (Guidotti et al., 2000; Dracheva et al., 2004), and one study in temporal cortex reported a non-significant 27% decrease in GAD65 compared to controls (Impagnatiello et al., 1998). Differences between these reports of GAD65 protein levels and our own could be due to cohort-specific differences in subject characteristics such as age and post-mortem interval, but most likely can be attributed to the different methods used. We may have observed a larger reduction in GAD65 protein expression because in contrast to the Western blot studies where GAD65 protein from a less specific region was analyzed, we measured GAD65 protein at its site of action within boutons. For example, in a recent study using a similar approach to assess GAD67 protein, a larger deficit was found within boutons than within total gray matter when both were assessed in the same subjects (Curley et al., 2011). A potential biological explanation for the

discrepancy between total gray matter and within-bouton levels of GAD65 and GAD67 protein is that transport of GAD65/67 protein from the soma to the axon bouton is impaired in subjects with schizophrenia. This could result in relatively normal levels of protein detected unless within-bouton protein levels are examined exclusively. Future immunohistochemistry studies could test this possibility by quantifying GAD65 fluorescence within the somata of inhibitory neurons. Another possible source of discrepancy is that different cortical regions were examined, and reduction of GAD65 protein may not occur universally, but may be more pronounced in auditory cortex. Future studies will be necessary to evaluate whether reduced GAD65 protein within inhibitory boutons is specific to deep layer 3 or is a feature across cortical layers in primary auditory cortex and other regions.

3.4.2 GAD65-IR bouton density, number, and volume

We found that the density of GAD65-IR inhibitory boutons was unaltered in deep layer 3 of primary auditory cortex, despite significantly reduced bouton fluorescence intensity. Our finding that GAD65-IR bouton density is unchanged in schizophrenia agrees with a previous report that GAD65-IR puncta density is unaltered in the anterior cingulate and prefrontal cortices (Benes et al., 2000). A potential difficulty in interpreting a lack of change in bouton density between groups is that gray matter volume, particularly in the STG, is consistently reported to be reduced in schizophrenia (McCarley et al., 1999; Hirayasu et al., 2000; Kasai et al., 2003; Rajarethinam et al., 2004; Salisbury et al., 2007; Takahashi et al., 2009). Therefore, even though we identified no change in bouton density in schizophrenia, it is possible that the number of boutons is reduced, and an accompanying reduction in regional gray matter volume masks this effect when bouton density is calculated—this is known as “the reference trap” (Braendgaard and Gundersen,

1986). The stereological techniques described in Dorph-Petersen et al. (Dorph-Petersen et al., 2009b) that we used to generate the tissue sections for cohort 2 allowed us to systematic randomly sample the entire primary auditory cortex. Our previous study showed no significant reduction in auditory cortex layer 3 gray matter volume in schizophrenia (Dorph-Petersen et al., 2009b). Similarly, using unbiased stereological principles of sampling we estimated the number of GAD65-IR boutons in auditory cortex deep layer 3 for each subject and found that the absolute numbers of GAD65-IR boutons were not altered in schizophrenia.

We identified a reduction in mean bouton volume in subjects with schizophrenia, which was significant within one cohort (cohort 2) of schizophrenia subjects relative to matched controls. Given the difference between control and schizophrenia subject GAD65-IR bouton fluorescence intensity in cohort 2 pairs, we tested whether reduced intensity mediated the reduction in volume. Instead, we found that after correcting for bouton fluorescence intensity the association of reduced GAD65-IR bouton volume with schizophrenia was strengthened. This evidence suggests that the reduction in GAD65-IR bouton volume is not fully attributable to reduced GAD65 fluorescence intensity and may be an effect of schizophrenia. If so, reduced bouton volume may further contribute to inhibitory bouton impairment and lead to reduced inhibitory neurotransmission, as bouton size is positively correlated with the number of active zones (Ruiz et al., 2011; Chen et al., 2011a). However, caution must be used in the interpretation of this finding, as reduced bouton volume in schizophrenia subjects was only observed in one of our two cohorts studied.

3.4.3 Clinical factors

We assessed the association between GAD65-IR bouton alterations and a number of clinical factors, including whether the subject had a diagnosis of schizoaffective disorder or schizophrenia, died by suicide, was living independently at time of death, had a history of cannabis use or alcohol or other substance abuse. We found that the percent reduction in GAD65-IR bouton fluorescence intensity was greater in those subjects who were not living independently at time of death. One study has shown that tone matching ability is particularly impaired in schizophrenia subjects who require long-term residential care (Rabinowicz et al., 2000), and reductions in auditory MMN amplitude are correlated with impairments in daily function in patients (Rasser et al., 2011). Social perception and emotion responsivity are independently correlated with functional outcome in schizophrenia patients (Mathews and Barch, 2010). Taken together, these findings indicate that reduction of GAD65 protein levels within inhibitory boutons, auditory processing, and social and emotional cognition are all associated with poor functional outcome in schizophrenia.

A number of our subjects were taking antipsychotics, benzodiazepines, antidepressants, or anticonvulsant medications at time of death. For a discussion of the association of these medications with GAD65 bouton characteristics see **Appendix B.2 Discussion.**

3.4.4 Implications for regulation of the synthesis of GABA by GAD65 in schizophrenia

GAD65 exists predominantly in the inactive apoenzyme form and readily associates with synaptic vesicle membranes (Chang and Gottlieb, 1988), localizing it to the presynaptic bouton where it is available to synthesize GABA for release. Association of inactive GAD65 with its

cofactor PLP to form the active holoenzyme form of GAD65 is promoted by increased metabolism during periods of synaptic activity (reviewed in (Martin et al., 1991)). GAD65 thus serves as a molecular switch, allowing GABA synthesis to be up-regulated during conditions of high GABA demand, i.e. during periods of high interneuron firing rates (Tian et al., 1999). Impairments in inhibitory transmission during increased neuronal activity have been demonstrated in GAD65 knockout mice, which despite having no difference in baseline levels of GABA (Asada et al., 1996), exhibit impaired neural plasticity (Choi et al., 2002) and behavioral deficits (Kash et al., 1999). Our finding of reduced GAD65 protein within inhibitory boutons in schizophrenia therefore suggests that up-regulation of GABA production would be impaired when interneurons fire at high rates, leading to depletion of GABA and depression of inhibitory synapses under these conditions.

3.4.5 Implications for specific inhibitory neuron populations

Evidence suggests that GAD65 is the predominant GAD isoform expressed in the cannabinoid (CB1) receptor-IR boutons of cholecystokinin (CCK) expressing interneurons, whereas GAD65 and GAD67 are co-expressed in the boutons of parvalbumin (PV) -IR basket cells and GAD67 is the predominant isoform in the axon cartridges of chandelier neurons (Fish et al., 2011). Therefore, reduced GAD65 protein expression in CCK boutons is likely to greatly impair the function of these interneurons. Activating CB1 receptors decreases GABA release from CCK-IR neurons, and disrupts the M100 component of auditory evoked potentials, as well as hippocampal and cortical theta and gamma range oscillatory activity in rats (Hajos et al., 2000). Further, reduced event related gamma activity is observed in chronic cannabis users (Edwards et al., 2009), paralleling electrophysiological disruptions observed in schizophrenia (Javitt et al.,

1994; Kwon et al., 1999b; Brenner et al., 2003; Light et al., 2006; Spencer et al., 2008; Krishnan et al., 2009; Hamm et al., 2011). Decreased GAD65 protein within CCK boutons would reduce GABA available for release from these neurons, which would have a similar effect to that of CB1 receptor agonists, suggesting that such an alteration could at least in part be responsible for the disrupted oscillatory activity and auditory evoked potentials associated with schizophrenia. Reduced GAD65 protein could also impair PV-IR basket cell function. PV-IR basket cells exhibit high firing rates (reviewed in (Markram et al., 2004)), a condition under which GAD65 is thought to be necessary for maintaining adequate levels of GABA needed for release (Tian et al., 1999; Patel et al., 2006). These fast-spiking interneurons are important for modulating the responses of primary auditory cortex pyramidal neurons to auditory stimuli (Wu et al., 2008) and for the induction of gamma oscillations (Cardin et al., 2009; Sohal et al., 2009), which are abnormal in schizophrenia. In contrast, chandelier cells, the terminals of which express predominantly GAD67 (Fish et al., 2011), would probably be less affected by reduced GAD65 protein than PV-IR and CCK-IR interneurons. Taken together, impairment of GABA release as the result of decreased GAD65 protein in CCK-IR and PV-IR boutons may contribute to some features of abnormal auditory cortex function and auditory processing in schizophrenia. Future studies determining whether reduced GAD65 expression is common to all GABAergic boutons in schizophrenia or specific to a certain population of interneurons will provide more information as to how reduced within-bouton expression of GAD65 protein impacts inhibitory neuron circuitry in schizophrenia.

3.4.6 Impaired GAD65-mediated GABA synthesis could disrupt auditory processing

Impaired GABAergic neurotransmission resulting from loss of GAD65 may impair the processing of stimuli in auditory cortex. Altering inhibition impairs the frequency tuning and response properties of auditory cortex neurons (Chen and Jen, 2000; Wang et al., 2000; Wang et al., 2002). An auditory stimulus elicits both excitation and inhibition in auditory cortex which shape the postsynaptic response to the stimulus. Inhibition which roughly balances excitation contributes to the frequency selectivity of pyramidal neurons by scaling down the level of excitation in response to non-characteristic frequencies (Wehr and Zador, 2003) and by narrowing the tuning curve of the postsynaptic response through a lateral inhibition mechanism (Wu et al., 2008). Reduced inhibition caused by reduced GAD65 in schizophrenia may broaden frequency tuning of auditory cortex neurons and thus, impair stimulus discrimination.

Reduced GABA available for release resulting from loss of GAD65 protein could also contribute to alterations in gamma-range aSSRs to modulated tones and noise measured in subjects with schizophrenia (Krishnan et al., 2009; Hamm et al., 2011). Rapid adjustments in levels of inhibition balance large fluctuations in excitation during gamma oscillations and regulate the oscillation frequency (Atallah and Scanziani, 2009; Mann and Mody, 2010). If insufficient GABA is available for release during this process due to reduced GAD65 protein, this could lead to the reductions of gamma band power and phase synchrony in schizophrenia (Krishnan et al., 2009). Interestingly, in human visual cortex, GABA concentration is directly proportional to the frequency of gamma oscillations, and is inversely related to stimulus discrimination threshold (Edden et al., 2009). If the same is true for auditory cortex, reduced GABA synthesis resulting from decreased GAD65 protein may contribute to disruptions in gamma oscillations and auditory discrimination impairments in schizophrenia. However, the

relationship between steady state GABA levels and GAD65 protein remains to be determined, and studies of GABA levels in human cortex in report conflicting findings (Choe et al., 1994; Stanley et al., 1995; Yoon et al., 2010).

3.4.7 Reduced GAD65 protein levels may compensate for reduced excitatory activity

We observed a correlation between GAD65-IR bouton fluorescence intensity and dendritic spine density reductions, a finding that is consistent with other studies which have demonstrated that GAD expression and spine density are often co-regulated in cerebral cortex. Additionally, we found that dendritic spine density and percent reduction were significantly correlated with GAD65-IR bouton density and percent reductions in schizophrenia subjects. Reduced dendritic spine density occurs in multiple cortical regions in schizophrenia (Lewis and Sweet, 2009), and reduced expression of GABAergic markers is also conserved across cortical regions (Lewis et al., 2005; Hashimoto et al., 2008; Fung et al., 2010). Further, correlation between expression levels of excitatory and inhibitory synapse markers in the prefrontal cortex appears to be stronger in schizophrenia subjects than in controls (Fung et al., 2011). We also observed stronger correlations between spine density and both within-bouton GAD65 protein and GAD65-IR bouton density in schizophrenia subjects compared with control subjects. This raises the possibility that reduced inhibition and reduced spine density are related pathologies in schizophrenia.

Several lines of evidence indicate that reducing or disrupting GAD activity can have stability-promoting effects on dendritic spines. Monocular deprivation results in elimination of spines in layer 2/3 of visual cortex, but when GAD65 is disrupted, monocular deprivation-induced loss of spines does not occur (Mataga et al., 2004). Further, GAD65 knockout mice are

reported to have elevated spine density (Mataga et al., 2004), and spine density increases when cultured neurons are exposed to the GAD inhibitor mercaptopropionic acid (Murphy et al., 1998). Conversely, studies using a variety of methods have demonstrated that reducing neuronal activity or sensory input decreases expression of GAD (Hendry and Jones, 1988; Welker et al., 1989; Patz et al., 2003; Hartman et al., 2006). Therefore, our finding of correlated reductions in within-bouton GAD65 protein and spine density would be unlikely to indicate that reduced GAD65 expression causes spine loss in schizophrenia. Instead, reduced excitatory drive from the loss of dendritic spines may lead to a compensatory reduction in GAD65 protein expression. This could be evaluated by determining whether a reduction in within-bouton GAD65 expression occurs subsequent to accelerated loss of spines, e.g. during normal adolescent spine pruning (Huttenlocher, 1979; Rakic et al., 1986) or in animal models of adolescent onset spine reduction (Cahill et al., 2009).

3.4.8 Conclusions

In summary, our study is the first to find that GAD65 protein levels are reduced within GAD65-expressing boutons of primary auditory cortex in subjects with schizophrenia. This reduction may impair inhibitory transmission auditory processing, causing impaired oscillatory activity and disrupting stimulus discrimination. Understanding the cell types in which GAD65 expression is reduced in schizophrenia will be important for the future design of therapies directed at this pathological feature. Similarly, studies that investigate the temporal relationship between GAD65 protein and excessive dendritic spine loss will be important to determine how to best target these features for prevention.

4.0 DEVELOPMENTAL TRAJECTORIES OF EXCITATORY SYNAPTIC STRUCTURES AND WITHIN-BOUTON GAD65 PROTEIN IN MOUSE AUDITORY CORTEX BETWEEN EARLY ADOLESCENCE AND YOUNG ADULTHOOD

Abstract

Schizophrenia onset often occurs during adolescence and young adulthood, leading to the hypothesis that an increase in the normal pruning of excitatory synapses that occurs in the cortex during adolescence contributes to symptom development. Previously, we have identified disruptions of dendritic spines and within-bouton levels of GAD65 protein in the primary auditory cortex of individuals with schizophrenia, suggesting that excitatory and inhibitory synapse pathology could be related. Based on this relationship between alterations of dendritic spines and GAD65 protein levels in schizophrenia, we wanted to determine whether decreases in levels of GAD65 occur subsequent to spine pruning in auditory cortex during adolescence. We used immunohistochemistry and quantitative fluorescence microscopy to measure spines, VGluT1-expressing excitatory boutons and GAD65-expressing inhibitory boutons at 4, 8 and 12 weeks postnatal in auditory cortex of wild type mice and mice lacking kalirin, a protein which is implicated in schizophrenia and is important for adolescent spine development in frontal cortex. We observed reductions in numbers of spines and VGluT1-positive boutons in auditory cortex between early adolescence and young adulthood, consistent with other reports of excitatory

synapse pruning in mice. We observed a decrease in levels of within-bouton GAD65 protein between late adolescence and young adulthood, suggesting that spines and GAD65 protein levels undergo coordinated reductions during adolescence as well as in schizophrenia. Surprisingly, there were only subtle alterations in spines and excitatory boutons in mice lacking kalirin, indicating that molecular regulators of spine pruning may be slightly different in auditory compared to frontal cortex. Future work is necessary to explore whether adolescence represents a developmental window when synapses are vulnerable to schizophrenia pathophysiology as well as accessible to preventative measures.

4.1 INTRODUCTION

The onset of schizophrenia symptoms typically occurs during late adolescence and young adulthood (Tandon et al., 2009), an observation which has led to the hypothesis that abnormal adolescent developmental processes in regions undergoing relatively protracted maturation may contribute to the emergence of schizophrenia symptoms (Feinberg, 1982; McGlashan and Hoffman, 2000). Imaging studies have shown evidence for accelerated gray matter loss around the time of first psychotic episode (Kasai et al., 2003; Pantelis et al., 2007). A key adolescent neurodevelopmental process is the pruning of synapses in the cortex, where synapse density peaks prior to adolescence, then declines during adolescence before reaching adult levels (Huttenlocher, 1979; Rakic et al., 1986; Zecevic et al., 1989; Glantz et al., 2007). Reduced dendritic spine density is a feature of multiple brain regions in schizophrenia, including auditory cortex (Sweet et al., 2009). Abnormal or excessive synapse pruning during adolescence could

cause reduced dendritic spine density and decreased gray matter volume in individuals with schizophrenia (Bennett, 2011).

Schizophrenia is associated with disruptions in both excitatory and inhibitory cortical synapses (Lewis, 2009; Penzes et al., 2013), and alterations in markers for inhibitory neurotransmission are reported in several cortical regions in schizophrenia (Hashimoto et al., 2008). In the primary auditory cortex of subjects with schizophrenia, we have shown that within-bouton protein levels of the 65 kDa isoform of glutamate decarboxylase (GAD65) are reduced, and that this reduction is correlated with reduced dendritic spine density (Moyer et al., 2012) (see chapter 3). This raises the possibility that reduced inhibition and reduced spine density are related features of auditory cortex pathology in schizophrenia. However, evidence for co-existence of excitatory and inhibitory synapse disruption in schizophrenia does not reveal whether a primary reduction in spine density could lead to secondary changes in inhibitory boutons, or vice versa.

GAD65 expression has been shown to be activity dependent (Wei and Wu, 2008). If reduced spine density in individuals with schizophrenia is indicative of altered excitatory circuit activity, expression of GAD65 may be affected as a consequence. Studies have demonstrated that decreased neuronal activity or sensory input are associated with reduced expression of GAD (Hendry and Jones, 1988; Welker et al., 1989; Patz et al., 2003). Thus, dendritic spine loss in auditory cortex in subjects with schizophrenia could precipitate a reduction in within-bouton GAD65 protein. On the contrary, there is a lack of support for the reverse direction and experimental evidence suggests that a primary decrease in GAD65 would be unlikely to cause decreased spine density. For example, it has been shown that GAD65 KO mice, which exhibit decreased inhibitory transmission during sustained neuronal activity (Tian et al., 1999), are

reported to have elevated, rather than reduced, dendritic spine density (Mataga et al., 2004). Also, spine density increases when cultured hippocampal neurons are exposed to mercaptopropionic acid, a GAD inhibitor (Murphy et al., 1998). Together, this suggests that if a causal relationship between reduced spine density and GAD65 expression exists, it is unlikely that reduced GAD65 expression would cause spine loss in individuals with schizophrenia. Rather, reduced spine density in individuals with schizophrenia may lead to a subsequent reduction in GAD65 levels.

Adolescence is a time when a relationship between spines and GAD65 may be particularly dynamic, as this is when pruning of spines occurs. If changes in GAD65 levels occur subsequent to spine pruning during this time, then increased pruning during adolescence may also lead to reduced GAD65 levels in individuals with schizophrenia. Therefore, adolescence may be a period during which preventative interventions to reduce spine loss and inhibitory bouton impairment in auditory cortex could be implemented. However, we must first understand the anatomical and molecular changes of auditory cortex excitatory and inhibitory synapses that result from spine pruning.

The molecular mechanisms regulating excitatory synapse pruning during adolescence in the cortex are largely unknown, although factors involved in regulating spine stability and elimination could potentially be involved (Tada and Sheng, 2006). Knock-out (KO) mice for the gene encoding the protein kalirin have an adolescent-onset deficit in dendritic spine density in frontal cortex (Cahill et al., 2009). Kalirin is a guanine nucleotide exchange factor (GEF) localized to spines and dendrites in the brain, and is responsible for activation of Rho GTPases, such as Rac1 (Penzes and Jones, 2008), which increases dendritic spine stability and spine growth (Yoshihara et al., 2009a). In the auditory cortex of subjects with schizophrenia, protein

levels of the kalirin-9 isoform are increased (Deo et al., 2012), while studies in frontal cortex suggest that kalirin levels may be reduced (Hill et al., 2006; Rubio et al., 2012). Therefore, we sought to determine whether kalirin loss has an effect on adolescent synapse pruning in auditory cortex of mice, as it does in frontal cortex.

In the present study, we hypothesized that within-bouton GAD65 protein levels decline subsequent to adolescent spine pruning in the primary auditory cortex. To evaluate this, we quantified the trajectories of excitatory and inhibitory synapse components in the superficial layers of the mouse primary auditory cortex between early adolescence and young adulthood. To model the effects of a genetically mediated dendritic spine disruption during adolescent auditory cortex development, we also quantified markers of spines, and excitatory and inhibitory boutons across adolescence in the kalirin KO mouse. We found that levels of GAD65 protein within inhibitory boutons decrease between late adolescence and young adulthood in wild type mouse auditory cortex, subsequent to the onset of excitatory synapse pruning. Kalirin KO mice did not demonstrate reduced spine number compared to WT mice, and demonstrate no decrease in spine number between early adolescence and young adulthood, suggesting that adolescent spine pruning is disrupted in the absence of kalirin. These findings provide clues to the molecular processes that may be important for normal adolescent development of excitatory and inhibitory synapses in auditory cortex and how disruptions in adolescent synapse pruning can contribute excitatory and inhibitory synapse pathology in schizophrenia.

4.2 MATERIALS AND METHODS

4.2.1 Experimental animals

Experiments were carried out using kalirin knockout (KO) and wild type (WT) mice. KO mice were generated as described previously by inserting the neomycin resistance cassette in place of exons 27-28, the site of the GEF1 domain (Cahill et al., 2009). Mice were rederived on the C57Bl/6NJ background at The Jackson Laboratory. Heterozygous breeders were crossed to generate KO and WT experimental animals. Animals were identified with metal ear tags and tail snip DNA samples were obtained for genotyping prior to weaning at approximately postnatal day 24. Only male animals were included in experiments because of the effects of estrogen on dendritic spine density and GAD protein (Murphy et al., 1998), and its interactions with kalirin (Ma et al., 2011). Animals were housed in standard microisolator caging in groups of up to 4, maintained on a 12 hour light / dark cycle (lights on at 7 a.m.) and were provided with food and water *ad libitum*. Cohorts of mice were used for behavioral testing (see chapter 5) and then sacrificed at postnatal day 31, 58, or 85 +/- 4 days (hereafter referred to as 4, 8, and 12 weeks of age). These ages correspond in general to early adolescence, late adolescence, and young adulthood in rodents (Spear and Brake, 1983; Spear, 2000; Kilb, 2012). All experimental procedures were approved by the Institutional Animal Care and Use Committee at the University of Pittsburgh.

4.2.2 Tissue generation

Mice were weighed and deeply anaesthetized with Nembutal (150 mg/kg) and transcardially perfused with ice cold normal saline. Brains were rapidly extracted, bisected, and left hemispheres were immersed in 4% paraformaldehyde for 48 hours at 4ºC. Hemispheres were allowed to sink in a 30% sucrose solution before being coronally sectioned at 40 µm on a cryostat. Sections were stored in ethylene glycol cryoprotectant at -30ºC until use. Brains from 6 animals per genotype x age group were analyzed.

4.2.3 Auditory cortex mapping

Every sixth section was stained for Nissl substance using a 0.1% thionin solution in acetate buffer to identify primary auditory cortex and laminar boundaries. Animals were blocked into groups of six (one genotype x age group member per block) and coded during mapping so that the investigator was blind to genotype and age group. Area Au1 was identified on the Nissl sections using a mouse brain atlas (Paxinos and Franklin, 2004). Using StereoInvestigator (MicroBrightField), a contour outline of cortical layers 2 through 4 was drawn, and the volume of these layers in left hemisphere Au1 was estimated for each subject (**Figure 4.1A).** Three auditory cortex containing sections per subject were randomly selected, and adjacent sections were used for immunohistochemistry.

4.2.4 Immunohistochemistry

All sections were processed in a single immunohistochemistry assay run. Sections were rinsed in 0.1 M phosphate buffer, and incubated in 1% $NaBH_4$ in phosphate buffer for 30 minutes to reduce tissue autofluorescence. Sections were thoroughly rinsed and incubated for 3 hours in blocking buffer containing 5% normal goat serum, 1% bovine serum albumin, 0.1% lysine, 0.1% glycine, and 0.3% Triton-X. The sections were incubated overnight at 4ºC in blocking buffer containing unconjugated goat anti-mouse monovalent Fab-fragment IgG to reduce goat anti-mouse secondary antibody labeling of blood vessels. Sections were then incubated for 48 hours in blocking buffer containing the primary antibodies: anti-spinophilin antibody raised in rabbit at 1:1,000 (Millipore, Billerica, MA), anti-VGluT1 antibody raised in guinea pig at 1:250 (Millipore, Billerica, MA), anti-GAD65 antibody raised in mouse at 1:250 (Millipore, MAB351). Following the primary incubation, sections were rinsed and incubated for 24 hours at 4ºC in secondary antibody solution in blocking buffer: Alexa Fluor 488 conjugated anti-rabbit antibody raised in goat at 1:500 (Invitrogen, Carlsbad, CA), biotinylated anti-guinea pig antibody raised in goat at 1:200 (Vector Laboratories, Burlingame, CA), Alexa Fluor 405 conjugated anti-mouse antibody raised in goat at 1:500 (Invitrogen, Carlsbad, CA). Sections were rinsed again and incubated in 1.5 µl/ml Alexa Fluor 568 conjugated phalloidin and 1:500 dilution of Alexa Fluor 647 conjugated streptavidin for 24 hours at 4ºC. Finally sections were rinsed again, mounted on gel coated slides, allowed to dry for 1 hour at room temperature, rehydrated for 10 min and coverslipped with Vectashield Hard Set mounting medium (Vector Laboratories, Burlingame, CA).

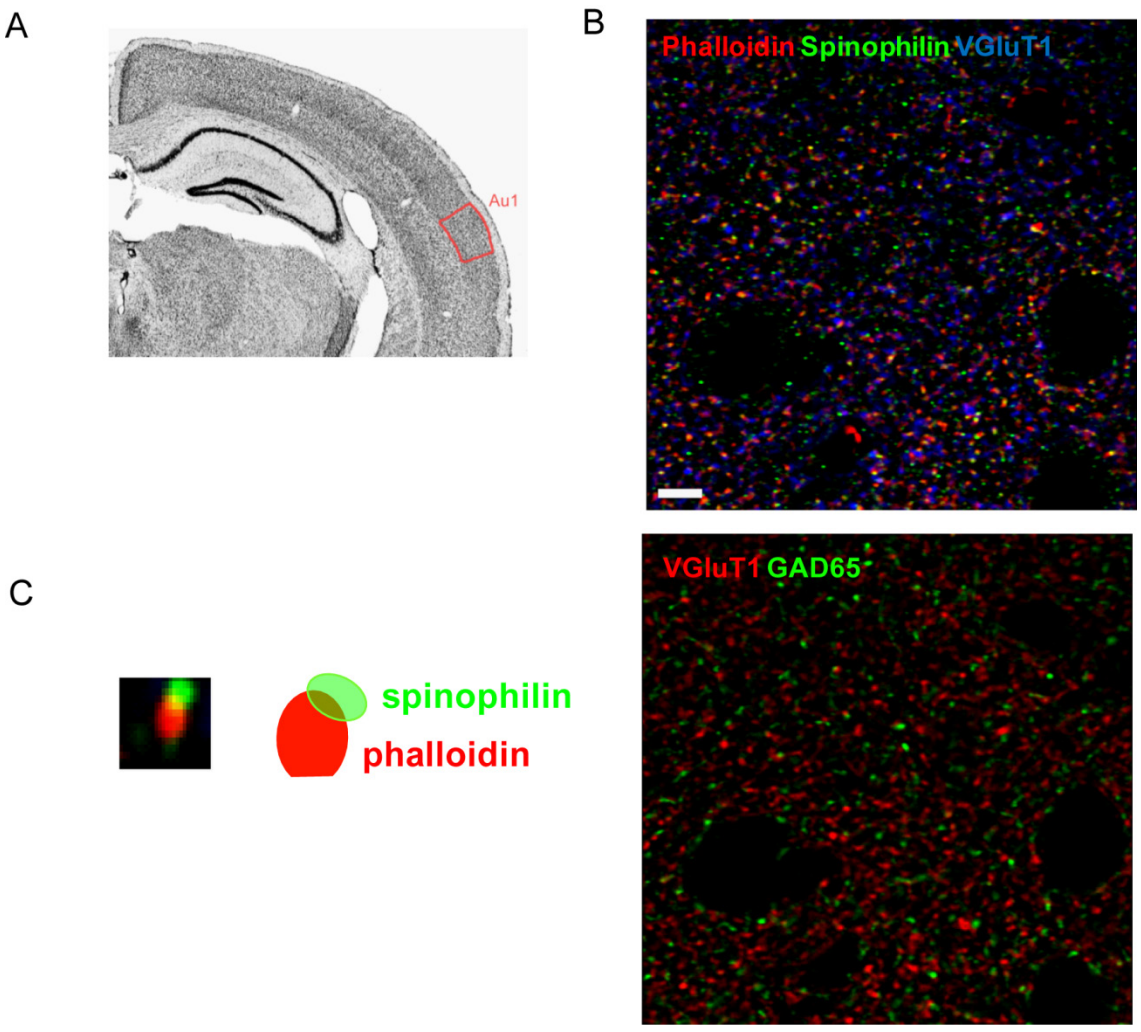

Figure 4.1. Example of contouring of layers 2 through 4 of mouse area Au1, blind deconvolution of immunoreactive puncta, and schemating depicting overlap of phalloidin and spinophilin labels for dendritic spine quantification. A.Coronal section stained for Nissl substance. An outline including cortical layers 2, 3, and 4 of area Au1 is shown in red. B. Projection image taken from a confocal Z stack after blind deconvolution, showing puncta fluorescently labeled to identify f-actin (red), spinophilin (green), and VGluT1 (blue) in the left image, and VGluT1 (red) and GAD65 (green) in the right image. Scale bar is 10 µm. C. Enlargement of presumptive spine from image in B and illustration of overlap between spinophilin and f-actin immunoreactivity. At least one voxel of overlap was required to include an immunoreactive object as a spine in our analysis.

4.2.5 Microscopy

Image collection was carried out using an Olympus (Center Valley, PA) BX51 WI upright microscope equipped with an Olympus DSU spinning disk confocal, super corrected Olympus PlanAPON 1.42 N.A. oil immersion objective, ORCA-R2 CCD camera (Hamamatsu, Bridgewater, NJ), MBF CX9000 front-mounted digital camera (MicroBrightField, Inc., Natick, MA), BioPrecision2 XYZ motorized stage with linear XYZ encoders (Ludl Electronic Products, Ltd., Hawthorne, NY), excitation and emission filter wheels (Ludl Electronic Products, Ltd., Hawthorne, NY), Sedat Quad 89000 filter set (Chroma Technology Corp., Bellows Falls, VT) and Lumen 220 metal halide lamp (Prior Scientific, Rockland, MA). The microscope was controlled using StereoInvestigator (MicroBrightField, Inc.) and SlideBook (Intelligent Imaging Innovations, Denver, CO) software. Confocal sampling sites were generated based on the Au1 layer 2-4 contour total areas for each mouse such that approximately 15 sites were sampled per animal. For imaging, animals were randomly blocked into groups of six, with one mouse from each genotype/age group combination in each block. At each sampling site, total tissue thickness was measured. Image stacks were collected with a step size of 0.25 μm between Z axis planes in the stack, starting from 10 μm below the tissue surface closest to the coverglass and stepping up until the tissue surface was reached, yielding a 10 μm thick (Z axis depth) stack comprised of 40 individual 2-dimensional planes. Collected image planes were 512 x 512 pixels, and exposure times for 568, 488, and 405 channels were held constant. Due to a gradual decline of 647 channel fluorescence over the course of imaging, exposure time in the 647 channel was increased halfway through imaging (for animals in blocks 4 through 6). Therefore, statistical models involving 647 channel (VGluT1-immunoreactive objects) included exposure time as a factor.

Mean site thickness did not differ by genotype ($F_{1,30} = 0.380$; $p = 0.542$) but did differ by age ($F_{1,30} = 5.206$; $p = 0.011$) so mean site thickness was included in statistical models as a covariate.

4.2.6 Image processing and analysis

Collected image stacks were post-processed offline, using SlideBook and Automation Anywhere software (Automation Anywhere, Inc., San Jose, CA) to automate keystrokes and increase image processing efficiency. Intensity levels attributable to electrical fluctuations of the camera sensor was subtracted from each channel, by determining the mean intensities (gray scale values) for each channel with identical exposure and capture settings as the tissue image stacks, and subtracting these values from all pixel intensities in the image stacks. Images were then deconvolved using the autoquant (blind deconvolution) algorithm in SlideBook (see **Figure 4.1B** for example of deconvolved micrographs). Finally, a transformation was applied to each channel to enhance detection of object edges during the automated segmentation process. Gaussian filters with two different standard deviations ($\sigma = 2$ and $\sigma = 0.7$) were applied to each channel, and the intensities of the channel transformation with the larger standard deviation ($\sigma = 2$) were subtracted from the channel intensities transformed with the smaller ($\sigma = 0.7$), to yield a new channel used in segmentation. This deconvolved and edge-enhanced image stack was then subject to intensity segmentation coupled with morphological selection using our iterative masking approach (Fish et al., 2008). For each channel, the initial intensity threshold was determined in advance by the experimenter, and with each subsequent iteration the intensity threshold was increased. For the 405 channel, the initial intensity threshold was set to 150, increased by 50 gray levels until 500 was reached, increased by 100 until 1000 was reached, increased by 500 until 3000 was reached, and increased by 1000 until 8000 was reached. For the

488 channel, the initial intensity threshold was set to 400, increased by 50 until 1000 was reached, increased by 100 until 2000 was reached, increased by 500 until 5000 was reached, and increased by 1000 until 14000 was reached. For the 568 channel, the initial intensity threshold was set to 100, increased by 50 until 500 was reached, increased by 100 until 2000 was reached, increased by 500 until 3000 was reached, and increased by 1000 until 8000 was reached. For the 647 channel, the initial threshold was set at 200, increased by 50 until 500 was reached, increased by 100 until 2000 was reached, increased by 500 until 3000 was reached, and increased by 1000 until 8000 was reached. After each segmentation step, mask objects were size gated (405, 568, and 647: 0.03 to 1 μm^3; 488: 0.03 to 0.5 μm^3) were selected and merged with the mask generated in the prior segmentation step. Immunoreactive (IR) puncta data (mean intensity, mean volume) were extracted from these image stacks using the generated mask to identify objects of interest. To obtain accurate intensity information, object intensities were derived from the deconvolved, but not Gaussian-filtered channels.

One limitation of using phalloidin to label dendritic spines is that it has a high affinity for the f-actin found in astrocytic end feet surrounding blood vessels (Capani et al., 2001) as well as that found in dendritic spines (Fifkova and Delay, 1982). Therefore, not all phalloidin-positive objects in our images are dendritic spines, as blood vessels are reported to account for 4% of the total cortical volume in mice (Schuz and Palm, 1989). Similarly, although spinophilin is highly concentrated in dendritic spines (Ouimet et al., 2004), it is also localized to the dendrites of parvalbumin interneurons (Muly et al., 2004). Therefore, we required that phalloidin-positive objects quantified as dendritic spines have at least one voxel of overlap with the spinophilin-IR object mask, and that the spinophilin-IR objects have at least one voxel of overlap with the

phalloidin-positive object mask. This increases the likelihood that we are quantifying dendritic spines, as they are f-actin enriched objects expressing spinophilin protein (**Figure 4.1C**).

Density of mask objects was determined by taking the total number of mask objects for each animal, divided by the sum of the total volumes of each sampling site. The volume of each sampling site was (256 pixels x 0.108 μm/pixel)^2 or 2,823 μm^2 multiplied by the height of the disector (10 μm). Puncta number for each animal was then generated using the N_v x V_{ref} approach by multiplying the density by the estimated volume of left hemisphere area Au1 layers 2-4.

4.2.7 Statistical analyses

ANOVA models with age and genotype as between subjects factors were used to examine group differences in body weight and gray matter volume of area Au1 layers 2 through 4. ANCOVA models with genotype as between subjects factors and mean site thickness as a covariate were used to test for age and genotype differences in spine and bouton number, mean fluorescence intensity, and volume. In VGluT1-IR puncta models, 647 channel exposure time was also included as a fixed factor in the model, to control for an adjustment made in imaging this channel halfway through the animals. Genotype comparisons between age groups, and age comparisons within genotypes were carried out using Bonferroni correction for multiple comparisons.

4.3 RESULTS

4.3.1 Au1 layer 2, 3 and 4 cortical volume reduced in kalirin KO

Unexpectedly, we did not find a significant overall effect of age on Au1 layers 2, 3 and 4 volume ($F_{(2,30)} = 1.884$; $p = 0.169$). As the kalirin KO is reported to have reduced dendritic spine density (Cahill et al., 2009) in frontal cortex at 12 weeks of age, and neuropil including excitatory synapses comprises 85% of the mouse cortical volume, we wanted to determine whether gray matter volume of the region of interest was reduced. The estimated volume of cortical layers 2 through 4 of left hemisphere Au1 was reduced in the KO compared to the WT animals ($F_{(1,30)} = 4.561$; $p = 0.041$; **Figure 4.2A**). Body weight was also significantly reduced in the KO compared to the WT ($F_{(1,30)} = 5.090$; $p = 0.032$; **Figure 4.2B**); however, there was an age by genotype interaction ($F_{(2,30)} = 3.329$; $p = 0.049$), revealing that weight is not significantly reduced in KO until 12 weeks. This is consistent with impaired growth in another kalirin KO model (Mandela et al., 2012). However, we found that body weight does not predict regional volume overall ($F_{(1,35)} = 0.777$; $p = 0.384$) or within any individual age group (4 week: $F_{(1,11)} = 0.106$; $p = 0.752$; 8 week: $F_{(1,11)} = 0.027$; $p = 0.874$; 12 week: $F_{(1,11)} = 2.364$; $p = 0.155$). This suggests that reduced regional volume in the KO is not solely attributable to smaller body size. To account for the difference in regional volumes between genotypes, we report number rather than density of pre and post synaptic components.

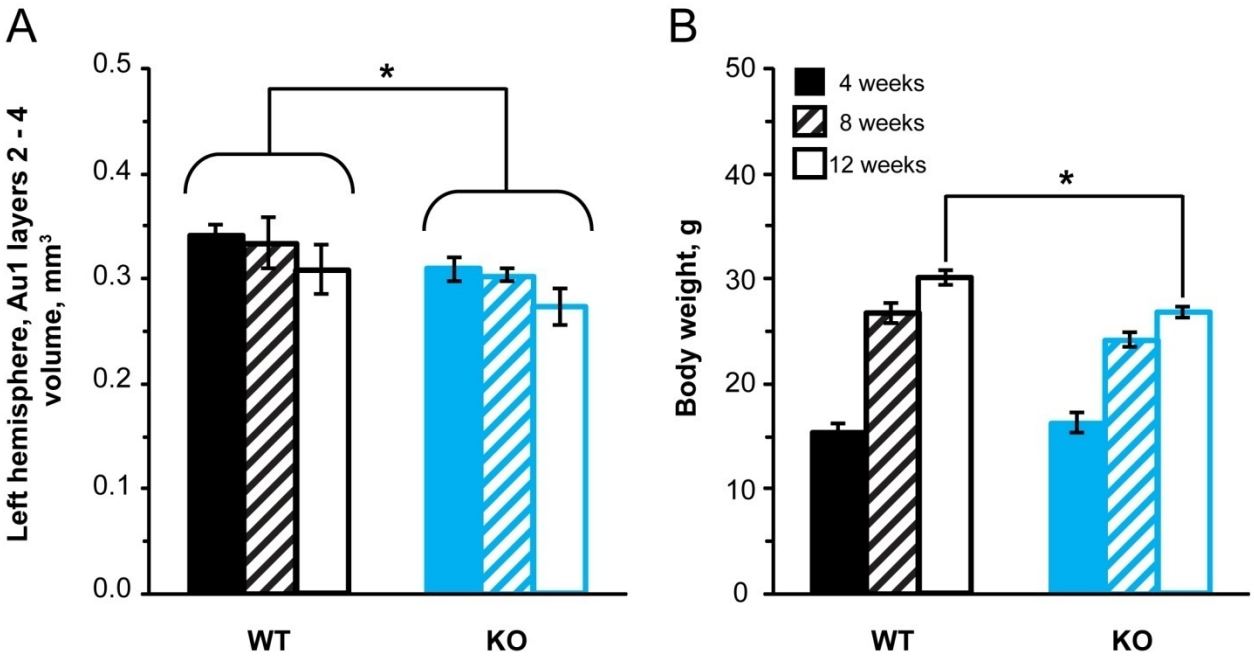

Figure 4.2. Superficial auditory cortex gray matter volume and body weight in kalirin KO and WT mice. A. Estimated gray matter volume of area Au1 layers 2 through 4 across adolescence in WT and kalirin KO mice. KO mice have reduced regional volume overall relative to WT. *$p < 0.05$. B. Weight of WT and KO mice across adolescence. 12 week old KO mice are smaller than 12 week old WT mice. *$p < 0.05$. N = 6 per age x genotype group. Error bars are ± SEM.

4.3.2 Numbers of presumptive spines and intracortical excitatory boutons decrease between early adolescence and early adulthood

To identify dendritic spines in the region of interest, we used fluorophore conjugated phalloidin, a mushroom toxin that binds f-actin. To enhance specificity for spines, we quantified phalloidin-labled puncta that exhibit overlap with spinophilin-immunoreactive (-IR) puncta. We found that numbers of phalloidin and spinophilin co-labled puncta significantly decreased between 4 and 12 weeks of age ($F_{(2,29)} = 6.720$; $p = 0.004$; **Figure 4.3A**). The same pattern was observed when we examined numbers of spinophilin-IR puncta that overlap with phalloidin-labeled puncta (**Appendix Figure C.1**). We examined numbers of VGluT1-IR puncta to determine if presynaptic components of excitatory synapses are also decreasing in number during this time. We saw that the number of VGluT1-IR puncta decreases between 4 and 12 weeks ($F_{(1,28)} = 6.191$; $p = 0.006$; **Figure 4.3B**).

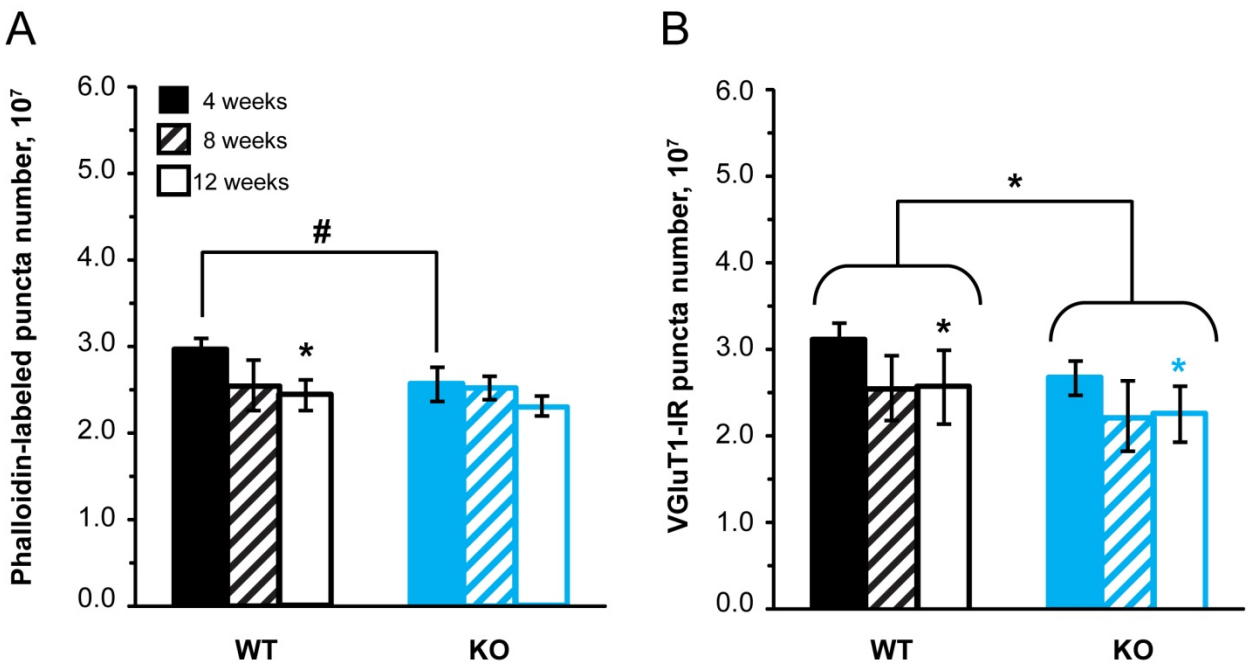

Figure 4.3. Evidence for 15-20% reduction of excitatory synapse number between early adolescence and young adulthood in superficial primary auditory cortex. A. The numbers of phalloidin-labeled puncta decrease between 4 and 12 weeks of age in WT mice. There is a trend-level reduction in puncta number in the KO compared to the WT at 4 weeks of age. *$p < 0.05$ vs 4 week old WT. #$p < 0.10$ 4 week old WT vs KO. B. The numbers of VGluT1-IR puncta decrease between 4 and 12 weeks in the WT and KO mice, and overall the number of VGluT1-IR puncta is reduced in the KO. *$p < 0.05$ vs 4 week old, asterisk color denotes genotype. Brackets and asterisk indicate $p < 0.05$ overall effect of genotype. N = 6 per age x genotype group. Error bars are ± SEM.

4.3.3 Spine number is not reduced in auditory cortex of kalirin KO mice

Spine density is reported to be lower in frontal cortex of young adult but not pre-adolescent kalirin KO mice (Cahill et al., 2009). We wanted to determine whether this also occurs in auditory cortex. There was a trend toward an overall reduction of phalloidin-labled puncta number in the KO mice ($F_{(1,29)} = 3.470$; $p = 0.073$), and we observed a trend toward a reduction in puncta number in the KO at 4 weeks compared to the WT ($F_{(1,29)} = 2.995$; $p = 0.096$). The developmental effect between the two genotypes was similar, in that there was a trend toward an effect of age on puncta number in the KO ($F_{(2,29)} = 2.928$; $p = 0.069$) and a significant effect of age in the WT ($F_{(2,29)} = 4.929$; $p = 0.014$; **Figure 4.3A**).

However, when we examined presumptive excitatory boutons, we found that kalirin KO mice had a reduced number of VGluT1-IR puncta compared to the WT ($F_{(2,28)} = 4.747$; $p = 0.038$; **Figure 4.3B).** The decrease in puncta number with age was significant in both genotypes: (WT: ($F_{(2,28)} = 3.569$; $p = 0.042$; KO ($F_{(2,28)} = 3.729$; $p = 0.037$)), suggesting the decrease in VGluT1-IR puncta with age occurs to a similar extent in both genotypes.

4.3.4 Changes in GAD65-IR puncta occur between late adolescence and early adulthood and are disrupted in kalirin KO mice

We found significant reductions in GAD65-IR puncta fluorescence intensity ($F_{(2,29)} = 10.769$; $p < 0.001$) and GAD65-IR puncta number between 4 and 12 weeks of age ($F_{(2,29)} = 5.439$; $p = 0.010$; **Figure 4.4A**). Specifically, the reductions in fluorescence intensity ($p=0.001$) and puncta number ($p=0.035$) were significant between 8 and 12 weeks of age.

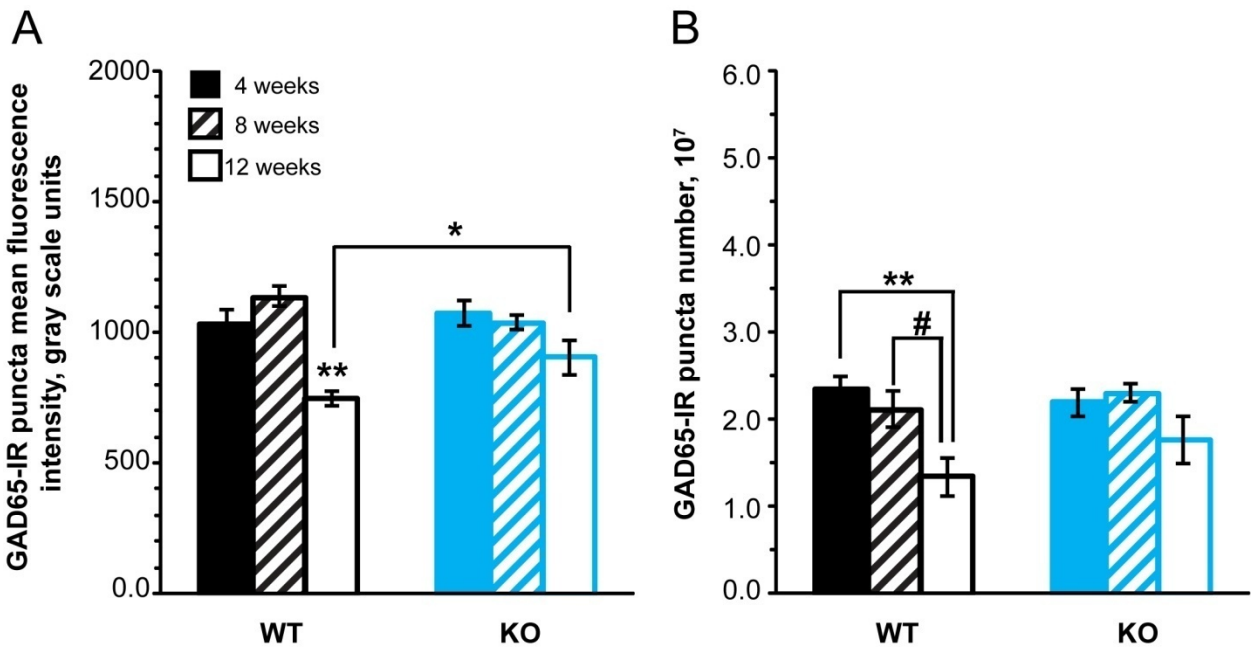

Figure 4.4. Changes in characteristics of GAD65-expressing boutons across adolescence and early adulthood. A. The mean GAD65 fluorescence intensity within GAD65-IR puncta significantly decreases between 8 and 12 weeks in WT mice. The mean GAD65 fluorescence intensity within GAD65-IR puncta is significantly greater in KO compared to WT at 12 weeks of age. *$p < 0.05$ KO vs WT at 12 weeks, **$p < 0.01$ vs 4 and 8 week old WT. B. The number of GAD65-IR puncta decreases between 4 and 12 weeks in the WT mice. #$p < 0.10$; **$p < 0.01$. N = 6 per age x genotype group. Error bars are ± SEM.

The mean GAD65-IR puncta fluorescence intensity was not different overall between KO and WT mice ($F_{(1,29)} = 0.776$; $p = 0.386$; **Figure 4.4B**). The decrease in GAD65 fluorescence with age was highly significant in the WT ($F_{(2,29)} = 12.633$; $p < 0.001$) but not in the KO ($F_{(2,29)} = 2.272$, $p = 0.121$). Further, the mean GAD65-IR puncta fluorescence intensity is significantly greater in the KO than the WT at 12 weeks ($F_{(1,29)} = 5.024$, $p = 0.033$), suggesting increased within-bouton GAD65 protein in young adult KO mice relative to WT. Numbers of GAD65-IR puncta did not differ between kalirin KO and WT mice ($F_{(1,29)} = 0.730$; $p = 0.400$). However, numbers of GAD65-IR puncta decreased with age in the WT ($F_{(2,29)} = 5.694$; $p = 0.008$) and did not decrease in the KO ($F_{(2,29)} = 1.519$; $p = 0.236$).

4.3.5 Within-spine spinophilin and f-actin fluorescence intensity

Spinophilin is a postsynaptic excitatory synapse protein that is prevalent in dendritic spines and serves a variety of structural and functional roles (reviewed in (Sarrouilhe et al., 2006)). Importantly, it has been shown that cortical spinophilin protein levels decline during adolescence in rat (Allen et al., 1997), and that spinophilin may play a role in spine elimination (Feng et al., 2000). Therefore, we wanted to know how levels of spinophilin protein per spine change during this time period. We found a significant reduction in spinophilin fluorescence intensity within phalloidin-labeled spines over adolescence ($F_{(2,29)} = 16.410$; $p < 0.001$).

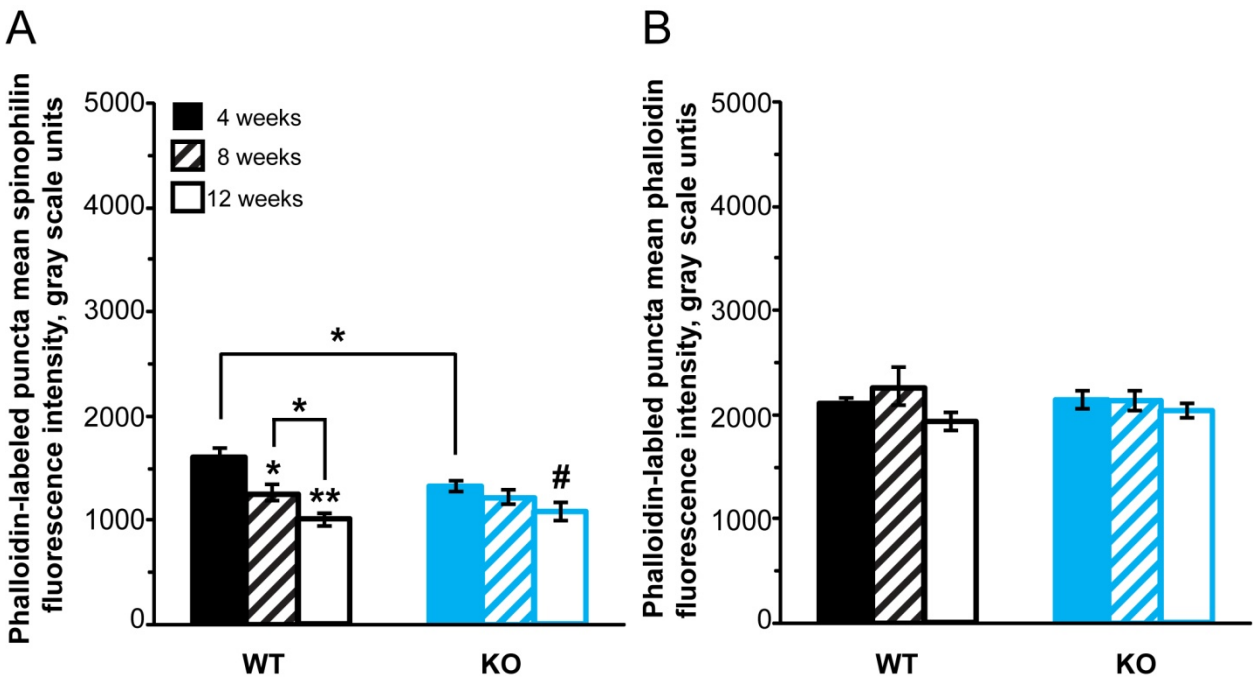

Figure 4.5. Changes in characteristics of dendritic spines across adolescence and early adulthood. A. The mean spinophilin-label fluorescence intensity within phalloidin-positive objects significantly decreases across adolescence in WT mice and reaches trend level significance between 4 and 12 weeks in KO mice. The mean spinophilin fluorescence intensity within phalloidin-labeled objects is significantly reduced in KO compared to WT at 4 weeks of age. *$p < 0.05$, **$p < 0.01$, vs 4 week old WT; #$p < 0.10$ vs 4 week old KO. B. The mean fluorescence intensity of the phalloidin label within phalloidin-positive objects does not change across adolescence. N = 6 per age x genotype group. Error bars are ± SEM.

The reduction in mean puncta spinophilin fluorescence intensity with age could be attributed to the increase in spine volume that we observed between 4 and 12 weeks (**Figure C.1**), without a corresponding increase in the size of the spinophilin immunoreactive portion of the spine. However, we found that the sum spinophilin intensity of all voxels in the spine also decreased with the same pattern as the mean intensity ($F_{(2,29)} = 13.716$; $p < 0.001$), whereas if the reduction in intensity was solely attributable to increasing spine volume, this would have increased or remained unchanged.

We hypothesized that kalirin loss could disrupt spinophilin levels within dendritic spines as the two proteins have been shown to interact (Penzes et al., 2001). Although we saw no overall difference in spinophilin fluorescence intensity between KO and WT mice ($F_{(1,29)} = 2.200$; $p = 0.149$) (**Figure 4.5A**), there was a trend toward an age by genotype interaction effect ($F_{(2,29)} = 3.073$; $p = 0.062$), and we found that spinophilin fluorescence intensity was significantly lower in the KO compared to the WT at 4 weeks of age ($F_{(2,29)} = 7.703$; $p = 0.010$). The reduction in within-spine spinophilin fluorescence intensity with age was significant in the WT mice ($F_{(2,29)} = 17.870$; $p < 0.001$) and was trend-level in the KO ($F_{(2,29)} = 3.143$; $p = 0.058$). In the WT mice, within-spine spinophilin fluorescence intensity decreased between 4 and 8 weeks, as well as between 8 and 12 weeks.

We examined the mean fluorescence intensity attributable to the phalloidin label to determine whether f-actin content of spines changes across adolescence or is altered in the absence of kalirin. However, we saw no change in puncta fluorescence intensity over adolescence ($F_{(2,29)} = 0.554$; $p = 0.581$; **Figure 4.5B**) and no effect of genotype ($F_{(1,29)} = 0.066$, $p=0.800$).

4.4 DISCUSSION

Here we report decreases in numbers of dendritic spines, intracortical excitatory boutons, and GAD65-expressing inhibitory boutons in mouse auditory cortex between early adolescence and young adulthood (summarized in **Figure 4.6**). In WT mice, we found that spine numbers decreased between early adolescence and young adulthood, while levels of GAD65 protein within inhibitory boutons decreased between late adolescence and young adulthood, suggesting that excitatory synapse pruning begins first and is followed by a subsequent reduction in GAD65 protein levels. This provides evidence that spines and GAD65 protein levels are co-regulated in development, and lends insight into potential developmental origins of the correlation between spine density and GAD65 protein levels in the auditory cortex of individuals with schizophrenia.

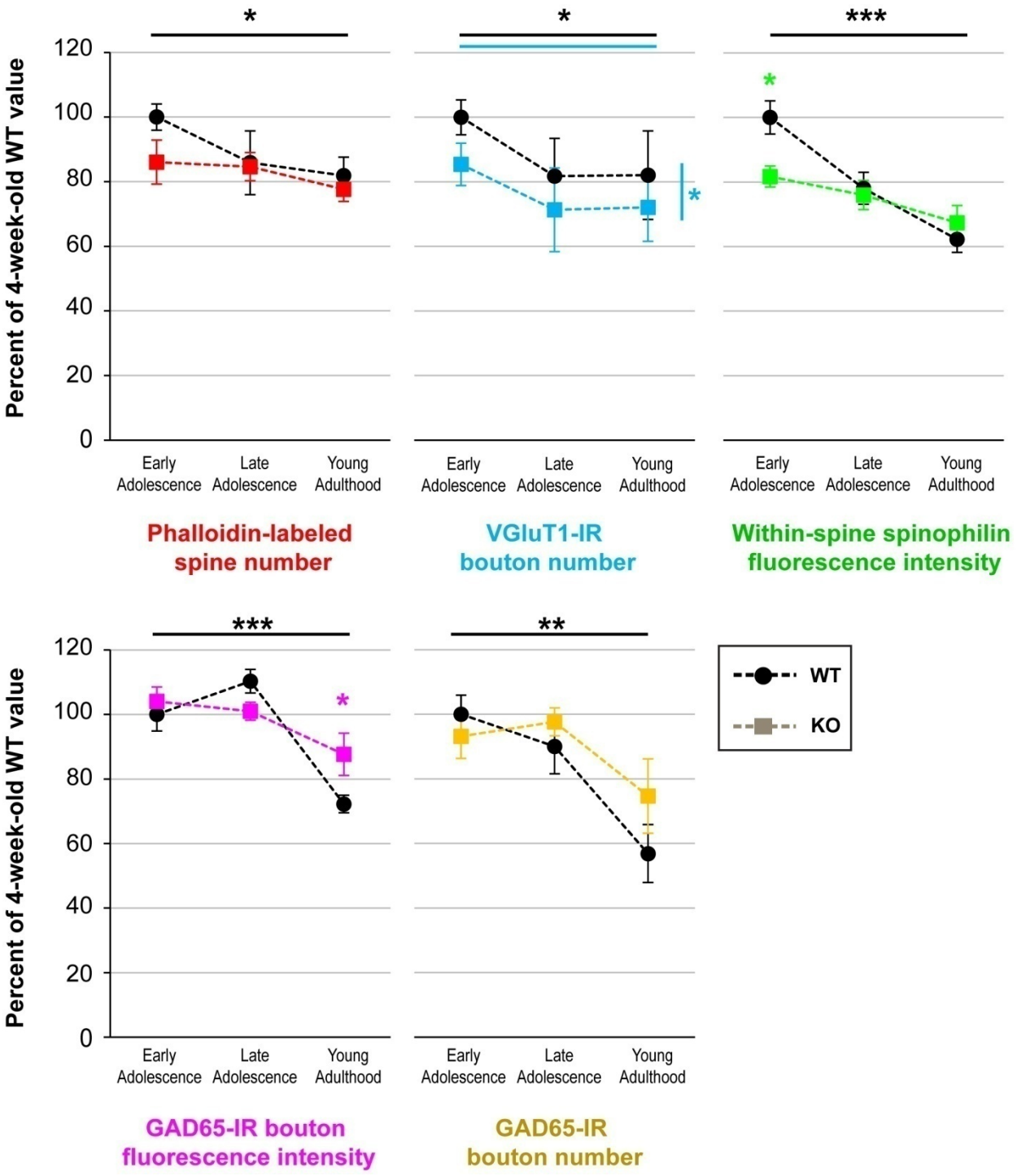

Figure 4.6. Summary of developmental trajectories, age and genotype effects for spines and intracortical excitatory bouton numbers, within-spine spinophilin protein, within-bouton GAD65 protein, and GAD65-expressing inhibitory bouton number. Values expressed as a percentage of the 4 week old WT values. Dotted lines connecting data points are used to illustrate developmental trajectories, but all markers were assessed in

independent groups of animals. Age effects denoted by horizontal lines above graph, with genotype indicated by line color. Genotype effects indicated by colored astericks, vertical line indicates overall genotype effect. *$p < 0.05$; **$p < 0.01$; ***$p < 0.001$.

4.4.1 Pre- and postsynaptic components of excitatory synapses are pruned in auditory cortex between early adolescence and young adulthood

We found that numbers of dendritic spines and VGluT1-IR intracortical excitatory boutons in layers 2, 3 and 4 of mouse auditory cortex decline by 15 to 20% between early adolescence and young adulthood. This is consistent with spine changes in mouse frontal cortex during this developmental period (20% decrease; (Zuo et al., 2005)) and likely represents adolescent excitatory synapse pruning as reported in other mammalian species (Huttenlocher, 1979; Rakic et al., 1986; Zecevic et al., 1989; Glantz et al., 2007). It is possible that excitatory synapse numbers continue to decline after 12 weeks of age; in mouse frontal cortex synapse numbers are found to stabilize by 4 months (Alvarez and Sabatini, 2007). Therefore, future studies should be done to determine whether spine and excitatory bouton numbers in auditory cortex continue to decline at ages later than 12 weeks.

4.4.2 GAD65 protein within inhibitory boutons decreases between late adolescence and young adulthood in auditory cortex

Our results indicate that within-bouton GAD65 protein decreases between late adolescence and young adulthood in auditory cortex. Importantly, our findings suggest that pre- and postsynaptic components of excitatory synapses are pruned between early adolescence and young adulthood,

while levels of GAD65 protein within inhibitory boutons decrease between the end of adolescence and young adulthood. This indicates within-bouton GAD65 protein reduction occurs subsequent to the onset of spine pruning during adolescence, and provides a neurodevelopmental context for the reduced within-bouton GAD65 protein observed in auditory cortex of subjects with schizophrenia.

Few studies have examined levels of GAD65 protein during adolescent development. GAD65 immunoreactivity in the rat primary somatosensory cortex increases slowly between postnatal day (P) 6 and P33 (Kiser et al., 1998). Xu et al. (Xu et al., 2010) examined protein levels of GAD65 in the rat auditory cortex and found an increase across postnatal development; however, the oldest age examined in the study was P56 (8 weeks), corresponding to the end of adolescence, whereas we also examined 12 week old young adult animals. GAD65 protein levels in human visual cortex also peak relatively late, at approximately age 20 (Pinto et al., 2010). However, in visual cortex, GAD65 levels slowly declined through old age, whereas we observed a more dramatic reduction between late adolescence and young adulthood.

Down-regulation of GAD65 protein during normal adolescent development could be a mechanism reducing the likelihood of spine elimination toward the end of adolescent spine pruning. GAD65 KO mice show impaired long term depression (LTD) (Choi et al., 2002) a plasticity mechanism that favors spine shrinkage and elimination (Bosch and Hayashi, 2012). Spine elimination in visual cortex in response to monocular deprivation does not occur in GAD65 KO mice (Kanold et al., 2009), suggesting that loss of GAD65 protects against plasticity-induced spine loss. Lower levels of within-bouton GAD65 protein in auditory cortex of subjects with schizophrenia may then be a compensatory response to excessive spine pruning during adolescence. The mechanisms regulating GAD65 expression are not yet fully understood,

but transcription is influenced by CREB-mediated BDNF signaling (Sanchez-Huertas and Rico, 2011) and also through epigenetic control (Zhang et al., 2011). Interestingly, BDNF levels in the cortex peak during adolescence and decline between 2 and 4 months of age in rats (Katoh-Semba et al., 1997) and there is some evidence that BDNF levels are abnormal in schizophrenia (reviewed in (Green et al., 2011)).

A potential confounding factor in our study is that the C57Bl/6 background is associated with young adult onset high frequency hearing loss, which could impact GAD expression in the auditory cortex. C57Bl/6 mice show substantial loss of cochlear hair cells by 12 weeks of age (Spongr et al., 1997), and begin to exhibit high frequency hearing loss beginning between 12 and 16 weeks of age, and remapping of frequency responsiveness in auditory cortex occurs at the same time (Willott et al., 1993). Induced high-frequency hearing loss has been shown to reduce GAD65 expression in areas of auditory cortex responding to high frequencies (Yang et al., 2011). However, another study reports increased GAD immunoreactivity following induction of hearing loss around the time of hearing onset (Sarro et al., 2008). Future studies should evaluate GAD65 protein levels between late adolescence and young adulthood in a strain with no known hearing loss during this time, such as the CBA/CaJ strain, to determine if the reduction in GAD65 protein is a feature of adolescent development or a consequence of peripheral hearing impairment.

We also identified a substantial decrease in GAD65-IR bouton number between late adolescence and adulthood. This is consistent with findings in rat visual cortex, where the number of type II synapses, which would include inhibitory synapses, decreases substantially between P28 and P90 (Blue and Parnavelas, 1983). A small decrease in symmetric synapse density is also reported during this time period in mouse somatosensory cortex (De Felipe et al., 1997). However, another report in rat somatosensory cortex indicates that inhibitory synapse

numbers do not decrease between postnatal days 30 and 60 (Micheva and Beaulieu, 1996). Yet, it may be that the reduction in inhibitory bouton number occurs later than P60 (approximately 8 weeks) which was the oldest age examined, as our data suggest that the reduction occurs primarily between 8 and 12 weeks of age. In general, most studies in primate cortex indicate that inhibitory synapses do not undergo pruning during adolescence. In monkey prefrontal cortex, parvalbumin-immunoreactive puncta density increases during adolescence (Erickson and Lewis, 2002). However, densities of parvalbumin and GABA transporter (GAT-1) labeled cartridges of chandelier neurons are reported to decrease over adolescence (Anderson et al., 1995), though this may be attributable to developmental changes in markers, rather than loss of synapses (Lewis and Gonzalez-Burgos, 2008). In the present study, it is possible that the decrease in within-bouton GAD65 protein led to reduced detectability of boutons, causing the apparent decrease in number. Future studies using alternative bouton inhibitory synapse markers, such as GAT-1 or postsynaptic $GABA_A$ receptor subunits, should be done to clarify the developmental trajectory of inhibitory synapse number in auditory cortex between early adolescence and young adulthood.

It is important to keep in mind that reduction in the number of GAD65-IR boutons between early adolescence and young adulthood does not necessarily indicate a reduction in the total population of inhibitory boutons, as we did not quantify inhibitory boutons that express only the 67 kDa isoform (Fish et al., 2011). Future studies are needed to determine how GAD67-expressing boutons and within-bouton GAD67 protein change in auditory cortex during this time. Also, future studies will be necessary to determine if the reduction in within-bouton GAD65 protein that occurs between late adolescence and young adulthood is specific to a

particular population of GABAergic interneurons, as this will provide insight into how function of different interneuron subtypes changes during late adolescence and young adulthood.

We found that within-spine spinophilin protein content decreases by about 30% between early adolescence and young adulthood. This is consistent with the reported decrease in spinophilin protein in rat total cortex homogenate between the third postnatal week and adulthood (Allen et al., 1997). Spinophilin plays a role in the PSD as a scaffolding protein, and interacts with a host of molecular factors involved in regulating spine function, such as protein phosphatase 1 (PP1) and f-actin (reviewed in (Sarrouilhe et al., 2006)). Spinophilin has been shown to be important for spine stability and formation, as well as long term depression (LTD) (Feng et al., 2000). If LTD contributes to spine elimination during adolescence (Selemon, 2013), and spinophilin plays a role in LTD, then higher within-spine spinophilin protein content earlier in adolescence could promote LTD-mediated spine elimination, while reduction in spinophilin protein over the course of adolescence may increase spine stability and slow down the process of spine elimination toward the end of adolescence and young adulthood.

4.4.3 Effects of kalirin loss on development of excitatory and inhibitory synapse components in auditory cortex between early adolescence and young adulthood

Previous work has found that protein levels of the kalirin-9 isoform are elevated, and other isoforms are unchanged, in the primary auditory cortex of subjects with schizophrenia (Deo et al., 2012). Therefore, the kalirin KO does not serve as a model of auditory cortex disruption in schizophrenia, but can provide insight into the roles of kalirin in the auditory cortex during adolescent development and in disease. In frontal cortex, dendritic spine density is no different between KO and WT mice prior to adolescence, but is significantly reduced in the KO by young

adulthood (Cahill et al., 2009). In contrast, there was no deficit in spine number in the superficial auditory cortex of kalirin KO mice. Our findings suggest that there may be differences in molecular factors important for regulating frontal and auditory cortex spines during adolescence. Future studies should determine whether distributions of other GEFs (Rossman et al., 2005) differ between frontal and auditory cortices and if so, can compensate for loss of kalirin in the auditory cortex. It is also possible that kalirin may have different functional roles in dendritic spine formation and stability in the primary auditory cortex compared to the frontal cortex. The kalirin KO also did not exhibit evidence of significant reduction in spine number between early adolescence and young adulthood. Numbers of spines were about 15% lower at early adolescence compared with wild type mice, although this was only a statistical trend. By late adolescence and young adulthood, numbers of spines in the KO were comparable to the WT. This is likely due to the different trajectories, where spine number decreases in the WT between early adolescence and young adulthood but does not change in the KO. Our results suggest that although there is no overall effect of kalirin loss on spine number in the auditory cortex, there may be subtle changes that alter spine pruning during adolescence in KO mice.

We did see that kalirin KO mice exhibit overall reduced numbers of VGluT1-IR boutons. This is consistent with *in vitro* work showing that transfection of cultured hippocampal neurons with kalirin-7 targeting shRNA leads to a reduction in the number of VGluT1-IR puncta (Ma et al., 2011). Our findings suggest that overall numbers of intracortical excitatory synapses may be reduced in auditory cortex of kalirin KO mice. Further, numbers of VGluT1-IR boutons decreaed between early adolescence and young adulthood in the KO as well as the WT mice. It is worth noting that the decrease in numbers of VGluT1-IR boutons between early adolescence and young adulthood in the KO were no different from WT, while the KO showed no significant

change in numbers of spines during this time. This finding suggests the possibility that pre- and postsynaptic components of excitatory synapses are pruned independently during adolescence. In the auditory cortex of individuals with schizophrenia spine density is reduced while excitatory boutons are unchanged (Chapter 2), which represents the opposite, but still discordant, relationship that we observed in the kalirin KO. Therefore, the kalirin KO may provide an opportunity to model the effects of disconnect between spine and excitatory bouton changes in auditory cortex of subjects with schizophrenia.

Kalirin protein appears to be necessary for the decrease in within-bouton GAD65 levels and number of GAD65-IR puncta between the end of adolescence and young adulthood. *In vitro* transfection of hippocampal interneurons with exogenous kalirin-7 reduces GAD65 immunoreactivity (Ma et al., 2011). Our findings support the opposite relationship, where loss of endogenous kalirin protein leads to a relative increase, or a failure to decrease, levels of GAD65 protein. The effects of kalirin on GAD65 protein are likely mediated by loss of kalirin at postsynaptic sites of excitatory synapses onto GABAergic interneurons, as kalirin is expressed in both glutamatergic and GABAergic neurons. In a global knockout model, it is difficult to tease apart whether the failure to downregulate GAD65 in young adulthood is attributable to kalirin at excitatory synapses onto interneuron dendrites versus changes in global circuit activity caused by loss of kalirin. We may gain more insight into this issue by studying mice with an interneuron-specific knockdown of kalirin, using a mouse line such as the parvalbumin-Cre line to restrict loss of kalirin to parvalbumin-expressing interneurons.

Spinophilin is known to interact with kalirin *in vitro* (Penzes et al., 2001), and consistent with this observation, we found that that spinophilin protein levels within spines are reduced in the KO at 4 weeks. The fact that we saw no alteration in spinophilin protein levels at 8 or 12

weeks suggests that kalirin is not necessary to maintain spinophilin in spines after 4 weeks of age, or other factors are able to compensate for kalirin loss in this regard. For example, spinophilin associates with Tiam1 (Buchsbaum et al., 2003), another Rac-GEF. Future work should investigate whether spinophilin protein levels in the auditory cortex of the kalirin KO fail to undergo upregulation during postnatal development (Allen et al., 1997), or develop normal levels followed by an earlier or accelerated decrease in within-spine protein levels.

4.4.4 Conclusions

In order to design preventative measures to mitigate spine and GAD65 reductions in auditory cortex of schizophrenia patients, we first need to understand whether one feature occurs as a consequence of the other. Here we report evidence that dendritic spine and excitatory bouton numbers decrease in mouse auditory cortex between early adolescence and young adulthood, with a subsequent reduction of within-bouton levels of GAD65 protein occurring between late adolescence and young adulthood. This supports the idea that the GAD65 protein deficit in schizophrenia is a consequence of dendritic spine loss in auditory cortex, and further suggests a developmental window when GAD65 protein reduction may occur. Our findings also suggest different roles of kalirin in regulating stability of dendritic spines during adolescence in frontal and auditory cortices. Together, these results enhance our understanding of regulation of excitatory and inhibitory synapses in auditory cortex during adolescence. Further investigation is needed to understand the molecular factors influencing development of excitatory and inhibitory synapses during adolescence, and how these factors contribute to the pathophysiology of schizophrenia.

5.0 DEVELOPMENT OF GAP-MEDIATED PREPULSE INHIBITION OF THE ACOUSTIC STARTLE REFLEX ACROSS ADOLESCENCE IN MICE

Abstract

Auditory sensory processing impairments in individuals with schizophrenia may underlie some symptoms and contribute to poor disease outcomes. We have reported alterations in primary auditory cortex synapses in subjects with schizophrenia. It has been suggested that abnormal synapse refinement in individuals with schizophrenia during adolescence could contribute to these alterations. In the mouse auditory cortex, we have observed that numbers and molecular features of excitatory and inhibitory synapses change between early adolescence and young adulthood. Therefore, we sought to characterize how auditory cortex function changes during adolescence in mice, and in kalirin KO mice that demonstrate disrupted excitatory and inhibitory synapse development during this time period. We used silent gap-prepulse inhibition of the acoustic startle reflex (gap-PPI), to assess auditory cortex function, as evidence has shown that gap-PPI depends on the integrity of the auditory cortex. To determine if changes in gap-PPI could be attributable to auditory cortex function and not a consequence of maturation of other PPI circuit components, we also measured noise-prepulse mediated PPI (noise-PPI). Finally, to determine whether observed developmental changes in gap-PPI might reflect non-specific consequences attributable to the relatively early onset of high frequency hearing loss evident in

some inbred mouse strains, we also examined gap-PPI in 3 mouse strains with differing temporal patterns of high frequency hearing loss. We observed an increase in gap-PPI between early and late adolescence in WT mice. Kalirin KO mice exhibited detectable gap-PPI responses, but did not show any increase between early adolescence and young adulthood. Gap-PPI responses increased during adolescent development in normal hearing CBA/CaJ mice and in C57Bl/6J mice, which exhibit young adult onset high-frequency hearing loss. In contrast, DBA/2J mice, which exhibit high-frequency hearing loss by early adolescence, showed a loss of gap-PPI responses by early adulthood. Our findings indicate that normal development leads to improvement in gap-PPI responses during adolescence. The timing of this improvement, and the lack of improvement in the kalirin KO mice, suggest excitatory synapse pruning in the auditory cortex may contribute to the improvement in gap processing, as kalirin KO mice do not demonstrate pruning of auditory cortex spines during adolescence.

5.1 INTRODUCTION

Individuals with schizophrenia exhibit auditory processing impairments that may contribute to deficits in verbal and social cognition, negative symptoms and ultimately poor disease outcome (Rabinowicz et al., 2000; Javitt, 2009). Excitation and inhibition in auditory cortex are important in generating the electrophysiological measures of auditory processing that are impaired in schizophrenia (Javitt et al., 1996; Krishnan et al., 2009), and excitatory and inhibitory synapse abnormalities contribute to auditory cortex pathology (Moyer et al., 2012; Moyer et al., 2013) (see chapters 2 and 3). Accelerated thinning of auditory cortex gray matter occurs around the time of schizophrenia onset in adolescence and young adulthood (Pantelis et al., 2007), when

synaptic pruning takes place in the cortex (Huttenlocher, 1979; Rakic et al., 1986; Zecevic et al., 1989; Glantz et al., 2007). Postmortem studies of auditory cortex of individuals with schizophrenia indicate that both spines and within-bouton GAD65 protein levels are reduced (Sweet et al., 2009; Moyer et al., 2012). In mouse auditory cortex, spine pruning occurs between early adolescence and young adulthood (Chapter 4), and within-bouton levels of GAD65 protein decrease between the end of adolescence and young adulthood. This suggests that excitatory and inhibitory synapses in auditory cortex continue to develop during adolescence and early adulthood, and their development may be disrupted in schizophrenia. A better understanding of the functional development of auditory cortex associated with adolescent excitatory and inhibitory synapse maturation may lead to development of tests for abnormal development of auditory cortex circuitry that could eventually be implemented in early schizophrenia diagnosis or prevention.

Detection of silent gaps embedded in noise depends in part on auditory cortex function. Bilateral silencing of the cortex with KCl (Ison et al., 1991) and more specifically, bilateral lesions of the auditory cortex (Bowen et al., 2003) impairs silent gap detection, while responses to noise offset and noise pulses are unaffected. Behavioral approaches for assessing silent gap detection utilizing prepulse inhibition of the acoustic startle reflex (PPI) have been used to evaluate auditory processing in mice (Truong et al., 2012). PPI can be used as a readout to assess stimulus detection without training or conditioning (Fitch et al., 2008). PPI occurs when a brief, non-startling stimulus (the prepulse) precedes and attenuates the response to a startle eliciting stimulus (Hoffman and Searle, 1965) which is typically a loud noise burst. Paradigms utilizing noise prepulses of increasing intensity over a low level background noise are used to assess PPI as a measure of sensorimotor gating (Swerdlow et al., 2001). Studies have shown that

while PPI responses to silent gap "prepulses" embedded in noise (gap-PPI) are impaired when the auditory cortex is compromised, PPI responses to noise-intensity prepulses (noise-PPI) remain intact (Ison et al., 1991; Bowen et al., 2003). This suggests that auditory cortex plays a role in gap-PPI, and gap-PPI may be an indicator of whether auditory cortex circuitry is functioning normally.

Silent gap detection improves over adolescence in rats (Friedman et al., 2004; Sun et al., 2008; Sun et al., 2011), suggesting that it may be a useful assessment of auditory cortex maturation during this developmental period, though it is not yet known if silent gap detection improves during adolescence in mice. We have found that kalirin KO mice exhibit subtle disruptions in adolescent development of auditory cortex synaptic components (see Chapter 4). If normal development of synaptic components is important for the maturation of gap-PPI responses, then gap-PPI responses might be abnormal in kalirin KO mice during this time period.

Assessment of silent gap detection has a great deal of translational relevance, as gap detection plays a role in speech comprehension (Elangovan and Stuart, 2008), and is impaired in subjects with schizophrenia (Thonnessen et al., 2008). Currently, a number of genetic mouse models of various aspects of schizophrenia neuropathology exist (O'Tuathaigh et al., 2007). Gap-PPI could be used to determine how schizophrenia-relevant genetic manipulations impact auditory processing in mice. However, a confounding factor of many genetic mouse models is the incidence of high-frequency hearing loss in several strains, including the popular C57Bl/6 strain background (Mikaelian, 1979). High frequency components of the carrier noise in which the silent gaps are embedded have been shown to be important for gap-PPI responses in mice (Radziwon et al., 2009). It is not known if gap-PPI responses differ between different inbred

strains commonly used as genetic backgrounds for disease models, particularly in those with pre-adolescent or young adult onset high frequency hearing loss.

In the present study, we ask whether gap-PPI responses improve over adolescence in mice, whether loss of kalirin is associated with alterations in gap-PPI responses, and whether gap-PPI during adolescence and young adulthood differs between different inbred strains with varying degrees of high frequency hearing loss. We found that gap-PPI responses increase in WT mice over adolescence, but not in mice lacking kalirin. This was not attributable to a general PPI increase, as noise-PPI responses did not increase during this time. Gap-PPI responses did not improve between adolescence and young adulthood, and in fact were reduced in adulthood in DBA/2J mice, which demonstrate high-frequency hearing loss beginning at about 4 weeks of age. Together, our findings suggest that increased gap-PPI responses in mice over adolescence could be an indicator of functional maturation of auditory cortex synapses. Importantly, gap-PPI responses vary by strain, which underscores the importance of considering strain background when evaluating genetic models of schizophrenia.

5.2 MATERIALS AND METHODS

5.2.1 Experimental animals

Experiments were carried out using kalirin knockout (KO) and wild type (WT) mice. KO mice were generated as described previously by inserting the neomycin resistance cassette in place of exons 27-28, the site of the GEF1 domain (Cahill et al., 2009). Mice were rederived on the C57Bl/6NJ background at The Jackson Laboratory. Heterozygous breeders were crossed to

generate KO and WT experimental animals. Only male animals were included in experiments to avoid effects of estrogen and estrous phase on prepulse inhibition of acoustic startle (Koch, 1998; Charitidi et al., 2012). Animals were maintained on a 12 hr light / dark cycle (lights on at 7 am) and were provided with food and water *ad libitum*. Mice were used for behavioral testing beginning at postnatal day 28, 55, or 82 +/- 4 days (hereafter referred to as 4, 8, and 12 weeks of age). Each mouse was tested at only a single age.

For comparison of inbred strains, male CBA/CaJ, C57Bl/6J, and DBA/2J mice were obtained from the Jackson Laboratory at 3, 7, and 11 weeks of age +/- 3 days. Animals were housed 4 per cage and remained undisturbed for 5 days before behavioral testing started to allow them to acclimate to the animal facility. Four animals of each strain/age combination underwent behavioral testing at a time in each cohort, for a total of 16 animals per age/strain group (N = 15 in the 4 week-old CBA/CaJ group). Mice were tested at only one age. All experimental procedures were approved by the Institutional Animal Care and Use Committee at the University of Pittsburgh.

5.2.2 Auditory testing

Mice received two days of acclimation prior to behavioral testing. On the first day, cages were carried from the colony holding room to the testing room, and the animal holding apparatus from the acoustic startle test chamber was placed in the home cage for approximately 30 minutes. On the second acclimation day, cages were again brought to the testing room and animals placed in the test chambers for approximately 30 minutes, with ambient noise (no auditory stimuli presented). The next day, acoustic startle testing began, with the gap detection-PPI session done the first day, the acoustic startle reflex and noise-intensity-PPI session the second day. Each day

the order in which mice were tested was randomized, and they were also randomly distributed between test chambers. Acclimation and test sessions were carried out at the same time of day, during the second half of the light portion of the cycle.

5.2.3 Acoustic startle reflex and noise-PPI

The acoustic startle reflex (ASR) is an involuntary response which occurs after exposure to a startle-eliciting acoustic stimulus. To assess this reflex, mice were placed on a force- sensing piezoelectric transducer enclosed within a sound attenuating chamber (14 x 19.5 x 10.875 in, -35 +/- 2 dB attenuation) (Kinder Scientific, Poway, CA). The platforms were calibrated to 1 +/- 0.05 N prior to each gap-PPI session. Acoustic stimuli (full range white noise) were delivered via a built-in speaker centered above the animal enclosure. Noise stimuli were calibrated using a digital sound pressure level meter (model 33-2055, accuracy +/- 2 dB at 114 dB, range 50- 126 dB, RadioShack, Fort Worth, TX). Animals were able to turn freely during the session, but were prevented from rearing by the height of the animal enclosure.

At the start of the session, mice were placed in the test chamber and acclimated in the chamber for 5 minutes while exposed to the background white noise (65 dB, A-weighting). Following the acclimation, mice were presented with a series of 3 different trial types: startle only trials, prepulse trials, and background only trials. During startle only trials, the background intensity lasted for a randomized intertrial interval (ITI) of 15 to 25 ms before the startle eliciting stimulus occurred. The startle-eliciting stimulus was an increase in the noise background intensity, up to 75, 85, 95, 105, or 115 dB, lasting for 40 ms. The mouse's startle response (displacement) was sampled in 1-ms bins for 70 ms beginning with the onset of the startle-eliciting stimulus. During prepulse trials, following the random ITI, an increase of 5, 10, 15, or

20 dB over the background noise intensity lasting for 40 ms preceded the 115 dB startle-eliciting stimulus by a 100-ms interstimulus interval (ISI). During background-only trials, only the background noise was played, and the animal's displacement was measured following the random ITI. The trials were pseudorandomized into 10 blocks, with one trial of each type per block. Five consecutive startle only trials were presented at the beginning and end of the session to assess startle response attenuation over the course of the session, which lasted approximately 40 minutes. The maximum startle response in the 70-ms recording window was calculated automatically by the Startle Monitor software (Kinder Scientific, Poway, CA).

5.2.4 Gap-PPI

To assess detection of silent gaps, we used a modified prepulse inhibition of acoustic startle reflex paradigm (Turner et al., 2006; Fitch et al., 2008). At the start of this session, mice were acclimated for 5 minutes in the chamber to a 70-dB white noise background. During the course of this session, mice were presented with 3 different trial types, startle-only trials, gap trials, and background-only trials. During the gap trials, a silent gap (1, 2, 4, 7, 10, 20, 40 or 100 ms in duration) was embedded in the background noise following a random ITI of 15 to 25 sec (**Figure 5.1**). The 70-dB background noise returned during the 100-ms ISI before the startle eliciting stimulus (105 dB, 40 ms noise pulse). During startle-only trials, no silent gap preceded the startle eliciting stimulus, and background only trials consisted of only background noise for the duration of the ITI. Trials were pseudorandomized in 10 blocks, each comprising one trial of each type. As above, 5 consecutive startle-only trials were presented at the beginning and end of the session to assess startle response attenuation over the course of the session, which lasted approximately 45 minutes.

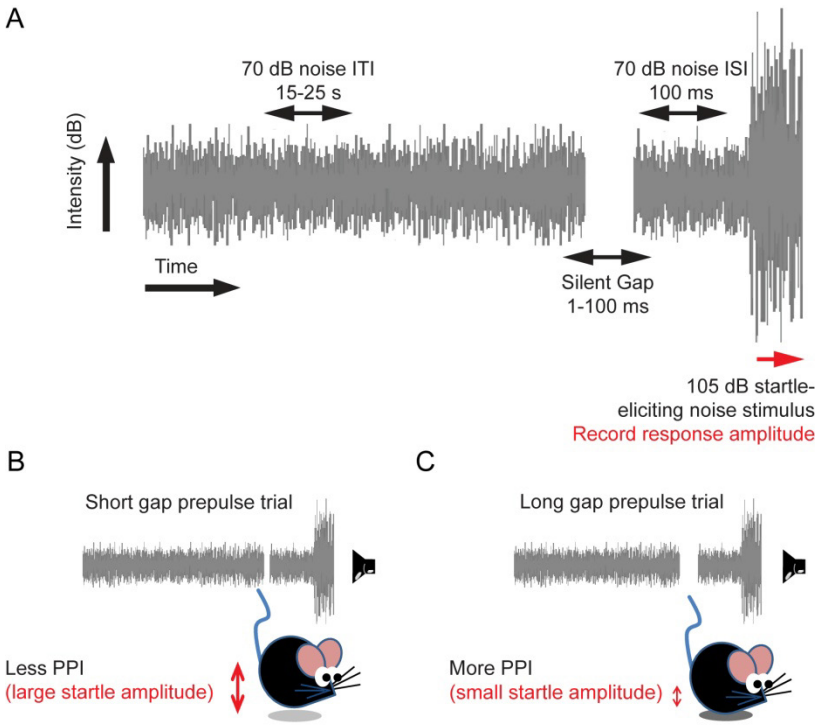

Figure 5.1. Diagram illustrating gap-PPI trial design and predicted responses. A. Gap-PPI trials consisted of a 70 dB white noise background that persisted for the duration of the random duration intertrial interval (ITI). The "prepulse" stimulus was a silent gap embedded in the background noise, which varied from 1 to 100 ms in duration. The offset of the gap was followed by a 100 ms interstimulus interval (ISI) during which the 70 dB background noise returned After the ISI, the startle eliciting noise stimulus occurred, which was a 105 dB noise pulse lasting 40 ms. The maximum displacement (response amplitude) of the mouse was recorded beginning at the onset of the startle-eliciting stimulus. As the magnitude of prepulse inhibition of the startle reflex (PPI) is proportional to the salience of the prepulse, a shorter gap duration trial (B) should elicit relatively less PPI, or a larger startle amplitude, than a longer gap duration trial (C), which should elicit relatively greater PPI, or a smaller startle response.

5.2.5 Statistical analyses

Effects of genotype and age on the acoustic startle responses in WT and KO mice were tested using repeated measures ANOVA, with startle eliciting stimulus intensity as the within-subjects factor, and age and genotype as between-subjects factors. For gap-PPI analyses, startle reflex amplitude from trials from gap durations 1 and 2 ms, 4 and 7 ms, 10 and 20 ms, and 40 and 100 ms were binned. Percent inhibition of startle response was calculated for each gap duration bin as 100*[(mean startle-only trial response – mean binned gap trial response)/mean startle-only trial response]. For the noise-PPI experiments, percent inhibition of startle response was calculated for each noise prepulse stimulus using a similar equation, as 100*[(mean startle-only response – mean noise prepulse trial response)/ mean startle-only trial response]. For both gap- and noise-PPI, genotype and age group comparisons of percent inhibition were tested using repeated measures ANOVA with gap duration bin or noise-prepulse intensity level as a within-subjects factor, and age and genotype as between-subjects factors. To control for variability between acoustic startle chambers, test chamber was included as a factor. Genotype and age comparisons within groups were carried out using Bonferroni correction for multiple comparisons.

Startle amplitude data from individual animals was evaluated with a repeated measures ANOVA model for within-animal effects of gap duration to identify which animals exhibited significant modulation of the startle response amplitude by silent gaps (significant main effect of gap). Proportions of each age/genotype or age/strain group that did and did not exhibit modulation of the startle reflex by gap were compared using χ^2 or Fisher's exact tests.

Group level gap detection thresholds were determined comparing the mean percent inhibition for each gap duration bin against zero using a one-sample t-test. The threshold was

defined as the first of at least two consecutive gap duration bins where the percent inhibition was significantly different from zero. Group level threshold to startle was assessed using t-tests determining whether the mean response amplitudes for each startle eliciting stimulus intensity were different from mean response-amplitudes during background only, no-stimulus trials. The lowest of two consecutive startle eliciting stimulus intensities to elicit a response different from the response during the background only trials was defined as the threshold to startle.

Statistical tests were conducted at the 0.05 significance level, and were done using SPSS software (IBM Corporation, Armonk, NY). When appropriate, degrees of freedom were corrected for deviations from sphericity using the Greenhouse-Geisser adjustment.

5.3 RESULTS

5.3.1 Gap-PPI improves over adolescence in WT but not kalirin KO mice

We found a significant effect of age on gap-PPI responses overall ($F_{(2,95)} = 5.346$, $p = 0.006$). We did not see any effect of genotype ($F_{(1,95)} = 0.592$, $p = 0.444$) or an age by genotype interaction ($F_{(2,95)} = 1.852$, $p = 0.163$). However, the effect of age was highly significant in the WT mice ($F_{(2,95)} = 6.730$, $p = 0.002$), but did not reach significance in the KO ($F_{(2,95)} = 1.013$, $p = 0.367$). Mean gap-PPI increased significantly in WT mice between 4 and 8 weeks of age ($p = 0.001$) (**Figure 5.2**). We examined group-level thresholds for gap-PPI as a secondary measure of gap detection ability. The group-level thresholds for gap-PPI decreased between 4 and 8 weeks of age in the WT mice, but did not change between age groups in the KO mice.

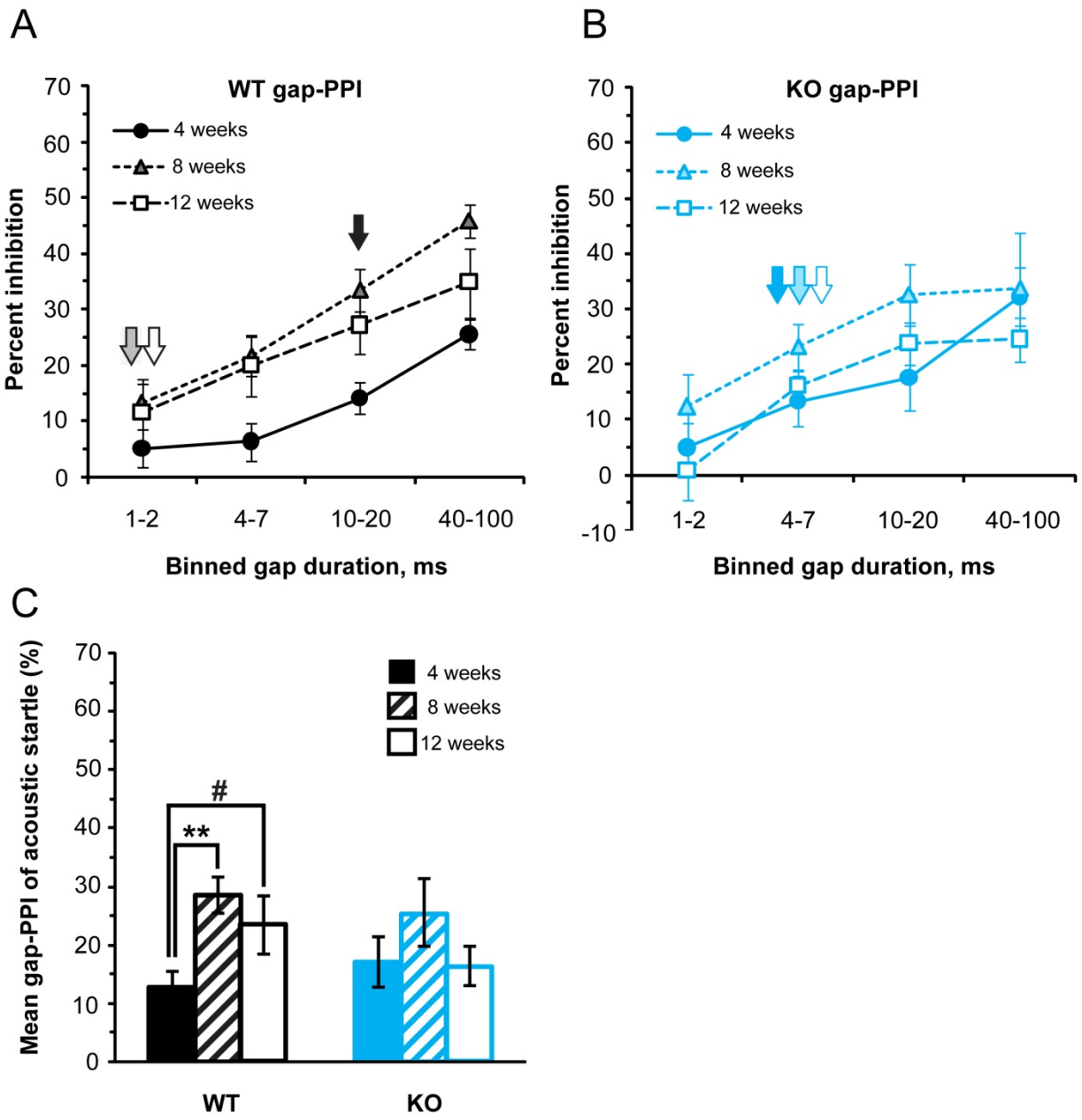

Figure 5.2. Gap-PPI in kalirin WT and KO mice at 4, 8, and 12 weeks of age. Magnitude of gap-PPI as a function of increasing binned gap durations in WT (A) and KO (B) mice. Block arrows indicate gap detection threshold for 4 week (solid) 8 week (light fill) and 12 week (white fill) groups. C. Average gap-PPI for all gap durations in WT and KO mice by age. Mean gap-PPI increases significantly between 4 and 8 weeks in WT mice but not in KO mice. Significance markers indicate comparisons vs. 4 week old WT. #$p < 0.10$, **$p < 0.01$. Animal

numbers per group- Genotype: Age (N): WT: 4 weeks (18), 8 weeks (17), 12 weeks (18); KO: 4 weeks (13), 8 weeks (15), 12 weeks (22). Error bars are ± SEM.

To determine whether the numbers of animals that do and do not demonstrate modulation of the startle response by gap-prepulses differed between age and genotype groups, we also evaluated the proportion of WT and KO animals in each age group that showed significant modulation of the acoustic startle reflex by silent gaps. We did not find a significant effect of age on the proportions of WT mice at 4, 8, and 12 weeks of age that demonstrated significant gap-PPI ($\chi^2 = 4.6$, df = 2, p = 0.102). Similar to the WT, we did not find any age differences on the proportions of KO animals that showed significant modulation of the startle reflex by silent gaps ($\chi^2 = 0.8$, df = 2, p = 0.660). Additionally, proportions of animals showing modulation of the startle reflex by gaps at each age did not differ by genotype (Fisher's exact test, 4 weeks: p = 1.000; 8 weeks: p = 0.383; 12 weeks: p = 0.747) (**Table 1**).

Table 5.1. Proportions of kalirin WT and KO animals that do and do not demonstrate significant modulation of acoustic startle by silent gap prepulses. Numbers of WT and KO animals that do (y) and do not (n) show significant modulation of startle by silent gap prepulses do not differ by age (rows). Further, proportions of animals that do and do not show modulation of acoustic startle do not differ by genotype at any age group (columns). % indicates percent of total number of animals tested that do show significant modulation of acoustic startle by silent gaps.

	4 week	8 week	12 week	age difference
WT (y/n) (%)	10/8 (56%)	15/2 (88%)	12/6 (67%)	p=0.102
KO (y/n) (%)	8/5 (62%)	11/4 (73%)	13/9 (59%)	p=0.660
genotype difference	p=1.00	p=0.383	p=0.747	

When we repeated the binned-gap repeated measures analysis including only the animals that did show significant effect of gap duration on startle response were included, the results were similar (**Appendix Figure D.1**). We again found a significant overall effect of age on gap-PPI responses ($F_{(2,61)}$ = 6.839; p = 0.002). We saw no overall differences in KO gap-PPI compared to WT mice ($F_{(1,61)}$ = 0.091; p = 0.764); however, there was a significant age by genotype interaction effect ($F_{(2,61)}$ = 3.757; p = 0.029). Again, we saw that although the effect of age on gap-PPI is highly significant in the WT animals, there was no effect of age on gap-PPI in the KO mice ($F_{(2,61)}$ = 1.481; p = 0.235). Specifically, gap-PPI increased between 4 and 8 weeks of age in WT mice (p = 0.007). Further, we observed trends toward increased gap-PPI in the KO relative to WT at 4 weeks of age (p = 0.051) and decreased gap-PPI in the KO at 12 weeks of age (p = 0.069).

5.3.2 Noise-PPI does not change during adolescence in WT and kalirin KO mice

To determine if the increase in gap-PPI responses during adolescence in WT mice was attributable to an overall increase in PPI responses during this time, we examined noise-prepulse inhibition of the acoustic startle reflex. There was no overall effect of age ($F_{(2,95)}$ = 0.674, p = 0.512). However, we observed a highly significant main effect of genotype ($F_{(1,95)}$ = 7.025, p = 0.009), and a significant age by genotype interaction effect ($F_{(2,95)}$ = 3.775, p = 0.026). There were no significant effects of age in either genotype (WT: $F_{(2,95)}$ = 2.230, p = 0.113; KO: $F_{(2,95)}$ = 2.454, p = 0.091). Genotype differences were present only in the 12 week group ($F_{(1,95)}$ = 15.830, p < 0.001) and not in the 4 week ($F_{(1,95)}$ = 0.034, p = 0.854) or 8 week groups ($F_{(1,95)}$ = 0.483, p = 0.489). (**Figure 5.3**). All age and genotype groups demonstrated significant prepulse inhibition in response to all noise prepulse intensities tested (p < 0.01).

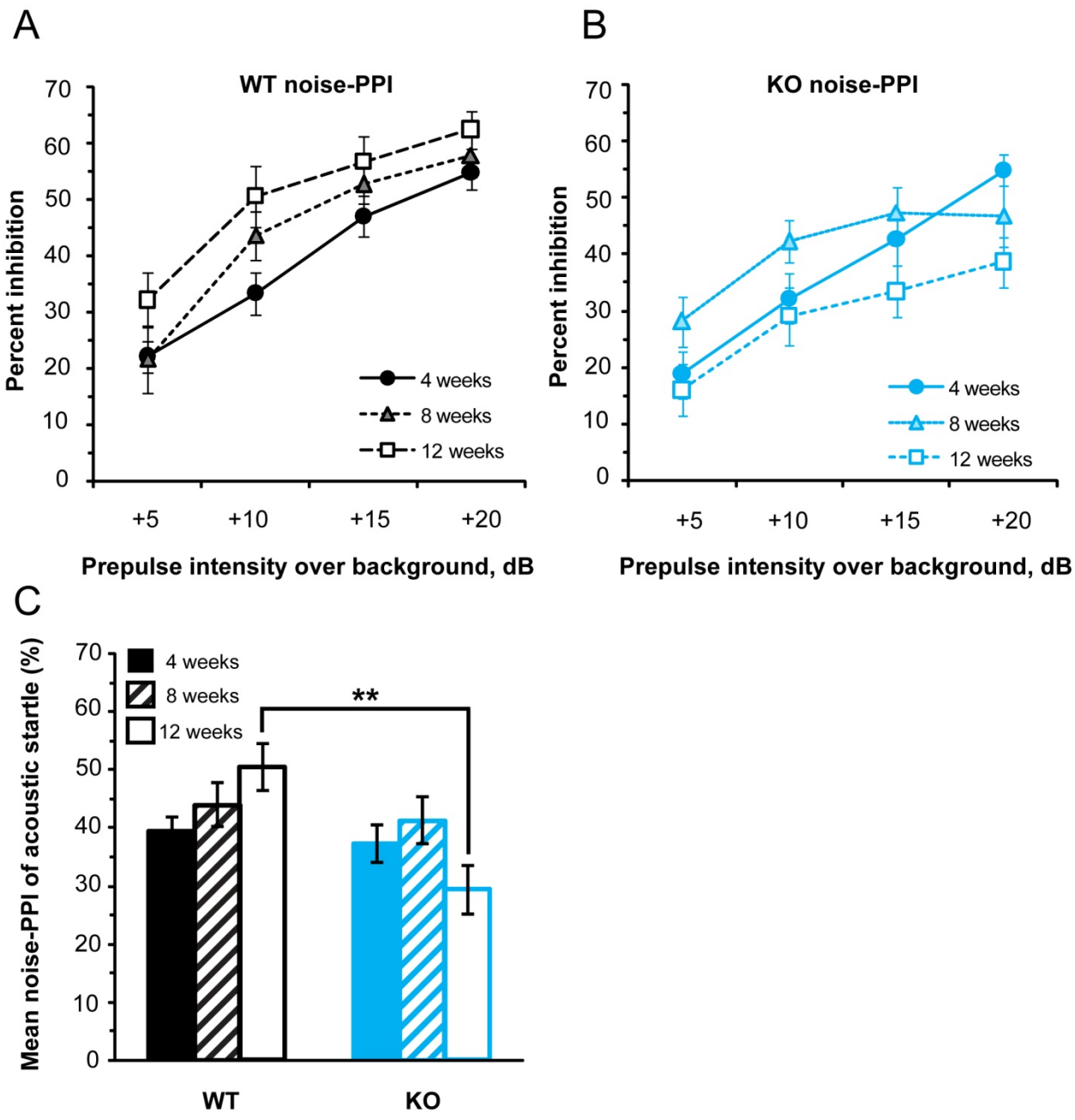

Figure 5.3. Noise-PPI in kalirin WT and KO mice at 4, 8, and 12 weeks of age. Magnitude of noise-PPI as a function of increasing prepulse intensity in WT(A) and KO (B) mice. C) Average noise-PPI for all prepulse intensities in WT and KO mice by age. **p < 0.01. Animal numbers per group- Genotype: Age (N): WT: 4 weeks (18), 8 weeks (17), 12 weeks (18); KO: 4 weeks (13), 8 weeks (15), 12 weeks (22). Error bars are ± SEM.

Acoustic startle reflex amplitude has been previously reported to be reduced in kalirin KO compared to WT mice (Cahill et al., 2009;Mandela et al., 2012). We also found an overall effect of genotype on acoustic startle reflex amplitude ($F_{(1,95)} = 24.685$, $p < 0.001$) (**Appendix Figure D.2**). The acoustic startle reflex was significantly reduced in the KO in the 8 week ($F_{(1,95)} = 14.756$, $p < 0.001$) and 12 week ($F_{(1,95)} = 15.265$, $p < 0.001$) but not in the 4 week old group ($F_{(1,95)} = 0.978$, $p = 0.325$). There was a trend toward an overall effect of age which did not reach significance ($F_{(2,95)} = 2.681$, $p = 0.074$). We defined threshold to startle as the first of two consecutive stimulus intensities to elicit a change in response amplitude compared to the background (no stimulus) trials. In the 12 week old animals, the KO threshold to startle was greater than the WT threshold, but threshold to startle in all groups was reached with either 85 or 95 dB noise pulses.

5.3.3 Gap-PPI increases between early adolescence and young adulthood in CBA/CaJ and C57Bl/6J, but not in DBA/2J mice

None of the strains exhibited significant changes in gap-PPI responses with age (CBA/CaJ: $F_{(2,42)} = 1.819$, $p = 0.175$; C57Bl/6J: $F_{(2,43)} = 1.695$, $p = 0.196$; DBA/2J: $F_{(2,43)} = 0.797$, $p = 0.457$). However, we observed age by gap interaction effects in the CBA/CaJ and C57Bl/6J strains (CBA/CaJ: $F_{(4.333, 90.985)} = 2.469$, $p = 0.046$; C57Bl/6J: $F_{(6,129)} = 2.397$, $p = 0.031$). Our analyses indicated a significant effect of age in these strains on the mean gap-PPI response to 40-100 ms gap durations (CBA/CaJ: $F_{(2, 42)} = 3.209$, $p = 0.050$; C57Bl/6J: $F_{(2,43)} = 4.682$, $p = 0.014$). No age by gap interaction effect was observed in the DBA/2J mice ($F_{(6,129)} = 1.195$, $p = 0.313$) (**Figure 5.4**); however, 12 week old DBA/2J mice failed to demonstrate significant PPI in response to any of the gap durations tested. Increasing background noise intensity in attempt to increase saliency

had no effect on prepulse inhibition in response to gaps in the DBA/2J mice of any age group (effect of background intensity: ($F_{(1,66)} = 0.041$, $p = 0.841$; intensity by age interaction: $F_{(2,66)} = 0.056$, $p = 0.945$) (Not shown).

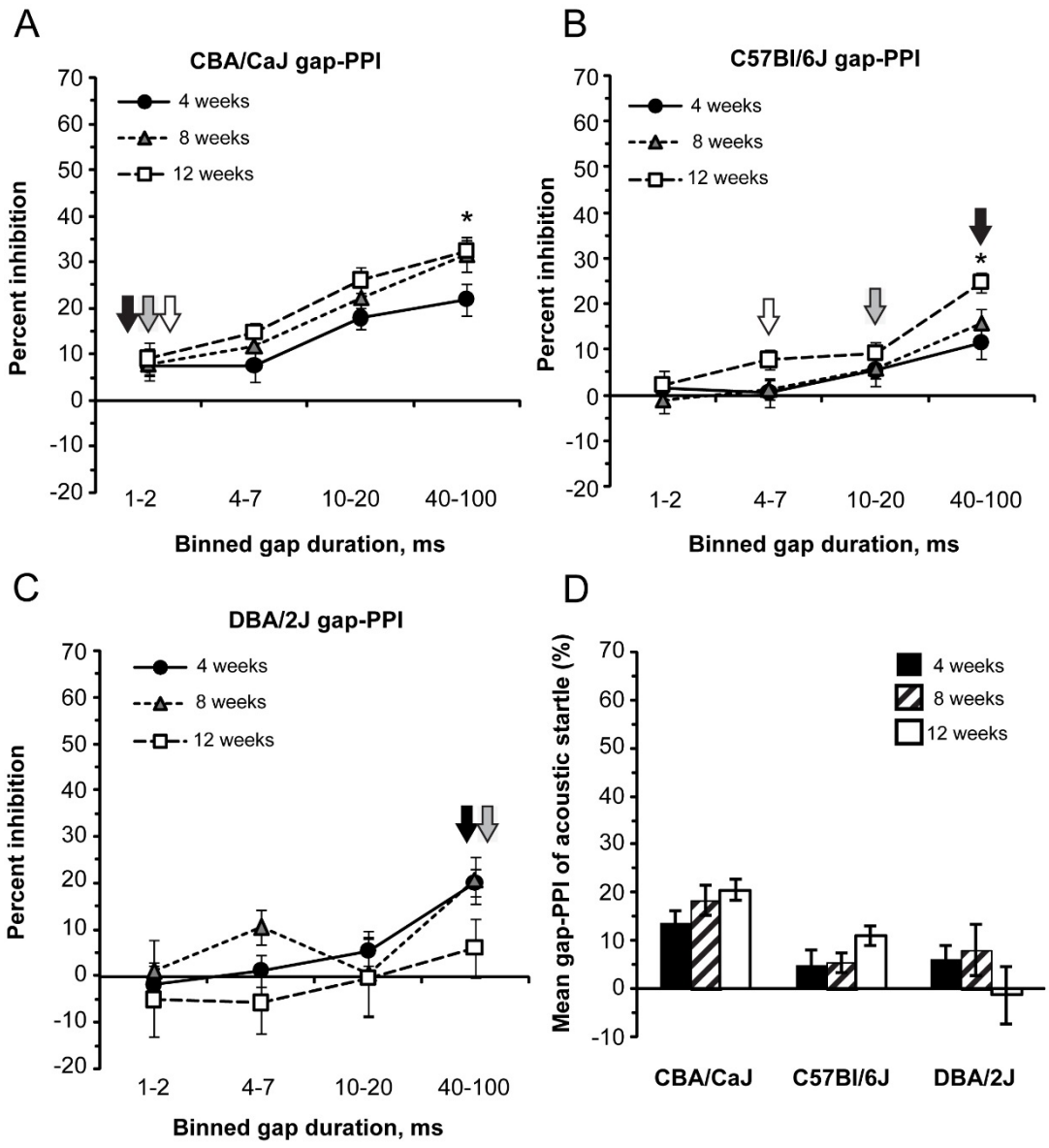

Figure 5.4. Gap-PPI in CBA/CaJ, C57Bl/6J, and DBA/2J at 4, 8, and 12 weeks of age. Mean gap-PPI in 4, 8, and 12 week old CBA/CaJ (A) C57Bl/6J (B) and DBA/2J (C). Significance markers indicate age effects within each strain that were present at indicated gap duration bins. *$p < 0.05$. Arrows indicate group gap detection thresholds in 4 week old (solid), 8 week old (light fill), and 12 week old (white fill) animals. D) Average gap-PPI for all gap durations in CBA/CaJ, C57Bl/6J and DBA/2J mice by age. No significant overall age effects were observed in any strain. Animal numbers per group- Strain: Age (N): CBA/CaJ: 4 weeks (15), 8 weeks (16), 12 weeks (16); C57Bl/6J: 4 weeks (16), 8 weeks (16), 12 weeks (16); DBA/2J: 4 weeks (16), 8 weeks (16), 12 weeks (16). Error bars are ± SEM.

We found that gap detection thresholds of CBA/CaJ mice were already maximal at 4 weeks and did not change between 4 and 12 weeks of age (4 weeks: 1-2 ms, 8 weeks: 1-2 ms, 12 weeks: 1-2 ms). However, gap detection thresholds of C57Bl/6J mice decreased between 4 and 12 weeks (4 weeks: 40-100 ms, 8 weeks: 10-20 ms, 12 weeks: 4-7 ms). In contrast, gap detection thresholds of DBA/2J mice did not decrease between 4 and 8 weeks of age (4 week: 40-100ms, 8 week: 40-100 ms) and could not be measured at 12 weeks, but our data suggest the threshold for this group is greater than 100 ms.

We also evaluated the proportion of animals in each strain by age group that showed modulation of the startle reflex by silent gaps. We did not observe any changes with age in the proportion of animals that showed gap responsiveness in CBA/CaJ ($\chi^2 = 2.69$, df = 2, p = 0.264), C57Bl/6J (Fisher's exact test: p = 1.00), or DBA/2J (Fisher's exact test: p = 1.00) (**Table D.1**). At 4 weeks, there were no differences in the proportions of each strain that showed modification of startle by gaps (Fisher's exact test: p = 0.103); however there were significant strain differences in proportions of animals that showed significant modification of startle by gaps at 8 (Fisher's exact test: p = 0.009) and 12 weeks (Fisher's exact test: p = 0.0007). No analyses were carried out on only the animals with significant modulation of startle by gaps due to the low numbers (< 50%) in the C57Bl/6J and DBA/2J groups.

5.4 DISCUSSION

Here we report that gap-PPI responses increase across the time period between early and late adolescence in wild type C57Bl/6NJ mice (**Figure 5.5**). This does not appear to be attributable to increased PPI in general, as noise-PPI responses did not significantly increase during this time.

Kalirin KO mice failed to show any significant changes in gap-PPI between early and late adolescence. It is possible that this is a functional indicator of abnormal auditory cortex synapse development in mice lacking kalirin (see chapter 4). Gap-PPI responses increased for long duration gaps between early adolescence and young adulthood in C57Bl/6J and CBA/CaJ mice. DBA/2J mice, which exhibit early adolescent onset high frequency hearing loss, did not show any increase in gap-PPI responses between early adolescence and young adulthood, probably reflecting the impact of high frequency hearing loss on detection of silent gaps.

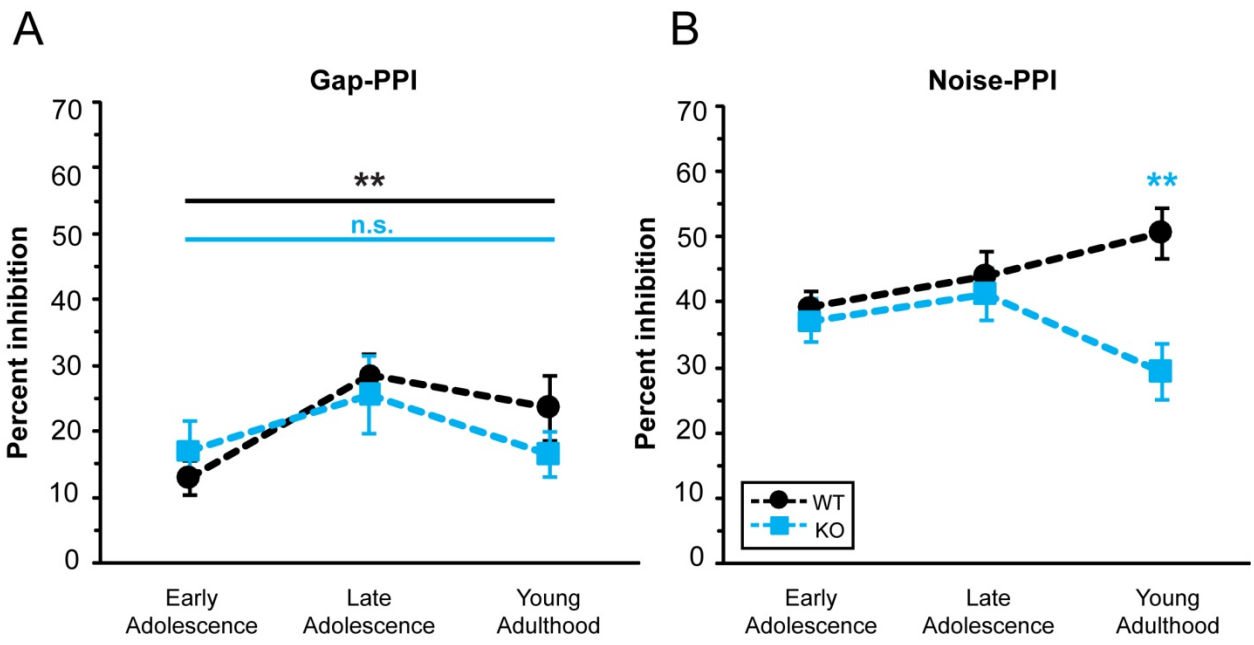

Figure 5.5. Trajectories of gap-PPI and noise-PPI magnitude across adolescence and young adulthood in WT and kalirin KO mice. A) Mean gap-PPI responses increase during adolescence in WT but not kalirin KO mice. Horizontal lines and significance markers indicate overall age effects for WT (black) and KO (blue). **p < 0.01; n.s. not significant. B) Mean noise-PPI responses do not change significantly with age in either WT or kalirin KO mice. Consistent with other studies, kalirin KO mice exhibit a deficit in noise-PPI in young adulthood. **p < 0.01 between WT and KO at 12 weeks. Error bars are ± SEM.

5.4.1 Improved gap-PPI in WT but not kalirin KO during adolescence

We found an increase in gap-PPI between 4 and 8 weeks of age in wild type mice of the C57Bl/6NJ background, suggesting that gap-PPI matures during adolescence in mice of this strain. This agrees with a previous study that gap detection threshold decreases between 1 and 2 months of age in rats (Friedman et al., 2004; Sun et al., 2008; Sun et al., 2011). As auditory cortex has been shown to be required for detection of silent gaps (Ison et al., 1991; Bowen et al., 2003) we speculate that pruning of excitatory synapses in auditory cortex during this time (see chapter 4) may contribute to maturation of gap-PPI.

In contrast to the WT mice, we saw no improvement of gap-PPI over adolescence in the kalirin KO mice. This suggests that the process of gap-PPI maturation is impaired in the absence of kalirin. Further, we observed a trend toward increased gap-PPI in 4 week old kalirin KO animals compared to WT when we included only animals that demonstrated significant gap-prepulse modulation of the startle reflex (**Figure D.1**). In this analysis, the gap detection threshold was higher in 4 week old WT compared to KO, suggesting that gap-PPI is already at "mature" levels in early adolescent kalirin KO mice, and then remains unchanged while WT gap-PPI matures across adolescence. This parallels our findings of auditory cortex spine numbers between early adolescence and young adulthood in WT and kalirin KO mice (see chapter 4). In WT mice, spine numbers decrease between early adolescence and young adulthood, while in spine numbers were already slightly reduced in early adolescence of mice lacking kalirin and did not decrease further by young adulthood. Thus, it may be that primary auditory cortex spine pruning contributes to the maturation of gap-PPI. Further studies to examine the relationship between auditory cortex spine pruning and gap-PPI should be done in other models of dendritic

spine disruption, such as mice lacking Abl-related gene (Arg) kinase, which exhibit a deficit in frontal cortex spine density throughout adolescence (Gourley et al., 2012).

Our data also suggest that the failure of kalirin KO mice to show improvement in gap-PPI over adolescence is not fully attributable to abnormal PPI responses in general (Cahill et al., 2009). We found that mice lacking kalirin do not demonstrate impaired noise-intensity PPI until young adulthood. Therefore, failure of gap-PPI responses to increase during adolescence is likely not attributable to general PPI impairment. Alternatively, it may be that gap-PPI is more sensitive to earlier impairments in mechanisms common to both noise and gap-PPI, and so it is possible that general impairment of PPI circuitry contributes to both observations. This could be confirmed using non-PPI paradigms, such as conditioned suppression (Heffner et al., 2006) to assess gap detection in adult kalirin KO mice.

5.4.2 Development of noise intensity-PPI and acoustic startle reflex impairments in kalirin KO mice

Cahill et al (2009) reported impaired prepulse inhibition of the acoustic startle reflex with noise prepulses of increasing intensity and reduced startle response in adult kalirin KO mice. A conflicting report using a different kalirin KO model reported a reduction in acoustic startle response, but no deficit in noise-intensity prepulse inhibition (Mandela et al., 2012) in animals between 2 and 3 months of age. We found that prepulse inhibition is impaired in kalirin KO mice beginning in young adulthood, while a deficit in acoustic startle reflex amplitude is apparent at the end of adolescence. Therefore, we have identified a potential developmental explanation which reconciles the previously reported conflicting findings. It may be possible to observe an overall impairment in acoustic startle reflex without an accompanying deficit in

noise-PPI prior to young adulthood. This highlights the need to consider developmental changes which may occur during and following adolescence when evaluating genetic animal models.

5.4.3 Improvement in gap-PPI during adolescence in CBA/CaJ and C57Bl/6J

We found that gap-PPI improves between early adolescence and young adulthood in CBA/CaJ and C57Bl/6J inbred strains, reflected in increased PPI for long duration gaps and, for the C57Bl/6J, by reduced gap-PPI thresholds. The improvement with age in these strains was not as robust as in the WT mice of the C57Bl/6NJ background. Differences in traditional noise-PPI between the C57Bl/6N and 6J substrains have been reported (Grottick et al., 2005). Similar to that study we observed greater magnitudes of noise-PPI and lower amplitude of the acoustic startle response in the C57Bl/6NJ-WT mice. It may be that the substrains also differ in gap-PPI, and further illustrates the importance of strain (and substrain) considerations when evaluating genetic animal models.

5.4.4 Impaired gap-PPI in DBA/2J mice during late adolescence and adulthood

Studies have shown that high frequency components of sound may contribute to the detection of silent gaps in noise by mice (Radziwon et al., 2009). The fact that DBA/2J mice show no increase in gap-PPI responses and no decrease in gap-PPI threshold over adolescence, and a lack of significant gap-PPI with gaps $\leq$ 100 ms by 12 weeks, is consistent with this observation. Mice of the DBA/2J strain background demonstrate high frequency hearing loss which begins at about 4 weeks of age (Willott et al., 1994). Therefore, the poor gap-PPI performance that we observed

is likely attributable to progressive inability to detect high frequency components of sound required for silent gap detection.

5.4.5 Methodological considerations

Modification of the acoustic startle reflex by silent gaps embedded in a constant acoustic background has been used as a behavioral measure to determine the presence of tinnitus (perception of ringing in the ears) in animals (Turner et al., 2006). Evidence to support the role of the auditory cortex in gap processing comes from experiments where the auditory cortex is lesioned (Bowen et al., 2003), or after functional decortication with potassium chloride (Ison et al., 1991). Gap-PPI deficits have also been identified in the rat microgyria model of cortical developmental disruption (Peiffer et al., 2004; Threlkeld et al., 2009), and a middle cerebral artery occlusion stroke mouse model (Truong et al., 2012). These studies all support the idea that compromised cortical function impairs gap-PPI. However, a potential caveat of our use of this technique is that auditory cortex may be necessary, but subcortical components regulating noise-PPI are probably also important. Therefore, the maturation in gap-PPI that we observed could be attributable to changes in any of those components, although in that case we might expect to observe the same increase in noise-PPI. In particular, inferior colliculus responses to silent gaps demonstrate similar gap detection thresholds as behaviorally measured thresholds. It is important to keep in mind that it is possible that maturation of other components of the auditory system, such as the inferior colliculus, may underlie the increase in gap-PPI we observed during adolescence.

5.4.6 Conclusions

In summary we have found that gap-PPI responses increase between early and late adolescence in WT mice, but not in mice lacking kalirin. Given that we have previously found subtle disruptions in trajectories of adolescent and early adulthood changes in excitatory and inhibitory synapses in auditory cortex of kalirin KO mice (see chapter 4), and auditory cortex is necessary for normal gap-PPI responses, it is possible that this finding reflects abnormal auditory cortex synapse development in mice lacking kalirin. Future studies of gap-PPI in other genetic animal models of schizophrenia relevant excitatory synapse pathology will contribute to our understanding of the circuitry underlying the increase in gap-PPI during adolescence in mice.

6.0 GENERAL DISCUSSION

6.1 SUMMARY OF FINDINGS

Individuals with schizophrenia demonstrate auditory processing impairments that range from the most basic levels of tone discrimination all the way up to complex perceptual tasks such as comprehension of speech prosody and semantics. These impairments likely contribute to some of the highly debilitating negative and cognitive symptoms of schizophrenia, for which there are few, if any, satisfactory treatments. In order to develop new treatments and preventions for these debilitating symptoms, we must first understand the neurobiology of their origin. As the clinical onset of schizophrenia commonly occurs later in adolescence and in young adulthood, adolescence represents a potential window where preventative measures could be implemented to mitigate or reverse neuropathological changes that contribute to symptom onset. However, the adolescent developmental trajectories of the synaptic features in auditory cortex that we may wish to target with future preventative strategies have not been fully characterized. The goals of these studies were to determine whether excitatory and inhibitory presynaptic bouton alterations contribute to schizophrenia primary auditory cortex synaptic pathology, and to evaluate, in a mouse model, adolescent developmental trajectories of auditory cortex synapse components affected in schizophrenia, and adolescent development of auditory cortex function. In the following sections we will review the findings of the experimental chapters, and then discuss the

broader implications of these findings in the context of an updated adolescent neurodevelopmental model of schizophrenia, highlighting the relationship between dendritic spines and within-bouton GAD65 protein in the primary auditory cortex. Finally, we will discuss implications for interpreting our findings beyond the auditory cortex, and caveats associated with genetic mouse models of schizophrenia.

6.1.1 Excitatory and inhibitory presynaptic components in auditory cortex in schizophrenia

Because dendritic spine density is reduced in primary auditory cortex of subjects with schizophrenia, we hypothesized that presynaptic excitatory boutons are also reduced, which could indicate excitatory synapse loss. In chapter 2, we determined that two populations of excitatory boutons in the primary auditory cortex, VGluT1-expressing intracortical excitatory and VGluT2-expressing thalamocortical boutons, are unaltered in density, number, and levels of VGluT protein in subjects with schizophrenia. Another recent study also failed to identify changes in protein levels of VGluT1 and VGluT2 in the STG (Shan et al., 2013), which is consistent with the idea that numbers of excitatory boutons and their levels of VGluT protein are unaltered in the auditory cortex. The lack of change in excitatory boutons was unexpected, given the previously observed reductions in auditory cortex deep layer 3 dendritic spines (Sweet et al., 2009), which are the primary postsynaptic targets of glutamatergic boutons in the cortex. Our findings could indicate a disproportionate number of excitatory boutons synapsing on dendritic shafts in the auditory cortex of subjects with schizophrenia. Future studies using both quantitative fluorescence microscopy and electron microscopy methods can address this question by quantifying the proportions of VGluT1 and VGluT2- expressing boutons which form

synapses with dendritic spines versus dendritic shafts in individuals with schizophrenia compared to healthy controls. We predict that there may be an increase in the proportion of dendritic shaft synapses in the auditory cortex relative to spine excitatory synapses, and results supporting this hypothesis have been described in other brain regions (Barksdale et al., 2012). Although the electrophysiological significance of shaft compared to spine synapses are not well understood, shaft synapses may elicit larger excitatory potentials in postsynaptic pyramidal neurons compared to spine synapses (Segal, 2010). The downstream consequences of this for neuronal activity are not clear, but this may render pyramidal cells more vulnerable to other insults (Fishbein and Segal, 2007), and could have an effect on firing rates and input summation (Shepherd et al., 1989; Jaslove, 1992; Tsay and Yuste, 2004). However, spines do contribute to segregation of frequency-specific inputs to neurons in primary auditory cortex (Chen et al., 2011b) and so loss of spines may impair frequency tuning of primary auditory cortex neurons and contribute to tone discrimination deficits in schizophrenia. Future studies should also determine whether protein levels of other glutamatergic synaptic components implicated in schizophrenia are altered (Mirnics et al., 2000), as this could impact excitatory synapse function independent of a reduction in the number of boutons, or levels of VGluT protein within boutons.

Given the electrophysiological evidence for disruptions in aSSR and auditory evoked oscillatory activity in individuals with schizophrenia, we hypothesized that GABAergic signaling may be impaired in the primary auditory cortex. In particular, we wanted to examine levels of the 65 kDa isoform of GAD, due to its role in fast, on-demand GABA production. In chapter 3, we demonstrated that levels of GAD65 protein are reduced within inhibitory boutons in deep layer 3 of the primary auditory cortex. Evidence suggests that primary auditory cortex is specialized for processing of fast temporal information, and inhibitory responses in auditory

cortex have been found to be faster than in other cortical areas (Hefti and Smith, 2000). Reduced levels of GAD65 protein may indicate a reduction of GABA synthesis within inhibitory terminals. This may be particularly detrimental during conditions requiring high rates of inhibitory neuron firing, when GAD65-mediated GABA synthesis is likely to be important (Tian et al., 1999). High rates of interneuron firing may contribute to generation of auditory steady state responses and gamma range oscillatory activity, which are impaired in schizophrenia. Therefore, we propose that reduced GAD65 protein in auditory cortex inhibitory neurons could contribute to the abnormal auditory evoked steady state responses and impairments in gamma-range oscillations observed in individuals with schizophrenia. In section 6.2.2, we outline some potential mechanisms by which GAD65 protein reduction could occur.

As balanced excitation and inhibition are important for processing auditory information (Wehr and Zador, 2003; Wu et al., 2008), we wanted to examine correlations between excitatory and inhibitory synaptic components in primary auditory cortex of subjects with schizophrenia. Interestingly, we observed that reductions in GAD65 protein are correlated with previously identified reductions in spinophilin-immunoreactive spine density in the same subjects (Sweet et al., 2009). This suggests a relationship between levels of GAD65 and dendritic spines in the auditory cortex. The implications of this relationship are discussed at length in section 6.2.

6.1.2 Adolescent development of excitatory and inhibitory synaptic components of mouse primary auditory cortex and functional implications

Given the evidence for correlated reductions in dendritic spines and GAD65 in auditory cortex of subjects with schizophrenia, we hypothesized that reductions in GAD65 occur following dendritic spine pruning in the auditory cortex during adolescence. We also wanted to determine

if excessive dendritic spine pruning occurs in the auditory cortex in the absence of kalirin, a regulator of dendritic spine development and stability. Additionally, we wanted to assess how the absence of kalirin affects development of excitatory and inhibitory synapse components in auditory cortex, which are disrupted in schizophrenia. In chapter 4, we observed evidence for pruning of dendritic spines in auditory cortex of wild type mice between early adolescence and young adulthood. This was accompanied by the subsequent onset of a marked reduction in within-bouton GAD65 protein between late adolescence and young adulthood. This temporal relationship suggests that spine pruning precedes the onset of the reduction in GAD65 protein, which lends insight into the directionality of the correlation we observed between dendritic spine density and GAD65 protein reductions in schizophrenia.

In contrast to what has been observed in the frontal cortex (Cahill et al., 2009), we did not find evidence for increased pruning of spines between early adolescence and young adulthood in the auditory cortex of the kalirin KO mice. In fact, there was no evidence for spine pruning during this time in the kalirin KO, suggesting one of a few possibilities. First, it may be that mice lacking kalirin fail to generate the normal number of dendritic spines in the auditory cortex during postnatal development, resulting in a reduced number of spines which are then not pruned during adolescence. Second, it may be that dendritic spine pruning in auditory cortex occurs earlier in mice lacking kalirin, so that by early adolescence, mature numbers of spines are already attained. It is also possible that either of these options is coupled with an adult phase of spine elimination (later than 12 weeks of age) that would ultimately lead to reduced spine density in the auditory cortex of the kalirin KO. We can distinguish between these possibilities in future studies expanding the time window to examine spine density in early postnatal development

through later in adulthood in order to determine whether spine pruning occurs outside of adolescence in the kalirin KO.

In chapter 5, we used gap-PPI as a measure of auditory cortex function, and hypothesized that abnormal adolescent spine development in the kalirin KO mice would be associated with impaired gap-PPI, while WT mice would show improvement in gap-PPI over adolescence. We found that gap-PPI responses increase during adolescence in WT mice, similar to improvements in gap-PPI observed in rats (Friedman et al., 2004; Sun et al., 2008; Sun et al., 2011). This was not attributable to a general increase in noise-PPI responses, suggesting that the improvement over adolescence is specific for gap-PPI and may indicate functional maturation of the auditory cortex. In the kalirin KO mice, which do not demonstrate spine pruning in auditory cortex between early adolescence and young adulthood, gap-PPI responses also do not increase. This suggests there may be subtle functional consequences for auditory cortex when adolescent spine pruning does not occur normally. However, further studies of auditory cortex in animal models where excessive spine pruning occurs should be done to evaluate whether excessive adolescent spine pruning in the auditory cortex causes impairments in schizophrenia-relelvant auditory cortex function.

Although inactivation and lesion studies in animals have demonstrated a role for the auditory cortex in gap-PPI (Ison et al., 1991; Bowen et al., 2003), the physiological mechanisms underlying cortical contributions to gap-PPI are not known. A potential avenue by which the primary auditory cortex could influence PPI circuitry is via subcortical projections from layer 5 neurons. The inferior colliculus is an important component of the circuitry mediating PPI (Fendt et al., 2001). The lack of an increase in gap-PPI with age in mice lacking kalirin could be mediated by the effects of kalirin loss in primary auditory cortex layer 5 pyramidal neurons, as

layer 5 neurons project back to the inferior colliculus (Mitani and Shimokouchi, 1985). Further, kalirin protein expression in the cortex is particularly prominent in layer 5 pyramidal neurons (Ma et al., 2001). The subtle disruptions in the development of excitatory and inhibitory synaptic components that we observed in layers 2 through 4 of the auditory cortex in the kalirin KO could influence layer 5 output to the inferior colliculus via feed forward projections to layer 5 neurons from layer 2 and 3 pyramidal neurons. Future studies will be necessary to elucidate the laminar contributions of primary auditory cortex to gap-PPI responses.

6.2 CONSIDERATION OF AUDITORY CORTEX NEUROPATHOLOGY IN THE CONTEXT OF ADOLESCENT NEURODEVELOPMENT

The fact that late adolescence and young adulthood typically correspond to emergence of psychotic symptoms in schizophrenia suggests that this period of postnatal development factors heavily in the pathogenesis of the disease. A better understanding of the normal developmental processes occurring in the auditory cortex during this time will inform the development of preventative measures to counteract the pathophysiological mechanisms which lead to schizophrenia. In the following sections we will discuss an updated model of synapse pathology in the auditory cortex of subjects with schizophrenia in the context of what we have learned about adolescent synaptic component development in the mouse auditory cortex.

6.2.1 Developmental context for the relationship between dendritic spine and GAD65 protein reductions in auditory cortex of subjects with schizophrenia

Dendritic spines are anatomical substrates for neural circuit plasticity, and growth and retraction of spines are associated with induced forms of plasticity such as long term potentiation and depression (LTP and LTD), respectively (Bosch and Hayashi, 2012). We found that reduced within-bouton GAD65 protein levels are correlated with reduced dendritic spine density in deep layer 3 of primary auditory cortex of subjects with schizophrenia. The correlation suggests that they may be related pathological features of schizophrenia. In mouse auditory cortex, we found evidence that dendritic spine pruning occurs between early adolescence and young adulthood, while a reduction in within-bouton GAD65 protein levels occurs between the end of adolescence and early adulthood. We cannot infer directionality of a relationship between dendritic spines and GAD65 protein based on the correlation we observed in schizophrenia. However, the timing of the two features during adolescent development in the mouse suggests that a reduction in GAD65 protein could follow a reduction in dendritic spines. Experimental evidence also favors this direction. Decreased excitatory activity, which can accompany reductions in spines in cultured hippocampal neurons after treatment with pharmacological convulsants (Muller et al., 1993), or decreases in sensory input, which alters sensory cortex excitability (Lambo and Turrigiano, 2013), lead to decreased GAD expression (Hendry and Jones, 1988; Welker et al., 1989; Huntsman et al., 1995; Patz et al., 2003). In contrast, a model where a primary deficit in GAD65 protein occurs first and subsequently elicits a reduction in dendritic spines is less favorable based on existing evidence. For example, GAD65 KO mice, which exhibit decreased inhibitory transmission during sustained neural activity (Tian et al., 1999), are reported to have elevated, rather than reduced, dendritic spine density (Mataga et al., 2004). Also, spine density

increases when cultured hippocampal neurons are exposed to mercaptopropionic acid, a GAD inhibitor (Murphy et al., 1998). Finally, in the visual cortex, monocular deprivation-induced loss of dendritic spines in cortical layers 2 and 3 does not occur in the absence of GAD65 (Fagiolini and Hensch, 2000). This suggests that reduction of GAD65 protects against plasticity-induced loss of dendritic spines. Taken together, this evidence suggests that a primary deficit in inhibition would *increase* the density of dendritic spines, which is not the case in the auditory cortex of individuals with schizophrenia. Therefore, if a causal relationship between reduced spine density and GAD65 expression in schizophrenia does exist, it is unlikely that spine loss is a consequence of reduced GAD65 levels in schizophrenia. In contrast, there is more evidence to support the idea that a primary reduction in dendritic spines could elicit subsequent reductions in GAD65 protein levels.

We propose a developmental model of auditory cortex excitatory and inhibitory synapse impairment in schizophrenia, summarized in **Figure 6.1**. Normally, dendritic spine pruning occurs during adolescence, and is followed by a reduction in within-bouton GAD65 protein levels between the end of adolescence and early adulthood. In individuals with schizophrenia, excessive dendritic spine pruning is followed by a parallel excessive decrease in within-bouton levels of GAD65 protein. It may be that the reduction in GAD65-mediated GABA synthesis is a compensatory response to reduced excitatory drive induced by a reduction of dendritic spines. In the following sections, we present potential mechanisms by which excitatory activity can alter levels of GAD65 protein. Also, we review evidence suggesting that the down-regulation of GAD65 protein at the end of adolescence could be a mechanism for decreasing the rate of spine elimination at the end of adolescence. It should be noted that our findings are not by any means sufficient to determine a causal relationship between spine pruning and reduction of GAD65

during adolescence or in schizophrenia. However, identification of the association between excitatory and inhibitory synaptic components in development and in schizophrenia lays the groundwork for future studies to further investigate the potential for a causal relationship, and what the mechanisms regulating such a relationship might be. Further, we have identified the transition between the end of adolescence and the beginning of early adulthood as a developmental time period during which GAD65 protein levels in the auditory cortex are changing and could be vulnerable to perturbation. The validity of the model should be tested in future studies, using convergent models to both increase and decrease the extent of cortical spine elimination to test whether spines and GAD65 are co-regulated.

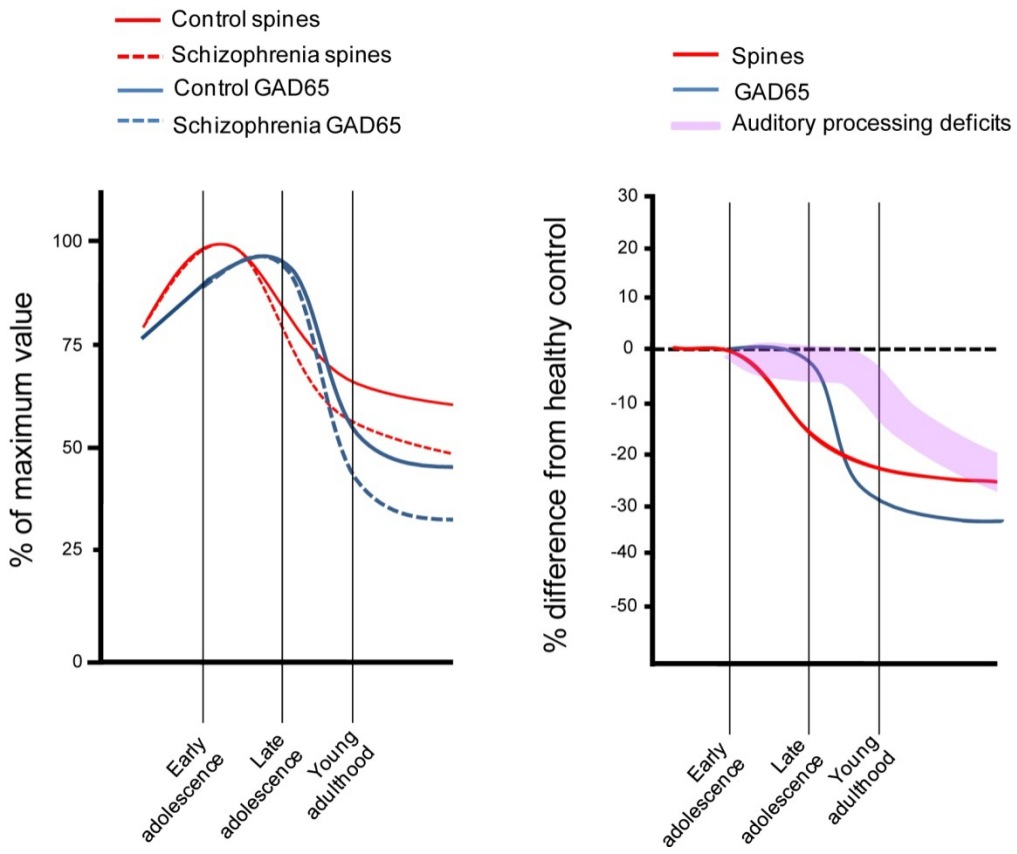

Figure 6.1. Proposed adolescent developmental model for spine and GAD65 protein reductions in auditory cortex during adolescence and in schizophrenia. Left. Spines (red) decrease in auditory cortex between early adolescence and young adulthood, followed by a reduction in within-bouton GAD65 protein levels (blue) between late adolescence and young adulthood. In schizophrenia, deficits in within-bouton GAD65 protein develop subsequent to deficits in dendritic spine density (dashed lines). Right. Time course depicting deficits (difference from healthy controls). Deficits in dendritic spines develop first (red), followed by deficits in GAD65 protein levels (blue). We speculate that electrophysiological deficits (purple) in auditory processing develop subsequent to synapse pathology in auditory cortex.

6.2.2 Mechanisms for GAD65 reduction in development and in disease

The mechanisms regulating GAD65 expression are not yet fully understood, but multiple studies have demonstrated that GAD65 is regulated by excitatory activity. First, there is evidence from studies of kalirin that excitatory synapses onto inhibitory interneurons influence levels of GAD65 protein. Kalirin-7 protein is expressed adjacent to VGluT1-expressing puncta in cultured hippocampal interneurons (Ma et al., 2008), indicating that kalirin is a component of excitatory synapses onto the dendritic shafts of interneurons. In chapter 4, we describe that between late adolescence and young adulthood the within-bouton levels of GAD65 protein decrease in the auditory cortex of WT mice. However, in mice lacking kalirin, we did not observe a significant reduction in within-bouton GAD65 during this time. Complementary to our results, expression of exogenous kalirin-7 in cultured hippocampal interneurons results in a decrease in GAD65 protein levels (Ma et al., 2011). Together, this evidence suggests that kalirin expressed at postsynaptic sites of excitatory synapses onto interneurons is important for regulating GAD65 protein levels, and disruption of excitatory synapses by removing kalirin leads to altered regulation of GAD65 protein levels between late adolescence and young adulthood.

Blocking the NMDA subtype of ionotropic glutamate receptor has been shown to exert a substantial impact on interneuron activity (Homayoun and Moghaddam, 2007). Decreased expression of GAD by blocking neuronal activity chemically or through sensory deprivation (Hendry and Jones, 1988; Welker et al., 1989; Huntsman et al., 1995; Patz et al., 2003) could be mediated through the NMDA subtype of ionotropic glutamate receptor. In support of this, MK-801 administration decreases levels of GAD65 mRNA in rat frontal and cingulate cortex (Laprade and Soghomonian, 1995). Although comparatively less work has been done

investigating consequences of NMDA signaling on GAD65, findings that blocking NMDA receptors reduces the expression of the 67 kDa isoform of GAD are well replicated (Qin et al., 1994; Bacci et al., 2002; Paulson et al., 2003; Turner et al., 2010). Evidence for NMDA receptor involvement in schizophrenia stems from observations that pharmacological antagonists, such as PCP and ketamine, that target NMDA receptors, recapitulate some of the symptoms of schizophrenia in otherwise healthy individuals, and exacerbate symptoms in individuals with schizophrenia (Javitt, 2007). It may be that one of the long term consequences of altered glutamatergic signaling in schizophrenia (Moghaddam and Javitt, 2012) is a decrease in the levels of GAD65 protein in the auditory cortex of subjects with schizophrenia.

GAD65 gene transcription is influenced by CREB-mediated BDNF signaling (Sanchez-Huertas and Rico, 2011). Pyramidal neurons secrete BDNF in an activity dependent manner (Cellerino et al., 1996; Marty et al., 1997) which then interacts with the trkB receptor expressed in GABAergic inhibitory neurons (Cellerino et al., 1996; Gorba and Wahle, 1999). BDNF levels are sensitive to sensory input, as expression in visual cortex is decreased after monocular deprivation, and increased by exposure to light (Castren et al., 1992; Bozzi et al., 1995). In the hippocampus, increased BDNF signal is correlated with increased GAD65 protein following a contextual fear conditioning paradigm (Chen et al., 2007). Further, manipulating levels of BDNF in rat primary auditory cortex distorts development of tonotopic representations in the cortex, and alters expression of $GABA_A$ receptors (Anomal et al., 2013). This suggests that BDNF is tightly linked to plasticity and inhibitory signaling in sensory cortices.

The developmental trajectory of BDNF expression in auditory cortex is not yet known in detail; however, in general, levels of BDNF in the rat auditory cortex increase between P12 and 14 weeks (Zhou et al., 2011), although levels were not assessed during adolescence. However, in

rat, BDNF levels in the cortex peak during adolescence and decline between 2 and 4 months of age (Katoh-Semba et al., 1997). Future studies should determine whether the decline in BDNF expression between late adolescence and young adulthood also occurs in auditory cortex. This decline in BDNF levels parallels the decrease we observed in GAD65 protein levels between late adolescence and young adulthood, consistent with the idea that BDNF signaling influences expression of GAD65. Interestingly, there is some evidence that BDNF levels are abnormal in schizophrenia (Green et al., 2011). If reduced BDNF signaling in schizophrenia plays a role in the reduction in GAD65 protein levels within boutons, a reduction in GAD65 mRNA, and cognate protein, within inhibitory neurons in the auditory cortex of subjects with schizophrenia may be a consequence.

It is important to consider alternative mechanisms beyond gene transcription that could contribute to a change in GAD65 protein levels during development and in schizophrenia. Although translational mechanisms involved in GAD65 protein synthesis have not yet been elucidated, regulation of this process could change during development or be affected in schizophrenia. Future studies comparing GAD65 mRNA and protein levels in deep layer 3 of primary auditory cortex of subjects with schizophrenia may be able to distinguish between transcriptional and translational mechanisms of GAD65 protein reduction in schizophrenia, or during development. Another important step in GAD65 protein availability is its targeting to the presynaptic bouton, where it synthesizes GABA for packaging into vesicles. A dynamic palmitoylation and depalmitoylaion cycle is responsible for shuttling GAD65 back and forth between the golgi apparatus and the presynaptic bouton (Kanaani et al., 2008). It will be important to further determine whether neuronal activity, developmental influences, and schizophrenia impact the mechanism targeting GAD65 to the presynaptic bouton. Future studies

could address this by quantifying levels of GAD65 protein within the cell soma to determine if there is a relative increase in somal GAD65 protein in schizophrenia, which would be suggestive of a failed transport mechanism. Further, it may be that protein degradation is altered in individuals with schizophrenia. GAD65 is reported to have a relatively longer half-life when compared to GAD67 (Christgau et al., 1991), however if protein stability or degradation is affected in schizophrenia this could potentially cause a reduction in within-bouton GAD65 protein.

Finally, it must be noted that we cannot definitively infer GABA synthesis activity from levels of GAD65 protein. Several activity-dependent mechanisms are in place to regulate the GABA synthesizing activity of GAD65. First, GABA synthesis by GAD65 is highly activity dependent (Martin et al., 1991). GAD65 exists mainly in the inactive apoenzyme form, and binding to its cofactor, pyridoxal 5'-phosphate (PLP), is required for conversion to the active holoenzyme form. Factors promoting formation of the holoenzyme include free inorganic phosphate, which may originate from the breakdown of ATP during synaptic activity, while ATP itself actually competes for the PLP binding site and prevents formation of the holoenzyme (Battaglioli et al., 2003). Therefore, increased metabolism of ATP during high levels of synaptic activity favors the conversion of apoGAD65 to holoGAD65 to promote increased GABA synthesis. In vitro, GAD65 is activated via phosphorylation by protein kinase C (PKC) (Wei et al., 2004), thought to be mediated by PKCε, which is highly localized to presynaptic boutons in the brain (Tanaka and Nishizuka, 1994). Interestingly, inhibition of PKC *in vivo* protects against stress-induced cortical spine loss in rats (Hains et al., 2009). This could be further, albeit indirect, evidence that a decrease in GAD65 activity reduces the likelihood of spine elimination in the cortex. Regulator of G-protein signaling-4 (RGS4) is reported to be disrupted in

schizophrenia and plays a role in inhibiting PKC signaling (Mirnics et al., 2001). Excessive PKC signaling in individuals with schizophrenia would promote activation of GAD65, which could possibly offset the effects of reduced GAD65 protein on GABA synthesis. The complex regulation of GAD65-mediated GABA synthesis suggests that considering factors such as protein phosphorylation and synaptic bouton energy metabolism will aid our understanding of inhibitory transmission in schizophrenia and adolescent development.

6.2.3 Decrease in GAD65 protein as a signal for the end of adolescence

We cannot say with any certainty what the biological relevance of a reduction of GAD65 protein within inhibitory boutons at the end of adolescence might be. It has been proposed that LTD mechanisms play a role in adolescent spine pruning (Selemon, 2013). Therefore, the end of adolescence may be characterized by a down-regulation in LTD-promoting mechanisms in the cortex until rates of spine elimination and formation are balanced in adulthood (Zuo et al., 2005). Given the impairment in LTD in mice lacking GAD65 (Choi et al., 2002), and the observation that one form of LTD in the prefrontal cortex during adolescence is dependent on GABAergic signaling (Caballero et al., 2013), we speculate that a reduction in GAD65 at the end of adolescence could reduce the propensity for LTD-induced spine elimination and bring adolescent spine pruning to a close. Of interest, spinophilin, like GAD65, is necessary for long term depression (LTD), as knockout animals for either protein show LTD impairments (Feng et al., 2000;Choi et al., 2002). Evidence suggests that both proteins are important for LTD as well as spine elimination, as spinophilin knockout mice actually show an increase in spine density in the CA3 region of the hippocampus (Feng et al., 2000), and GAD65 KO mice are also reported to have an increased density of spines (Mataga et al., 2004). We propose that, if LTD contributes

to spine elimination during adolescence (Selemon, 2013), and spinophilin and GAD65 are necessary for LTD, then increased levels of spinophilin and GAD65 protein prior to or early in adolescence may induce a favorable environment for adolescent spine pruning. It is interesting that both within-spine levels of spinophilin protein and within-bouton levels of GAD65 protein decrease between early adolescence and young adulthood in mouse auditory cortex (chapter 4). When we consider our results together with results from a study of spinophilin protein in rat cortical homogenate (Allen et al., 1997) we see that spinophilin protein levels in cortex increase during postnatal development, and then decrease between early adolescence until adulthood. Similarly, when we interpret our GAD65 protein findings together with a study of GAD65 protein levels in the auditory cortex during postnatal development (Xu et al., 2010), we see that GAD65 protein levels increase through the end of adolescence, then decline by young adulthood. Reductions in levels of spinophilin and GAD65 protein during the course of adolescence and young adulthood may shift the balance away from spine elimination and promote spine stability to slow down the process of spine pruning. It will be important to determine in future studies if the within-spine and within-bouton trajectories of these two proteins occurs across cortical regions during adolescence or is a feature unique to auditory cortex. The reduction in GAD65 protein in auditory cortex of subjects with schizophrenia could stem from an increased reduction in GAD65 levels as a consequence of spine over-pruning, as a compensatory response to excessive spine elimination. If spinophilin levels are also co-regulated with spine loss, then there may also be a reduction in within-spine levels of spinophilin protein in individuals with schizophrenia. This has not yet been thoroughly addresssed in auditory cortex; however, spinophilin protein levels in auditory cortex homogenate appear to be unchanged in schizophrenia (Deo et al., 2013), consistent with evidence that spinophilin mRNA levels are

unaltered in prefrontal cortex (Weickert et al., 2004; Ide and Lewis, 2010). Unaltered levels of spinophilin may be evidence of a failed compensatory mechanism in schizophrenia. If a decrease in within-spine spinophilin protects against loss of spines, then this could represent a potential therapeutic target for preventing or mitigating spine loss in schizophrenia. Future studies done to determine if spinophilin is altered within dendritic spines in individuals with schizophrenia will further inform our understanding of the relationship between spinophillin protein levels and spine loss in schizophrenia.

6.2.4 Evidence for independent regulation of excitatory boutons and spines

We observed a reduction in numbers of VGluT1-expressing presumptive excitatory boutons between early adolescence and young adulthood in the mouse in Chapter 4, suggesting that these components of auditory cortex circuits undergo refinement during adolescence in parallel with dendritic spine pruning. A caveat to our interpretation is that our findings of unchanged density and number of excitatory boutons in primary auditory cortex of subjects with schizophrenia does not support a model where pre and postsynaptic components of excitatory axospinous synapses are concurrently over-pruned during adolescence. Despite the fact that they did not demonstrate evidence of dendritic spine reduction between early adolescence and young adulthood, we observed evidence of reduction in intracortical excitatory bouton number in the kalirin KO mice, paralleling the changes in WT mice. Both the human postmortem schizophrenia findings and the findings from adolescent development in the kalirin KO suggest that dendritic spines can be eliminated without a corresponding elimination of presynaptic excitatory boutons. Evidence supporting differential regulation of spines and bouton dynamics comes from *in vivo* imaging in mouse sensory cortex, where spines exhibit higher rates of turnover than boutons (Majewska et

al., 2006). It may be that independent LTD mechanisms contribute to spine and bouton loss during adolescent excitatory synapse pruning. For example, a form of presynaptic NMDA receptor-mediated LTD has been shown to operate independently of postsynaptic signaling, and could be a mechanism for presynaptic depression prior to synapse elimination during development (Rodriguez-Moreno et al., 2013). Different postsynaptic contacts of excitatory boutons may also impact the stability of the bouton. In monkey primary visual cortex, numbers of shaft and spine synapse reach a developmental plateau at approximately the same age, but numbers of spine synapses undergo a much more dramatic reduction during puberty than shaft synapses (Bourgeois and Rakic, 1993). Variation in the ratios between shaft and spine excitatory synapses during pre- and postnatal development suggests that there could be different mechanisms regulating these two synapse types. Taken together, these findings suggest differential regulation of spines and boutons during adolescent development and potentially also in schizophrenia. Future studies should be done to examine levels of proteins which have been shown to mediate shaft synapse formation, such as GRIP1 and ephrinB3 (Aoto et al., 2007) in auditory cortex of subjects with schizophrenia. Further work examining the molecular mechanisms which regulate pruning of excitatory boutons, and importantly, spine- versus shaft-targeting boutons, will further inform interpretations of the disconnect between excitatory boutons and spines in auditory cortex of individuals with schizophrenia.

6.2.5 Adolescence as a window of opportunity for preventative measures

Evidence suggests that neuropathological changes are occurring in auditory cortex during the time building up to onset of schizophrenia. Reductions in gray matter volume of Heschl's gyrus and planum temporale are reported in patients in both cross-sectional and longitudinal studies

(Kwon et al., 1999a; Hirayasu et al., 2000; Kasai et al., 2003; Smiley et al., 2009). First episode psychosis patients and ultra-high risk individuals who later develop psychosis show longitudinal reductions in superior temporal gyrus gray matter (Takahashi et al., 2009). Longitudinal gray matter deficits that develop across adolescence in very early onset (< 12 years of age) schizophrenia patients progress in a manner that recapitulates what is reported in normal development, with deficits in superior temporal gyrus and prefrontal cortex appearing last (Thompson et al., 2001). These changes in gray matter likely have functional consequences, as reductions in MMN responses to frequency and duration deviants are correlated with reduction in volume of Heschl's gyrus (Rasser et al., 2011) and this relationship is already present at the first psychotic episode (Salisbury et al., 2007). Also, groups at high risk of developing schizophrenia demonstrate impairments in auditory working memory, verbal memory, and verbal processing (Simon et al., 2007). This evidence suggests that alterations in auditory cortex gray matter and symptoms which might stem from abnormal auditory processing are beginning to take shape during adolescence, and suggest that this is a time when prevention is needed to halt or reverse pathological processes.

We have presented evidence suggesting that adolescence is a time when both dendritic spine density and within bouton levels of GAD65 protein are decreasing in auditory cortex. Both of these are reduced in deep layer 3 of the auditory cortex of subjects with schizophrenia, and furthermore, the reductions are correlated. We have proposed that abnormal regulation of adolescent synapse pruning may lead to excessive reductions in dendritic spines and GAD65 protein in auditory cortex of subjects with schizophrenia. Based on the review in the previous sections, it may be that GAD65 reduction within inhibitory boutons is a consequence of dendritic spine pruning and occurs as a compensatory mechanism to balance excitation and inhibition, or

to reduce the likelihood of spine elimination. Blocking GAD activity and genetic ablation of GAD65 in animals increases spine density (Murphy et al., 1998; Mataga et al., 2004), or prevents plasticity-induced spine loss (Fagiolini and Hensch, 2000). Therefore, manipulating levels of GAD65 in the prodromal phase or early stages of the illness could be a strategy to prevent or mitigate spine loss.

6.3 DIFFERENCES BETWEEN PREFRONTAL AND AUDITORY CORTEX SYNAPSE DEFICITS IN SCHIZOPHRENIA: INSIGHTS FROM KALIRIN

An important question that arises from the experimental results presented here is, are the findings we observed in auditory cortex in subjects with schizophrenia consistent across brain regions? Similarly, do our findings of development of synaptic components in auditory cortex between early adolescence and young adulthood generalize across cortical regions? Primary auditory cortex shares many features common to all neocortical regions, and in particular shares similarity with other primary sensory regions such as primary somatosensory and visual cortices (Linden and Schreiner, 2003). An important difference between sensory areas, at least in humans, is that imaging studies suggest that postnatal developmental changes in auditory cortex gray matter volume are more protracted than in primary visual and primary somatosensory cortices (Gogtay et al., 2004; Shaw et al., 2008), so in this respect auditory cortex is more similar to frontal cortical regions. In humans, spine density in primary auditory cortex peaks at a later age than in visual cortex, but at a slightly earlier age compared to frontal cortex (Huttenlocher and Dabholkar, 1997).

A number of the excitatory and inhibitory synapse abnormalities that have been identified in primary auditory cortex of subjects with schizophrenia have been recapitulated in the prefrontal cortex, but some features appear to differ between the two regions (**Table 6.1**). Some of the similarities in findings between the two regions include a decrease in pyramidal neuron somal volume (Pierri et al., 2001; Sweet et al., 2004) with no accompanying reduction in pyramidal neuron number (Thune et al., 2001; Dorph-Petersen et al., 2009b). A deficit in dendritic spine density exists in both the dorsolateral prefrontal cortex and auditory cortex in subjects with schizophrenia (Glantz and Lewis, 2000; Sweet et al., 2009). Reduced density of synaptophysin-immunoreactive axon boutons is present in primary auditory cortex of subjects with schizophrenia (Sweet et al., 2007) while immunoreactivity for synaptophysin is decreased in prefrontal cortex (Glantz and Lewis, 1997). In prefrontal cortex neurons, levels of synaptophysin mRNA per neuron are unchanged (Glantz et al., 2007), suggesting it is not likely that reduced bouton density is attributable to reduction in within-bouton synaptophysin content, although this has not been ruled out. The density of GAD65-expressing boutons is unchanged in both auditory and prefrontal cortex of subjects with schizophrenia (Moyer et al., 2012) (chapter 3); (Benes et al., 2000). In the auditory cortex, we found that densities of VGluT1-expressing intracortical excitatory and VGluT2-expressing thalamocortical excitatory boutons, and within-bouton VGluT protein levels, are unaltered in individuals with schizophrenia (Moyer et al., 2013) (chapter 2). Intracortical excitatory and thalamocortical bouton densities and VGluT protein levels have not yet been assessed in prefrontal cortex, however findings of both unchanged and decreased VGluT1 mRNA have been reported for individuals with schizophrenia (Oni-Orisan et al., 2008; Fung et al., 2011). Results are also conflicting for levels of GAD65 mRNA in prefrontal cortex, although two reports agree that protein levels are unchanged in

prefrontal cortex in schizophrenia (Guidotti et al., 2000; Dracheva et al., 2004). This is in contrast to what we have observed in the auditory cortex (Moyer et al., 2012) (chapter 3) where within-bouton GAD65 protein is significantly reduced.

Studies of kalirin in schizophrenia have also yielded results that differ between auditory and prefrontal cortical areas. One study has reported reduced mRNA expression of kalirin in the prefrontal cortex of subjects with schizophrenia, correlated with reduced spine density in the same region (Hill et al., 2006). This study was done using probes specific for the kalirin-7 and kalirin-5 isoforms, suggesting that expression of these two isoforms is reduced in schizophrenia. A Western blot study evaluated levels of kalirin-7 protein in the anterior cingulate and dorsolateral prefrontal cortex and found reductions in both regions in subjects with schizophrenia (Rubio et al., 2012). In contrast, a recent study found no change in levels of kalirin-7 protein in primary auditory cortex of subjects with schizophrenia and an increase in protein levels of kalirin-9 (Deo et al., 2012). This indicates that kalirin isoforms are differentially altered in different cortical regions in schizophrenia. Further support for different functional roles of kalirin between frontal and auditory cortex comes from evidence demonstrating that global loss of kalirin reduces spine density in the frontal cortex, but does not alter density of dendritic spines in the hippocampus (Cahill et al., 2009). However, it should be noted that kalirin-7 specific knockout mice are reported to have reduced dendritic spine density in the hippocampus (Ma et al., 2008); although this could be attributable to up-regulation in kalirin-9 and kalirin-12 expression (Penzes and Remmers, 2012). Our findings indicate that global loss of kalirin also does not lead to an overall reduction in dendritic spine density in the superficial layers of the auditory cortex (chapter 4). Therefore, kalirin expression may be particularly important in regulating spine stability in frontal cortex, and global loss of kalirin (Cahill et al., 2009) or

reduced kalirin expression in schizophrenia (Hill et al., 2006) may decrease spine stability and lead to spine loss in that region. In contrast, kalirin, may not be critical for regulating stability of spines in primary auditory cortex, and kalirin expression may be affected in schizophrenia in such a way that the kalirin-9 isoform is actually overexpressed. Further in support of differential regulation of kalirin between cortical regions in schizophrenia, levels of PAK1, a downstream target of kalirin signaling, are unchanged in the auditory cortex (Deo et al., 2013), and are reported to be elevated, although with decreased phosphorylation in the prefrontal cortex of subjects with schizophrenia (Rubio et al., 2012). Taken together, the above evidence suggests that while there may be some global pathological features common to multiple cortical regions in schizophrenia, it should be noted that not all postmortem findings from schizophrenia studies can be assumed to be consistent between cortical regions.

Table 6.1. Comparison of results of postmortem studies of synapse components in primary auditory cortex of subjects with schizophrenia with findings from prefrontal cortex.

Component	Primary auditory cortex	Prefrontal cortex
Pyramidal neuron somal volume	↓ (Sweet et al., 2004)	↓ (Pierri et al., 2001)
Pyramidal neuron number	↔ (Dorph-Petersen et al., 2009)	↔ (Thune et al., 2001)
Spines	↓ spine density (Sweet et al., 2009)	↓ spine density (Glantz and Lewis, 2000)
Boutons **Intracortical excitatory** **Thalamocortical** **Inhibitory**	↓ synaptophysin bouton density (Sweet et al., 2007) ↔ Intracortical excitatory bouton density (Moyer et al., 2013) ↔ Thalamocortical bouton density (Moyer et al., 2013) ↔ GAD65-expressing bouton density (Moyer et al., 2012)	↓ synaptophysin bouton density (Glantz and Lewis, 1997) ↔ GAD65-expressing bouton density (Benes et al., 2000)
GAD65	↓ protein (Moyer et al., 2012)	↔ mRNA, protein (Guidotti et al., 2000) ↑ mRNA, ↔ protein (Dracheva et al, 2004)
VGluT	↔ VGluT1 protein (Moyer et al., 2013) ↔ VGluT2 protein (Moyer et al., 2013)	↓ VGluT1 mRNA (Eastwood and Harrison, 2005) ↔ VGluT1 mRNA (Fung et al, 2011)
Kalirin	↑ protein (kalirin-9) (Deo et al., 2012) ↔ protein (kal-7, -5, -12) (Deo et al., 2012)	↓ protein (kalirin-7) (Rubio et al., 2012) ↓ mRNA (kalirin-7) (Hill et al., 2006)
PAK1	↔ protein (Deo et al., 2013)	↓ PAK1 phosphorylation (Rubio et al., 2012) ↑ PAK1 protein (Rubio et al., 2012)

6.4 CONSIDERATIONS IN THE USE OF GENETIC MOUSE MODELS OF SCHIZOPHRENIA NEUROPATHOLOGY

There are no animal models that are able to recapitulate all of the clinical features observed in individuals suffering from schizophrenia (Arguello and Gogos, 2006). Modeling the heterogeneous symptoms of a complex and uniquely human neurodevelopmental disorder such as schizophrenia is a particularly challenging task (Powell and Miyakawa, 2006). Animal models of schizophrenia have been developed using four main approaches: developmental, pharmacological, lesion, or genetic manipulation (Jones et al., 2011). Genetic models have been developed to replicate genomic, mRNA, and protein-level changes observed in schizophrenia. Some of the most well-characterized genetic models are knock-out and knock-down models for DISC1 (Jaaro-Peled, 2009), neuregulin and ErbB4 (Mei and Xiong, 2008), dysbindin (Karlsgodt et al., 2011), and reelin (Krueger et al., 2006). In the present studies, we have used the kalirin KO model to assess the consequences of genetically-mediated spine disruption on development of excitatory and inhibitory synapse components in auditory cortex and auditory cortex function between adolescence and young adulthood. In the following section we will discuss a number of caveats associated with the use of genetic mouse models which are relevant for the interpretations of our results.

To date, three different mouse models of kalirin loss of function have been developed. The knockout model that we used was generated through insertion of the neomycin resistance gene in place of exons 27 and 28, which encode the first GEF domain (KO) (Cahill et al., 2009). Another model is specific for the kalirin-7 isoform, and is generated by deleting its unique 3'-exon ($Kal7^{KO/KO}$) (Ma et al., 2008). A third model is another global knockout ($KalSR^{KO/KO}$) generated by targeting exon 13, within the spectrin repeat region (Mandela et al., 2012). This

group also examined a variation where the knockout was restricted to the nervous system under control of the nestin promoter, to distinguish between nervous system specific and peripheral effects of kalirin loss.

When interpreting findings in global gene knockout animal models, it is important to consider that effects could be attributable to loss of the gene throughout embryonic and postnatal development. In the present studies, we examined auditory cortex synaptic components and function in the kalirin KO during a developmental window between early adolescence and young adulthood. However, absence of kalirin protein likely contributes to effects outside of this developmental window. For example, expression of kalirin-7 is up-regulated during postnatal development in the hippocampus and suggests a role of kalirin-7 in synaptogenesis (Ma et al., 2003; Ma et al., 2008). Although evidence suggests that a normal number of dendritic spines are present in the frontal cortex of kalirin KO mice prior to adolescence (Cahill et al., 2009) we cannot conclude that spinogenesis in the auditory cortex of mice lacking kalirin occurred normally. Therefore, future studies will be necessary to determine whether synaptogenesis occurs normally in the auditory cortex of mice lacking kalirin. Another potential confounding factor is that compensatory changes can occur when loss of the gene of interest induces alterations in related or interacting factors. This makes it difficult to determine whether phenotypes are attributable to the loss of the gene of interest or compensatory changes in function of other genes. For this reason, expression levels of other GEFs in auditory cortex should be examined, to determine if changes in any of these could elicit the effects we observed in the kalirin KO mice. Despite these confounds, global gene knockout models do have translational relevance. Genetic disruptions that contribute to human disease are likely to be present throughout all stages of development, and may elicit some of the same compensatory

changes and alterations in developmental processes that occur in a mouse model (Gingrich and Hen, 2000).

The unique molecular and physiological environments of different brain regions are also important to consider when interpreting the consequences of a genetic manipulation. For example, the effects of loss of kalirin on spines appear to differ between brain regions. The $Kal7^{KO/KO}$ mice demonstrate a reduction in hippocampal spine density, while the kalirin KO have reductions in frontal cortex spine density, but do not show alterations in hippocampal spine density (Cahill et al., 2009). However, the differences between these two models may be attributable to up-regulation of the kalirin-9 and kalirin-12 isoforms reported in the $Kal7^{KO/KO}$ mice, which only demonstrate a 25% loss of total kalirin protein despite the fact that kalirin-7 is thought to account for 75% of forebrain kalirin levels in adult mice (Ma et al., 2008). Kalirin-9 and kalirin-12 possess the second GEF domain capable of activating RhoA, activation of which is reported to enhance spine elimination (Newey et al., 2005). Up-regulation of these two isoforms may contribute to hippocampal spine elimination in $Kal7^{KO/KO}$, but not in kalirin KO mice. Kalirin disruption in schizophrenia also appears to differ between brain regions, as the kalirin-7 isoform is reduced in the prefrontal cortex of subjects with schizophrenia (Hill et al., 2006; Rubio et al., 2012) while the kalirin-9 isoform is increased in the primary auditory cortex (Deo et al., 2012). The global kalirin gene knockout eliminates all isoforms of the kalirin protein, which removes the potential confound that certain isoforms could be up-regulated to compensate for loss of another isoform. However, in future studies it will be of interest to examine effects of loss of specific kalirin isoforms on primary auditory cortex synapse components and function. Future studies specifically targeting the kalirin-9 isoform will be

useful to determine whether we can model schizophrenia-relevant effects of kalirin-9 in the mouse auditory cortex.

Strain background has long been recognized as a potential confounding factor in interpreting studies of genetic models (Gerlai, 1996). There are numerous genetic differences between inbred mouse strains that have the potential to interact with the phenotypic effects attributable to loss of kalirin (Taft et al., 2006). Therefore, kalirin ablation could yield different phenotypic effects in different mouse strains. It is also possible that the changes in synaptic components across adolescence in the WT mice that we presented may vary between strains. However, the influence of background strain on knockout mouse phenotype does contribute translational relevance, as humans with disease also have varying genetic backgrounds. Therefore, studying knockout models of kalirin and other relevant genes in multiple strain backgrounds may help to identify gene interaction effects that contribute to the expression of schizophrenia symptoms (Gingrich and Hen, 2000).

An important consideration in our study is the effect of inbred strain background on the function of the auditory system. The C57Bl/6 background demonstrate progressive hearing loss and associated auditory cortex plasticity that is evident behaviorally beginning around 3-4 months of age (Willott et al., 1993), while anatomical changes in the cochlea are already present at 3 months of age (Spongr et al., 1997). Therefore, a caveat of our interpretation that excitatory and inhibitory synapse components in the auditory cortex change across adolescence and young adulthood is that they could be attributable to plasticity in the auditory cortex induced by the early stages of high frequency hearing loss. Future studies should be done to examine auditory cortex changes across adolescence in a strain which does not exhibit high frequency hearing loss

during adolescence, such as the CBA/CaJ, which would differentiate between changes attributable to adolescence and to hearing loss.

Finally, it is important to consider that inbred strains differ in performance in behavioral tasks used to evaluate validity of schizophrenia models. For example, and most relevant for interpretation of our findings, magnitude of the acoustic startle reflex and prepulse inhibition varies substantially between different inbred strains (Paylor and Crawley, 1997; Bullock et al., 1997; Willott et al., 2003). Although hearing loss would be expected to impair measurement of acoustic startle reflex and PPI using acoustic stimuli, ASR and PPI are not correlated with measures of hearing ability such as the acoustic brainstem response within strains (Willott et al., 2003). Considered together with many other strains, the C57Bl/6J strain is reported to have low to middle range ASR and PPI responses. A mid-range level of PPI is ideal because it allows for evaluation of genetic manipulations that result in both increased and decreased levels of PPI. However, we observed relatively lower PPI responses to gap compared to noise prepulse stimuli, which may have made it more difficult to observe reductions in gap-PPI in kalirin KO. Further, an already reduced level of noise-PPI in general in young adult kalirin KO mice contributes substantial ambiguity to our assessment of gap-PPI. Finally, the range of PPI may be constrained in the kalirin KO mice due to reduced ASR, which could further confound PPI comparisons between KO and WT mice. Therefore, future studies should be done using an alternate behavioral paradigm to assess gap detection, such as conditioned suppression (Heffner et al., 2006).

6.5 CONCLUSIONS

In summary, evidence from electrophysiological, *in vivo* imaging, and postmortem tissue studies all suggest disruptions of the primary auditory cortex in individuals with schizophrenia. Improper functioning of the auditory cortex is likely to underlie behavioral deficits in auditory processing, contributing to certain aspects of negative and cognitive symptoms. In this thesis, we investigated the contributions of excitatory and inhibitory presynaptic boutons to primary auditory cortex neuropathology. We also examined the developmental trajectories of excitatory and inhibitory synapse components in the mouse primary auditory cortex. This facilitates the interpretation of our findings of excitatory and inhibitory synaptic structure deficits in the context of the adolescent neurodevelopmental hypothesis of schizophrenia. Our results indicate that there are correlated reductions in within-bouton GAD65 protein and dendritic spine density in the primary auditory cortex of subjects with schizophrenia. In mouse auditory cortex, we found that within-bouton GAD65 protein decreases between late adolescence and young adulthood, subsequent to the onset of dendritic spine pruning in the auditory cortex between early adolescence and young adulthood. The fact that we observed increases in a behavioral readout of auditory cortex functional integrity in the mouse during adolescence suggests that normal pruning of excitatory synaptic components in primary auditory cortex across adolescence may be important for auditory cortex function.

Based on our findings, we propose a model where spines may be over-pruned in the auditory cortex of subjects with schizophrenia, accompanied by a subsequent excessive reduction in GAD65 protein. Co-occurring deficits in components of excitatory and inhibitory synapses likely contribute to the auditory processing impairments that may underlie features of schizophrenia such as abnormal perception of semantic and emotional aspects of language,

ultimately contributing to poor functional outcome in patients. As both spines and GAD65 protein levels undergo changes during and following adolescence, the time period between early adolescence and young adulthood may be a developmental window of opportunity for mitigating or reversing these pathological features of primary auditory cortex in schizophrenia. For example, our findings suggest that early adolescence may be a time period to intervene to prevent excessive spine pruning, and the late adolescent period could be targeted with measures to prevent excessive within-bouton GAD65 reduction. Preventing the deficit in spine pruning may help to normalize electrophysiological measures of auditory processing that are dysfunctional in schizophrenia, such as the mismatch negativity response, which may depend on activity of supragranular excitatory synapses. To inform the development of strategies to prevent the dendritic spine deficit in schizophrenia, future work should be done to increase our understanding of how molecular factors such as GAD65 and spinophilin may be involved in processes which promote or prevent spine elimination during adolescence.

Lower levels of GAD65 protein within inhibitory boutons may contribute to the abnormal oscillatory and steady state responses observed in individuals with schizophrenia, and this could be determined using animal models. It is possible that normalizing GAD65 protein levels within inhibitory boutons in auditory cortex could improve auditory processing in individuals with schizophrenia. However, future studies are needed to determine whether decreased GAD65 protein in the auditory cortex in schizophrenia is a compensatory response to mitigate excessive spine loss. If so, blocking the reduction in GAD65 during adolescence could lead to an even greater reduction of spines in the auditory cortex of individuals with schizophrenia. In this case, promoting an earlier onset of, or enhancing the reduction in GAD65 protein within auditory cortex inhibitory boutons may prove to be an effective strategy to slow excess spine pruning.

Future mechanistic studies in animal models and *in vitro* studies will aid the development of strategies to address deficits in both dendritic spines and within-bouton GAD65 protein in primary auditory cortex, and may help to reduce the severity of symptoms affected by poor auditory processing and ultimately improve long term functional outcome of individuals with schizophrenia.

APPENDIX A

CHAPTER 2 SUPPLEMENTAL MATERIALS

A.1 SUPPLEMENTAL METHODS

Table A.1. Control and schizophrenia subject characteristics for cohort 1 (top, green) and cohort 2 (bottom, blue). Abbreviations: S/R/A, Sex/Race/Age; PMI, postmortem interval; Hand, handedness; Meds ATOD, medications used at time of death; ASCVD, atherosclerotic coronoary vascular disease; AAC, Alcohol Abuse, current at time of death; AAR, Alcohol Abuse, in remission at time of death; ADC, Alcohol Dependence, current at time of death; ADR, Alcohol Dependence, in remission at time of death; OAC, Other Substance Abuse, current at time of death; ODC, Other Substance Dependence, current at time of death; ODR, Other Substance Dependence, in remission at time of death; L, Left; M, Mixed; R, Right; U, Unknown; B, Benzodiazepines; C, Anticonvulsants; D, Antidepressants; L, Lithium; N, No medications; O, Other medication(s); P, Antipsychotic; PA, Atypical Antipsychotic; PT, Typical Antipsychotic; U, Unknown; antipsychotic medication denoted by lowercase letter: ch, chlorpromazine; cl, clozapine; f, fluphenazine; h, haloperidol; l, loxapine; m, mesoridazine; o, olanzapine; p, perphenazine; r, risperidone; th, thiothixene; tr trifluoperazine; un, unspecified. Living independently ATOD: Y, yes; N, no. Tobacco use current ATOD: Y, yes; N, no; U, unknown. *Control subject 396 tested positive for benzodiazepines at autopsy; **Control subject 987 diagnosed with post traumatic stress disorder- in remission 39 years. ‡Schizophrenia subject 1010 diagnosed with mild mental retardation.

Control Subjects								Schizophrenia Subjects									
Pair	Case	S/R/A	Hand	PMI (h)	Storage Time (mos)	Cause of Death	Tobacco ATOD	Case	S/R/A	Hand	PMI (h)	Storage Time (mos)	Cause of Death	Diagnosis	Meds ATOD	Living Independently ATOD	Tobacco ATOD
Cohort 1																	
1	250	F/W/47	R	5.3	211.2	ASCVD	N	398	F/W/41	U	10.3	166.9	Pulmonary embolism	Schizoaffective disorder	B,C,O,P_T: th	N	U
2	620	M/W/64	R	17.3	139.3	Accidental drowning	U	566	M/W/63	R	18.3	148.7	ASCVD	Undifferentiated schizophrenia, AAR	B,D,O,P_A: r	N	Y
3	681	M/W/51	R	11.6	131.6	Hypertrophic cardiomyopathy	N	234	M/W/51	R	12.8	214.1	Cardiomyopathy	Paranoid schizophrenia	N	Y	N
4	643	M/W/50	R	24	136.4	ASCVD	U	581	M/W/46	M	28.1	146.3	Accidental combined drug overdose	Paranoid schizophrenia, ADC, OAC	B,C,O,P_T: h	Y	U
5	634	M/W/52	L	16.2	137.5	ASCVD	U	625	M/B/49	R	23.5	138.7	ASCVD	Disorganized schizophrenia, AAC	D,O,P_T: f	N	Y
6	474	F/B/49	U	13.4	166.8	Hypertensive cardiovascular disease	U	656	F/B/47	R	20.1	134.9	Suicide by gun shot	Schizoaffective disorder, ADC	O,P_A: o	Y	Y
7	396*	M/W/41	L	17.5	167.1	ASCVD	Y	408	M/W/46	R	19.8	185.5	ASCVD	Paranoid schizophrenia	B,D,O,P_T: tr	Y	Y
8	449	F/W/47	L	4.3	170.3	Accidental CO poisoning	U	517	F/W/48	R	3.7	155.7	Intracerebral hemorrhage	Disorganized schizophrenia, ADC	P_A: cl	N	Y
9	451	M/W/48	L	12	170.0	ASCVD	U	317	M/W/48	U	8.3	201.4	Bronchopneumonia	Undifferentiated schizophrenia	D,L,O,P_T: l	N	U
10	178	M/W/48	R	7.8	221.9	ASCVD	U	377	M/W/52	R	10.0	192.7	GI bleeding	Undifferentiated schizophrenia, ADC	O,P_T: h	Y	N
11	412	M/W/42	R	14.2	184.5	Aortic stenosis	N	466	M/B/48	U	19.0	168.0	ASCVD	Undifferentiated schizophrenia	O,P_A: cl	N	U
12	285	F/W/27	R	16.5	206.6	Trauma	U	587	F/B/38	R	17.8	144.9	Myocardial hypertrophy	Undifferentiated schizophrenia, AAR	B,L,O,P_A: cl, P_T: h	N	Y
13	575	F/B/55	R	11.3	146.8	ASCVD	Y	597	F/W/46	L	10.1	143.4	Pneumonia	Schizoaffective disorder	D,O,P_T: m	Y	Y
14	592	M/B/41	R	22.1	144.1	ASCVD	Y	450	M/B/48	L	22.0	170.2	Suicide by jumping	Undifferentiated schizophrenia, ADR, ODR, OAR	N	N	Y
15	452	F/W/40	R	14.3	169.9	ASCVD	N	341	F/W/47	L	14.5	198.8	Suicide by chlorpromazine overdose	Undifferentiated schizophrenia, AAC	O,P_T: ch	Y	Y
Cohort 2																	
1	700	M/W/42	R	26.1	131.6	ASCVD	U	533	M/W/40	R	29.1	156.7	Accidental asphyxiation	Undifferentiated schizophrenia	P_T: ch	N	U
2	806	M/W/57	R	24.0	113.1	Pulmonary thromboembolism	N	665	M/B/59	R	28.1	137.2	Intestinal hemorrhage	Paranoid schizophrenia, ADC	D,O,P_T: h	Y	Y
3	739	M/W/40	R	15.8	126.6	ASCVD	Y	1088	M/W/49	R	21.5	63.1	Accidental combined drug overdose	Undifferentiated schizophrenia, ADC, OAC	D,O,P: un	N	Y
4	822	M/B/28	L	25.3	110.5	ASCVD	N	787	M/B/27	L	19.2	116.7	Suicide by gunshot	Schizoaffective disorder, ODC	O,P_T: f	N	N
5	727	M/B/19	R	7.0	127.5	Trauma	N	829	M/W/25	U	5.0	108.4	Suicide by salicylate overdose	Schizoaffective disorder, ADC, OAR	B,C	N	Y
6	659	M/O/46	R	22.3	137.9	Peritonitis	Y	930	M/W/47	R	15.3	88.2	ASCVD	Disorganized schizophrenia, ADR, OAR	C,O,P_T: th	N	Y
7	1047	M/W/43	R	12.4	69.3	ASCVD	N	933	M/W/44	U	8.3	87.6	Myocarditis	Disorganized schizophrenia	C,D,O,P_A: o	N	N
8	852	M/W/54	R	8.0	102.9	Cardiac tamponade	Y	722	M/B/45	R	9.1	128.0	Upper GI bleed	Undifferentiated schizophrenia, ODR, OAR	B,O,P_T: h	N	Y
9	685	M/W/56	R	14.5	134.0	Hypoplastic coronary artery disease	U	1105	M/W/53	R	7.9	61.2	ASCVD	Schizoaffective disorder	P_A: o	N	Y
10	686	F/W/52	R	22.6	133.7	ASCVD	Y	802	F/W/63	M	29.0	113.7	Right ventricular dysplasia	Schizoaffective disorder, ADC, ODR	C,O,P_A: o, P_T: ch,f	Y	Y
11	987**	F/W/65	R	21.5	78.5	ASCVD	N	917	F/W/71	U	23.8	91.6	ASCVD	Undifferentiated schizophrenia	O,P_T: h,p	N	Y
12	1092	F/B/39	R	16.6	62.7	Mitral valve prolapse	N	1010‡	F/B/44	L	18.7	75.4	Sudden unexpected death	Undifferentiated schizophrenia	C,D,P_A: o	N	N

A.2 SUPPLEMENTAL RESULTS

A.2.1 VGluT1-IR puncta morphology

The mean volume ($F_{(1, 24.9)} = 2.70$, $p = 0.113$, 95% CI: (-0.03, 0.003)) and surface area ($F_{(1, 23.7)} = 1.72$, $p = 0.202$, 95% CI: (-0.05, 0.21)) of VGluT1-IR puncta were not different between schizophrenia and control subjects (data not shown). However, the mean shape complexity of VGluT1-IR puncta was significantly reduced by 1.3% in subjects with schizophrenia compared to controls ($F_{(1, 24.5)} = 4.74$, $p = 0.039$, 95% CI: (-0.02, -0.001)) (**Figure A.1**). We observed no effect of chronic haloperidol exposure on volume ($F_{(1, 3.02)} = 0.20$; $p = 0.684$, 95% CI: (-0.10, 0.07)), surface area ($F_{(1, 3.05)} = 0.24$; $p = 0.656$, 95% CI: (-0.81, 0.59)), or shape complexity ($F_{(1, 3)} = 0.27$; $p = 0.641$, 95% CI: (-0.01, 0.01)) of VGluT1-IR puncta in deep layer 3 of primary auditory cortex of the antipsychotic-exposed macaques (data not shown).

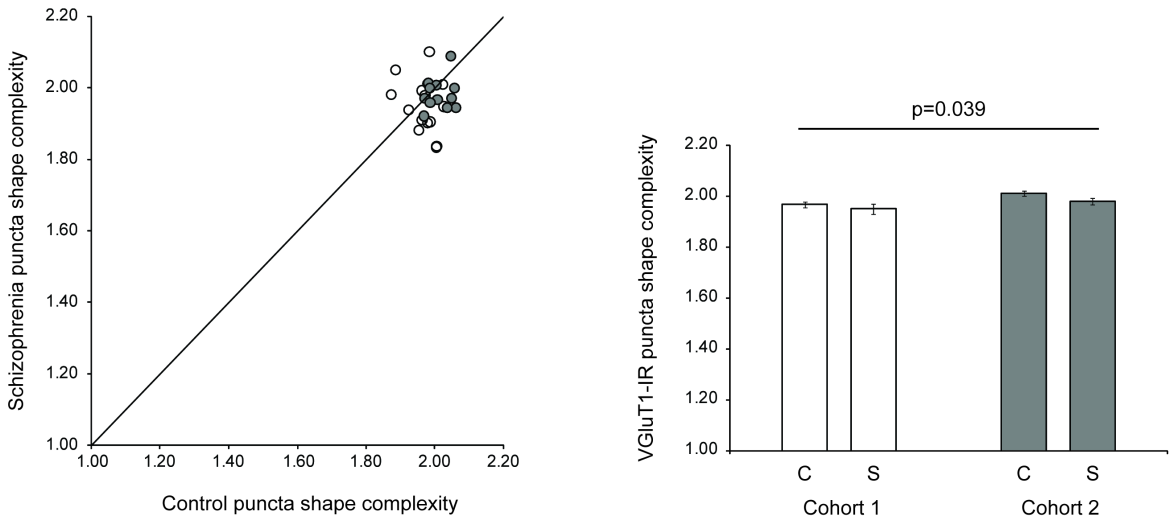

Figure A.1. VGluT1-IR bouton shape complexity. (Left) Mean VGluT1-IR puncta shape complexity for each schizophrenia-control subject pair in cohort 1 (open circles) and cohort 2 (gray circles). Reference line represents schizophrenia = control values, where points below the line indicate a pair where control > schizophrenia, and points above the line indicate schizophrenia > control. (Right) Diagnostic group mean puncta shape complexity for control (c) and schizophrenia (s) subjects in cohort 1 (open bars) and cohort 2 (gray bars). Error bars are ± SEM.

A.2.2 VGluT2-IR puncta morphology

There were no diagnostic group differences in primary auditory cortex deep layer 3 VGluT2-IR puncta volume ($F_{(1,142)} = 0.15$, $p = 0.702$, 95% CI: (-0.02, 0.01)), surface area ($F_{(1, 22.6)} = 0.27$, $p = 0.605$, 95% CI: (-0.16, 0.09)), or shape complexity ($F_{(1, 24.1)} = 1.52$, $p = 0.230$, 95% CI: (-0.001, 0.005)) (data not shown). Also, there were no changes in VGluT2- IR puncta volume ($F_{(1, 3.15)} = 2.60$; $p = 0.201$), surface area ($F_{(1, 3.09)} = 1.14$; $p = 0.361$), or shape complexity ($F_{(1, 6.95)} = 2.50$; $p = 0.158$) in the antipsychotic exposed monkeys (data not shown).

A.2.3 Association of clinical factors with VGluT1- and VGluT2-IR puncta measures

We tested for associations between VGluT1- and VGluT2-IR bouton characteristics and a number of clinical factors to determine if bouton alterations were associated with any sub-groups of schizophrenia subjects. Subjects living independently at time of death had a relative percent reduction in the fluorescence intensity of VGluT1-IR boutons, compared to those who were not living independently (living independently at time of death, mean percent change in fluorescence intensity (SD), Yes = 19.9 (29.3) % reduction relative to controls, No = 6.1 (29.1) % increase relative to controls; $t_{25} = -2.20$, $p = 0.037$). We also found that schizophrenia subjects living independently at time of death showed a relative reduction in the density of VGluT2-IR boutons compared to those subjects who were not living independently at time of death (living independent at time of death; mean percent change in density (SD), Yes = 14.2 (19.1) % reduction relative to controls, No = 5.7 (22.5) % increase relative to controls; $t_{25} = -2.27$; $p = 0.032$). These findings should be interpreted with caution as the analyses were not corrected for multiple comparisons. We did not identify any other significant relationships between other

bouton measures and clinical factors including living independently at time of death, diagnosis of schizoaffective disorder, antipsychotic use at time of death, class of antipsychotic, history of alcohol or other substance abuse, or death by suicide (**See Tables A.2 and A.3**). A number of both control and schizophrenia subjects were known to be using tobacco at time of death. We did not observe any associations between VGluT1- and VGluT2-IR bouton characteristics and tobacco use status at time of death (data not shown), suggesting tobacco use at time of death does not alter the characteristics of VGluT-IR boutons.

Table A.2. Relationship between VGluT1-IR puncta measurements and clinical variables. T test results showing that relative percent reductions in VGluT1-IR puncta density, fluorescence intensity, volume, surface area, and shape complexity are not different depending on whether the schizophrenia subject was living independently at time of death, had antipsychotic use current at time of death (ATOD), was taking typical or atypical antipsychotics ATOD, had a history of alcohol or substance abuse, died by suicide, or had a diagnosis of schizoaffective disorder (with the exception of independent living status and VGluT1-IR puncta fluorescence intensity, shown in bold).

	VGluT1-IR bouton density				VGluT1-IR bouton intensity				VGluT1-IR bouton volume				VGluT1-IR bouton surface area				VGluT1-IR bouton shape complexity			
	No Mean (SD)	Yes Mean (SD)	t_{25}	p	No Mean (SD)	Yes Mean (SD)	t_{25}	p	No Mean (SD)	Yes Mean (SD)	t_{25}	p	No Mean (SD)	Yes Mean (SD)	t_{25}	p	No Mean (SD)	Yes Mean (SD)	t_{25}	p
Living Independently ATOD	-6.10 (34.70)	4.61 (40.97)	-0.712	0.483	**-6.14 (29.10)**	**19.97 (29.32)**	**-2.20**	**0.037**	-7.74 (12.55)	-0.029 (8.79)	-1.65	0.112	-3.07 (6.82)	0.503 (6.30)	-1.31	0.201	1.53 (2.31)	0.373 (6.37)	0.693	0.495
Schizoaffective Disorder	0.365 (30.38)	-10.79 (52.28)	0.690	0.497	-4.16 (31.27)	21.77 (23.14)	-2.00	0.056	-6.17 (12.65)	-2.31 (9.41)	-0.74	0.469	-2.38 (7.13)	-0.453 (5.78)	-0.642	0.527	1.25 (3.90)	0.824 (4.71)	0.238	0.814
Antipsychotic ATOD	-12.10 (59.39)	-1.33 (34.40)	-0.475	0.639	-18.43 (5.73)	5.19 (32.11)	-1.25	0.223	-11.60 (19.75)	-4.36 (10.89)	-0.998	0.328	-4.20 (9.74)	-1.59 (6.52)	-0.624	0.538	2.53 (2.28)	0.968 (4.20)	0.626	0.537
History of Alcohol / Substance Abuse	5.71 (37.54)	-8.19 (35.80)	0.972	0.340	13.12 (29.34)	-4.70 (31.20)	1.49	0.148	-8.05 (10.47)	-3.19 (12.65)	-1.050	0.304	-3.78 (5.90)	-0.571 (7.17)	-1.23	0.231	1.19 (4.35)	1.11 (3.95)	0.056	0.956
Death by suicide	-3.38 (33.84)	1.24 (51.12)	-0.25	0.804	1.15 (32.52)	8.77 (26.59)	-0.486	0.631	-5.28 (10.88)	-4.69 (17.06)	-0.097	0.923	-1.94 (5.85)	-1.63 (10.79)	-0.09	0.928	1.21 (3.80)	0.857 (5.47)	0.172	0.865
	Typical Mean (SD)	Atypical Mean (SD)	t_{19}	p	Typical Mean (SD)	Atypical Mean (SD)	t_{19}	p	Typical Mean (SD)	Atypical Mean (SD)	t_{19}	p	Typical Mean (SD)	Atypical Mean (SD)	t_{19}	p	Typical Mean (SD)	Atypical Mean (SD)	t_{19}	p
Antipsychotic Class	-1.97 (31.38)	-3.86 (39.37)	-0.119	0.906	-3.38 (34.06)	-6.17 (22.71)	-0.194	0.848	-4.28 (15.76)	-7.53 (10.75)	-0.560	0.582	-1.78 (7.44)	-3.01 (7.52)	-0.357	0.725	0.676 (4.57)	1.52 (1.89)	0.466	0.646

Table A.3. Relationship between VGluT2-IR puncta measurements and clinical variables. T test results showing that relative percent reductions in VGluT2-IR puncta density, fluorescence intensity, volume, surface area, and shape complexity are not different depending on whether the schizophrenia subject was living independently at time of death (ATOD), had antipsychotic use current at time of death, was taking typical or atypical antipsychotics ATOD, had a history of alcohol or substance abuse, died by suicide, or had a diagnosis of schizoaffective disorder (with the exception of independent living status and VGluT2-IR puncta density, shown in bold).

	VGluT2-IR bouton density				VGluT2-IR bouton intensity				VGluT2-IR bouton volume				VGluT2-IR bouton surface area				VGluT2-IR bouton shape complexity			
	No Mean (SD)	Yes Mean (SD)	t_{25}	p	No Mean (SD)	Yes Mean (SD)	t_{25}	p	No Mean (SD)	Yes Mean (SD)	t_{25}	p	No Mean (SD)	Yes Mean (SD)	t_{25}	p	No Mean (SD)	Yes Mean (SD)	t_{25}	p
Living Independently ATOD	**-5.67 (22.46)**	**14.21 (19.06)**	**-2.27**	**0.032**	-5.23 (13.54)	-7.90 (29.00)	0.329	0.745	-4.45 (28.22)	-23.40 (48.04)	1.30	0.206	-4.14 (22.47)	-17.05 (32.63)	1.21	0.238	-0.633 (2.46)	-1.715 (2.58)	1.060	0.299
Schizoaffective Disorder	4.54 (18.57)	-9.29 (32.43)	1.39	0.177	-9.39 (20.03)	3.22 (15.48)	-1.51	0.144	-15.43 (39.43)	2.58 (22.11)	-1.14	0.265	-11.51 (28.58)	0.328 (17.59)	-1.02	0.316	-1.15 (2.54)	-0.536 (2.55)	-0.554	0.585
Antipsychotic ATOD	-10.78 (14.04)	2.42 (23.77)	-0.932	0.360	-9.93 (37.54)	-5.65 (17.47)	-0.353	0.727	3.10 (42.47)	-12.50 (36.05)	0.696	0.493	1.10 (36.64)	-9.64 (25.63)	0.657	0.517	-0.335 (4.15)	-1.08 (2.35)	0.476	0.638
History of Alcohol / Substance Abuse	3.75 (21.71)	-0.96 (24.49)	0.513	0.612	-12.82 (21.71)	-1.52 (17.00)	-1.52	0.142	-11.57 (47.52)	-10.21 (27.76)	-0.094	0.926	-8.58 (33.59)	-8.35 (21.32)	-0.021	0.983	-0.946 (3.17)	-1.03 (2.04)	0.081	0.936
Death by suicide	2.68 (20.46)	-6.63 (34.29)	0.809	0.426	-8.29 (18.97)	3.40 (21.07)	-1.22	0.233	-14.86 (37.25)	7.27 (27.46)	-1.25	0.225	-11.43 (26.74)	4.69 (22.54)	-1.25	0.224	-1.18 (2.48)	-0.161 (2.74)	-0.818	0.421
	Typical Mean (SD)	**Atypical Mean (SD)**	t_{19}	p	**Typical Mean (SD)**	**Atypical Mean (SD)**	t_{19}	p	**Typical Mean (SD)**	**Atypical Mean (SD)**	t_{19}	p	**Typical Mean (SD)**	**Atypical Mean (SD)**	t_{19}	p	**Typical Mean (SD)**	**Atypical Mean (SD)**	t_{19}	p
Antipsychotic Class	3.87 (24.94)	-5.65 (20.79)	-0.867	0.397	-14.03 (18.83)	-0.90 (17.69)	1.53	0.141	-21.51 (39.84)	3.54 (38.95)	1.37	0.187	-16.45 (27.79)	3.50 (30.42)	1.50	0.149	-1.78 (2.36)	0.60 (3.09)	1.97	0.063

A.3 SUPPLEMENTAL DISCUSSION

A.3.1 Methodological considerations

One must be cautious in the interpretation of measures of puncta volume and surface area (and the resulting shape complexity calculated from these two measures) using our approach. First, vesicular glutamate transporters are located in the vesicle membrane; therefore, VGluT-IR puncta may be more indicative of vesicle pools and do not necessarily reflect the entire volume and shape of the bouton. Second, the voxel size of our data set is 0.215 x 0.215 x 0.220 μm^3 resulting in a digitized estimation of the volume of each puncta that is derived from relatively few voxels, and is necessarily biased to some extent (Ziegel and Kiderlen, 2010). Moreover, the use of voxel-based measurements to estimate surface area is likely to be very biased, even when based upon high resolution data (Ziegel and Kiderlen, 2010). Because there is no way to estimate the magnitude of the bias, or whether it may differ between schizophrenia and control subjects, our finding of a significant difference in shape complexity should be interpreted conservatively pending replication via another approach.

A.3.2 Clinical and therapeutic implications of disconnect between spine loss and bouton preservation

It should be noted that antipsychotic treatment may up-regulate the expression of VGluT2. We observed nonsignificant increases in VGluT2-IR bouton density and fluorescence intensity in the chronic haloperidol exposed macaques relative to control macaques. This is not surprising given that previous studies have reported that VGluT2 protein expression is increased in prefrontal

cortex of mice after chronic haloperidol exposure (Moutsimilli et al., 2008). The haloperidol-induced increase in VGluT2 protein in auditory cortex boutons of antipsychotic-exposed macaques is likely mediated by the D_2 subtype of dopamine receptors located in the medial geniculate nucleus of the thalamus (Rieck et al., 2004). Increased expression of VGluT2 mRNA has been reported in the thalamus of subjects with schizophrenia (Smith et al., 2001), and one could speculate that this is a result of chronic antipsychotic treatment. We did not observe an increase in VGluT2 protein levels in our subjects with schizophrenia, although both cohorts trended in that direction. It is possible that VGluT2 protein expression is decreased in subjects with schizophrenia and chronic antipsychotic exposure normalized this effect by elevating VGluT2 expression. It is interesting that antipsychotic treatment is associated with increased VGluT2 expression, while our data suggest that decreased VGluT1 expression and decreased VGluT2-IR bouton density in the auditory cortex to be associated with better functional outcome (living independently at time of death). However, studies report that antipsychotic treatment has no effect on auditory MMN in patients with schizophrenia (Umbricht et al., 1998; Schall et al., 1998; Umbricht et al., 1999; Korostenskaja et al., 2005), while glutamatergic drugs do affect MMN (Javitt et al., 1996; Gunduz-Bruce et al., 2012). Therefore, up-regulation of VGluT2 mRNA in the thalamus may not have much of an effect on auditory stimulus processing in the primary auditory cortex of schizophrenia subjects treated with antipsychotics, despite beneficial effects of antipsychotic drugs on positive symptoms.

APPENDIX B

CHAPTER 3 SUPPLEMENTAL INFORMATION

B.1 SUPPLEMENTAL METHODS

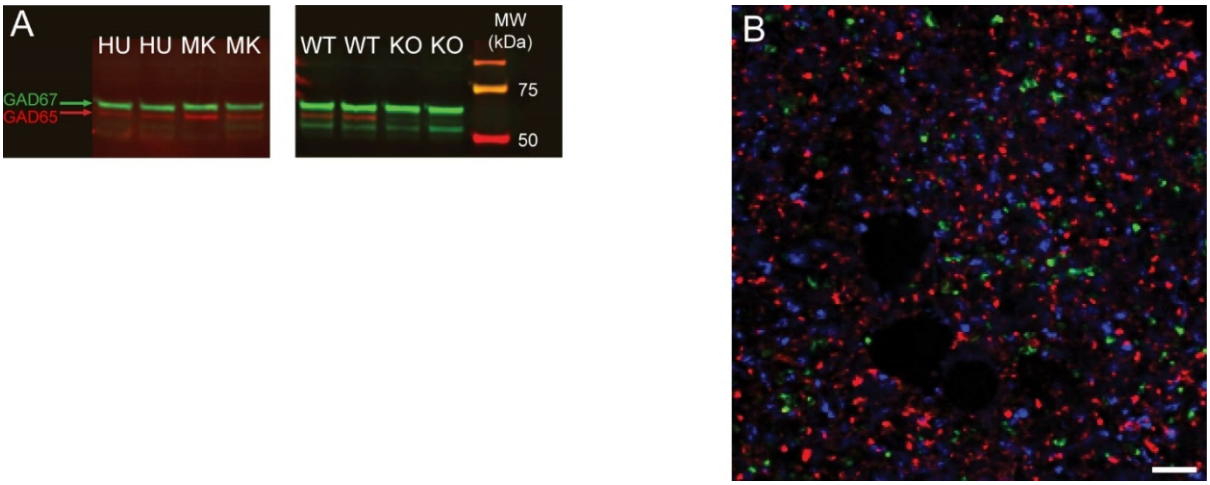

Figure B.1 Specificity of GAD65 antibody. (A) Western blot demonstrating labeling with mouse anti-GAD65 monoclonal antibody (Millipore) (red) showing specificity for the lower molecular weight isoform of GAD in human (HU) and monkey (MK). To demonstrate antibody specificity for the 65 kDa isoform, blots were labeled with rabbit anti-GAD67 antibody (Sigma-Aldrich) (green). Red channel intensity is shown increased for visualization purposes on left half of blot. Right half of blot shows GAD65 antibody labeling in wild type (WT) and GAD65-knockout (KO) mouse cortical gray matter. GAD65 immunoreactivity is absent in the GAD65-KO tissue, as expected. (B) Human auditory cortex labeled with the GAD65 antibody (blue), as well as antibodies against vesicular glutamate transporters, VGluT1 (red) and VGluT2 (green), to label intracortical and thalamocortical glutamatergic boutons, respectively. Projection image was processed with background subtraction and constrained iterative deconvolution (see **Chapter 3.2.5**). No colocalization is observed between GAD65 antibody and excitatory bouton markers. Scale bar is 10 μm.

B.2 SUPPLEMENTAL RESULTS

B.2.1 Clinical factors

We tested for associations between pair-wise changes in GAD65-IR mean bouton density, fluorescence intensity, and volume and a number of clinical confounds including: whether the subject had a diagnosis of schizophrenia or schizoaffective disorder, died by suicide, had a history of alcohol or other substance abuse, or was on or off antipsychotics, anticonvulsants, or benzodiazepines at time of death (**Figure B.2**). We found a significant relationship between benzodiazepine use at time of death and percent change in GAD65-IR bouton density ($t_{23} = 2.64$, $p = 0.015$). The mean (95% CI) percent change in bouton density for subject pairs in which the schizophrenia subject was taking benzodiazepines at time of death was a 17.7% (3.3%, 32.0%) increase relative to normal controls, and a 2.7% (-4.6%, 10%) decrease for subject pairs in which the schizophrenia subject was not taking benzodiazepines at time of death. Additionally, we determined that there was no effect of subjects' history of cannabis use or antidepressant use at time of death on the percent change in GAD65-IR mean bouton density, fluorescence intensity, or volume (data not shown; *Cannabis*: Intensity, $t_{22} = 0.06$, $p = 0.953$; Density, $t_{22} = 0.42$, $p = 0.677$; Volume, $t_{22} = 0.72$, $p = 0.481$; *Antidepressants*: Intensity, $t_{24} = -0.4$, $p = 0.692$; Density, $t_{24} = -0.22$, $p = 0.829$; Volume, $t_{24} = -1.52$, $p = 0.140$).

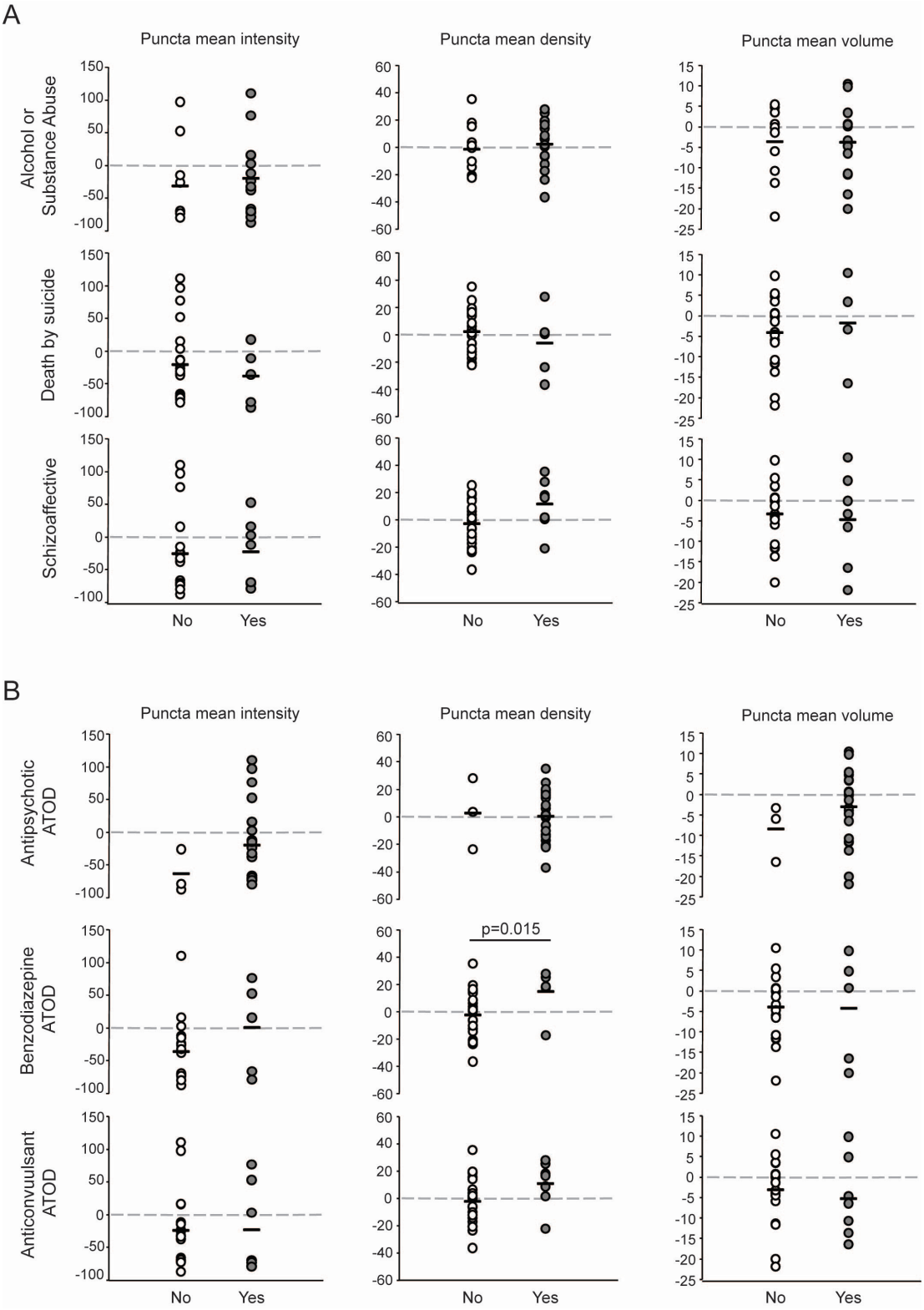

Figure B.2. Percent change in GAD65-immunoreactive (IR) puncta features associated with schizophrenia subject clinical features and medication status at time of death. (A) Percent change in GAD65-IR puncta

fluorescence intensity (left), density (middle) and volume (right) as a function of history of alcohol or substance abuse, death by suicide or diagnosis of schizoaffective disorder. (B) Percent change in GAD65-IR puncta fluorescence intensity (left), density (middle) and volume (right) as a function of current antipsychotic use at time of death, benzodiazepine use at time of death, or anticonvulsant drug use at time of death (ATOD). Dotted line at 0% indicates no difference between schizophrenia and control subject. Horizontal bars indicate group means.

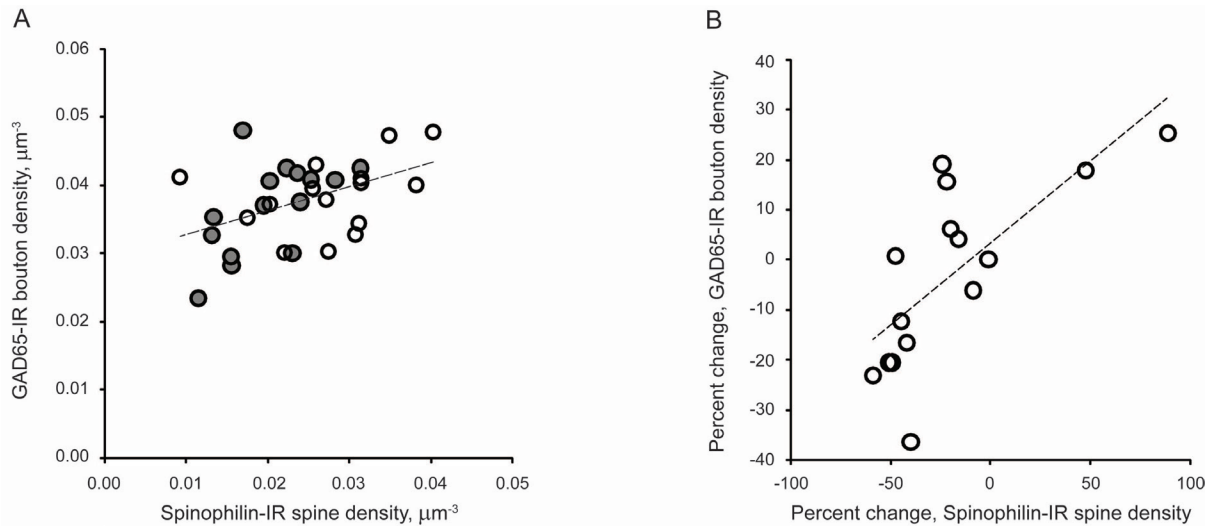

Figure B.3. Correlations between subject mean values and schizophrenia subject relative percent changes in GAD65-immunoreactive (IR) puncta density and spine density in primary auditory cortex. (A) Mean GAD65-IR puncta density plotted as a function of spinophilin-IR puncta density for each subject in cohort 1. Open circles = control, filled circles = schizophrenia. Dashed line represents the regression line (Pearson r = 0.457, p = 0.01). (B) The percent change in GAD65-IR puncta density plotted as a function of the percent change in spinophilin-IR puncta density for pairs in cohort 1 (schizophrenia subjects relative to matched controls). Dashed line represents the regression line (Pearson r = 0.718, p = 0.003).

B.3 SUPPLEMENTAL DISCUSSION

B.3.1 Clinical factors

GAD65-IR bouton fluorescence intensity, density, and volume did not differ between schizophrenia subjects who were on or off antipsychotic medication at time of death, or between monkeys chronically exposed to haloperidol and control monkeys. This suggests that the reduction in GAD65-IR bouton fluorescence intensity observed in subjects with schizophrenia is not an effect of antipsychotic medications. On the contrary, use of antipsychotic medications in our subjects may actually result in underestimation of the effect of disease on GAD65 fluorescence intensities, as we observed a non-significant trend toward increased GAD65-IR bouton fluorescence intensity in the antipsychotic exposed monkeys.

A number of our subjects were taking benzodiazepines, antidepressants, or anticonvulsant medications at time of death (see **Table A.1**). Because of the potential impact of these medications on the GABAergic system ((Mijnster et al., 1998), reviewed in (Costa and Guidotti, 1979; Treiman, 2001)) we tested for significant effects of their use at time of death. We did not find any significant effects of benzodiazepines, anticonvulsants, or antidepressants on the fluorescence intensity of GAD65-IR boutons. From this, we conclude that our finding of decreased within-bouton GAD65 protein is not caused by exposure to these medications. However, we found that schizophrenia subjects who were on benzodiazepines at time of death had a significantly larger percent increase (relative to controls) in the density of GAD65-IR boutons compared to schizophrenia subjects who were not on benzodiazepines at time of death, who actually had a percent decrease. This association could indicate that benzodiazepines increase the density of GAD65-IR boutons, or that those subjects with greater GAD65-IR bouton

density are more likely to be treated with benzodiazepines; however, the most probable interpretation is that benzodiazepine exposure leads to a non-significant increase in GAD65 protein levels within boutons, causing us to detect more GAD65-IR boutons in schizophrenia subjects who were taking benzodiazepines at time of death. In support of this, chronic benzodiazepine exposure increases GAD65 mRNA (Izzo et al., 2001), and our data trend toward increased GAD65-IR bouton fluorescence intensity in subjects on benzodiazepines at time of death (**Figure B.2**).

APPENDIX C

CHAPTER 4 SUPPLEMENTAL MATERIALS

C.1 SUPPLEMENTAL RESULTS

C.1.1 Phalloidin-labeled puncta volume increases over adolescence

We found that mean phalloidin-labled puncta volume increased significantly between early adolescence and young adulthood ($F_{(2,29)} = 5.922$; $p = 0.007$; **Figure C.1**). However, there was no difference in volume between KO and WT mice at any age ($F_{(1,29)} = 0.013$; $p = 0.910$). We observed that the increase in volume over adolescence is highly significant in the WT mice ($F_{(2,29)} = 5.608$; $p = 0.009$) but not significant in the KO ($F_{(2,29)} = 1.371$; $p = 0.270$).

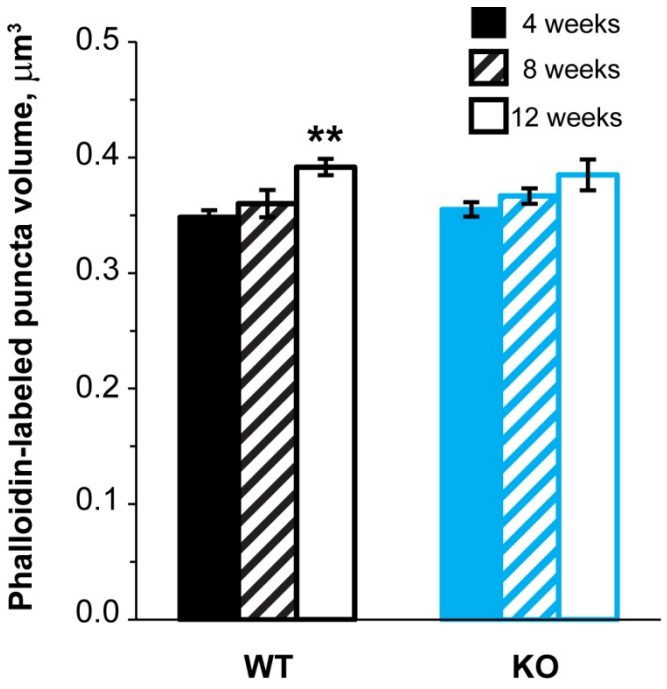

Figure C.1. Phalloidin-labeled spine volume increases across adolescence and early adulthood in WT mice. Mean phalloidin-labled spine volume significantly increases between 4 and 12 weeks in WT mice. **p < 0.01, vs 4 week old WT. N = 6 per age x genotype group. Error bars are ± SEM.

C.1.2 VGluT1-IR puncta mean fluorescence intensity and volume between early adolescence and young adulthood

We found that mean VGluT1-IR puncta fluorescence intensity decreased significantly between early adolescence and young adulthood ($F_{(2,28)} = 4.720$; $p = 0.017$; **Figure C.2.A**), and there were no genotype differences in VGluT1-IR puncta fluorescence intensity ($F_{(1,28)} = 0.371$; $p = 0.547$). However, the decrease in fluorescence intensity with age was significant in the KO ($F_{(2,28)} = 4.220$; $p = 0.025$) but not in the WT ($F_{(2,28)} = 1.287$; $p = 0.292$). This could indicate that

reduction in within-bouton VGluT1 fluorescence intensity is not a normal developmental process of adolescence and is a consequence of kalirin loss.

We found that mean VGluT1-IR puncta volume decreased significantly between 4 and 12 weeks of age ($F_{(2,28)} = 12.194$; $p < 0.001$; **Figure C.2.B**). There were no differences between WT and KO animals in mean volume of VGluT1-IR puncta ($F_{(1,28)} = 1.238$; $p = 0.275$). The decrease in puncta volume with age was highly significant in both genotypes (WT: ($F_{(2,28)} = 7.995$; $p = 0.002$); KO: ($F_{(2,28)} = 7.102$; $p = 0.003$)).

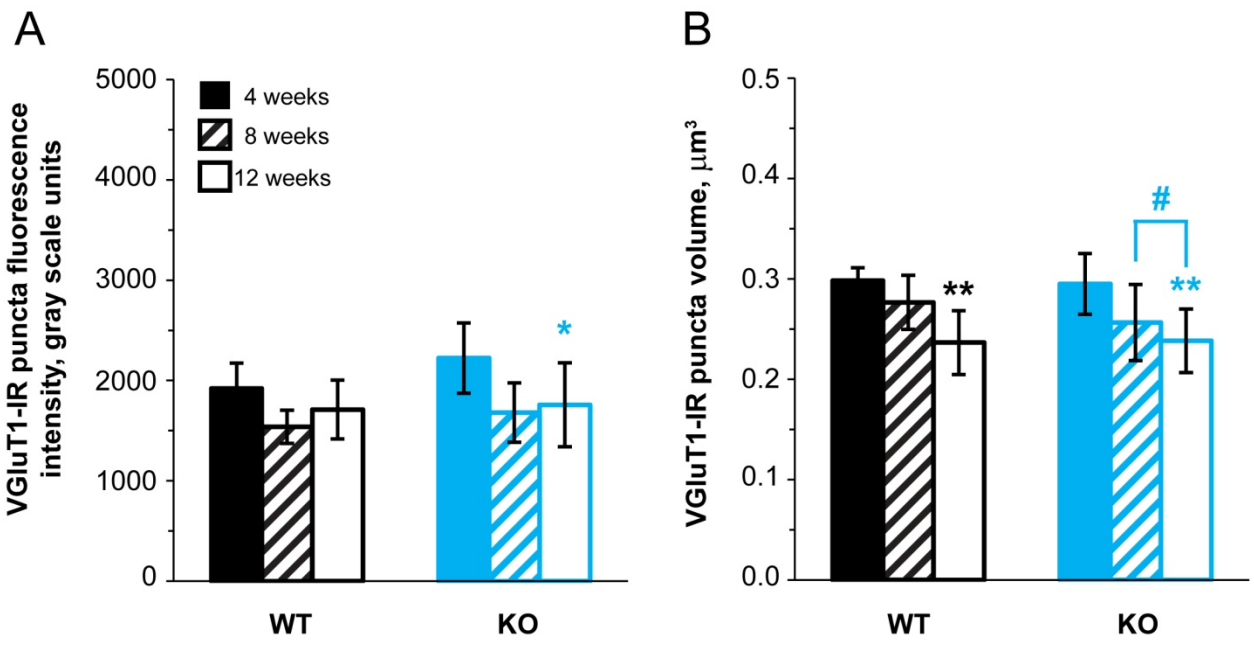

Figure C.2. Changes in VGluT1-IR boutons across adolescence and early adulthood. A. Mean VGluT1-IR fluoresncence intensity decreases significantly between 4 and 12 weeks in KO mice. *p < 0.05, vs 4 week old KO. B. Mean VGluT1-IR bouton volume decreases significantly between 4 and 12 weeks in KO and between 8 and 12 weeks in WT. **p < 0.01; #p < 0.10 between 8 and 12 week old KO. N = 6 per age x genotype group. Error bars are ± SEM.

C.1.3 Spinophilin-IR puncta measures between early adolescence and young adulthood

The numbers of spinophilin-IR puncta decreased overall between 4 and 12 weeks of age ($F_{(2,29)}$ = 5.389; p = 0.010) (**Figure C.3A**). Similar to the phalloidin-labeled puncta results, we found a trend toward an overall decrease in spinophilin-IR puncta number in the KO compared to the WT ($F_{(1,29)}$ = 3.575 p = 0.069) and a trend toward reduced spinophilin-IR puncta number in the KO compared to the WT at 4 weeks ($F_{(1,29)}$ = 3.265; p = 0.081). The decrease in spinophilin-IR

puncta number across adolescence was similar in the two genotypes, but was significant only in the WT ($F_{(2,29)} = 3.930$; $p = 0.031$) and was trend level in the KO ($F_{(2,29)} = 2.594$; $p = 0.092$).

To verify the changes in spinophilin mean intensity within phalloidin-labled objects we also evaluated the mean spinophilin-IR puncta fluorescence intensity. Similar to the results of spinophilin immunofluorescence within phalloidin-labeled spines, we found a highly significant reduction in mean spinophilin-IR puncta fluorescence intensity over adolescence ($F_{(2,29)} = 17.360$; $p < 0.001$). We found no overall difference in spinophilin-IR puncta fluorescence intensity between WT and KO ($F_{(1,29)} = 1.285$, $p = 0.266$; **Figure C.3B**), but there was a trend toward an age by genotype interaction ($F_{(2,29)} = 3.185$; $p = 0.056$). Spinophilin-IR puncta fluorescence intensity was significantly lower at 4 weeks in the KO compared to the WT ($F_{(1,29)} = 4.460$; $p = 0.043$), confirming a relative reduction in spinophilin protein levels in early adolescence in the KO. The reduction in spinophilin-IR puncta mean intensity with age was significant for both genotypes (KO: ($F_{(2,29)} = 3.477$; $p = 0.044$); WT ($F_{(2,29)} = 18.711$; $p < 0.001$)).

Spinophilin-IR puncta volume decreased from early adolescence to young adulthood ($F_{(2,29)} = 23.275$; $p < 0.001$) **Figure C.3C**). We did not see any difference in spinophilin-IR puncta volume between KO and WT ($F_{(1,29)} = 0.098$ $p = 0.757$); however, we observed a trend toward an age by genotype interaction ($F_{(2,29)} = 2.541$; $p = 0.096$). The effect of age on spinophilin-IR puncta volume was highly significant in both genotypes (KO:($F_{(2,29)} = 6.146$; $p = 0.006$);WT ($F_{(2,29)} = 22.215$; $p < 0.001$)). However, the changes in spinophilin-IR puncta volume and fluorescence intensity are highly correlated, so we cannot rule out whether the change in volume is independent of changes in fluorescence intensity or caused by changes in fluorescence intensity.

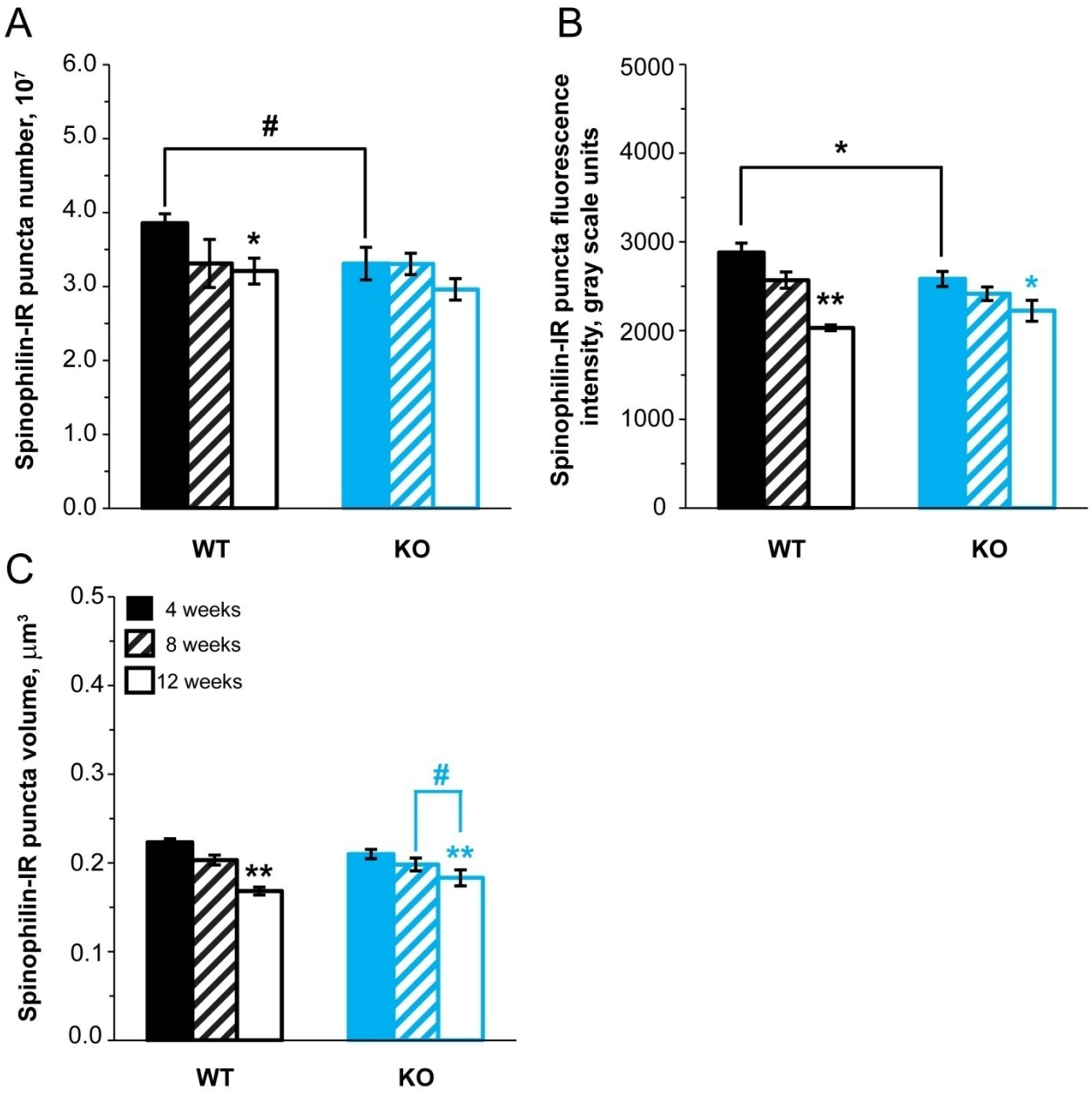

Figure C.3. Changes in spinophilin-IR puncta across adolescence and early adulthood. A. Mean spinophilin-IR puncta numbers decrease between 4 and 12 weeks in WT mice and are reduced with trend level significance at 4 weeks in the KO mice. *$p < 0.05$ vs 4 week WT; # $p < 0.10$ 4 week WT vs KO. B. Mean spinophilin-IR fluorescence intensity decreases significantly between 4 and 12 weeks in WT and KO mice. **$p < 0.01$ vs 4 and 8 week WT; *$p < 0.05$, vs 4 week old KO. Spinophilin intensity is significantly reduced in 4 week old KO compared to WT. *$p < 0.05$. C. Mean spinophilin-IR bouton volume decreases significantly between 8 and 12 weeks in WT

and 4 and 12 weeks in KO. **p < 0.01; #p < 0.10 between 8 and 12 week old KO. N = 6 per age x genotype group. Error bars are ± SEM.

C.1.4 GAD65-IR puncta volume decreases over adolescence

There was a significant reduction in the mean puncta volume across adolescence ($F_{(2,29)} = 14.577$; $p < 0.001$) (**Figure C.4**). There was no difference in GAD65-IR puncta volume between KO and WT mice ($F_{(1,29)} = 1.580$; $p = 0.219$), although there was a trend toward an age by genotype interaction ($F_{(2,29)} = 3.336$; $p = 0.050$). We found that mean puncta volume was significantly greater in the KO at 12 weeks of age ($F_{(1,29)} = 7.365$; $p = 0.011$), and the reduction with age was trend level in the KO ($F_{(2,29)} = 2.986$; $p = 0.066$) but highly significant in the WT ($F_{(2,29)} = 16.545$; $p < 0.001$). However, it should be noted that mean fluorescence intensity and volume are correlated and may not be independent.

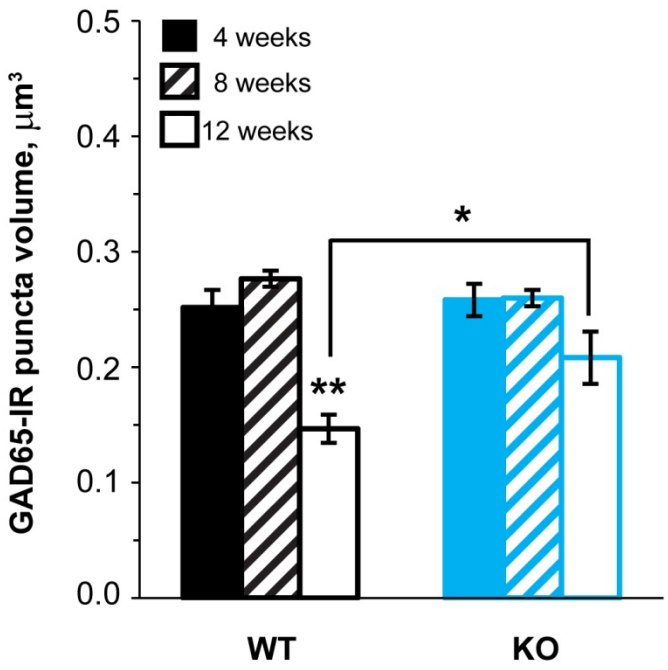

Figure C.4. GAD65-IR bouton volume decreases between 8 and 12 weeks in WT mice. Mean GAD65-IR bouton volume decreases significantly between 8 and 12 weeks in WT mice, and is significantly greater in 12 week old KO compared to WT mice. **$p < 0.01$, vs 4 and 8 week old KO, *$p < 0.05$ 12 week old WT vs KO. N = 6 per age x genotype group. Error bars are ± SEM.

APPENDIX D

CHAPTER 5 SUPPLEMENTAL MATERIALS

D.1 SUPPLEMENTAL FIGURES

Table D.1. Proportions of CBA/CaJ, C57Bl/6J, and DBA/2J that do and do not demonstrate significant modulation of acoustic startle by silent gap prepulses. Numbers of CBA/CaJ, C57Bl/6J, and DBA/2J that do (y) and do not (n) show significant modulation of startle by silent gap prepulses do not differ by age (rows). Further, proportions of animals that do and do not show modulation of acoustic startle do not differ by strain at any age group (columns). % indicates percent of the total number of animals tested that do show significant modulation of acoustic startle by silent gaps.

	4 week	8 week	12 week	Age difference
CBA/CaJ (y/n) (%)	7/8 (47%)	9/7 (56%)	12/4 (75%)	p=0.264
C57Bl/6J (y/n) (%)	3/13 (19%)	3/13 (19%)	4/12 (25%)	p=1.00
DBA/2J (y/n) (%)	2/14 (13%)	1/15 (6%)	2/14 (13%)	p=1.00
Strain difference	p=0.103	p=0.009	p=0.0007	

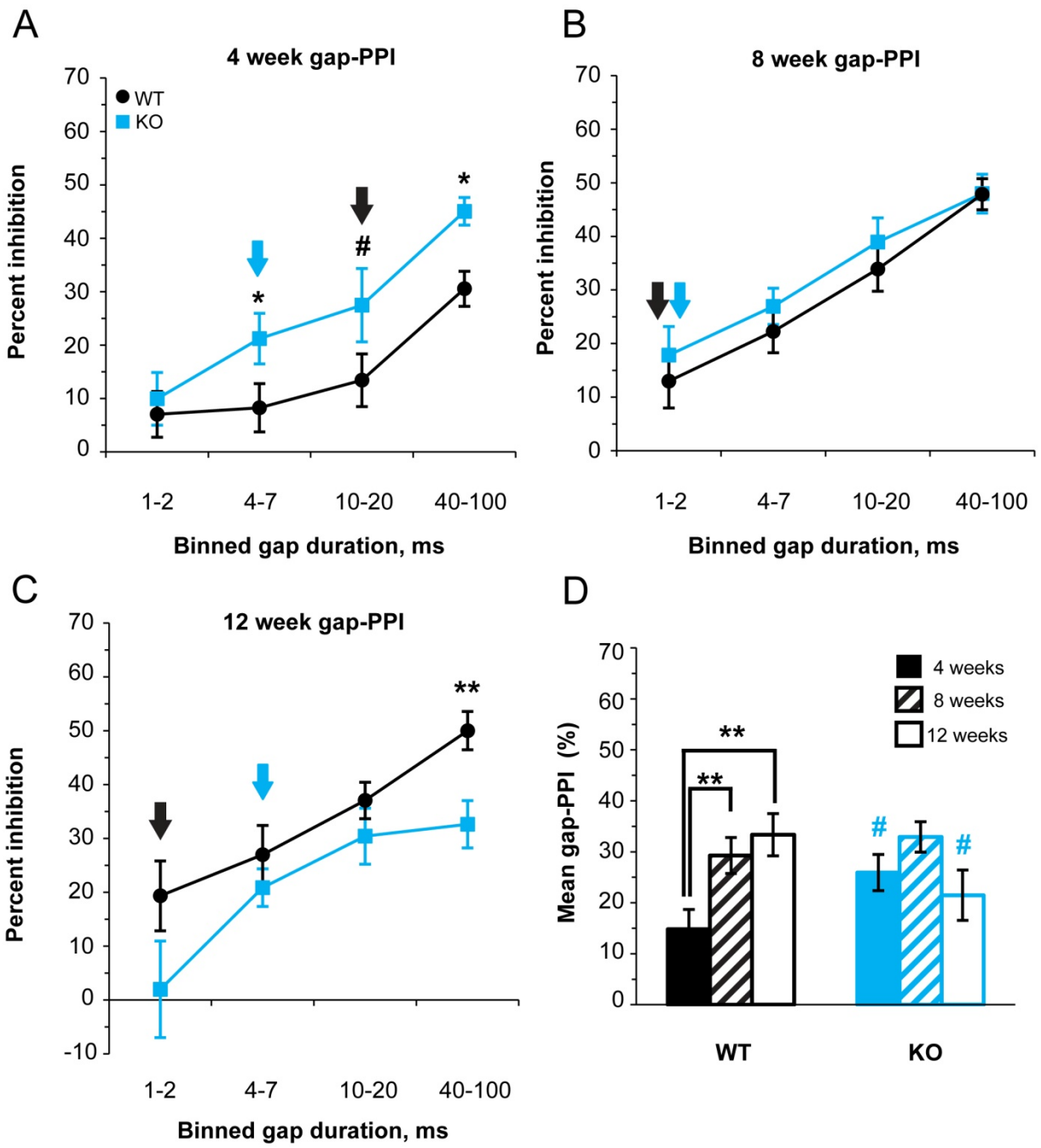

Figure D.1. Gap-PPI in WT and kalirin KO mice that individually demonstrated modulation of startle reflex by gap prepulses. Magnitude of gap-PPI as a function of increasing binned gap durations in 4 week (A), 8 week (B) and 12 week (C) WT (black) and KO (blue) mice. Arrows indicate gap detection threshold for each group, and arrow color indicates genotype. D. Average gap-PPI for all gap durations in WT and KO mice by age. Mean gap-PPI increases significantly between 4 and 8 weeks in WT mice but not in KO mice. Significance markers indicate

genotype comparisons, unless otherwise indicated. #$p < 0.10$, *$p < 0.05$, **$p < 0.01$. Animal numbers per group-Genotype: Age (N): WT: 4 weeks (10), 8 weeks (15), 12 weeks (12); KO: 4 weeks (8), 8 weeks (11), 12 weeks (13). Error bars are ± SEM.

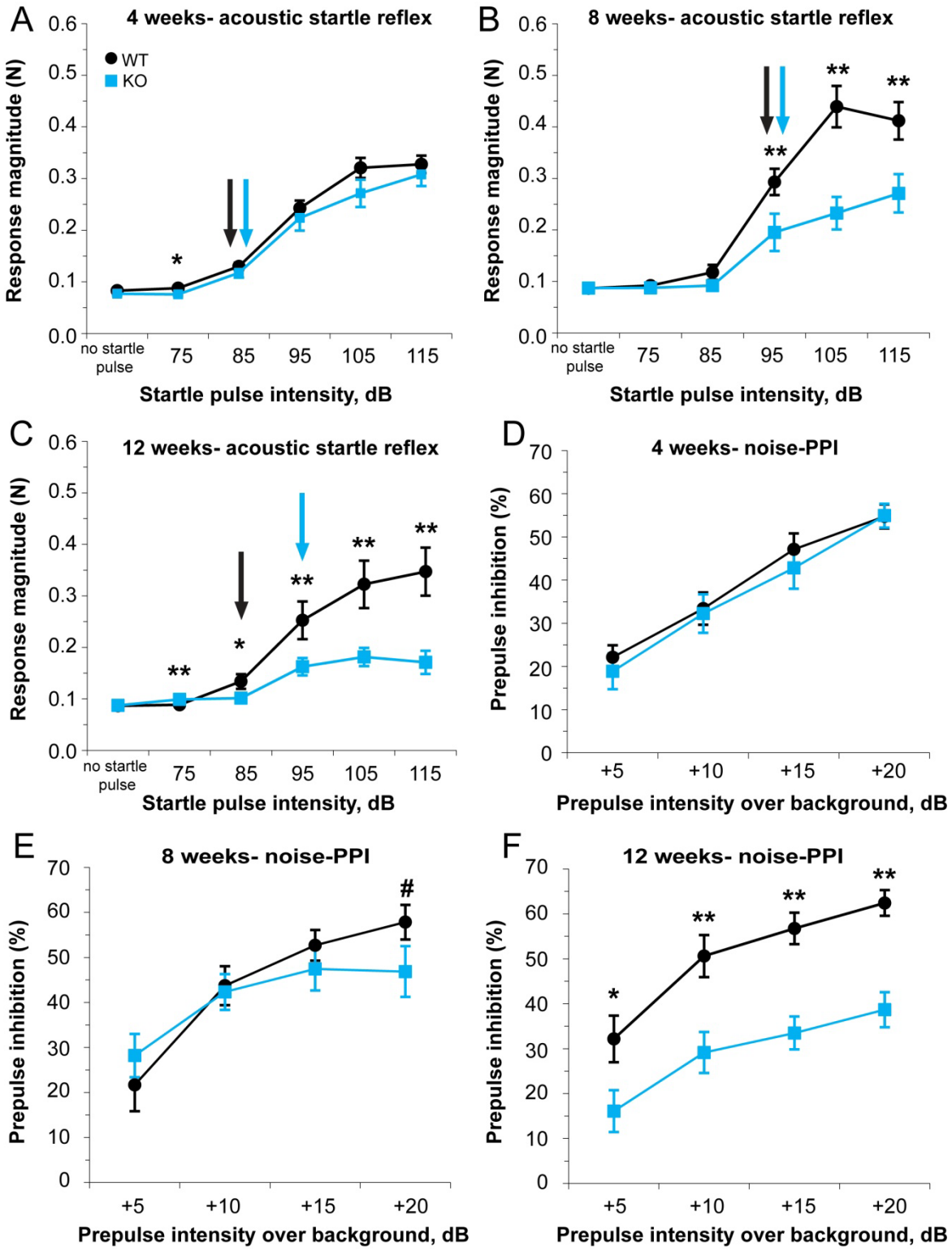

Figure D.2. Acoustic startle reflex and noise-PPI in 4, 8 and 12 week old WT and kalirin KO mice. Acoustic startle reflex in kalirin KO mice is no different from WT at 4 weeks (A) but is reduced at 8 (B) and 12 (C) weeks of

age. Threshold to startle is higher in kalirin KO mice at 12 weeks of age. Noise-PPI in kalirin KO mice is not different from WT at 4 weeks (D) and 8 weeks (E) but is significantly reduced at 12 weeks (F). Significance markers indicate genotype comparisons, #$p < 0.1$, *$p < 0.05$, **$p < 0.01$. Animal numbers per group- Genotype: Age (N): WT: 4 weeks (18), 8 weeks (17), 12 weeks (18); KO: 4 weeks (13), 8 weeks (15), 12 weeks (22). Error bars are ± SEM.

BIBLIOGRAPHY

Adcock RA, Dale C, Fisher M, Aldebot S, Genevsky A, Simpson GV, Nagarajan S, Vinogradov S (2009) When top-down meets bottom-up: auditory training enhances verbal memory in schizophrenia. Schizophr Bull 35: 1132-1141.

Alho K, Woods DL, Algazi A (1994) Processing of auditory stimuli during auditory and visual attention as revealed by event-related potentials. Psychophysiology 31: 469-479.

Allen PB, Ouimet CC, Greengard P (1997) Spinophilin, a novel protein phosphatase 1 binding protein localized to dendritic spines. Proc Natl Acad Sci U S A 94: 9956-9961.

Alvarez VA, Sabatini BL (2007) Anatomical and physiological plasticity of dendritic spines. Annu Rev Neurosci 30: 79-97.

American Psychiatric Association (1994) Diagnostic and Statistical Manual of Mental Disorders, 4th ed. Washington, D.C.: American Psychiatric Press.

Anderson SA, Classey JD, Conde F, Lund JS, Lewis DA (1995) Synchronous development of pyramidal neuron dendritic spines and parvalbumin-immunoreactive chandelier neuron axon terminals in layer III of monkey prefrontal cortex. Neuroscience 67: 7-22.

Anggono V, Huganir RL (2012) Regulation of AMPA receptor trafficking and synaptic plasticity. Curr Opin Neurobiol 22: 461-469.

Anomal R, Villers-Sidani E, Merzenich MM, Panizzutti R (2013) Manipulation of BDNF signaling modifies the experience-dependent plasticity induced by pure tone exposure during the critical period in the primary auditory cortex. PLoS One 8: e64208.

Aoto J, Ting P, Maghsoodi B, Xu N, Henkemeyer M, Chen L (2007) Postsynaptic ephrinB3 promotes shaft glutamatergic synapse formation. J Neurosci 27: 7508-7519.

Arguello PA, Gogos JA (2006) Modeling madness in mice: one piece at a time. Neuron 52: 179-196.

Asada H, Kawamura Y, Maruyama K, Kume H, Ding R, Ji FY, Kanbara N, Kuzume H, Sanbo M, Yagi T, Obata K (1996) Mice lacking the 65 kDa isoform of glutamic acid decarboxylase (GAD65) maintain normal levels of GAD67 and GABA in their brains but are susceptible to seizures. Biochem Biophys Res Commun 229: 891-895.

Atallah BV, Scanziani M (2009) Instantaneous modulation of gamma oscillation frequency by balancing excitation with inhibition. Neuron 62: 566-577.

Auquier P, Lancon C, Rouillon F, Lader M (2007) Mortality in schizophrenia. Pharmacoepidemiol Drug Saf 16: 1308-1312.

Bacci JJ, Salin P, Kerkerian-Le Goff L (2002) Systemic administration of dizocilpine maleate (MK-801) or L-dopa reverses the increases in GAD65 and GAD67 mRNA expression in the globus pallidus in a rat hemiparkinsonian model. Synapse 46: 224-234.

Baddeley A, Jensen EBV (2004) Stereology for Statisticians. Taylor & Francis.

Barbour DL, Callaway EM (2008) Excitatory local connections of superficial neurons in rat auditory cortex. J Neurosci 28: 11174-11185.

Barksdale KA, Roche JK, Lahti AC, and Roberts, R. C. Synaptic and mitochondrial changes in the postmortem anterior cingulate cortex in schizophrenia. Neuroscience Meeting Planner. 2012.

Battaglioli G, Liu H, Martin DL (2003) Kinetic differences between the isoforms of glutamate decarboxylase: implications for the regulation of GABA synthesis. J Neurochem 86: 879-887.

Benes FM, Todtenkopf MS, Logiotatos P, Williams M (2000) Glutamate decarboxylase(65)-immunoreactive terminals in cingulate and prefrontal cortices of schizophrenic and bipolar brain. J Chem Neuroanat 20: 259-269.

Bennett MR (2011) Schizophrenia: susceptibility genes, dendritic-spine pathology and gray matter loss. Prog Neurobiol 95: 275-300.

Blue ME, Parnavelas JG (1983) The formation and maturation of synapses in the visual cortex of the rat. II. Quantitative analysis. J Neurocytol 12: 697-712.

Bosch M, Hayashi Y (2012) Structural plasticity of dendritic spines. Curr Opin Neurobiol 22: 383-388.

Bourgeois JP, Rakic P (1993) Changes of synaptic density in the primary visual cortex of the macaque monkey from fetal to adult stage. J Neurosci 13: 2801-2820.

Bowen GP, Lin D, Taylor MK, Ison JR (2003) Auditory cortex lesions in the rat impair both temporal acuity and noise increment thresholds, revealing a common neural substrate. Cereb Cortex 13: 815-822.

Boyer C, Schikorski T, Stevens CF (1998) Comparison of hippocampal dendritic spines in culture and in brain. J Neurosci 18: 5294-5300.

Bozzi Y, Pizzorusso T, Cremisi F, Rossi FM, Barsacchi G, Maffei L (1995) Monocular deprivation decreases the expression of messenger RNA for brain-derived neurotrophic factor in the rat visual cortex. Neuroscience 69: 1133-1144.

Braendgaard H, Gundersen HJ (1986) The impact of recent stereological advances on quantitative studies of the nervous system. J Neurosci Methods 18: 39-78.

Brenner CA, Krishnan GP, Vohs JL, Ahn WY, Hetrick WP, Morzorati SL, O'Donnell BF (2009) Steady state responses: electrophysiological assessment of sensory function in schizophrenia. Schizophr Bull 35: 1065-1077.

Brenner CA, Sporns O, Lysaker PH, O'Donnell BF (2003) EEG synchronization to modulated auditory tones in schizophrenia, schizoaffective disorder, and schizotypal personality disorder. Am J Psychiatry 160: 2238-2240.

Broadbelt K, Byne W, Jones LB (2002) Evidence for a decrease in basilar dendrites of pyramidal cells in schizophrenic medial prefrontal cortex. Schizophr Res 58: 75-81.

Brown AS (2011) The environment and susceptibility to schizophrenia. Prog Neurobiol 93: 23-58.

Brown AS, Derkits EJ (2010) Prenatal infection and schizophrenia: a review of epidemiologic and translational studies. Am J Psychiatry 167: 261-280.

Buchsbaum RJ, Connolly BA, Feig LA (2003) Regulation of p70 S6 kinase by complex formation between the Rac guanine nucleotide exchange factor (Rac-GEF) Tiam1 and the scaffold spinophilin. J Biol Chem 278: 18833-18841.

Budinger E, Laszcz A, Lison H, Scheich H, Ohl FW (2008) Non-sensory cortical and subcortical connections of the primary auditory cortex in Mongolian gerbils: bottom-up and top-down processing of neuronal information via field AI. Brain Res 1220: 2-32.

Bullock AE, Slobe BS, Vazquez V, Collins AC (1997) Inbred mouse strains differ in the regulation of startle and prepulse inhibition of the startle response. Behav Neurosci 111: 1353-1360.

Caballero A, Thomases DR, Flores-Barrera E, Cass DK, Tseng KY (2013) Emergence of GABAergic-dependent regulation of input-specific plasticity in the adult rat prefrontal cortex during adolescence. Psychopharmacology (Berl).

Cahill ME, Xie Z, Day M, Photowala H, Barbolina MV, Miller CA, Weiss C, Radulovic J, Sweatt JD, Disterhoft JF, Surmeier DJ, Penzes P (2009) Kalirin regulates cortical spine morphogenesis and disease-related behavioral phenotypes. Proc Natl Acad Sci U S A 106: 13058-13063.

Campbell MJ, Lewis DA, Foote SL, Morrison JH (1987) Distribution of choline acetyltransferase-, serotonin-, dopamine-beta-hydroxylase-, tyrosine hydroxylase-immunoreactive fibers in monkey primary auditory cortex. J Comp Neurol 261: 209-220.

Cannon TD, van Erp TG, Bearden CE, Loewy R, Thompson P, Toga AW, Huttunen MO, Keshavan MS, Seidman LJ, Tsuang MT (2003) Early and late neurodevelopmental influences in the prodrome to schizophrenia: contributions of genes, environment, and their interactions. Schizophr Bull 29: 653-669.

Capani F, Martone ME, Deerinck TJ, Ellisman MH (2001) Selective localization of high concentrations of F-actin in subpopulations of dendritic spines in rat central nervous system: a three-dimensional electron microscopic study. J Comp Neurol 435: 156-170.

Cardin JA, Carlen M, Meletis K, Knoblich U, Zhang F, Deisseroth K, Tsai LH, Moore CI (2009) Driving fast-spiking cells induces gamma rhythm and controls sensory responses. Nature 459: 663-667.

Castren E, Zafra F, Thoenen H, Lindholm D (1992) Light regulates expression of brain-derived neurotrophic factor mRNA in rat visual cortex. Proc Natl Acad Sci U S A 89: 9444-9448.

Catts SV, Shelley AM, Ward PB, Liebert B, McConaghy N, Andrews S, Michie PT (1995) Brain potential evidence for an auditory sensory memory deficit in schizophrenia. Am J Psychiatry 152: 213-219.

Cellerino A, Maffei L, Domenici L (1996) The distribution of brain-derived neurotrophic factor and its receptor trkB in parvalbumin-containing neurons of the rat visual cortex. Eur J Neurosci 8: 1190-1197.

Chance SA, Casanova MF, Switala AE, Crow TJ (2008) Auditory cortex asymmetry, altered minicolumn spacing and absence of ageing effects in schizophrenia. Brain 131: 3178-3192.

Chang YC, Gottlieb DI (1988) Characterization of the proteins purified with monoclonal antibodies to glutamic acid decarboxylase. J Neurosci 8: 2123-2130.

Charitidi K, Meltser I, Canlon B (2012) Estradiol treatment and hormonal fluctuations during the estrous cycle modulate the expression of estrogen receptors in the auditory system and the prepulse inhibition of acoustic startle response. Endocrinology 153: 4412-4421.

Chen J, Kitanishi T, Ikeda T, Matsuki N, Yamada MK (2007) Contextual learning induces an increase in the number of hippocampal CA1 neurons expressing high levels of BDNF. Neurobiol Learn Mem 88: 409-415.

Chen J, Mizushige T, Nishimune H (2011a) Active zone density is conserved during synaptic growth but impaired in aged mice. J Comp Neurol.

Chen QC, Jen PH (2000) Bicuculline application affects discharge patterns, rate-intensity functions, and frequency tuning characteristics of bat auditory cortical neurons. Hear Res 150: 161-174.

Chen X, Leischner U, Rochefort NL, Nelken I, Konnerth A (2011b) Functional mapping of single spines in cortical neurons in vivo. Nature 475: 501-505.

Choe BY, Kim KT, Suh TS, Lee C, Paik IH, Bahk YW, Shinn KS, Lenkinski RE (1994) 1H magnetic resonance spectroscopy characterization of neuronal dysfunction in drug-naive, chronic schizophrenia. Acad Radiol 1: 211-216.

Choi SY, Morales B, Lee HK, Kirkwood A (2002) Absence of long-term depression in the visual cortex of glutamic Acid decarboxylase-65 knock-out mice. J Neurosci 22: 5271-5276.

Christgau S, Schierbeck H, Aanstoot HJ, Aagaard L, Begley K, Kofod H, Hejnaes K, Baekkeskov S (1991) Pancreatic beta cells express two autoantigenic forms of glutamic acid decarboxylase, a 65-kDa hydrophilic form and a 64-kDa amphiphilic form which can be both membrane-bound and soluble. J Biol Chem 266: 23516.

Cobb SR, Buhl EH, Halasy K, Paulsen O, Somogyi P (1995) Synchronization of neuronal activity in hippocampus by individual GABAergic interneurons. Nature 378: 75-78.

Costa E, Guidotti A (1979) Recent studies on the mechanism whereby benzodiazepines facilitate GABA-ergic transmission. Adv Exp Med Biol 123: 371-378.

Curley AA, Arion D, Volk DW, Asafu-Adjei JK, Sampson AR, Fish KN, Lewis DA (2011) Cortical deficits of glutamic Acid decarboxylase 67 expression in schizophrenia: clinical, protein, and cell type-specific features. Am J Psychiatry 168: 921-929.

Dale CL, Findlay AM, Adcock RA, Vertinski M, Fisher M, Genevsky A, Aldebot S, Subramaniam K, Luks TL, Simpson GV, Nagarajan SS, Vinogradov S (2010) Timing is everything: neural response dynamics during syllable processing and its relation to higher-order cognition in schizophrenia and healthy comparison subjects. Int J Psychophysiol 75: 183-193.

Davies G, Welham J, Chant D, Torrey EF, McGrath J (2003) A systematic review and meta-analysis of Northern Hemisphere season of birth studies in schizophrenia. Schizophr Bull 29: 587-593.

De Felipe J, Marco P, Fairen A, Jones EG (1997) Inhibitory synaptogenesis in mouse somatosensory cortex. Cereb Cortex 7: 619-634.

De Gois S, Schafer MK, Defamie N, Chen C, Ricci A, Weihe E, Varoqui H, Erickson JD (2005) Homeostatic scaling of vesicular glutamate and GABA transporter expression in rat neocortical circuits. J Neurosci 25: 7121-7133.

De Paola, V, Holtmaat A, Knott G, Song S, Wilbrecht L, Caroni P, Svoboda K (2006) Cell type-specific structural plasticity of axonal branches and boutons in the adult neocortex. Neuron 49: 861-875.

Deo AJ, Cahill ME, Li S, Goldszer I, Henteleff R, Vanleeuwen JE, Rafalovich I, Gao R, Stachowski EK, Sampson AR, Lewis DA, Penzes P, Sweet RA (2012) Increased expression of Kalirin-9 in the auditory cortex of schizophrenia subjects: its role in dendritic pathology. Neurobiol Dis 45: 796-803.

Deo AJ, Goldszer IM, Li S, DiBitetto JV, Henteleff R, Sampson A, Lewis DA, Penzes P, Sweet RA (2013) PAK1 protein expression in the auditory cortex of schizophrenia subjects. PLoS One 8: e59458.

Dierks T, Linden DE, Jandl M, Formisano E, Goebel R, Lanfermann H, Singer W (1999) Activation of Heschl's gyrus during auditory hallucinations. Neuron 22: 615-621.

Dorph-Petersen KA, Caric D, Saghafi R, Zhang W, Sampson AR, Lewis DA (2009a) Volume and neuron number of the lateral geniculate nucleus in schizophrenia and mood disorders. Acta Neuropathol 117: 369-384.

Dorph-Petersen KA, Delevich KM, Marcsisin MJ, Zhang W, Sampson AR, Gundersen HJ, Lewis DA, Sweet RA (2009b) Pyramidal neuron number in layer 3 of primary auditory cortex of subjects with schizophrenia. Brain Res 1285: 42-57.

Dorph-Petersen KA, Nyengaard JR, Gundersen HJ (2001) Tissue shrinkage and unbiased stereological estimation of particle number and size. J Microsc 204: 232-246.

Dracheva S, Elhakem SL, McGurk SR, Davis KL, Haroutunian V (2004) GAD67 and GAD65 mRNA and protein expression in cerebrocortical regions of elderly patients with schizophrenia. J Neurosci Res 76: 581-592.

Eastwood SL, Harrison PJ (2005) Decreased expression of vesicular glutamate transporter 1 and complexin II mRNAs in schizophrenia: further evidence for a synaptic pathology affecting glutamate neurons. Schizophr Res 73: 159-172.

Edden RA, Muthukumaraswamy SD, Freeman TC, Singh KD (2009) Orientation discrimination performance is predicted by GABA concentration and gamma oscillation frequency in human primary visual cortex. J Neurosci 29: 15721-15726.

Edwards CR, Skosnik PD, Steinmetz AB, O'Donnell BF, Hetrick WP (2009) Sensory gating impairments in heavy cannabis users are associated with altered neural oscillations. Behav Neurosci 123: 894-904.

Eggermont JJ (1999) Neural correlates of gap detection in three auditory cortical fields in the Cat. J Neurophysiol 81: 2570-2581.

Eggermont JJ (2000) Neural responses in primary auditory cortex mimic psychophysical, across-frequency-channel, gap-detection thresholds. J Neurophysiol 84: 1453-1463.

Elangovan S, Stuart A (2008) Natural boundaries in gap detection are related to categorical perception of stop consonants. Ear Hear 29: 761-774.

Erickson SL, Lewis DA (2002) Postnatal development of parvalbumin- and GABA transporter-immunoreactive axon terminals in monkey prefrontal cortex. J Comp Neurol 448: 186-202.

Erlander MG, Tillakaratne NJ, Feldblum S, Patel N, Tobin AJ (1991) Two genes encode distinct glutamate decarboxylases. Neuron 7: 91-100.

Evans JD, Bond GR, Meyer PS, Kim HW, Lysaker PH, Gibson PJ, Tunis S (2004) Cognitive and clinical predictors of success in vocational rehabilitation in schizophrenia. Schizophr Res 70: 331-342.

Fagiolini M, Hensch TK (2000) Inhibitory threshold for critical-period activation in primary visual cortex. Nature 404: 183-186.

Feinberg I (1982) Schizophrenia: caused by a fault in programmed synaptic elimination during adolescence? J Psychiatr Res 17: 319-334.

Fendt M, Li L, Yeomans JS (2001) Brain stem circuits mediating prepulse inhibition of the startle reflex. Psychopharmacology (Berl) 156: 216-224.

Feng J, Yan Z, Ferreira A, Tomizawa K, Liauw JA, Zhuo M, Allen PB, Ouimet CC, Greengard P (2000) Spinophilin regulates the formation and function of dendritic spines. Proc Natl Acad Sci U S A 97: 9287-9292.

Fiala JC, Feinberg M, Popov V, Harris KM (1998) Synaptogenesis via dendritic filopodia in developing hippocampal area CA1. J Neurosci 18: 8900-8911.

Fifkova E, Delay RJ (1982) Cytoplasmic actin in neuronal processes as a possible mediator of synaptic plasticity. J Cell Biol 95: 345-350.

Fish KN, Sweet RA, Deo AJ, Lewis DA (2008) An automated segmentation methodology for quantifying immunoreactive puncta number and fluorescence intensity in tissue sections. Brain Res 1240: 62-72.

Fish KN, Sweet RA, Lewis DA (2011) Differential Distribution of Proteins Regulating GABA Synthesis and Reuptake in Axon Boutons of Subpopulations of Cortical Interneurons. Cereb Cortex.

Fishbein I, Segal M (2007) Miniature synaptic currents become neurotoxic to chronically silenced neurons. Cereb Cortex 17: 1292-1306.

Fitch RH, Threlkeld SW, McClure MM, Peiffer AM (2008) Use of a modified prepulse inhibition paradigm to assess complex auditory discrimination in rodents. Brain Res Bull 76: 1-7.

Frazier L, Carlson K, Clifton C, Jr. (2006) Prosodic phrasing is central to language comprehension. Trends Cogn Sci 10: 244-249.

Fremeau RT, Jr., Kam K, Qureshi T, Johnson J, Copenhagen DR, Storm-Mathisen J, Chaudhry FA, Nicoll RA, Edwards RH (2004a) Vesicular glutamate transporters 1 and 2 target to functionally distinct synaptic release sites. Science 304: 1815-1819.

Fremeau RT, Jr., Troyer MD, Pahner I, Nygaard GO, Tran CH, Reimer RJ, Bellocchio EE, Fortin D, Storm-Mathisen J, Edwards RH (2001) The expression of vesicular glutamate transporters defines two classes of excitatory synapse. Neuron 31: 247-260.

Fremeau RT, Jr., Voglmaier S, Seal RP, Edwards RH (2004b) VGLUTs define subsets of excitatory neurons and suggest novel roles for glutamate. Trends Neurosci 27: 98-103.

Friedman JT, Peiffer AM, Clark MG, Benasich AA, Fitch RH (2004) Age and experience-related improvements in gap detection in the rat. Brain Res Dev Brain Res 152: 83-91.

Fung SJ, Sivagnanasundaram S, Weickert CS (2011) Lack of change in markers of presynaptic terminal abundance alongside subtle reductions in markers of presynaptic terminal plasticity in prefrontal cortex of schizophrenia patients. Biol Psychiatry 69: 71-79.

Fung SJ, Webster MJ, Sivagnanasundaram S, Duncan C, Elashoff M, Weickert CS (2010) Expression of interneuron markers in the dorsolateral prefrontal cortex of the developing human and in schizophrenia. Am J Psychiatry 167: 1479-1488.

Garey LJ. 1999. Description of individual brain maps. In: GareyLJ, editor. Brodmann's "localisation in the cerebral cortex." London: Imperial College Press. p 122–125.

Gerlai R (1996) Gene-targeting studies of mammalian behavior: is it the mutation or the background genotype? Trends Neurosci 19: 177-181.

Gingrich JA, Hen R (2000) The broken mouse: the role of development, plasticity and environment in the interpretation of phenotypic changes in knockout mice. Curr Opin Neurobiol 10: 146-152.

Glantz LA, Gilmore JH, Hamer RM, Lieberman JA, Jarskog LF (2007) Synaptophysin and postsynaptic density protein 95 in the human prefrontal cortex from mid-gestation into early adulthood. Neuroscience 149: 582-591.

Glantz LA, Lewis DA (1997) Reduction of synaptophysin immunoreactivity in the prefrontal cortex of subjects with schizophrenia. Regional and diagnostic specificity. Arch Gen Psychiatry 54: 943-952.

Glantz LA, Lewis DA (2000) Decreased dendritic spine density on prefrontal cortical pyramidal neurons in schizophrenia. Arch Gen Psychiatry 57: 65-73.

Gogtay N, Giedd JN, Lusk L, Hayashi KM, Greenstein D, Vaituzis AC, Nugent TF, III, Herman DH, Clasen LS, Toga AW, Rapoport JL, Thompson PM (2004) Dynamic mapping of human cortical development during childhood through early adulthood. Proc Natl Acad Sci U S A 101: 8174-8179.

Gonzalez-Burgos G, Kroener S, Zaitsev AV, Povysheva NV, Krimer LS, Barrionuevo G, Lewis DA (2008) Functional maturation of excitatory synapses in layer 3 pyramidal neurons during postnatal development of the primate prefrontal cortex. Cereb Cortex 18: 626-637.

Gonzalez-Burgos G, Lewis DA (2008) GABA neurons and the mechanisms of network oscillations: implications for understanding cortical dysfunction in schizophrenia. Schizophr Bull 34: 944-961.

Gorba T, Wahle P (1999) Expression of TrkB and TrkC but not BDNF mRNA in neurochemically identified interneurons in rat visual cortex in vivo and in organotypic cultures. Eur J Neurosci 11: 1179-1190.

Gottesman II, Shields J (1967) A polygenic theory of schizophrenia. Proc Natl Acad Sci U S A 58: 199-205.

Gourley SL, Olevska A, Warren MS, Taylor JR, Koleske AJ (2012) Arg kinase regulates prefrontal dendritic spine refinement and cocaine-induced plasticity. J Neurosci 32: 2314-2323.

Graziano A, Liu XB, Murray KD, Jones EG (2008) Vesicular glutamate transporters define two sets of glutamatergic afferents to the somatosensory thalamus and two thalamocortical projections in the mouse. J Comp Neurol 507: 1258-1276.

Green MF (1996) What are the functional consequences of neurocognitive deficits in schizophrenia? Am J Psychiatry 153: 321-330.

Green MF, Penn DL, Bentall R, Carpenter WT, Gaebel W, Gur RC, Kring AM, Park S, Silverstein SM, Heinssen R (2008) Social cognition in schizophrenia: an NIMH workshop on definitions, assessment, and research opportunities. Schizophr Bull 34: 1211-1220.

Green MJ, Matheson SL, Shepherd A, Weickert CS, Carr VJ (2011) Brain-derived neurotrophic factor levels in schizophrenia: a systematic review with meta-analysis. Mol Psychiatry 16: 960-972.

Griffiths TD, Warren JD (2002) The planum temporale as a computational hub. Trends Neurosci 25: 348-353.

Grottick AJ, Bagnol D, Phillips S, McDonald J, Behan DP, Chalmers DT, Hakak Y (2005) Neurotransmission- and cellular stress-related gene expression associated with prepulse inhibition in mice. Brain Res Mol Brain Res 139: 153-162.

Guidotti A, Auta J, Davis JM, Giorgi-Gerevini V, Dwivedi Y, Grayson DR, Impagnatiello F, Pandey G, Pesold C, Sharma R, Uzunov D, Costa E (2000) Decrease in reelin and glutamic acid decarboxylase67 (GAD67) expression in schizophrenia and bipolar disorder: a postmortem brain study. Arch Gen Psychiatry 57: 1061-1069.

Gundersen HJ (1977) Notes on the estimation of the numerical density of arbitrary profiles: the edge effect. Journal of Microscopy 111: 219-223.

Gunduz-Bruce H, Reinhart RM, Roach BJ, Gueorguieva R, Oliver S, D'Souza DC, Ford JM, Krystal JH, Mathalon DH (2012) Glutamatergic modulation of auditory information processing in the human brain. Biol Psychiatry 71: 969-977.

Hackett TA, Stepniewska I, Kaas JH (1998) Subdivisions of auditory cortex and ipsilateral cortical connections of the parabelt auditory cortex in macaque monkeys. J Comp Neurol 394: 475-495.

Hackett TA, Stepniewska I, Kaas JH (1999) Prefrontal connections of the parabelt auditory cortex in macaque monkeys. Brain Res 817: 45-58.

Hackett TA, Takahata T, Balaram P (2011) VGLUT1 and VGLUT2 mRNA expression in the primate auditory pathway. Hear Res 274: 129-141.

Hafner H, Behrens S, De Vry J, Gattaz WF (1991) Oestradiol enhances the vulnerability threshold for schizophrenia in women by an early effect on dopaminergic neurotransmission. Evidence from an epidemiological study and from animal experiments. Eur Arch Psychiatry Clin Neurosci 241: 65-68.

Hafner H, Maurer K, Loffler W, Riecher-Rossler A (1993) The influence of age and sex on the onset and early course of schizophrenia. Br J Psychiatry 162: 80-86.

Hagiwara A, Fukazawa Y, Deguchi-Tawarada M, Ohtsuka T, Shigemoto R (2005) Differential distribution of release-related proteins in the hippocampal CA3 area as revealed by freeze-fracture replica labeling. J Comp Neurol 489: 195-216.

Hains AB, Vu MA, Maciejewski PK, van Dyck CH, Gottron M, Arnsten AF (2009) Inhibition of protein kinase C signaling protects prefrontal cortex dendritic spines and cognition from the effects of chronic stress. Proc Natl Acad Sci U S A 106: 17957-17962.

Hajos N, Katona I, Naiem SS, MacKie K, Ledent C, Mody I, Freund TF (2000) Cannabinoids inhibit hippocampal GABAergic transmission and network oscillations. Eur J Neurosci 12: 3239-3249.

Hamm JP, Gilmore CS, Picchetti NA, Sponheim SR, Clementz BA (2011) Abnormalities of neuronal oscillations and temporal integration to low- and high-frequency auditory stimulation in schizophrenia. Biol Psychiatry 69: 989-996.

Harnett MT, Makara JK, Spruston N, Kath WL, Magee JC (2012) Synaptic amplification by dendritic spines enhances input cooperativity. Nature 491: 599-602.

Hartman KN, Pal SK, Burrone J, Murthy VN (2006) Activity-dependent regulation of inhibitory synaptic transmission in hippocampal neurons. Nat Neurosci 9: 642-649.

Hashimoto T, Bazmi HH, Mirnics K, Wu Q, Sampson AR, Lewis DA (2008) Conserved regional patterns of GABA-related transcript expression in the neocortex of subjects with schizophrenia. Am J Psychiatry 165: 479-489.

Heffner HE, Heffner RS (1986) Hearing loss in Japanese macaques following bilateral auditory cortex lesions. J Neurophysiol 55: 256-271.

Heffner HE, Koay G, Heffner RS (2006) Behavioral assessment of hearing in mice--conditioned suppression. Curr Protoc Neurosci Chapter 8: Unit8.

Hefti BJ, Smith PH (2000) Anatomy, physiology, and synaptic responses of rat layer V auditory cortical cells and effects of intracellular GABA(A) blockade. J Neurophysiol 83: 2626-2638.

Hendry SH, Jones EG (1988) Activity-dependent regulation of GABA expression in the visual cortex of adult monkeys. Neuron 1: 701-712.

Hill JJ, Hashimoto T, Lewis DA (2006) Molecular mechanisms contributing to dendritic spine alterations in the prefrontal cortex of subjects with schizophrenia. Mol Psychiatry 11: 557-566.

Hirayasu Y, McCarley RW, Salisbury DF, Tanaka S, Kwon JS, Frumin M, Snyderman D, Yurgelun-Todd D, Kikinis R, Jolesz FA, Shenton ME (2000) Planum temporale and Heschl gyrus volume reduction in schizophrenia: a magnetic resonance imaging study of first-episode patients. Arch Gen Psychiatry 57: 692-699.

Hoffman HS, Searle JL (1965) Acoustic variables in the modification of startle reaction in the rat. J Comp Physiol Psychol 60: 53-58.

Holt LL, Lotto AJ (2008) Speech Perception Within an Auditory Cognitive Science Framework. Curr Dir Psychol Sci 17: 42-46.

Homayoun H, Moghaddam B (2007) NMDA receptor hypofunction produces opposite effects on prefrontal cortex interneurons and pyramidal neurons. J Neurosci 27: 11496-11500.

Hong LE, Summerfelt A, McMahon R, Adami H, Francis G, Elliott A, Buchanan RW, Thaker GK (2004) Evoked gamma band synchronization and the liability for schizophrenia. Schizophr Res 70: 293-302.

Huntsman MM, Leggio MG, Jones EG (1995) Expression patterns and deprivation effects on GABAA receptor subunit and GAD mRNAs in monkey lateral geniculate nucleus. J Comp Neurol 352: 235-247.

Huttenlocher PR (1979) Synaptic density in human frontal cortex - developmental changes and effects of aging. Brain Res 163: 195-205.

Huttenlocher PR, Dabholkar AS (1997) Regional differences in synaptogenesis in human cerebral cortex. J Comp Neurol 387: 167-178.

Ide M, Lewis DA (2010) Altered cortical CDC42 signaling pathways in schizophrenia: implications for dendritic spine deficits. Biol Psychiatry 68: 25-32.

Ikeda M, Aleksic B, Kinoshita Y, Okochi T, Kawashima K, Kushima I, Ito Y, Nakamura Y, Kishi T, Okumura T, Fukuo Y, Williams HJ, Hamshere ML, Ivanov D, Inada T, Suzuki M, Hashimoto R, Ujike H, Takeda M, Craddock N, Kaibuchi K, Owen MJ, Ozaki N, O'Donovan MC, Iwata N (2011) Genome-wide association study of schizophrenia in a Japanese population. Biol Psychiatry 69: 472-478.

Impagnatiello F, Guidotti AR, Pesold C, Dwivedi Y, Caruncho H, Pisu MG, Uzunov DP, Smalheiser NR, Davis JM, Pandey GN, Pappas GD, Tueting P, Sharma RP, Costa E (1998) A decrease of reelin expression as a putative vulnerability factor in schizophrenia. Proc Natl Acad Sci U S A 95: 15718-15723.

Ison JR, O'Connor K, Bowen GP, Bocirnea A (1991) Temporal resolution of gaps in noise by the rat is lost with functional decortication. Behav Neurosci 105: 33-40.

Izzo E, Auta J, Impagnatiello F, Pesold C, Guidotti A, Costa E (2001) Glutamic acid decarboxylase and glutamate receptor changes during tolerance and dependence to benzodiazepines. Proc Natl Acad Sci U S A 98: 3483-3488.

Jaaro-Peled H (2009) Gene models of schizophrenia: DISC1 mouse models. Prog Brain Res 179: 75-86.

Jaslove SW (1992) The integrative properties of spiny distal dendrites. Neuroscience 47: 495-519.

Javitt DC (2007) Glutamate and schizophrenia: phencyclidine, N-methyl-D-aspartate receptors, and dopamine-glutamate interactions. Int Rev Neurobiol 78: 69-108.

Javitt DC (2009) When doors of perception close: bottom-up models of disrupted cognition in schizophrenia. Annu Rev Clin Psychol 5: 249-275.

Javitt DC, Doneshka P, Zylberman I, Ritter W, Vaughan HG, Jr. (1993) Impairment of early cortical processing in schizophrenia: an event-related potential confirmation study. Biol Psychiatry 33: 513-519.

Javitt DC, Shelley A, Ritter W (2000) Associated deficits in mismatch negativity generation and tone matching in schizophrenia. Clin Neurophysiol 111: 1733-1737.

Javitt DC, Steinschneider M, Schroeder CE, Arezzo JC (1996) Role of cortical N-methyl-D-aspartate receptors in auditory sensory memory and mismatch negativity generation: implications for schizophrenia. Proc Natl Acad Sci U S A 93: 11962-11967.

Javitt DC, Steinschneider M, Schroeder CE, Vaughan HG, Jr., Arezzo JC (1994) Detection of stimulus deviance within primate primary auditory cortex: intracortical mechanisms of mismatch negativity (MMN) generation. Brain Res 667: 192-200.

Jeschke M, Lenz D, Budinger E, Herrmann CS, Ohl FW (2008) Gamma oscillations in gerbil auditory cortex during a target-discrimination task reflect matches with short-term memory. Brain Res 1220: 70-80.

Johnson RC, Penzes P, Eipper BA, Mains RE (2000) Isoforms of kalirin, a neuronal Dbl family member, generated through use of different 5'- and 3'-ends along with an internal translational initiation site. J Biol Chem 275: 19324-19333.

Jones CA, Watson DJ, Fone KC (2011) Animal models of schizophrenia. Br J Pharmacol 164: 1162-1194.

Jones EG (2000) Microcolumns in the cerebral cortex. Proceedings of the National Academy of Sciences 97: 5019-5021.

Jones TA, Klintsova AY, Kilman VL, Sirevaag AM, Greenough WT (1997) Induction of multiple synapses by experience in the visual cortex of adult rats. Neurobiol Learn Mem 68: 13-20.

Kaas JH, Hackett TA (2000) Subdivisions of auditory cortex and processing streams in primates. Proc Natl Acad Sci U S A 97: 11793-11799.

Kanaani J, Patterson G, Schaufele F, Lippincott-Schwartz J, Baekkeskov S (2008) A palmitoylation cycle dynamically regulates partitioning of the GABA-synthesizing enzyme GAD65 between ER-Golgi and post-Golgi membranes. J Cell Sci 121: 437-449.

Kaneko T, Fujiyama F (2002) Complementary distribution of vesicular glutamate transporters in the central nervous system. Neurosci Res 42: 243-250.

Kanold PO, Kim YA, GrandPre T, Shatz CJ (2009) Co-regulation of ocular dominance plasticity and NMDA receptor subunit expression in glutamic acid decarboxylase-65 knock-out mice. J Physiol 587: 2857-2867.

Kantrowitz JT, Leitman DI, Lehrfeld JM, Laukka P, Juslin PN, Butler PD, Silipo G, Javitt DC (2013) Reduction in tonal discriminations predicts receptive emotion processing deficits in schizophrenia and schizoaffective disorder. Schizophr Bull 39: 86-93.

Karlsgodt KH, Robleto K, Trantham-Davidson H, Jairl C, Cannon TD, Lavin A, Jentsch JD (2011) Reduced dysbindin expression mediates N-methyl-D-aspartate receptor hypofunction and impaired working memory performance. Biol Psychiatry 69: 28-34.

Kasai K, Nakagome K, Itoh K, Koshida I, Hata A, Iwanami A, Fukuda M, Kato N (2002) Impaired cortical network for preattentive detection of change in speech sounds in schizophrenia: a high-resolution event-related potential study. Am J Psychiatry 159: 546-553.

Kasai K, Shenton ME, Salisbury DF, Hirayasu Y, Onitsuka T, Spencer MH, Yurgelun-Todd DA, Kikinis R, Jolesz FA, McCarley RW (2003) Progressive decrease of left Heschl gyrus and planum temporale gray matter volume in first-episode schizophrenia: a longitudinal magnetic resonance imaging study. Arch Gen Psychiatry 60: 766-775.

Kash SF, Tecott LH, Hodge C, Baekkeskov S (1999) Increased anxiety and altered responses to anxiolytics in mice deficient in the 65-kDa isoform of glutamic acid decarboxylase. Proc Natl Acad Sci U S A 96: 1698-1703.

Katoh-Semba R, Takeuchi IK, Semba R, Kato K (1997) Distribution of brain-derived neurotrophic factor in rats and its changes with development in the brain. J Neurochem 69: 34-42.

Kaur S, Rose HJ, Lazar R, Liang K, Metherate R (2005) Spectral integration in primary auditory cortex: laminar processing of afferent input, in vivo and in vitro. Neuroscience 134: 1033-1045.

Kawakubo Y, Kamio S, Nose T, Iwanami A, Nakagome K, Fukuda M, Kato N, Rogers MA, Kasai K (2007) Phonetic mismatch negativity predicts social skills acquisition in schizophrenia. Psychiatry Res 152: 261-265.

Keshavan MS, Tandon R, Boutros NN, Nasrallah HA (2008) Schizophrenia, "just the facts": what we know in 2008 Part 3: neurobiology. Schizophr Res 106: 89-107.

Kilb W (2012) Development of the GABAergic system from birth to adolescence. Neuroscientist 18: 613-630.

Kirby AE, Middlebrooks JC (2012) Unanesthetized auditory cortex exhibits multiple codes for gaps in cochlear implant pulse trains. J Assoc Res Otolaryngol 13: 67-80.

Kiser PJ, Cooper NG, Mower GD (1998) Expression of two forms of glutamic acid decarboxylase (GAD67 and GAD65) during postnatal development of rat somatosensory barrel cortex. J Comp Neurol 402: 62-74.

Koch M (1998) Sensorimotor gating changes across the estrous cycle in female rats. Physiol Behav 64: 625-628.

Korostenskaja M, Dapsys K, Siurkute A, Maciulis V, Ruksenas O, Kahkonen S (2005) Effects of olanzapine on auditory P300 and mismatch negativity (MMN) in schizophrenia spectrum disorders. Prog Neuropsychopharmacol Biol Psychiatry 29: 543-548.

Krishnan GP, Hetrick WP, Brenner CA, Shekhar A, Steffen AN, O'Donnell BF (2009) Steady state and induced auditory gamma deficits in schizophrenia. Neuroimage 47: 1711-1719.

Krueger DD, Howell JL, Hebert BF, Olausson P, Taylor JR, Nairn AC (2006) Assessment of cognitive function in the heterozygous reeler mouse. Psychopharmacology (Berl) 189: 95-104.

Kushima I, Nakamura Y, Aleksic B, Ikeda M, Ito Y, Shiino T, Okochi T, Fukuo Y, Ujike H, Suzuki M, Inada T, Hashimoto R, Takeda M, Kaibuchi K, Iwata N, Ozaki N (2012) Resequencing and association analysis of the KALRN and EPHB1 genes and their contribution to schizophrenia susceptibility. Schizophr Bull 38: 552-560.

Kwon JS, McCarley RW, Hirayasu Y, Anderson JE, Fischer IA, Kikinis R, Jolesz FA, Shenton ME (1999a) Left planum temporale volume reduction in schizophrenia. Arch Gen Psychiatry 56: 142-148.

Kwon JS, O'Donnell BF, Wallenstein GV, Greene RW, Hirayasu Y, Nestor PG, Hasselmo ME, Potts GF, Shenton ME, McCarley RW (1999b) Gamma frequency-range abnormalities to auditory stimulation in schizophrenia. Arch Gen Psychiatry 56: 1001-1005.

Lambo ME, Turrigiano GG (2013) Synaptic and intrinsic homeostatic mechanisms cooperate to increase L2/3 pyramidal neuron excitability during a late phase of critical period plasticity. J Neurosci 33: 8810-8819.

Laprade N, Soghomonian JJ (1995) MK-801 decreases striatal and cortical GAD65 mRNA levels. Neuroreport 6: 1885-1889.

Leitman DI, Foxe JJ, Butler PD, Saperstein A, Revheim N, Javitt DC (2005) Sensory contributions to impaired prosodic processing in schizophrenia. Biol Psychiatry 58: 56-61.

Leitman DI, Laukka P, Juslin PN, Saccente E, Butler P, Javitt DC (2010a) Getting the cue: sensory contributions to auditory emotion recognition impairments in schizophrenia. Schizophr Bull 36: 545-556.

Leitman DI, Sehatpour P, Higgins BA, Foxe JJ, Silipo G, Javitt DC (2010b) Sensory deficits and distributed hierarchical dysfunction in schizophrenia. Am J Psychiatry 167: 818-827.

Leitman DI, Ziwich R, Pasternak R, Javitt DC (2006) Theory of Mind (ToM) and counterfactuality deficits in schizophrenia: misperception or misinterpretation? Psychol Med 36: 1075-1083.

Lenz D, Jeschke M, Schadow J, Naue N, Ohl FW, Herrmann CS (2008) Human EEG very high frequency oscillations reflect the number of matches with a template in auditory short-term memory. Brain Res 1220: 81-92.

Lewis DA (2009) Neuroplasticity of excitatory and inhibitory cortical circuits in schizophrenia. Dialogues Clin Neurosci 11: 269-280.

Lewis DA (2011) The chandelier neuron in schizophrenia. Dev Neurobiol 71: 118-127.

Lewis DA, Gonzalez-Burgos G (2008) Neuroplasticity of neocortical circuits in schizophrenia. Neuropsychopharmacology 33: 141-165.

Lewis DA, Hashimoto T, Volk DW (2005) Cortical inhibitory neurons and schizophrenia. Nat Rev Neurosci 6: 312-324.

Lewis DA, Sweet RA (2009) Schizophrenia from a neural circuitry perspective: advancing toward rational pharmacological therapies. J Clin Invest 119: 706-716.

Light GA, Hsu JL, Hsieh MH, Meyer-Gomes K, Sprock J, Swerdlow NR, Braff DL (2006) Gamma band oscillations reveal neural network cortical coherence dysfunction in schizophrenia patients. Biol Psychiatry 60: 1231-1240.

Linden JF, Schreiner CE (2003) Columnar transformations in auditory cortex? A comparison to visual and somatosensory cortices. Cereb Cortex 13: 83-89.

Liu BH, Wu GK, Arbuckle R, Tao HW, Zhang LI (2007) Defining cortical frequency tuning with recurrent excitatory circuitry. Nat Neurosci 10: 1594-1600.

Lysaker P, Bell M (1995) Negative symptoms and vocational impairment in schizophrenia: repeated measurements of work performance over six months. Acta Psychiatrica Scandinavica 91: 205-208.

Ma XM, Huang J, Wang Y, Eipper BA, Mains RE (2003) Kalirin, a multifunctional Rho guanine nucleotide exchange factor, is necessary for maintenance of hippocampal pyramidal neuron dendrites and dendritic spines. J Neurosci 23: 10593-10603.

Ma XM, Huang JP, Kim EJ, Zhu Q, Kuchel GA, Mains RE, Eipper BA (2011) Kalirin-7, an important component of excitatory synapses, is regulated by estradiol in hippocampal neurons. Hippocampus 21: 661-677.

Ma XM, Johnson RC, Mains RE, Eipper BA (2001) Expression of kalirin, a neuronal GDP/GTP exchange factor of the trio family, in the central nervous system of the adult rat. J Comp Neurol 429: 388-402.

Ma XM, Wang Y, Ferraro F, Mains RE, Eipper BA (2008) Kalirin-7 is an essential component of both shaft and spine excitatory synapses in hippocampal interneurons. J Neurosci 28: 711-724.

Majewska AK, Newton JR, Sur M (2006) Remodeling of synaptic structure in sensory cortical areas in vivo. J Neurosci 26: 3021-3029.

Mandela P, Yankova M, Conti LH, Ma XM, Grady J, Eipper BA, Mains RE (2012) Kalrn plays key roles within and outside of the nervous system. BMC Neurosci 13: 136.

Mann EO, Mody I (2010) Control of hippocampal gamma oscillation frequency by tonic inhibition and excitation of interneurons. Nat Neurosci 13: 205-212.

Markram H, Toledo-Rodriguez M, Wang Y, Gupta A, Silberberg G, Wu C (2004) Interneurons of the neocortical inhibitory system. Nat Rev Neurosci 5: 793-807.

Martin DL, Martin SB, Wu SJ, Espina N (1991) Regulatory properties of brain glutamate decarboxylase (GAD): the apoenzyme of GAD is present principally as the smaller of two molecular forms of GAD in brain. J Neurosci 11: 2725-2731.

Marty S, Berzaghi M, Berninger B (1997) Neurotrophins and activity-dependent plasticity of cortical interneurons. Trends Neurosci 20: 198-202.

Marty S, Wehrle R, Fritschy JM, Sotelo C (2004) Quantitative effects produced by modifications of neuronal activity on the size of GABAA receptor clusters in hippocampal slice cultures. Eur J Neurosci 20: 427-440.

Mataga N, Mizuguchi Y, Hensch TK (2004) Experience-dependent pruning of dendritic spines in visual cortex by tissue plasminogen activator. Neuron 44: 1031-1041.

Mateos JM, Luthi A, Savic N, Stierli B, Streit P, Gahwiler BH, McKinney RA (2007) Synaptic modifications at the CA3-CA1 synapse after chronic AMPA receptor blockade in rat hippocampal slices. J Physiol 581: 129-138.

Mathews JR, Barch DM (2010) Emotion responsivity, social cognition, and functional outcome in schizophrenia. J Abnorm Psychol 119: 50-59.

McCann CM, Nguyen QT, Santo NH, Lichtman JW (2007) Rapid synapse elimination after postsynaptic protein synthesis inhibition in vivo. J Neurosci 27: 6064-6067.

McCarley RW, Faux SF, Shenton ME, Nestor PG, Adams J (1991) Event-related potentials in schizophrenia: their biological and clinical correlates and a new model of schizophrenic pathophysiology. Schizophr Res 4: 209-231.

McCarley RW, Nakamura M, Shenton ME, Salisbury DF (2008) Combining ERP and structural MRI information in first episode schizophrenia and bipolar disorder. Clin EEG Neurosci 39: 57-60.

McCarley RW, Wible CG, Frumin M, Hirayasu Y, Levitt JJ, Fischer IA, Shenton ME (1999) MRI anatomy of schizophrenia. Biol Psychiatry 45: 1099-1119.

McGlashan TH, Hoffman RE (2000) Schizophrenia as a disorder of developmentally reduced synaptic connectivity. Arch Gen Psychiatry 57: 637-648.

Mei L, Xiong WC (2008) Neuregulin 1 in neural development, synaptic plasticity and schizophrenia. Nat Rev Neurosci 9: 437-452.

Micheva KD, Beaulieu C (1996) Quantitative aspects of synaptogenesis in the rat barrel field cortex with special reference to GABA circuitry. J Comp Neurol 373: 340-354.

Mijnster MJ, Galis-de-Graaf Y, Voorn P (1998): Serotonergic regulation of neuropeptide and glutamic acid decarboxylase mRNA levels in the rat striatum and globus pallidus: studies with fluoxetine and DOI. Brain Res Mol Brain Res 54: 64-73.

Mikaelian DO (1979) Development and degeneration of hearing in the C57/b16 mouse: relation of electrophysiologic responses from the round window and cochlear nucleus to cochlear anatomy and behavioral responses. Laryngoscope 89: 1-15.

Mirnics K, Middleton FA, Marquez A, Lewis DA, Levitt P (2000) Molecular characterization of schizophrenia viewed by microarray analysis of gene expression in prefrontal cortex. Neuron 28: 53-67.

Mirnics K, Middleton FA, Stanwood GD, Lewis DA, Levitt P (2001) Disease-specific changes in regulator of G-protein signaling 4 (RGS4) expression in schizophrenia. Mol Psychiatry 6: 293-301.

Mitani A, Shimokouchi M (1985) Neuronal connections in the primary auditory cortex: an electrophysiological study in the cat. J Comp Neurol 235: 417-429.

Miyamoto S, Duncan GE, Marx CE, Lieberman JA (2005) Treatments for schizophrenia: a critical review of pharmacology and mechanisms of action of antipsychotic drugs. Mol Psychiatry 10: 79-104.

Moghaddam B, Javitt D (2012) From revolution to evolution: the glutamate hypothesis of schizophrenia and its implication for treatment. Neuropsychopharmacology 37: 4-15.

Molholm S, Martinez A, Ritter W, Javitt DC, Foxe JJ (2005) The neural circuitry of pre-attentive auditory change-detection: an fMRI study of pitch and duration mismatch negativity generators. Cereb Cortex 15: 545-551.

Molinari M, Dell'Anna ME, Rausell E, Leggio MG, Hashikawa T, Jones EG (1995) Auditory thalamocortical pathways defined in monkeys by calcium-binding protein immunoreactivity. J Comp Neurol 362: 171-194.

Morris HM, Hashimoto T, Lewis DA (2008) Alterations in somatostatin mRNA expression in the dorsolateral prefrontal cortex of subjects with schizophrenia or schizoaffective disorder. Cereb Cortex 18: 1575-1587.

Moutsimilli L, Farley S, El Khoury MA, Chamot C, Sibarita JB, Racine V, El Mestikawy S, Mathieu F, Dumas S, Giros B, Tzavara ET (2008) Antipsychotics increase vesicular glutamate transporter 2 (VGLUT2) expression in thalamolimbic pathways. Neuropharmacology 54: 497-508.

Moyer CE, Delevich KM, Fish KN, Asafu-Adjei JK, Sampson AR, Dorph-Petersen KA, Lewis DA, Sweet RA (2012) Reduced glutamate decarboxylase 65 protein within primary auditory cortex inhibitory boutons in schizophrenia. Biol Psychiatry 72: 734-743.

Moyer CE, Delevich KM, Fish KN, Asafu-Adjei JK, Sampson AR, Dorph-Petersen KA, Lewis DA, Sweet RA (2013) Intracortical excitatory and thalamocortical boutons are intact in primary auditory cortex in schizophrenia. Schizophr Res 149: 127-134.

Muller M, Gahwiler BH, Rietschin L, Thompson SM (1993) Reversible loss of dendritic spines and altered excitability after chronic epilepsy in hippocampal slice cultures. Proc Natl Acad Sci U S A 90: 257-261.

Muly EC, Allen P, Mazloom M, Aranbayeva Z, Greenfield AT, Greengard P (2004) Subcellular distribution of neurabin immunolabeling in primate prefrontal cortex: comparison with spinophilin. Cereb Cortex 14: 1398-1407.

Murphy DD, Cole NB, Greenberger V, Segal M (1998) Estradiol increases dendritic spine density by reducing GABA neurotransmission in hippocampal neurons. J Neurosci 18: 2550-2559.

Naatanen R, Kahkonen S (2009) Central auditory dysfunction in schizophrenia as revealed by the mismatch negativity (MMN) and its magnetic equivalent MMNm: a review. Int J Neuropsychopharmacol 12: 125-135.

Naatanen R, Paavilainen P, Alho K, Reinikainen K, Sams M (1989) Do event-related potentials reveal the mechanism of the auditory sensory memory in the human brain? Neurosci Lett 98: 217-221.

Naatanen R, Picton T (1987) The N1 wave of the human electric and magnetic response to sound: a review and an analysis of the component structure. Psychophysiology 24: 375-425.

Navone F, Jahn R, Di Gioia G, Stukenbrok H, Greengard P, De Camilli P (1986) Protein p38: an integral membrane protein specific for small vesicles of neurons and neuroendocrine cells. J Cell Biol 103: 2511-2527.

Newey SE, Velamoor V, Govek EE, Van Aelst L (2005) Rho GTPases, dendritic structure, and mental retardation. J Neurobiol 64: 58-74.

O'Tuathaigh CM, Babovic D, O'Meara G, Clifford JJ, Croke DT, Waddington JL (2007) Susceptibility genes for schizophrenia: characterisation of mutant mouse models at the level of phenotypic behaviour. Neurosci Biobehav Rev 31: 60-78.

Oni-Orisan A, Kristiansen LV, Haroutunian V, Meador-Woodruff JH, McCullumsmith RE (2008) Altered vesicular glutamate transporter expression in the anterior cingulate cortex in schizophrenia. Biol Psychiatry 63: 766-775.

Ouimet CC, Katona I, Allen P, Freund TF, Greengard P (2004) Cellular and subcellular distribution of spinophilin, a PP1 regulatory protein that bundles F-actin in dendritic spines. J Comp Neurol 479: 374-388.

Owen MJ, Williams NM, O'Donovan MC (2004) The molecular genetics of schizophrenia: new findings promise new insights. Mol Psychiatry 9: 14-27.

Pantelis C, Velakoulis D, Wood SJ, Yucel M, Yung AR, Phillips LJ, Sun DQ, McGorry PD (2007) Neuroimaging and emerging psychotic disorders: the Melbourne ultra-high risk studies. Int Rev Psychiatry 19: 371-381.

Pastor MA, Artieda J, Arbizu J, Marti-Climent JM, Penuelas I, Masdeu JC (2002) Activation of human cerebral and cerebellar cortex by auditory stimulation at 40 Hz. J Neurosci 22: 10501-10506.

Patel AB, de Graaf RA, Martin DL, Battaglioli G, Behar KL (2006) Evidence that GAD65 mediates increased GABA synthesis during intense neuronal activity in vivo. J Neurochem 97: 385-396.

Patz S, Wirth MJ, Gorba T, Klostermann O, Wahle P (2003) Neuronal activity and neurotrophic factors regulate GAD-65/67 mRNA and protein expression in organotypic cultures of rat visual cortex. Eur J Neurosci 18: 1-12.

Paulson L, Martin P, Persson A, Nilsson CL, Ljung E, Westman-Brinkmalm A, Eriksson PS, Blennow K, Davidsson P (2003) Comparative genome- and proteome analysis of cerebral cortex from MK-801-treated rats. J Neurosci Res 71: 526-533.

Paus T, Keshavan M, Giedd JN (2008) Why do many psychiatric disorders emerge during adolescence? Nat Rev Neurosci 9: 947-957.

Paxinos G, Franklin K (2004) The Mouse Brain in Stereotaxic Coordinates: Compact Second Edition. San Diego: Elsevier Academic Press.

Paylor R, Crawley JN (1997) Inbred strain differences in prepulse inhibition of the mouse startle response. Psychopharmacology (Berl) 132: 169-180.

Peiffer AM, Friedman JT, Rosen GD, Fitch RH (2004) Impaired gap detection in juvenile microgyric rats. Brain Res Dev Brain Res 152: 93-98.

Penzes P, Buonanno A, Passafaro M, Sala C, Sweet RA (2013) Developmental vulnerability of synapses and circuits associated with neuropsychiatric disorders. J Neurochem 126: 165-182.

Penzes P, Johnson RC, Sattler R, Zhang X, Huganir RL, Kambampati V, Mains RE, Eipper BA (2001) The neuronal Rho-GEF Kalirin-7 interacts with PDZ domain-containing proteins and regulates dendritic morphogenesis. Neuron 29: 229-242.

Penzes P, Jones KA (2008) Dendritic spine dynamics--a key role for kalirin-7. Trends Neurosci 31: 419-427.

Penzes P, Rafalovich I (2012) Regulation of the actin cytoskeleton in dendritic spines. Adv Exp Med Biol 970: 81-95.

Penzes P, Remmers C (2012) Kalirin signaling: implications for synaptic pathology. Mol Neurobiol 45: 109-118.

Picton TW, John MS, Dimitrijevic A, Purcell D (2003) Human auditory steady-state responses. Int J Audiol 42: 177-219.

Pierri JN, Volk CL, Auh S, Sampson A, Lewis DA (2001) Decreased somal size of deep layer 3 pyramidal neurons in the prefrontal cortex of subjects with schizophrenia. Arch Gen Psychiatry 58: 466-473.

Pinto JG, Hornby KR, Jones DG, Murphy KM (2010) Developmental changes in GABAergic mechanisms in human visual cortex across the lifespan. Front Cell Neurosci 4: 16.

Powell CM, Miyakawa T (2006) Schizophrenia-relevant behavioral testing in rodent models: a uniquely human disorder? Biol Psychiatry 59: 1198-1207.

Prieto JJ, Peterson BA, Winer JA (1994) Morphology and spatial distribution of GABAergic neurons in cat primary auditory cortex (AI). J Comp Neurol 344: 349-382.

Qin ZH, Zhang SP, Weiss B (1994) Dopaminergic and glutamatergic blocking drugs differentially regulate glutamic acid decarboxylase mRNA in mouse brain. Brain Res Mol Brain Res 21: 293-302.

Rabiner CA, Mains RE, Eipper BA (2005) Kalirin: a dual Rho guanine nucleotide exchange factor that is so much more than the sum of its many parts. Neuroscientist 11: 148-160.

Rabinowicz EF, Silipo G, Goldman R, Javitt DC (2000) Auditory sensory dysfunction in schizophrenia. Imprecision or distractibility? Arch Gen Psychiatry 57: 1149-1155.

Racenstein JM, Harrow M, Reed R, Martin E, Herbener E, Penn DL (2002) The relationship between positive symptoms and instrumental work functioning in schizophrenia: a 10 year follow-up study. Schizophr Res 56: 95-103.

Radziwon KE, June KM, Stolzberg DJ, Xu-Friedman MA, Salvi RJ, Dent ML (2009) Behaviorally measured audiograms and gap detection thresholds in CBA/CaJ mice. J Comp Physiol A Neuroethol Sens Neural Behav Physiol 195: 961-969.

Rajarethinam R, Sahni S, Rosenberg DR, Keshavan MS (2004) Reduced superior temporal gyrus volume in young offspring of patients with schizophrenia. Am J Psychiatry 161: 1121-1124.

Rakic P, Bourgeois JP, Eckenhoff MF, Zecevic N, Goldman-Rakic PS (1986) Concurrent overproduction of synapses in diverse regions of the primate cerebral cortex. Science 232: 232-235.

Rasser PE, Schall U, Todd J, Michie PT, Ward PB, Johnston P, Helmbold K, Case V, Soyland A, Tooney PA, Thompson PM (2011) Gray matter deficits, mismatch negativity, and outcomes in schizophrenia. Schizophr Bull 37: 131-140.

Rauschecker JP, Tian B, Hauser M (1995) Processing of complex sounds in the macaque nonprimary auditory cortex. Science 268: 111-114.

Read HL, Winer JA, Schreiner CE (2002) Functional architecture of auditory cortex. Curr Opin Neurobiol 12: 433-440.

Revheim N, Butler PD, Schechter I, Jalbrzikowski M, Silipo G, Javitt DC (2006) Reading impairment and visual processing deficits in schizophrenia. Schizophr Res 87: 238-245.

Rieck RW, Ansari MS, Whetsell WO, Jr., Deutch AY, Kessler RM (2004) Distribution of dopamine D2-like receptors in the human thalamus: autoradiographic and PET studies. Neuropsychopharmacology 29: 362-372.

Ripley B, Otto S, Tiglio K, Williams ME, Ghosh A (2011) Regulation of synaptic stability by AMPA receptor reverse signaling. Proc Natl Acad Sci U S A 108: 367-372.

Rocco, BR and Fish, K. N. Differential GAD65 and GAD67 expression in somatostatin-positive axon terminals. Society for Neuroscience Annual Meeting, San Diego, CA . 2010.

Rockel AJ, Hiorns RW, Powell TP (1980) The basic uniformity in structure of the neocortex. Brain 103: 221-244.

Rodriguez-Moreno A, Gonzalez-Rueda A, Banerjee A, Upton AL, Craig MT, Paulsen O (2013) Presynaptic self-depression at developing neocortical synapses. Neuron 77: 35-42.

Rossman KL, Der CJ, Sondek J (2005) GEF means go: turning on RHO GTPases with guanine nucleotide-exchange factors. Nat Rev Mol Cell Biol 6: 167-180.

Rubio MD, Haroutunian V, Meador-Woodruff JH (2012) Abnormalities of the Duo/Ras-related C3 botulinum toxin substrate 1/p21-activated kinase 1 pathway drive myosin light chain phosphorylation in frontal cortex in schizophrenia. Biol Psychiatry 71: 906-914.

Ruiz R, Cano R, Casanas JJ, Gaffield MA, Betz WJ, Tabares L (2011) Active zones and the readily releasable pool of synaptic vesicles at the neuromuscular junction of the mouse. J Neurosci 31: 2000-2008.

Rybalko N, Suta D, Nwabueze-Ogbo F, Syka J (2006) Effect of auditory cortex lesions on the discrimination of frequency-modulated tones in rats. Eur J Neurosci 23: 1614-1622.

Saletu B, Itil TM, Saletu M (1971) Auditory evoked response, EEG, and thought process in schizophrenics. Am J Psychiatry 128: 336-344.

Salisbury DF (2008) Semantic activation and verbal working memory maintenance in schizophrenic thought disorder: insights from electrophysiology and lexical ambiguity. Clin EEG Neurosci 39: 103-107.

Salisbury DF, Kuroki N, Kasai K, Shenton ME, McCarley RW (2007) Progressive and interrelated functional and structural evidence of post-onset brain reduction in schizophrenia. Arch Gen Psychiatry 64: 521-529.

Salisbury DF, Shenton ME, Griggs CB, Bonner-Jackson A, McCarley RW (2002) Mismatch negativity in chronic schizophrenia and first-episode schizophrenia. Arch Gen Psychiatry 59: 686-694.

Sanchez-Huertas C, Rico B (2011) CREB-Dependent Regulation of GAD65 Transcription by BDNF/TrkB in Cortical Interneurons. Cereb Cortex 21: 777-788.

Sarro EC, Kotak VC, Sanes DH, Aoki C (2008) Hearing loss alters the subcellular distribution of presynaptic GAD and postsynaptic GABAA receptors in the auditory cortex. Cereb Cortex 18: 2855-2867.

Sarrouilhe D, di Tommaso A, Metaye T, Ladeveze V (2006) Spinophilin: from partners to functions. Biochimie 88: 1099-1113.

Schall U, Catts SV, Chaturvedi S, Liebert B, Redenbach J, Karayanidis F, Ward PB (1998) The effect of clozapine therapy on frontal lobe dysfunction in schizophrenia: neuropsychology and event-related potential measures. Int J Neuropsychopharmacol 1: 19-29.

Schmidt SJ, Mueller DR, Roder V (2011) Social cognition as a mediator variable between neurocognition and functional outcome in schizophrenia: empirical review and new results by structural equation modeling. Schizophr Bull 37 Suppl 2: S41-S54.

Schuz A, Palm G (1989) Density of neurons and synapses in the cerebral cortex of the mouse. J Comp Neurol 286: 442-455.

Segal M (2010) Dendritic spines, synaptic plasticity and neuronal survival: activity shapes dendritic spines to enhance neuronal viability. Eur J Neurosci 31: 2178-2184.

Selemon LD (2013) A role for synaptic plasticity in the adolescent development of executive function. Transl Psychiatry 3: e238.

Shan D, Lucas EK, Drummond JB, Haroutunian V, Meador-Woodruff JH, McCullumsmith RE (2013) Abnormal expression of glutamate transporters in temporal lobe areas in elderly patients with schizophrenia. Schizophr Res 144: 1-8.

Shaw P, Kabani NJ, Lerch JP, Eckstrand K, Lenroot R, Gogtay N, Greenstein D, Clasen L, Evans A, Rapoport JL, Giedd JN, Wise SP (2008) Neurodevelopmental trajectories of the human cerebral cortex. J Neurosci 28: 3586-3594.

Shea TL, Sergejew AA, Burnham D, Jones C, Rossell SL, Copolov DL, Egan GF (2007) Emotional prosodic processing in auditory hallucinations. Schizophr Res 90: 214-220.

Shelley AM, Ward PB, Catts SV, Michie PT, Andrews S, McConaghy N (1991) Mismatch negativity: an index of a preattentive processing deficit in schizophrenia. Biol Psychiatry 30: 1059-1062.

Shenton ME, Dickey CC, Frumin M, McCarley RW (2001) A review of MRI findings in schizophrenia. Schizophr Res 49: 1-52.

Shepherd GM, Harris KM (1998) Three-dimensional structure and composition of CA3-->CA1 axons in rat hippocampal slices: implications for presynaptic connectivity and compartmentalization. J Neurosci 18: 8300-8310.

Shepherd GM, Woolf TB, Carnevale NT (1989) Comparisons between Active Properties of Distal Dendritic Branches and Spines: Implications for Neuronal Computations. Journal of Cognitive Neuroscience 1: 273-286.

Simon AE, Cattapan-Ludewig K, Zmilacher S, Arbach D, Gruber K, Dvorsky DN, Roth B, Isler E, Zimmer A, Umbricht D (2007) Cognitive functioning in the schizophrenia prodrome. Schizophr Bull 33: 761-771.

Smiley JF, Rosoklija G, Mancevski B, Mann JJ, Dwork AJ, Javitt DC (2009) Altered volume and hemispheric asymmetry of the superficial cortical layers in the schizophrenia planum temporale. Eur J Neurosci 30: 449-463.

Smit F, Bolier L, Cuijpers P (2004) Cannabis use and the risk of later schizophrenia: a review. Addiction 99: 425-430.

Smith PH, Populin LC (2001) Fundamental differences between the thalamocortical recipient layers of the cat auditory and visual cortices. J Comp Neurol 436: 508-519.

Smith RE, Haroutunian V, Davis KL, Meador-Woodruff JH (2001) Vesicular glutamate transporter transcript expression in the thalamus in schizophrenia. Neuroreport 12: 2885-2887.

Sohal VS, Zhang F, Yizhar O, Deisseroth K (2009) Parvalbumin neurons and gamma rhythms enhance cortical circuit performance. Nature 459: 698-702.

Spear LP (2000) The adolescent brain and age-related behavioral manifestations. Neurosci Biobehav Rev 24: 417-463.

Spear LP, Brake SC (1983) Periadolescence: age-dependent behavior and psychopharmacological responsivity in rats. Dev Psychobiol 16: 83-109.

Spencer KM, Salisbury DF, Shenton ME, McCarley RW (2008) Gamma-band auditory steady-state responses are impaired in first episode psychosis. Biol Psychiatry 64: 369-375.

Spongr VP, Flood DG, Frisina RD, Salvi RJ (1997) Quantitative measures of hair cell loss in CBA and C57BL/6 mice throughout their life spans. J Acoust Soc Am 101: 3546-3553.

Stanley JA, Drost DJ, Williamson PC, Carr TJ (1995) In vivo proton MRS study of glutamate and schizophrenia. Nasrallah HA and Pettegrew JW (Eds.), NMR Spectroscopy in Psychiatric Brain Disorders., American Psychiatric Press, Washington, DC. pp. 21–44.

Steinschneider M, Schroeder CE, Arezzo JC, Vaughan HG, Jr. (1994) Speech-evoked activity in primary auditory cortex: effects of voice onset time. Electroencephalogr Clin Neurophysiol 92: 30-43.

Steinschneider M, Schroeder CE, Arezzo JC, Vaughan HG, Jr. (1995) Physiologic correlates of the voice onset time boundary in primary auditory cortex (A1) of the awake monkey: temporal response patterns. Brain Lang 48: 326-340.

Steinschneider M, Volkov IO, Noh MD, Garell PC, Howard MA, III (1999) Temporal encoding of the voice onset time phonetic parameter by field potentials recorded directly from human auditory cortex. J Neurophysiol 82: 2346-2357.

Strous RD, Cowan N, Ritter W, Javitt DC (1995) Auditory sensory ("echoic") memory dysfunction in schizophrenia. Am J Psychiatry 152: 1517-1519.

Sullivan PF, Kendler KS, Neale MC (2003) Schizophrenia as a complex trait: evidence from a meta-analysis of twin studies. Arch Gen Psychiatry 60: 1187-1192.

Sun W, Hansen A, Zhang L, Lu J, Stolzberg D, Kraus KS (2008) Neonatal nicotine exposure impairs development of auditory temporal processing. Hear Res 245: 58-64.

Sun W, Tang L, Allman BL (2011) Environmental noise affects auditory temporal processing development and NMDA-2B receptor expression in auditory cortex. Behav Brain Res 218: 15-20.

Sweet RA, Bergen SE, Sun Z, Marcsisin MJ, Sampson AR, Lewis DA (2007) Anatomical evidence of impaired feedforward auditory processing in schizophrenia. Biol Psychiatry 61: 854-864.

Sweet RA, Bergen SE, Sun Z, Sampson AR, Pierri JN, Lewis DA (2004) Pyramidal cell size reduction in schizophrenia: evidence for involvement of auditory feedforward circuits. Biol Psychiatry 55: 1128-1137.

Sweet RA, Dorph-Petersen KA, Lewis DA (2005) Mapping auditory core, lateral belt, and parabelt cortices in the human superior temporal gyrus. J Comp Neurol 491: 270-289.

Sweet RA, Fish KN, Lewis DA (2010) Mapping Synaptic Pathology within Cerebral Cortical Circuits in Subjects with Schizophrenia. Frontiers in Human Neuroscience 4.

Sweet RA, Henteleff RA, Zhang W, Sampson AR, Lewis DA (2009) Reduced dendritic spine density in auditory cortex of subjects with schizophrenia. Neuropsychopharmacology 34: 374-389.

Sweet RA, Pierri JN, Auh S, Sampson AR, Lewis DA (2003) Reduced pyramidal cell somal volume in auditory association cortex of subjects with schizophrenia. Neuropsychopharmacology 28: 599-609.

Swerdlow NR, Geyer MA, Braff DL (2001) Neural circuit regulation of prepulse inhibition of startle in the rat: current knowledge and future challenges. Psychopharmacology (Berl) 156: 194-215.

Tada T, Sheng M (2006) Molecular mechanisms of dendritic spine morphogenesis. Curr Opin Neurobiol 16: 95-101.

Taft RA, Davisson M, Wiles MV (2006) Know thy mouse. Trends Genet 22: 649-653.

Takahashi T, Wood SJ, Yung AR, Soulsby B, McGorry PD, Suzuki M, Kawasaki Y, Phillips LJ, Velakoulis D, Pantelis C (2009) Progressive Gray Matter Reduction of the Superior Temporal Gyrus During Transition to Psychosis. Arch Gen Psychiatry 66: 366-376.

Tanaka C, Nishizuka Y (1994) The protein kinase C family for neuronal signaling. Annu Rev Neurosci 17: 551-567.

Tandon R, Keshavan MS, Nasrallah HA (2008) Schizophrenia, "just the facts" what we know in 2008. 2. Epidemiology and etiology. Schizophr Res 102: 1-18.

Tandon R, Nasrallah HA, Keshavan MS (2009) Schizophrenia, "just the facts" 4. Clinical features and conceptualization. Schizophr Res 110: 1-23.

Thomases DR, Cass DK, Tseng KY (2013) Periadolescent exposure to the NMDA receptor antagonist MK-801 impairs the functional maturation of local GABAergic circuits in the adult prefrontal cortex. J Neurosci 33: 26-34.

Thompson PM, Vidal C, Giedd JN, Gochman P, Blumenthal J, Nicolson R, Toga AW, Rapoport JL (2001) Mapping adolescent brain change reveals dynamic wave of accelerated gray matter loss in very early-onset schizophrenia. Proc Natl Acad Sci U S A 98: 11650-11655.

Thonnessen H, Zvyagintsev M, Harke KC, Boers F, Dammers J, Norra C, Mathiak K (2008) Optimized mismatch negativity paradigm reflects deficits in schizophrenia patients. A combined EEG and MEG study. Biol Psychol 77: 205-216.

Threlkeld SW, Hill CA, Rosen GD, Fitch RH (2009) Early acoustic discrimination experience ameliorates auditory processing deficits in male rats with cortical developmental disruption. Int J Dev Neurosci 27: 321-328.

Thune JJ, Uylings HB, Pakkenberg B (2001) No deficit in total number of neurons in the prefrontal cortex in schizophrenics. J Psychiatr Res 35: 15-21.

Tian N, Petersen C, Kash S, Baekkeskov S, Copenhagen D, Nicoll R (1999) The role of the synthetic enzyme GAD65 in the control of neuronal gamma-aminobutyric acid release. Proc Natl Acad Sci U S A 96: 12911-12916.

Tootell RB, Hamilton SL, Silverman MS (1985) Topography of cytochrome oxidase activity in owl monkey cortex. J Neurosci 5: 2786-2800.

Tramo MJ, Shah GD, Braida LD (2002) Functional role of auditory cortex in frequency processing and pitch perception. J Neurophysiol 87: 122-139.

Treiman DM (2001) GABAergic mechanisms in epilepsy. Epilepsia 42 Suppl 3: 8-12.

Truong DT, Venna VR, McCullough LD, Fitch RH (2012) Deficits in auditory, cognitive, and motor processing following reversible middle cerebral artery occlusion in mice. Exp Neurol 238: 114-121.

Tsay D, Yuste R (2004) On the electrical function of dendritic spines. Trends Neurosci 27: 77-83.

Turner CP, DeBenedetto D, Ware E, Stowe R, Lee A, Swanson J, Walburg C, Lambert A, Lyle M, Desai P, Liu C (2010) Postnatal exposure to MK801 induces selective changes in GAD67 or parvalbumin. Exp Brain Res 201: 479-488.

Turner JG, Brozoski TJ, Bauer CA, Parrish JL, Myers K, Hughes LF, Caspary DM (2006) Gap detection deficits in rats with tinnitus: a potential novel screening tool. Behav Neurosci 120: 188-195.

Uezato A, Meador-Woodruff JH, McCullumsmith RE (2009) Vesicular glutamate transporter mRNA expression in the medial temporal lobe in major depressive disorder, bipolar disorder, and schizophrenia. Bipolar Disord 11: 711-725.

Uhlhaas PJ, Singer W (2010) Abnormal neural oscillations and synchrony in schizophrenia. Nat Rev Neurosci 11: 100-113.

Umbricht D, Javitt D, Novak G, Bates J, Pollack S, Lieberman J, Kane J (1998) Effects of clozapine on auditory event-related potentials in schizophrenia. Biol Psychiatry 44: 716-725.

Umbricht D, Javitt D, Novak G, Bates J, Pollack S, Lieberman J, Kane J (1999) Effects of risperidone on auditory event-related potentials in schizophrenia. Int J Neuropsychopharmacol 2: 299-304.

Vassos E, Pedersen CB, Murray RM, Collier DA, Lewis CM (2012) Meta-analysis of the association of urbanicity with schizophrenia. Schizophr Bull 38: 1118-1123.

Vierling-Claassen D, Siekmeier P, Stufflebeam S, Kopell N (2008) Modeling GABA alterations in schizophrenia: a link between impaired inhibition and altered gamma and beta range auditory entrainment. J Neurophysiol 99: 2656-2671.

Villa AE, Rouiller EM, Simm GM, Zurita P, de Ribaupierre Y, de Ribaupierre F (1991) Corticofugal modulation of the information processing in the auditory thalamus of the cat. Exp Brain Res 86: 506-517.

Wadell H (1935) Volume, Shape, and Roundness of Quartz Particles. The Journal of Geology 43: 250-280.

Wang J, Caspary D, Salvi RJ (2000) GABA-A antagonist causes dramatic expansion of tuning in primary auditory cortex. Neuroreport 11: 1137-1140.

Wang J, McFadden SL, Caspary D, Salvi R (2002) Gamma-aminobutyric acid circuits shape response properties of auditory cortex neurons. Brain Res 944: 219-231.

Weedman DL, Ryugo DK (1996) Projections from auditory cortex to the cochlear nucleus in rats: synapses on granule cell dendrites. J Comp Neurol 371: 311-324.

Wehr M, Zador AM (2003) Balanced inhibition underlies tuning and sharpens spike timing in auditory cortex. Nature 426: 442-446.

Wei J, Davis KM, Wu H, Wu JY (2004) Protein phosphorylation of human brain glutamic acid decarboxylase (GAD)65 and GAD67 and its physiological implications. Biochemistry 43: 6182-6189.

Wei J, Wu JY (2008) Post-translational regulation of L-glutamic acid decarboxylase in the brain. Neurochem Res 33: 1459-1465.

Weickert CS, Straub RE, McClintock BW, Matsumoto M, Hashimoto R, Hyde TM, Herman MM, Weinberger DR, Kleinman JE (2004) Human dysbindin (DTNBP1) gene expression in normal brain and in schizophrenic prefrontal cortex and midbrain. Arch Gen Psychiatry 61: 544-555.

Welker E, Soriano E, Van der LH (1989) Plasticity in the barrel cortex of the adult mouse: effects of peripheral deprivation on GAD-immunoreactivity. Exp Brain Res 74: 441-452.

Whittington MA, Traub RD, Kopell N, Ermentrout B, Buhl EH (2000) Inhibition-based rhythms: experimental and mathematical observations on network dynamics. Int J Psychophysiol 38: 315-336.

Willott JF, Aitkin LM, McFadden SL (1993) Plasticity of auditory cortex associated with sensorineural hearing loss in adult C57BL/6J mice. J Comp Neurol 329: 402-411.

Willott JF, Carlson S, Chen H (1994) Prepulse inhibition of the startle response in mice: relationship to hearing loss and auditory system plasticity. Behav Neurosci 108: 703-713.

Willott JF, Tanner L, O'Steen J, Johnson KR, Bogue MA, Gagnon L (2003) Acoustic startle and prepulse inhibition in 40 inbred strains of mice. Behav Neurosci 117: 716-727.

Wilson NR, Kang J, Hueske EV, Leung T, Varoqui H, Murnick JG, Erickson JD, Liu G (2005) Presynaptic regulation of quantal size by the vesicular glutamate transporter VGLUT1. J Neurosci 25: 6221-6234.

Winer JA (1985) Structure of layer II in cat primary auditory cortex (AI). J Comp Neurol 238: 10-37.

Winer JA, Diehl JJ, Larue DT (2001) Projections of auditory cortex to the medial geniculate body of the cat. J Comp Neurol 430: 27-55.

Winer JA, Larue DT (1989) Populations of GABAergic neurons and axons in layer I of rat auditory cortex. Neuroscience 33: 499-515.

Winer JA, Larue DT, Diehl JJ, Hefti BJ (1998) Auditory cortical projections to the cat inferior colliculus. J Comp Neurol 400: 147-174.

Winer JA, Prieto JJ (2001) Layer V in cat primary auditory cortex (AI): cellular architecture and identification of projection neurons. J Comp Neurol 434: 379-412.

Winkler I, Karmos G, Naatanen R (1996) Adaptive modeling of the unattended acoustic environment reflected in the mismatch negativity event-related potential. Brain Res 742: 239-252.

Woods GF, Oh WC, Boudewyn LC, Mikula SK, Zito K (2011) Loss of PSD-95 enrichment is not a prerequisite for spine retraction. J Neurosci 31: 12129-12138.

World Health Organization. (2013). *Schizophrenia*. Retrieved August 9, 2013, from http://www.who.int/mental_health/management/schizophrenia/en/

Wu GK, Arbuckle R, Liu BH, Tao HW, Zhang LI (2008) Lateral sharpening of cortical frequency tuning by approximately balanced inhibition. Neuron 58: 132-143.

Wynn JK, Sugar C, Horan WP, Kern R, Green MF (2010) Mismatch negativity, social cognition, and functioning in schizophrenia patients. Biol Psychiatry 67: 940-947.

Xie Z, Srivastava DP, Photowala H, Kai L, Cahill ME, Woolfrey KM, Shum CY, Surmeier DJ, Penzes P (2007) Kalirin-7 controls activity-dependent structural and functional plasticity of dendritic spines. Neuron 56: 640-656.

Xu J, Yu L, Zhang J, Cai R, Sun X (2010) Early continuous white noise exposure alters l-alpha-amino-3-hydroxy-5-methyl-4-isoxazole propionic acid receptor subunit glutamate receptor 2 and gamma-aminobutyric acid type a receptor subunit beta3 protein expression in rat auditory cortex. J Neurosci Res 88: 614-619.

Yan J, Ehret G (2002) Corticofugal modulation of midbrain sound processing in the house mouse. Eur J Neurosci 16: 119-128.

Yang L, Chen S, Chen CM, Khan F, Forchelli G, Javitt DC (2012) Schizophrenia, culture and neuropsychology: sensory deficits, language impairments and social functioning in Chinese-speaking schizophrenia patients. Psychol Med 42: 1485-1494.

Yang S, Weiner BD, Zhang LS, Cho SJ, Bao S (2011) Homeostatic plasticity drives tinnitus perception in an animal model. Proc Natl Acad Sci U S A 108: 14974-14979.

Yoon JH, Maddock RJ, Rokem A, Silver MA, Minzenberg MJ, Ragland JD, Carter CS (2010) GABA concentration is reduced in visual cortex in schizophrenia and correlates with orientation-specific surround suppression. J Neurosci 30: 3777-3781.

Yoshihara Y, De Roo M, Muller D (2009b) Dendritic spine formation and stabilization. Curr Opin Neurobiol 19: 146-153.

Yoshihara Y, De Roo M, Muller D (2009a) Dendritic spine formation and stabilization. Curr Opin Neurobiol 19: 146-153.

Zecevic N, Bourgeois JP, Rakic P (1989) Changes in synaptic density in motor cortex of rhesus monkey during fetal and postnatal life. Brain Res Dev Brain Res 50: 11-32.

Zecevic N, Rakic P (1991) Synaptogenesis in monkey somatosensory cortex. Cereb Cortex 1: 510-523.

Zhang Y, Suga N (1997) Corticofugal amplification of subcortical responses to single tone stimuli in the mustached bat. J Neurophysiol 78: 3489-3492.

Zhang Z, Cai YQ, Zou F, Bie B, Pan ZZ (2011) Epigenetic suppression of GAD65 expression mediates persistent pain. Nat Med 17: 1448-1455.

Zhou X, Panizzutti R, Villers-Sidani E, Madeira C, Merzenich MM (2011) Natural restoration of critical period plasticity in the juvenile and adult primary auditory cortex. J Neurosci 31: 5625-5634.

Ziegel J, Kiderlen M (2010) Estimation of surface area and surface area measure of three-dimensional sets from digitizations. Image and Vision Computing 28: 64-77.

Zuo Y, Lin A, Chang P, Gan WB (2005) Development of long-term dendritic spine stability in diverse regions of cerebral cortex. Neuron 46: 181-189.